Heat and Mass Transfer

De-Yi Shang
Liang-Cai Zhong

Heat Transfer of Laminar Mixed Convection of Liquid

Springer

Heat and Mass Transfer

More information about this series at http://www.springer.com/series/4247

De-Yi Shang · Liang-Cai Zhong

Heat Transfer of Laminar Mixed Convection of Liquid

Springer

De-Yi Shang
Dr. of Tsinghua University and former professor of Northeastern University, China
136 Ingersoll Cres., Ottawa, ON, Canada
e-mail: deyishang@yahoo.ca

Liang-Cai Zhong
Department of Ferrous Metallurgy
Northeastern University
Shenyang
China

ISSN 1860-4846 ISSN 1860-4854 (electronic)
Heat and Mass Transfer
ISBN 978-3-319-27958-9 ISBN 978-3-319-27959-6 (eBook)
DOI 10.1007/978-3-319-27959-6

Library of Congress Control Number: 2015959944

Printed on acid-free paper

This Springer imprint is published by SpringerNature
The registered company is Springer International Publishing AG Switzerland

Preface

Three years ago, just after our book "Free convection film flows and heat transfer—models of laminar free convection with phase change for heat and mass transfer analysis" was published, our research interests were transferred to the more challenging field of laminar mixed convection heat and mass transfer. This is a cross field of free and forced convection with more difficult issues than free or forced convections. Strictly speaking, all forced convection heat transfer is mixed convection heat transfer. In fact, net forced convection heat transfer does never exist. It is because in fluid medium of so-called forced convection heat transfer, there should be temperature difference, which leads to fluid buoyancy. While, the fluid buoyancy will cause free convection. There have been numerous previous studies on mixed convection, however, for such a difficult field, engineers still have to deal with many unresolved problems. Due to these unresolved difficult problems, so far there is a lack of studies on the development of reliable theoretical or experiment achievements for heat transfer application of mixed convection. These difficulties prompted us to think deeply. Finally, we knew that to resolve these problems we needed to focus on the following issues: (i) developing an advanced theoretical and mathematical model; (ii) carefully considering and treating the variable physical properties of fluids; (iii) obtaining systems of rigorous numerical solutions; and (iv) on these bases, creating optimal formalized equations of heat transfer coefficient. In fact, these focused issues are interrelated. An advanced theoretical and mathematical model is the basic condition for successful investigation of mixed convection heat transfer. To address this issue, our innovative similarity transformation on velocity field would be taken as a better alternative. While, in our system of studies on free and forced convection heat and mass transfer, our innovative similarity transformation was conveniently and reliably applied. On the other hand, the variable physical properties will be taken into account in this study, and the polynomial model will be induced for treatment of the variable physical properties of liquids. Although there could be different models selected for consideration of the variable physical properties of liquids, the polynomial model should be the most convenient one combined with the transformed governing ordinary differential

equations used for simultaneous solutions.Through our comparison on the values of mixed convection heat transfer coefficient predicted for consideration of coupled effect of variable physical properties with those for consideration of Boussinesq approximation, we found their deviations are as high as over 8.4 %. It proves that proper consideration of the variable physical properties of fluids is very important for enhancement of the theoretical and practical value of convection heat transfer. Hence, it is important to face up the variable physical properties of fluids in rigorous theoretical study on clarification of convection heat transfer. Actually, since two decades ago, we have been committed to consider effect of fluid's variable physical properties on convection heat transfer in our studies. We deeply feel that it is necessary to consider coupled effect of variable physical properties for assurance of the theoretical and practical value for research of convection heat transfer. While, Boussinesq approximation or ignoring fluid's variable physical properties will severely weakened the theoretical and practical value of convection heat transfer. Furthermore, creation of the optimal formalized equations of heat transfer coefficient will be an important indicator on study with theoretical and application value for convection heat transfer application.

With this opportunity we thank Springer-Verlag for publishing our book "Heat Transfer of Laminar Mixed Convection of Liquid". We hope, based on our above efforts, this book will have a special theoretical and practical value for mixed convection heat transfer application, and will be of benefit to engineers, researchers, professors, and Ph.D. and master students in their engineering design, research work and teaching courses on thermal fluids and engineering fields related to convection heat and mass transfer.

Canada
August 2015

De-Yi Shang
Liang-Cai Zhong

Contents

Nomenclature

A	Area, m^2
c_p	Specific heat, J/(kg K)
g	Gravity acceleration, m/s^2
$Gr_{x,f}$	Local Grashof number for consideration of Boussinesq approximation
$Gr_{x,\infty}$	Local Grashof number for consideration of variable physical properties
$Mc_{x,f}$	Local mixed convection parameter for consideration of Boussinesq approximation
$Mc_{x,\infty}$	Local mixed convection parameter for consideration of variable physical properties
$Nu_{x,f}$	Local Nusselt number for consideration of Boussinesq approximation
$\overline{Nu}_{x,f}$	Average Nussel number for consideration of Boussinesq approximation
$Nu_{x,w}$	Local Nusselt number for consideration of variable physical properties
$\overline{Nu}_{x,w}$	Average Nusselt number for consideration of variable physical properties
Pr	Prandtl number
Pr_f	Mean Prandtl number at average temperature
Pr_w	Local Prandtl number at wall temperature
Pr_∞	Local Prandtl number at bulk local temperature
Q	Heat transfer rate, W
$q_{x,f}$	Local heat transfer rate for consideration of Boussinesq approximation, W/m^2
$Q_{x,f}$	Total heat transfer rate for consideration of Boussinesq approximation, W
$q_{x,w}$	Local heat transfer rate for consideration of variable physical properties, W/m^2

$Q_{x,w}$	Tocal heat transfer rate for consideration of variable physical properties, W
$Re_{x,f}$	Local Reynolds number with consideration of Boussinesq approximation
$Re_{x,\infty}$	Local Reynolds number with consideration of variable physical properties
t	Temperature, °C
T	Absolute temperature, K
Δt	Temperature difference, $t_w - t_\infty$, °C
t_f	Average temperature, °C
t_w	Wall temperature, °C
t_∞	Fluid bulk temperature, °C
w_x, w_y	Velocity components respectively in x and y directions, m/s
$w_{x,\infty}$	Velocity component beyond the boundary layer, m/s
$W_x(\eta, x)$, $W_y(\eta, x)$	Similarity velocity component, m/s
$W_x(\eta, Mc_{x,f}), /, W_y(\eta, Mc_{x,f})$	Equivalent similarity velocity components with consideration of Boussinesq approximation, m/s
$W_x(\eta, Mc_{x,\infty}), /, W_y(\eta, Mc_{x,\infty})$	Equivalent similarity velocity components with consideration of variable physical properties
x, y	Two-dimensional coordinate variables

Greek Symbols

ρ	Density, kg/m^3
μ	Absolute viscosity, kg/(m s)
λ	Thermal conductivity, W/(m K)
v	Kinetic viscosity, m^2/s
β	Expansion coefficient, 1/K
η	Similarity coordinate variable
θ	Similarity temperature
$\alpha_{x,f}$	Local heat transfer coefficient with consideration of Boussinesq approximation, W/(m^2 K)
$\overline{\alpha}_{x,f}$	Average heat transfer coefficient with consideration of Boussinesq approximation, W/(m^2 K)
$\alpha_{x,w}$	Local heat transfer coefficient with consideration of variable physical properties, W/(m^2 K)
$\overline{\alpha}_{x,w}$	Average heat transfer coefficient with consideration of variable physical properties, W/(m^2 K)
$\left(-\frac{\partial\theta(\eta,Mc)}{\partial\eta}\right)_{\eta=0}$	Wall similarity temperature gradient for consideration of Boussinesq approximation

$\left(-\frac{\partial\theta(\eta,Mc)}{\partial\eta}\right)_{\eta=0}$	Wall similarity temperature gradient for consideration of variable physical properties
$\frac{1}{\rho}\frac{d\rho}{d\eta}$	Fluid density factor
$\frac{1}{\mu}\frac{d\mu}{d\eta}$	Fluid viscosity factor
$\frac{1}{\lambda}\frac{d\lambda}{d\eta}$	Fluid thermal conductivity factor

Subscripts

f	At average temperature
w	At wall
∞	In fluid bulk

Chapter 1
Introduction

Abstract This chapter introduces recent advanced study on laminar mixed convection of liquid with focusing on its hydrodynamics and heat transfer. Taking water laminar mixed convection as an example enables researchers to targeted study of this book. On this basis, three activities are performed in order for enhancement of the theoretical and practical value of the study. First, for simplification of the study, the governing partial differential equations are equivalently transformed into the ordinary differential equations by using an innovative similarity transformation model of velocity field. Based on such simplification, the study can focus on successive even difficult and complicated issues of heat transfer. Second, coupled effect of variable physical properties is considered. It is an assurance that the systems of numerical solutions have their practical value. Third, based on the theoretical equations and the systems of rigorous numerical solutions, the optimal formalized equations of Nusselt number are created for convenient and reliable application of heat transfer, in view of that so far, there is still lack of such reliable theoretical achievements. These theoretical achievements with the optimal formalized equations are base on the systems of reliable numerical solutions with a better consideration of variable physical properties, they have solidly theoretical and practical value for heat transfer application.

Keywords Mixed convection · Heat transfer · Innovative similarity transformation · Mixed convection parameter · Positive flow · Variable physical properties · Theoretical and practical value

1.1 Universality of Mixed Convection

Free and forced mixed (or combined) convection, for short, mixed convection, is a coupled phenomenon of free and forced convection. As general case, the mixed convection is formed simultaneously by an outer forcing flow and inner volumetric

D.-Y. Shang and L.-C. Zhong, *Heat Transfer of Laminar Mixed Convection of Liquid*, Heat and Mass Transfer, DOI 10.1007/978-3-319-27959-6_1

(mass) force, while the latter is caused by the no-uniform density distribution of a fluid medium in a gravity field. In fact, so-called forced convection actually belongs to mixed convection if there is temperature difference between the wall surface and fluid bulk. Obviously, there has been much challenge in research of mixed convection over that of net free or forced convection.

For investigation of mixed convection, an important parameter, mixed convection parameter (i.e. Richardson number *Ri*) $Mc = Gr_x/Re_x^2$, where *Gr* is the Grashof number and *Re* the Reynolds number, has been induced for conveniently evaluating the ratio of intensity of free convection to that of forced convection. Numerically, the value of mixed convection parameter can be defined in a range $-\infty < Mc < +\infty$. As a special case with $Mc = 0$, the flow becomes net forced convection. With increasing the absolute value of the mixed convection parameter, the effect of free convection will increase. Here, it is an interesting issue that how a big value of the mixed convection parameter will lead to that free convection dominates whole flow and its heat transfer. Although there has been some studies involving this issue, it will still be touched in the research of this book as an interesting topic.

Generally, the mixed convection is divided to two types, positive (adding) and negative (opposing) flows. For the former flow, free and forced convections are in the same direction, and the mixed convection parameter *Mc* is positive. For the latter flow, free and forced convections are in the opposite directions, and the combined convection parameter *Mc* will be negative. In this book, the former phenomenon will be taken into account in our research area.

1.2 Application Backgrounds

The application of mixed convection flow can be found in several industrial departments, such as the metallurgical engineering, chemical engineering, mechanical engineering, energy engineering, electrical engineering and food engineering, etc. The thermal process on surfaces such as those of boilers, heating and smelting furnaces, heat exchangers placed in a low-velocity environment, nuclear reactors cooled during emergency shutdown, solar central receivers exposed to winds, electronic devices cooled by fans, and other various industrial and civic equipments are often caused by various forms of mixed convection. The heat transfer rate affects the related industrial heating process. While, in some thermal processes, for instance for them of electronic devices, cooling process occurs with mixed convection on the surface of integrated circuits, and tends to restrict the surface temperature to below the allowable value. The optimal design of the corresponding heating equipments as well as the optimal control of the heat transfer process of the cooling devices depend on correct prediction on heat transfer of mixed convection.

1.3 Previous Studies

As a most common form of convective flow, mixed convection has wide application in various industrial departments and human life, and the research of its fluid mechanics and heat transfer has been carried out since a half century years ago. In the books of Gebhart et al. [1], Bejan [2] and Pop and Ingham [3] the detailed reviews were done for research of mixed convective flow. Meanwhile, numerous academic papers were published for investigation of its heat transfer, and only some of them, such as Refs. [4–79], are listed here for saving space. In these investigations, the mixed convection in a boundary layer flow was analysed. These studies cover different flow types of mixed convection, for instance mixed convection in external flow [4–29], with continuously moving surface [30–33], from the sphere [34–41], along horizontal cylinders [42], towards a plate [43, 44], with suction or injection [45, 46], on permeable flat plate [47, 48], with utilizing nanofluids [49], with viscous dissipating fluid [50, 51], with micropolar fluid [52, 53], with MHD (magneto-hydrodynamic) flow [54, 55], with internal flow [56–58], for experimental investigation [59–65], and in a porous medium [66 –78]. Meanwhile, some studies such as those in [16, 17, 19, 79] were done for trying creation of the correlation equations on prediction of mixed convection heat transfer.

1.4 Big Challenge Associated with In-Depth Study on Heat Transfer of Mixed Convection

1.4.1 Limitation of Traditional Falkner-Skan Transformation

The aim of this book is to analyze and calculate heat transfer of laminar mixed convection. Theoretically, there could be different numerical methods that can be used for dealing with the problem. However, to resolve such problem, similarity and equivalent transformation (i.e. scaling transformation) of the governing partial differential equations is a key work in order to simplify the analysis and calculation of mixed convection. Moreover, the similarity analysis method by means of dimensionless parameters constituted by dimensional variables can greatly simplify these analysis and calculations on heat transfer.

However, so far, the related popular approach is still traditional method called Falkner-Skan type transformation. With this method a stream function and group theory have to be induced at first, and then, the dimensionless function variable $f(\eta)$ and its derivatives are induced for transformation of the governing partial differential equations. However, with such dimensionless function variable, the traditional Falkner-Skan type transformation becomes complicated, and even difficult to consider variable physical properties.

For more description about Falkner-Skan method and its limitations of application, please refer to books [80, 81]. Up to now, these limitations of the Falkner-Skan type transformation have hampered extensive study on mixed convection even with consideration of fluid's variable physical properties.

1.4.2 Challenge Associated with Consideration of Variable Physical Properties

Due to the universality of mixed convection with large temperature difference, the consideration of coupled effect of variable thermo-physical properties is necessary for enhancement of theoretical and practical value of the related research. To this end, for study of heat transfer of water mixed convection, in this book, the temperature-dependent models of the physical properties should be built up, which is based on the typical values of the experimental measurement. Moreover, the studies should be further conducted for investigation of coupled effects of the whole variable thermo-physical properties, such as viscosity, thermal conductivity, and density on heat transfer of mixed convection. About the more description of treatment of variable physical properties, please refer to books [80, 81]. It will be proved that with such approach for treatment of variable physical properties, the difficult situation caused by consideration of the variable thermo-physical properties can be resolved well for extensive analysis and calculation of heat transfer of mixed convection.

1.4.3 Challenge Associated with Practical Value on Study of Heat Transfer

Another challenge is formulization of a systematic prediction equations for heat transfer application of mixed convection, which is based on the system of numerical solution groups on heat transfer with practical application value. The difficult point for that work is that the various variable physical properties and their interaction should be taken into account to ensure the practical value of the theoretical analysis and numerical solutions on fluid flow and heat transfer. Unfortunately, in the previous study, there has been a lack of such rigorous consideration on these issues, and then it leads to a lack of the practical value of research on heat transfer application. Therefore, the current achievements of traditional theory of mixed convection heat transfer are still not adapted to the practical requirements. For a simple example, a lot of calculation correlations on mixed convection heat transfer application are still empirical or semi-empirical from experiment.

1.4.4 Key Measures to Ensure Theoretical and Practical Value on Study of Heat Transfer

To ensure theoretical and practical value of study on heat transfer, first, by using our innovative similarity transformation, the governing partial differential equations of laminar mixed convection are so similarly transformed that the transformed ordinary differential equations are combined well with the physical property factors. Second, these physical property factor are transformed to the related theoretical expressions for matching the governing ordinary differential equations for simultaneous solution. Third, the theoretical equations of Nusselt number will be set up based on our innovative similarity transformation model. It is interesting to see in such theoretical equations of Nusselt number that the wall similarity temperature gradient as only unknown variable dominates the heat transfer coefficient evaluation. So, fourth, the investigation will focus on optimal formulization of the wall similarity temperature gradient based on the systems of the related rigorous numerical solutions. Through these processes, the optimal formalized equations of heat transfer coefficient will be created for assurance of theoretical and practical value of study on heat transfer of mixed convection.

1.5 Focused Studies in This Book

The study of heat transfer of mixed convection in this book focuses on laminar water mixed convection with positive (adding) flow. Meanwhile, the research contains consideration of coupled effect of variable physical properties. With growing importance of mixed convection heat transfer in industry and human life, the investigation in this book will apply boundary layer method and focus on the following issues for resolving the big challenges for hydrodynamics and heat transfer of mixed convection:

(i) On the basis of our advanced similarity (or scaling) analysis method reported in our book [80] for successful study on forced convection film flows, a big challenge of research in the present book is to develop the innovative similarity analysis method and models for extensive investigation of heat transfer with mixed convection.

(ii) On the basis of the innovative theoretical models for advanced research on hydrodynamics and heat and mass transfer of forced convection, another big challenge of the research is to develop a system of theoretical models for practical consideration and treatment of coupled effect of fluid variable thermo-physical properties on mixed convection heat transfer. Meanwhile, the investigation will be performed for the organic link of the physical property factors to the complete governing similarly models.

(iii) To obtain systems of numerical solutions for meeting the practical physical conditions in a wide range of the boundary temperatures, Prandtl number and mixed convection parameter including consideration of coupled effects of variable physical properties.
(iv) To develop the theoretical equations of heat transfer for heat transfer coefficient, so that the problem of prediction of heat transfer will actually become the issue for evaluation of the wall temperature gradient.
(v) To realize the formulization of the systems of numerical solutions of the wall temperature gradient meeting the practical physical conditions in the wide range of boundary temperatures, Prandtl number and combined convection parameter, in order to realize optimal formalized correlations of Nusselt number for heat transfer application.

1.6 Research Developments in This Book

The innovative research developments on heat transfer of mixed convection for dealing with the above difficult points have been realized, and are demonstrated in this book. They are summarized as below:

1.6.1 Application of Innovative Similarity Transformation in In-Depth Study of Fluid Mixed Convection

In this book, new similarity analysis methods reported in [81] for innovative study on hydrodynamics and heat transfer of forced convection boundary layer has been applied for development on a novel governing system of similarity mathematical models for mixed convection. Although due to its velocity boundary conditions of forced convection the transformed governing similarity mathematical models of mixed convection are nonlinear, they are still simplified more greatly than those transformed by the popular Fakner-Skan transformation. Such simplification will be even demonstrated for consideration of coupled effect of variable physical properties. With our similarity transformation method, all variable physical properties of the governing partial differential equations can be transformed to the related physical property factors, and organically combined with the governing similarity mathematical models. Thus, the system of innovative governing similarity models are completely obtained for practical analysis and calculation of mixed convection with consideration of coupled effect of variable physical properties.

1.6.2 For Treatment of Coupled Effect of Variable Physical Properties

Since two decades ago, we have been committed to consider effect of fluid's variable physical properties on convection heat transfer in our studies. These studies enable us to deeply recognize that it is necessary to consider coupled effect of variable physical properties for assurance of the theoretical and practical value for research of convection heat transfer, and Boussinesq approximation or ignoring fluid's variable physical properties will severely weakened the theoretical and practical value for these studies.

For research in this book, the polynomial formulations [80, 81] are applied for setting up the model of variable physical properties on liquid mixed convection. Such model of variable physical properties can describe the fluid physical property values at any local point with a certain temperature, well coincident to the related experimental measurement values.

In the transformed system of similarity governing models, all thermo-physical properties exist in the form of the physical property factors for practical treatment of the variable physical properties. By means of our similarity analysis method, these physical property factors are further treated to the functions of the dimensionless temperature and its derivatives suitable for simultaneous solutions of the complete similarity governing models.

1.6.3 Systems of Numerical Solutions for Consideration of Coupled Effect of Variable Physical Properties

By means of our innovative similarity analysis method and variable physical property model, this book contributed system of the complete similarity governing model of mixed convection. On this basis, through a huge amount of numerical calculation, systems of the rigorous numerical solutions on velocity and temperature fields of water mixed convection were obtained at the broad ranges of Prandtl number, mixed convection parameter and temperature boundary conditions. These numerical solutions dominate hydrodynamics and heat transfer of mixed convection. On the basis of rigorous consideration of complicated physical conditions and effect of variable thermo-physical properties, definite practical value is realized on heat transfer application of mixed convection.

1.6.4 Optimal Formalization for Groups of Numerical Solutions

For heat transfer application of mixed convection, it is necessary to do two tasks in order to set up the theoretical equation on heat transfer and formulize its unknown variable. First, by means of our innovative similarity analysis method, theoretical equations of Nusselt number are contributed, where only the wall similarity temperature gradient is the unknown variable for evaluation of heat transfer of mixed convection. Therefore the numerical solutions of the wall similarity temperature gradient are regarded as key numerical solutions on heat transfer application. The second work is to formulize the numerical solution groups of the wall similarity temperature gradient meeting the practical physical conditions including coupled effect of variable thermo-physical properties. After finishing such two tasks, the optimal formalized equations on Nusselt number of mixed convection is posted in this book for heat transfer application.

1.6.5 Theoretical and Practical Value of the Optimal Formalized Equations on Heat Transfer Coefficient

The optimal formalized equations on Nusselt number only contain one variable to be determined: the wall similarity temperature gradient. It depends on local Prandtl numbers and mixed convection parameter. The latter depends on local Reynolds number and local Grashof number, both of which depend on the related local physical properties of fluid. Then, the calculation of mixed convection heat transfer is finally attributed to calculate the algebraic formula with the fluid's local physical properties, and thus, it is realized to greatly simplify the evaluation of mixed convection heat transfer. Meanwhile, the optimal formalized equations of Nusselt number are based on the systems of numerical solutions groups with consideration of coupled effect of variable physical properties, and then have definitely theoretical and practical value on heat transfer application.

1.7 Remarks

Our innovative similarity analysis method is applied in this book with development of a new local similarity transformation approach for a deep investigation of heat transfer on mixed convection. The governing mathematical models consider well the coupled effect of variable thermo-physical properties. It would be found that the transformed similarity governing models are dominated by boundary Prandtl numbers and induced mixed convection parameter of fluid. A huge of amount of numerical calculation is conducted, and the systems of numerical solutions on

velocity and temperature fields are obtained in the wide arranges of mixed convection parameter and boundary Prandtl numbers of fluid. The theoretical equations of Nusselt number are derived based on the innovative similarity transformation model, where it is seen that wall temperature gradient is the only one no-given variable for heat transfer prediction, so that the heat transfer problem is attributed to the issue to evaluate the wall similarity temperature gradient. The systems of numerical solutions of the wall similarity temperature gradient are formulized to the related formulated equations. Then, the heat transfer evaluation is finally attributed to an algebraic formula dependent on mixed convection parameter as well as the fluid physical boundary conditions. Since the governing mathematical models consider the coupled effect of variable thermo-physical properties, the systems of numerical solutions, and formulized equations on hydrodynamics and heat transfer have theoretical and practical value for mixed convection.

References

1. Gebhart, B., Jaluria, Y., Mahajan, R.L., Sammakia, B.: Buoyancy-induced Flows and Transport. Hemisphere, New York (1988)
2. Bejan, A.: Convective Heat Transfer. Wiley Inter Science, New York (1994)
3. Pop, I., Ingham, D.B.: Convective Heat Transfer: Mathematical and Computational Modelling of Viscous Fluids and Porous Media. Elsevier UK (2001)
4. Sparrow, E.M., Eichhorn, R., Gregg, J.L.: Combined forced and free convection in a boundary layer flow. Phys. Fluids **2**, 319–328 (1959)
5. Szewcyk, A.A.: Combined forced and free convection laminar flow. J. Heat Transf., Trans. ASME, Ser. C **86**(4), 501–507 (1964)
6. Metais, B., Eckert, E.R.G.: Forced, mixed, and free convection regimes. J. Heat Transf. **86**, 295–296 (1964)
7. Acrivos, A.: On the combined effect of forced and free convection heat transfer in laminar boundary layer flows. Chem. Eng. Sci. **21**(4), 343–352 (1966)
8. Acrivos, A.: Combined laminar free and forced convection heat transfer in external flows. AIChE J. **4**, 285–289 (1958)
9. Wilks, G.: Combined forced and free convection flow on vertical surfaces. Int. J. Heat Mass Transf. **16**, 1958–1966 (1973)
10. Lloyd, J.R., Sparrow, E.M.: Combined forced and free convection flow on vertical surfaces. Int. J. Heat Mass Transf. **13**(2), 434–438 (1970)
11. Robertson, G.E., Seinfield, J.H., Leal, L.G.: Combined forced and free convection flow past horizontal plate. AIChE J. **19**, 998–1008 (1972)
12. Oosthuizen, P.H., Hart, R.: A numerical study of laminar combined convection flow over flat plates. J. Heat Transf. **95**, 60–63 (1973)
13. Wilks, G.: Combined forced and free convection flow on vertical surfaces. Int. J. Heat Mass Transf. **16**(10), 1958–1964 (1973)
14. Mucoglu, A., Chen, T.S.: Mixed convection on inclined surface. J. Heat Transf. **101**, 422–426 (1979)
15. Chen, T.S., Yuh, C.F., Moutsoglou, A.: Combined heat and mass transfer in mixed convection along vertical and inclined plates. Int. J. Heat Mass Transf. **23**(4), 527–537 (1980)
16. Tsuruno, S., Iguchi, I.: Prediction of combined free and forced convective heat transfer along a vertical plate with blowing. ASME J. Heat Transf. **102**, 168–170 (1980)

17. Raju, M.S., Liu, X.R., Law, C.K.: A formulation of combined forced and free convection past horizontal and vertical surfaces. Int. J. Heat Mass Transf. **27**(12), 2215–2224 (1984)
18. Afzal, N., Hussain, T.: Mixed convection over a horizontal plate. J. Heat Transf. **106**(1), 240–241 (1984)
19. Chen, T.S., Armaly, B.F., Ramachandran, N.: Correlations for laminar mixed convection flows on vertical, inclined, and horizontal flat plates. ASME J. Heat Transf. **108**, 835–840 (1986)
20. Yao, L.S.: Two-dimensional mixed convection along a flat plate. ASME J. Heat Transf. **109**, 440–445 (1987)
21. Wickern, G.: Mixed convection from an arbitrarily inclined semi-infinite flat plate-I. The influence of the inclination angle. Int. J. Heat Mass Transf. **34**, 1935–1945 (1991)
22. Wickern, G.: Mixed convection from an arbitrarily inclined semi-infinite flat plate-II. The influence of the Prandtl number. Int. J. Heat Mass Transf. **34**, 1947–1957 (1991)
23. Gorla, R.S.R.: Mixed convection in a micropolar fluid along a vertical surface with uniform heat flux. Int. J. Eng. Sci. **30**(3), 349–358 (1992)
24. Kafoussias, N.G., Williams, E.W.: The effect of temperature-dependent viscosity on free-forced convective laminar boundary layer flow past a vertical isothermal flat plate. Acta Mech. **110**(1–4), 123–137 (1995)
25. Lin, H.T., Hoh, H.L.: Mixed convection from an isothermal vertical flat plate moving in parallel or reversely to a free stream. Heat Mass Transf. **32**(6), 441–445 (1997)
26. Hossain, M.A., Munir, M.S.: Mixed convection flow from a vertical flat plate with temperature dependent viscosity. Int. J. Therm. Sci. **39**, 173–183 (2000)
27. Merkin, J.H., Pop, I.: Mixed convection along a vertical surface: similarity solutions for uniform flow. Fluid Dyn. Res. **30**, 233–250 (2002)
28. Steinrück, H.: About the physical relevance of similarity solutions of the boundary-layer flow equations describing mixed convection flow along a vertical plate. Fluid Dyn. Res. **32**, 1–13 (2003)
29. Ali, M.E.: The effect of variable viscosity on mixed convection heat transfer along a vertical moving surface. Int. J. Therm. Sci. **45**, 60–69 (2006)
30. Ali, M., Al-Yousef, F.: Laminar mixed convection from a continuously moving vertical surface with suction or injection. Heat Mass Transf. **33**(4), 301–306 (1998)
31. Chen, C.H.: Mixed convection cooling of a heated, continuously stretching surface. Heat Mass Transf. **36**(1), 79–86 (2000). View at Publisher · View at Google Scholar
32. Al-Sanea, S.A.: Mixed convection heat transfer along a continuously moving heated vertical plate with suction or injection. Int. J. Heat Mass Transf. **47**, 1445–1465 (2004)
33. Chen, C.H.: Laminar mixed convection adjacent to vertical, continuously stretching sheets. Heat Mass Transf. **33**(5/6), 471–476 (1998) (continue moving surface)
34. Hieber, C., Gebhart, B.: Mixed convection from a sphere at small Reynolds and Grashof numbers. J. Fluid Mech. **38**(1), 137–159 (1969)
35. Mucoglu, A., Chen, T.: Mixed convection about a sphere with uniform surface heat flux. J. Heat Transf. **100**, 542–544 (1978)
36. Dudek, D.R., Fletcher, T.H., Longwell, J.P., Sarofim, A.F.: Natural convection induced drag forces on spheres at low Grashof numbers: comparison of theory with experiment. Int. J. Heat Mass Transf. **31**(4), 863–873 (1988)
37. Tang, L., Johnson, A.T.: Flow visualization of mixed convection about a sphere. Int. Commun. Heat Mass Transf. **17**(1), 67–77 (1990)
38. Koizumi, H., Umemura, Y., Hando, S., Suzuki, K.: Heat transfer performance and the transition to chaos of mixed convection around an isothermally heated sphere placed in a uniform, downwardly directed flow. Int. J. Heat Mass Transf. **53**(13), 2602–2614 (2010)
39. Nazar, R., Amin, N., Pop, I.: On the mixed convection boundary-layer flow about a solid sphere with constant surface temperature. Arab. J. Sci. Eng. **27**(2), 117–135 (2002)
40. Nazar, R., Amin, N., Pop, I.: Mixed convection boundary layer flow about an isothermal sphere in a micropolar fluid. Int. J. Therm. Sci. **42**(3), 283–293 (2003)

41. Bhattacharyya, S., Singh, A.: Mixed convection from an isolated spherical particle. Int. J. Heat Mass Transf. **51**(5), 1034–1048 (2008)
42. Gebhart, B., Pera, L.: Mixed convection from long horizontal cylinders. J. Fluid Mech. **45**, 49–64 (1970)
43. Aman, F., Ishak, A.: Mixed convection boundary layer flow towards a vertical plate with a convective surface boundary condition. Math. Probl. Eng. 2012 (2012)
44. Ramachandran, N., Chen, T.S., Armaly, B.F.: Mixed convection in stagnation flows adjacent to vertical surfaces. J. Heat Transf. **110**(2), 373–377 (1988)
45. Ishak, A., Nazar, R., Pop, I.: Dual solutions in mixed convection boundary-layer flow with suction or injection. IMA J. Appl. Math. **72**(4), 451–463 (2007)
46. Watanabe, T.: Forced and free mixed convection boundary layer flow with uniform suction or injection on a vertical flat plate. Acta Mech. **89**, 123–132 (1991)
47. Ishak, A., Merkin, J.H., Nazar, R., Pop, I.: Mixed convection boundary layer flow over a permeable vertical surface with prescribed wall heat flux. Z. Angew. Math. Phys. **59**(1), 100–123 (2008)
48. Bachok, N., Ishak, A., Pop, I.: Mixed convection boundary layer flow over a permeable vertical flat plate embedded in an anisotropic porous medium. Math. Probl. Eng. 2010, Article ID 659023, 12 p. (2010)
49. Rana, P., Bhargava, R.: Numerical study of heat transfer enhancement in mixed convection flow along a vertical plate with heat source/sink utilizing nanofluids. Commun. Nonlinear Sci. Numer. Simul. **16**, 4318–4334 (2011)
50. Aydin, O., Kaya, A.: Mixed convection of a viscous dissipating fluid about a vertical flat plate. Appl. Math. Model. **31**, 843–853 (2007)
51. Partha, M.K., Murthy, P.V.S.N., Rajasekhar, G.P.: Effect of viscous dissipation on the mixed convection heat transfer from an exponentially stretching surface. Heat Mass Transf. **41**(4), 360–366 (2005)
52. Gorla, R.S.R., Lin, P.P., Yang, A.J.: Asymptotic boundary layer solutions for mixed convection from a vertical surface in a micropolar fluid. Int. J. Eng. Sci. **28**(6), 525–533 (1990)
53. Lok, Y.Y., Amin, N., Campean, D., Pop, I.: Steady mixed convection flow of a micropolar fluid near the stagnation point on a vertical surface. Int. J. Numer. Meth. Heat Fluid Flow **15** (7), 654–670 (2005)
54. Hossain, M.A., Ahmed, M.U.: MHD forced and free convection boundary layer flow near the leading edge. Int. J. Heat Mass Transf. **33**(3), 571–575 (1990)
55. Merkin, J.H., Mahmood, T.: Mixed convection boundary layer similarity solution: prescribed wall heat flux. ZAMP **40**, 61–68 (1989)
56. Sabbagh, J.A., Aziz, A., EI-Ariny, A.S., Hamad, G.: Combined free and forced convection in inclined circular tubes. J. Heat Transf. **98**, 322–324 (1976)
57. Lee, K.T., Yan, W.M.: Mixed convection heat transfer in horizontal ducts with wall temperature effect. Int. J. Heat Mass Transf. **41**, 411–424 (1998)
58. Barletta, A.: Analysis of combined forced and free convection in a vertical channel with viscous dissipation and isothermal-isoflux boundary conditions. ASME J. Heat Transf. **121**, 349–356 (1999)
59. Yuge, T.: Experiments on heat transfer from spheres including combined natural and forced convection. J. Heat Transf. **82**, 214–220 (1960)
60. Oosthuizen, P.H., Bassey, M.: An experimental study of combined forced and free convection heat transfer from flat plates to air at low Renolds number. J. Heat Transf. **95**, 120–121 (1973)
61. Marcos, S.M., Bergles, A.E.: Experimental investigation of combined forced and free laminar convection in horizontal tubes. J. Heat Transf. **97**, 212–219 (1975)
62. Ramachandran, N., Armaly, B.F., Chen, T.S.: Measurements and predictions of laminar mixed convection flow adjacent to a vertical surface. J. Heat Transf. **107**, 636–641 (1985)
63. Ramachandran, N., Armaly, B.F., Chen, T.S.: Measurements of laminar mixed convection flow adjacent to an inclined surface. J. Heat Transf. **109**, 146–151 (1987)

64. Mograbi, E., Ziskind, G., Katoshevski, D., Bar-Ziv, E.: Experimental study of the forces associated with mixed convection from a heated sphere at small Reynolds and Grashof numbers. Part II: assisting and opposing flows. Int. J. Heat Mass Transf. **45**(12), 2423–2430 (2002)
65. Ziskind, G., Zhao, B., Katoshevski, D., Bar-Ziv, E.: Experimental study of the forces associated with mixed convection from a heated sphere at small Reynolds and Grashof numbers. Part I: cross-flow. Int. J. Heat Mass Transf. **44**(23), 4381–4389 (2001)
66. Cheng, P.: Combined free and forced boundary layer flows about inclined surfaces in a porous medium. Int. J. Heat Mass Transf. **20**, 807–814 (1977)
67. Merkin, J.H.: Mixed convection boundary layer flow on a vertical surface in a saturated porous medium. J. Eng. Math. **14**(4), 301–313 (1980)
68. Hsieh, J.C., Chen, T.S., Armaly, B.F.: Non-similarity solutions for mixed convection from vertical surfaces in porous media: variable surface temperature or heat flux. Int. J. Heat Mass Transf. **36**, 1485–1493 (1993)
69. Chen, C.H.: Non-Darcy mixed convection over a vertical flat plate in porous media with variable wall heat flux. Int. Commun. Heat Mass Transf. **24**, 427–438 (1997)
70. Harris, S.D., Ingham, D.B., Pop, I.: Unsteady mixed convection boundary layer flow on a vertical surface in a porous medium. Int. J. Heat Mass Transf. **42**, 357–372 (1998)
71. Harris, S.D., Ingham, D.B., Pop, I.: Unsteady mixed convection boundary-layer flow on a vertical surface in a porous medium. Int. J. Heat Mass Transf. **42**, 357–372 (1999)
72. Harris, S.D., Ingham, D.B., Pop, I.: Unsteady mixed convection boundary layer flow on a vertical surface in a porous medium. Int. J. Heat Mass Transf. **42**(2), 357–372 (1999)
73. Kumari, M., Takhar, H.S., Nath, G.: Mixed convection flow over a vertical wedge embedded in a highly porous medium. Heat Mass Transf. **37**, 139–146 (2001)
74. Aly, E.H., Elliot, L., Ingham, D.B.: Mixed Convection boundary-layer flow over a Vertical surface embedded in a porous medium. Eur. J. Mech. B/Fluids **22**, 529–543 (2003)
75. Alam, M.S., Rahman, M., Samad, M.A.: Numerical study of the Combined free-forced convection and mass transfer flow past a vertical porous plate in a porous medium with heat generation and thermal diffusion. Nonlinear Anal. Model. Contr. **11**(4), 331–343 (2006)
76. Chin, K.E., Nazar, R., Arifin, N.M., Pop, I.: Effect of variable viscosity on mixed convection boundary layer flow over a vertical surface embedded in a porous medium. Int. Commun. Heat Mass Transf. **34**, 464–473 (2007)
77. Ishak, A., Nazar, R., Pop, I.: Dual solutions in mixed convection flow near a stagnation point on a vertical surface in a porous medium. Int. J. Heat Mass Transf. **51**(5–6), 1150–1155 (2008). View at Publisher · View at Google Scholar · View at Scopus
78. Ishak, A., Nazar, R., Arifin, N.M., Pop, I.: Dual solutions in mixed convection flow near a stagnation point on a vertical porous plate. Int. J. Therm. Sci. **47**(4), 417–422 (2008). View at Publisher · View at Google Scholar · View at Scopus
79. Churchill, S.W.: A comprehensive correlating equation for laminar assisting forced and free convection. AIChE J. **23**, 10–16 (1977)
80. Shang, D.Y.: Theory of heat transfer with forced convection film flows. Springer, Berlin, Heidelberg (2011)
81. Shang, D.Y.: Free Convection Film Flows and Heat Transfer—Models of Laminar Free Convection with Phase Change for Heat and Mass Transfer Analysis. Springer, Berlin, Heidelberg (2013)

Part I
Theoretical Foundation

Chapter 2
Theoretical Foundation on Conservation Equations of Laminar Mixed Convection

Abstract In this chapter, the basic conservation equations corresponding to laminar free and forced mixed convection are introduced. For this purpose, the related general laminar conservation equations on continuity, momentum and energy equations are presented by means of theoretical and mathematical derivation for deeply understanding fluid convection. From these general conservation equations of convection, the fluid's variable physical properties are fully taken into account. By using the quantity grade analysis, the mass, momentum, and energy equations of laminar mixed convection boundary layer are obtained with consideration of variable physical properties.

Keywords Control volume · Variable physical properties · Cartesian forms · Continuity equation · Navier-Stokes Equation · Energy equation · Mixed convection · Quantitative grade analysis · Conservation equations

2.1 Continuity Equation

The conceptual basis for the derivation of the continuity equation of fluid flow is the mass conservation law. The control volume for the derivation of continuity equation is shown in Fig. 2.1 in which the mass conservation principle is stated as

$$\dot{m}_{increment} = \dot{m}_{in} - \dot{m}_{out} \tag{2.1}$$

where $\dot{m}_{increment}$ expresses the mass increment per unit time in the control volume, $\dot{m}_{in}$ represents the mass flowing into the control volume per unit time, and $\dot{m}_{out}$ is the mass flowing out of the control volume per unit time. The dot notation signifies a unit time.

In the control volume, the mass of fluid flow is given by $\rho dxdydz$, and the mass increment per unit time in the control volume can be expressed as

$$\dot{m}_{increment} = \frac{\partial \rho}{\partial \tau} dxdydz. \tag{2.2}$$

D.-Y. Shang and L.-C. Zhong, *Heat Transfer of Laminar Mixed Convection of Liquid*, Heat and Mass Transfer, DOI 10.1007/978-3-319-27959-6_2

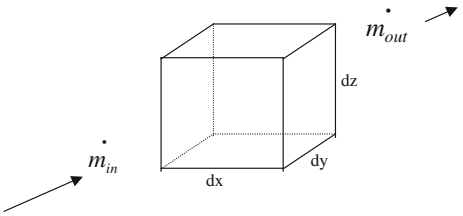

Fig. 2.1 Control volume for the derivation of the continuity equation

The mass flowing into the control volume per unit time in the x direction is given by $\rho w_x \mathrm{d}y\mathrm{d}z$. The mass flowing out of the control volume in a unit time in the x direction is given by $[\rho w_x + \partial(\rho w_x)/\partial x \cdot dx]dydz$. Thus, the mass increment per unit time in the x direction in the control volume is given by $\frac{\partial(\rho w_x)}{\partial x} dxdydz$. Similarly, the mass increments in the control volume in the y and z directions per unit time are given by $\frac{\partial(\rho w_y)}{\partial y} dydxdz$ and $\frac{\partial(\rho w_z)}{\partial z} dzdxdy$ respectively. Thus, we obtain

$$\dot{m}_{\mathrm{out}} - \dot{m}_{\mathrm{in}} = \left(\frac{\partial(\rho w_x)}{\partial x} + \frac{\partial(\rho w_y)}{\partial y} + \frac{\partial(\rho w_z)}{\partial z} \right) \mathrm{d}x\mathrm{d}y\mathrm{d}z. \tag{2.3}$$

Combining Eq. (2.1) with Eqs. (2.2) and (2.3) we obtain the following continuity equation in Cartesian coordinates:

$$\frac{\partial \rho}{\partial \tau} + \frac{\partial(\rho w_x)}{\partial x} + \frac{\partial(\rho w_y)}{\partial y} + \frac{\partial(\rho w_z)}{\partial z} = 0 \tag{2.4}$$

or in the vector notation

$$\frac{\partial \rho}{\partial \tau} + \nabla \cdot (\rho \vec{W}) = 0 \tag{2.5}$$

or

$$\frac{D\rho}{D\tau} + \rho \nabla \cdot (\vec{W}) = 0 \tag{2.6}$$

where $\vec{W} = iw_x + jw_y + kw_z$ is the fluid velocity.

For steady state, the vector and Cartesian forms of the continuity equation are given by

$$\frac{\partial}{\partial x}(\rho w_x) + \frac{\partial}{\partial y}(\rho w_y) + \frac{\partial}{\partial z}(\rho w_z) = 0 \tag{2.7}$$

or

$$\nabla \cdot (\rho \vec{W}) = 0 \tag{2.8}$$

2.2 Momentum Equation (Navier-Stokes Equation)

The control volume for the derivation of the momentum equation of fluid flow is shown in Fig. 2.2. Meanwhile, take an enclosed surface A that includes the control volume. According to momentum law, the momentum increment of the fluid flow per unit time equals the sum of the mass force and surface force acting on the fluid. The relationship is shown as below:

$$\dot{G}_{increment} = \vec{F}_m + \vec{F}_s \tag{2.9}$$

where $\vec{F}_m$ and $\vec{F}_s$ denote mass force and surface force respectively.

In the system the momentum increment $\dot{G}_{increment}$ of the fluid flow per unit time can be described as

$$\dot{G}_{increment} = \frac{D}{D\tau}\int_V \rho \vec{W}\, dV \tag{2.10}$$

In the system the sum of mass force F_m and surface force F_s acting on the fluid is expressed as

$$\vec{F}_m + \vec{F}_s = \int_V \rho \vec{F}\, dV + \int_A \vec{\tau}_n\, dA \tag{2.11}$$

where V and A are volume and surface area of the system respectively, and $\vec{\tau}_n$ is surface force acting on unit area.

Combining Eq. (2.9) with Eqs. (2.10) and (2.11), we have the following equation:

$$\frac{D}{D\tau}\int_V \rho \vec{W}\, dV = \int_V \rho \vec{F}\, dV + \int_A \vec{\tau}_n\, dA \tag{2.12}$$

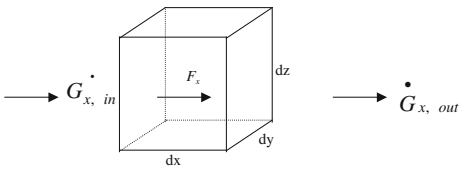

Fig. 2.2 Control volume for the derivation of momentum equation

According to tensor calculation, the right side of Eq. (2.12) is changed into the following form:

$$\int_V \rho \vec{F}\, dV + \int_A \vec{\tau}_n\, dA = \int_V \rho \vec{F}\, dV + \int_V \nabla \cdot [\tau] dV \tag{2.13}$$

where $\nabla \cdot [\tau]$ is divergence of the shear force tensor.

The left side of Eq. (2.12) can be rewritten as

$$\frac{D}{D\tau}\int_V \rho \vec{W}\, dV = \int_V \frac{D(\rho \vec{W})}{D\tau} dV \tag{2.14}$$

With Eqs. (2.13) and (2.14), Eq. (2.12) can be simplified as

$$\int_V \{\frac{D(\rho \vec{W})}{D\tau} - \rho \vec{F} - \nabla \cdot [\tau]\} dV = 0 \tag{2.15}$$

Therefore,

$$\frac{D(\rho \vec{W})}{D\tau} = \rho \vec{F} + \nabla \cdot [\tau] \tag{2.16}$$

This is the Navier-Stokes equations of fluid flow. For Cartesian Coordinates, Eq. (2.16) can be expressed as

$$\frac{D(\rho w_x)}{D\tau} = \frac{\partial \tau_{xx}}{\partial x} + \frac{\partial \tau_{yx}}{\partial y} + \frac{\partial \tau_{zx}}{\partial z} + \rho g_x \tag{2.17}$$

$$\frac{D(\rho w_y)}{D\tau} = \frac{\partial \tau_{xy}}{\partial x} + \frac{\partial \tau_{yy}}{\partial y} + \frac{\partial \tau_{zy}}{\partial z} + \rho g_y \tag{2.18}$$

$$\frac{D(\rho w_z)}{D\tau} = \frac{\partial \tau_{xz}}{\partial x} + \frac{\partial \tau_{yz}}{\partial y} + \frac{\partial \tau_{zz}}{\partial z} + \rho g_z \tag{2.19}$$

where

$$\frac{D(\rho w_x)}{D\tau} = \frac{\partial(\rho w_x)}{\partial \tau} + \frac{(\partial \rho w_x)}{\partial x} w_x + \frac{(\partial \rho w_x)}{\partial y} w_y + \frac{(\partial \rho w_x)}{\partial z} w_z$$

$$\frac{D(\rho w_y)}{D\tau} = \frac{\partial(\rho w_y)}{\partial \tau} + \frac{(\partial \rho w_y)}{\partial x} w_x + \frac{(\partial \rho w_y)}{\partial y} w_y + \frac{(\partial \rho w_y)}{\partial z} w_z$$

$$\frac{D(\rho w_z)}{D\tau} = \frac{\partial(\rho w_z)}{\partial \tau} + \frac{(\partial \rho w_z)}{\partial x} w_x + \frac{(\partial \rho w_z)}{\partial y} w_y + \frac{(\partial \rho w_z)}{\partial z} w_z$$

In Eqs. (2.17)–(2.19), g_x, g_y and g_z are gravity accelerations in x, y, and z directions respectively, while, the related shear forces are given below:

$$\tau_{xx} = -\left[p + \frac{2}{3}\mu\left(\frac{\partial w_x}{\partial x} + \frac{\partial w_y}{\partial y} + \frac{\partial w_z}{\partial z}\right)\right] + 2\mu\frac{\partial w_x}{\partial x}$$

$$\tau_{yy} = -[p + \frac{2}{3}\mu(\frac{\partial w_x}{\partial x} + \frac{\partial w_y}{\partial y} + \frac{\partial w_z}{\partial z})] + 2\mu\frac{\partial w_y}{\partial y}$$

$$\tau_{zz} = -[p + \frac{2}{3}\mu(\frac{\partial w_x}{\partial x} + \frac{\partial w_y}{\partial y} + \frac{\partial w_z}{\partial z})] + 2\mu\frac{\partial w_z}{\partial z}$$

$$\tau_{xy} = \tau_{yx} = \mu(\frac{\partial w_y}{\partial x} + \frac{\partial w_x}{\partial y})$$

$$\tau_{yz} = \tau_{zy} = \mu(\frac{\partial w_z}{\partial y} + \frac{\partial w_y}{\partial z})$$

$$\tau_{zx} = \tau_{xz} = \mu(\frac{\partial w_x}{\partial z} + \frac{\partial w_z}{\partial x})$$

Then, Eqs. (2.17)–(2.19) are rewritten as follows respectively:

$$\begin{aligned}&\frac{D(\rho w_x)}{D\tau}\\ &= -\frac{\partial p}{\partial x} + 2\frac{\partial}{\partial x}(\mu\frac{\partial w_x}{\partial x}) + \frac{\partial}{\partial y}[\mu(\frac{\partial w_x}{\partial y} + \frac{\partial w_y}{\partial x})] + \frac{\partial}{\partial z}[\mu(\frac{\partial w_x}{\partial z} + \frac{\partial w_z}{\partial x})]\\ &\quad -\frac{\partial}{\partial x}[\frac{2}{3}\mu(\frac{\partial w_x}{\partial x} + \frac{\partial w_y}{\partial y} + \frac{\partial w_z}{\partial z})] + \rho g_x\end{aligned} \tag{2.20}$$

$$\begin{aligned}&\frac{D(\rho w_y)}{D\tau}\\ &= -\frac{\partial p}{\partial y} + \frac{\partial}{\partial x}[\mu(\frac{\partial w_x}{\partial y} + \frac{\partial w_y}{\partial x})] + 2\frac{\partial}{\partial y}(\mu\frac{\partial w_y}{\partial y}) + \frac{\partial}{\partial z}[\mu(\frac{\partial w_y}{\partial z} + \frac{\partial w_z}{\partial y})]\\ &\quad -\frac{\partial}{\partial y}[\frac{2}{3}\mu(\frac{\partial w_x}{\partial x} + \frac{\partial w_y}{\partial y} + \frac{\partial w_z}{\partial z})] + \rho g_y\end{aligned} \tag{2.21}$$

$$\begin{aligned}&\frac{D(\rho w_z)}{D\tau}\\ &= -\frac{\partial p}{\partial z} + \frac{\partial}{\partial x}[\mu(\frac{\partial w_x}{\partial z} + \frac{\partial w_z}{\partial x})] + \frac{\partial}{\partial y}[\mu(\frac{\partial w_y}{\partial z} + \frac{\partial w_z}{\partial y})] + 2\frac{\partial}{\partial z}(\mu\frac{\partial w_z}{\partial z})\\ &\quad -\frac{\partial}{\partial z}[\frac{2}{3}\mu(\frac{\partial w_x}{\partial x} + \frac{\partial w_y}{\partial y} + \frac{\partial w_z}{\partial z})] + \rho g_z\end{aligned} \tag{2.22}$$

For steady state, the momentum Eqs. (2.20)–(2.22) are given as follows respectively:

$$\begin{aligned}&\rho(\frac{\partial w_x}{\partial x}w_x+\frac{\partial w_x}{\partial y}w_y+\frac{\partial w_x}{\partial z}w_z)+w_x(w_x\frac{\partial \rho}{\partial x}+w_y\frac{\partial \rho}{\partial y}+w_z\frac{\partial \rho}{\partial z})\\&=-\frac{\partial p}{\partial x}+2\frac{\partial}{\partial x}(\mu\frac{\partial w_x}{\partial x})+\frac{\partial}{\partial y}[\mu(\frac{\partial w_x}{\partial y}+\frac{\partial w_y}{\partial x})]+\frac{\partial}{\partial z}[\mu(\frac{\partial w_x}{\partial z}+\frac{\partial w_z}{\partial x})]\\&\quad-\frac{\partial}{\partial x}[\frac{2}{3}\mu(\frac{\partial w_x}{\partial x}+\frac{\partial w_y}{\partial y}+\frac{\partial w_z}{\partial z})]+\rho g_x\end{aligned}\tag{2.23}$$

$$\begin{aligned}&\rho(\frac{\partial w_y}{\partial x}w_x+\frac{\partial w_y}{\partial y}w_y+\frac{\partial w_y}{\partial z}w_z)+w_y(w_x\frac{\partial \rho}{\partial x}+w_y\frac{\partial \rho}{\partial y}+w_z\frac{\partial \rho}{\partial z})\\&=-\frac{\partial p}{\partial y}+\frac{\partial}{\partial x}[\mu(\frac{\partial w_x}{\partial y}+\frac{\partial w_y}{\partial x})]+2\frac{\partial}{\partial y}(\mu\frac{\partial w_y}{\partial y})+\frac{\partial}{\partial z}[\mu(\frac{\partial w_y}{\partial z}+\frac{\partial w_z}{\partial y})]\\&\quad-\frac{\partial}{\partial y}[\frac{2}{3}\mu(\frac{\partial w_x}{\partial x}+\frac{\partial w_y}{\partial y}+\frac{\partial w_z}{\partial z})]+\rho g_y\end{aligned}\tag{2.24}$$

$$\begin{aligned}&\rho(\frac{\partial w_z}{\partial x}w_x+\frac{\partial w_z}{\partial y}w_y+\frac{\partial w_z}{\partial z}w_z)+w_z(w_x\frac{\partial \rho}{\partial x}+w_y\frac{\partial \rho}{\partial y}+w_z\frac{\partial \rho}{\partial z})\\&=-\frac{\partial p}{\partial z}+\frac{\partial}{\partial x}[\mu(\frac{\partial w_x}{\partial z}+\frac{\partial w_z}{\partial x})]+\frac{\partial}{\partial y}[\mu(\frac{\partial w_y}{\partial z}+\frac{\partial w_z}{\partial y})]+2\frac{\partial}{\partial z}(\mu\frac{\partial w_z}{\partial z})\\&\quad-\frac{\partial}{\partial z}[\frac{2}{3}\mu(\frac{\partial w_x}{\partial x}+\frac{\partial w_y}{\partial y}+\frac{\partial w_z}{\partial z})]+\rho g_z\end{aligned}\tag{2.25}$$

Let us compare term $\rho(\frac{\partial w_x}{\partial x}w_x+\frac{\partial w_x}{\partial y}w_y+\frac{\partial w_x}{\partial z}w_z)$ with term $w_x(w_x\frac{\partial \rho}{\partial x}+w_y\frac{\partial \rho}{\partial y}+w_z\frac{\partial \rho}{\partial z})$. In general, derivatives $\frac{\partial w_x}{\partial x}$, $\frac{\partial w_x}{\partial y}$ and $\frac{\partial w_x}{\partial z}$ are much larger than the derivatives $\frac{\partial \rho_x}{\partial x}$, $\frac{\partial \rho_x}{\partial y}$ and $\frac{\partial \rho_x}{\partial z}$ respectively. In this case, the term $w_x(w_x\frac{\partial \rho}{\partial x}+w_y\frac{\partial \rho}{\partial y}+w_z\frac{\partial \rho}{\partial z})$ is omitted, and (2.23) is rewritten as generally

$$\begin{aligned}&\rho(\frac{\partial w_x}{\partial x}w_x+\frac{\partial w_x}{\partial y}w_y+\frac{\partial w_x}{\partial z}w_z)\\&=-\frac{\partial p}{\partial x}+2\frac{\partial}{\partial x}(\mu\frac{\partial w_x}{\partial x})+\frac{\partial}{\partial y}[\mu(\frac{\partial w_x}{\partial y}+\frac{\partial w_y}{\partial x})]+\frac{\partial}{\partial z}[\mu(\frac{\partial w_x}{\partial z}+\frac{\partial w_z}{\partial x})]\\&\quad-\frac{\partial}{\partial x}[\frac{2}{3}\mu(\frac{\partial w_x}{\partial x}+\frac{\partial w_y}{\partial y}+\frac{\partial w_z}{\partial z})]+\rho g_x\end{aligned}\tag{2.23a}$$

Similarly, in general, (2.24) and (2.25) are rewritten as respectively

$$\begin{aligned}&\rho(\frac{\partial w_y}{\partial x}w_x+\frac{\partial w_y}{\partial y}w_y+\frac{\partial w_y}{\partial z}w_z)\\&=-\frac{\partial p}{\partial y}+\frac{\partial}{\partial x}[\mu(\frac{\partial w_x}{\partial y}+\frac{\partial w_y}{\partial x})]+2\frac{\partial}{\partial y}(\mu\frac{\partial w_y}{\partial y})+\frac{\partial}{\partial z}[\mu(\frac{\partial w_y}{\partial z}+\frac{\partial w_z}{\partial y})]\\&\quad-\frac{\partial}{\partial y}[\frac{2}{3}\mu(\frac{\partial w_x}{\partial x}+\frac{\partial w_y}{\partial y}+\frac{\partial w_z}{\partial z})]+\rho g_y\end{aligned}\tag{2.24a}$$

$$\begin{aligned}&\rho(\frac{\partial w_z}{\partial x}w_x+\frac{\partial w_z}{\partial y}w_y+\frac{\partial w_z}{\partial z}w_z)\\&=-\frac{\partial p}{\partial z}+\frac{\partial}{\partial x}[\mu(\frac{\partial w_x}{\partial z}+\frac{\partial w_z}{\partial x})]+\frac{\partial}{\partial y}[\mu(\frac{\partial w_y}{\partial z}+\frac{\partial w_z}{\partial y})]+2\frac{\partial}{\partial z}(\mu\frac{\partial w_z}{\partial z})\\&\quad-\frac{\partial}{\partial z}[\frac{2}{3}\mu(\frac{\partial w_x}{\partial x}+\frac{\partial w_y}{\partial y}+\frac{\partial w_z}{\partial z})]+\rho g_z\end{aligned}\tag{2.25a}$$

2.3 Energy Equation

The control volume for derivation of the energy equation of fluid flow is shown in Fig. 2.3. Meanwhile, take an enclosed surface A that includes the control volume. According to the first law of thermodynamics, we have the following equation:

$$\Delta\dot{E}=\dot{Q}+\dot{W}_{out}\tag{2.26}$$

where $\Delta\dot{E}$ is energy increment in the system per unit time, $\dot{Q}$ is heat increment in the system per unit time, and $\dot{W}_{out}$ denotes work done by the mass force and surface force on the system per unit time.

The energy increment per unit time in the system is described as

$$\Delta\dot{E}=\frac{D}{D\tau}\int_V\rho(e+\frac{W^2}{2})\,dV\tag{2.27}$$

where τ denotes time, $\frac{W^2}{2}$ is the fluid kinetic energy per unit mass, W is fluid velocity, and the symbol e represents the internal energy per unit mass.

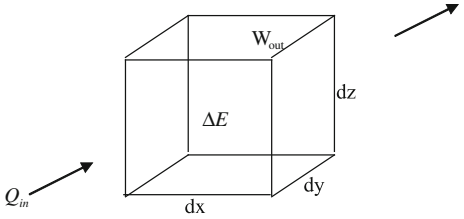

Fig. 2.3 Control volume for derivation of the energy equations of fluid flow

The work done by the mass force and surface force on the system per unit time is expressed as

$$\dot{W}_{out} = \int_V \rho \vec{F} \cdot \vec{W}\, dV + \int_A \vec{\tau_n} \cdot \vec{W}\, dA \tag{2.28}$$

where $\vec{F}$ is the mass force per unit mass, and $\vec{\tau_n}$ is surface force acting on unit area.

The heat increment entering into the system per unit time through thermal conduction is described by using Fourier's law as follows:

$$\dot{Q} = \int_A \lambda \frac{\partial t}{\partial n} dA \tag{2.29}$$

where n is normal line of the surface, t is temperature and here the heat conduction is considered only.

With Eqs. (2.27)–(2.29), Eq. (2.26) is rewritten as

$$\frac{D}{D\tau}\int_V \rho(e + \frac{W^2}{2})\, dV = \int_V \rho \vec{F} \cdot \vec{W}\, dV + \int_A \vec{\tau_n} \cdot \vec{W}\, dA + \int_A \lambda \frac{\partial t}{\partial n} dA \tag{2.30}$$

where

$$\frac{D}{D\tau}\int_V \rho(e + \frac{W^2}{2})\, dV = \int_V \frac{D}{D\tau}[\rho(e + \frac{W^2}{2})]\, dV \tag{2.31}$$

$$\int_A \vec{\tau_n} \cdot \vec{W}\, dA = \int_A \vec{n}[\tau] \cdot \vec{W}\, dA = \int_A \vec{n}([\tau] \cdot \vec{W})\, dA = \int_V \nabla \cdot ([\tau] \cdot \vec{W})\, dV \tag{2.32}$$

$$\int_A \lambda \frac{\partial t}{\partial n} dA = \int_V \nabla \cdot (\lambda \nabla t)\, dV \tag{2.33}$$

With Eqs. (2.31) to (2.33), Eq. (2.30) is rewritten as

$$\int_V \frac{D}{D\tau}[\rho(e + \frac{W^2}{2})]\, dV = \int_V \rho \vec{F} \cdot \vec{W}\, dV + \int_v \nabla \cdot ([\tau] \cdot \vec{W})\, dV + \int_V \nabla \cdot (\lambda \nabla t)\, dV. \tag{2.34}$$

Then,

$$\frac{D}{D\tau}[\rho(e + \frac{W^2}{2})] = \rho \vec{F} \cdot \vec{W} + \nabla \cdot ([\tau] \cdot \vec{W}) + \nabla \cdot (\lambda \nabla t) \tag{2.35}$$

where $[\tau]$ denotes tensor of shear force.

Equation (2.35) is the energy equation.

Through tensor and vector analysis, Eq. (2.35) can be further derived into the following form:

$$\frac{D(\rho e)}{D\tau} = [\tau] \cdot [\varepsilon] + \nabla \cdot (\lambda \nabla t) \tag{2.36}$$

Equation (2.36) is another form of the energy equation. Here, $[\tau] \cdot [\varepsilon]$ is the scalar quantity product of force tensor $[\tau]$ and deformation rate tensor $[\varepsilon]$, and represents the work done by fluid deformation surface force. The physical significance of Eq. (2.36) is that the internal energy increment of fluid with unit volume during the unit time equals the sum of the work done by deformation surface force of fluid with unit volume, $[\tau] \cdot [\varepsilon]$, and the heat entering the system.

The general Newtonian law is expressed as

$$[\tau] = 2\mu[\varepsilon] - (p + \frac{2}{3}\mu \nabla \cdot \vec{W})[I] \tag{2.37}$$

where $[I]$ is unit tensor.

According to Eq. (2.37) the following equation can be obtained:

$$[\tau] \cdot [\varepsilon] = -p\nabla \cdot \vec{W} - \frac{2}{3}\mu(\nabla \cdot \vec{W})^2 + 2\mu[\varepsilon]^2 \tag{2.38}$$

Then, Eq. (2.36) can be rewritten as

$$\frac{D(\rho e)}{D\tau} = -p\nabla \cdot \vec{W} + \Phi + \nabla \cdot (\lambda \nabla t) \tag{2.39}$$

where $\Phi = -\frac{2}{3}\mu(\nabla \cdot \vec{W})^2 + 2\mu[\varepsilon]^2$ is viscous dissipation function, which is further described as

$$\begin{aligned}\Phi = \mu\{&2(\frac{\partial w_x}{\partial x})^2 + 2(\frac{\partial w_y}{\partial y})^2 + 2(\frac{\partial w_z}{\partial z})^2 + (\frac{\partial w_x}{\partial y} + \frac{\partial w_y}{\partial x})^2 + (\frac{\partial w_y}{\partial z} + \frac{\partial w_z}{\partial y})^2 \\ &+ (\frac{\partial w_z}{\partial x} + \frac{\partial w_x}{\partial z})^2 - \frac{2}{3}[div(\vec{W})]^2\}\end{aligned} \tag{2.40}$$

Equation (2.6) can be rewritten as

$$\nabla \cdot \vec{W} = -\frac{1}{\rho}\frac{D\rho}{D\tau} = \rho\frac{D}{D\tau}(\frac{1}{\rho})$$

With the above equation, Eq. (2.39) is changed into the following form:

$$[\frac{D(\rho e)}{D\tau} + p\rho\frac{D}{D\tau}(\frac{1}{\rho})] = \Phi + \nabla \cdot (\lambda \nabla t) \tag{2.41}$$

According to thermodynamics equation of fluid

$$\frac{D(\rho h)}{D\tau} = \frac{D(\rho e)}{D\tau} + p\rho\frac{D}{D\tau}(\frac{1}{\rho}) + \frac{Dp}{D\tau} \tag{2.42}$$

Equation (2.41) can be expressed as the following enthalpy form:

$$\frac{D(\rho h)}{D\tau} = \frac{Dp}{D\tau} + \Phi + \nabla\cdot(\lambda\nabla t) \tag{2.43}$$

or

$$\frac{D(\rho c_p t)}{D\tau} = \frac{Dp}{D\tau} + \Phi + \nabla\cdot(\lambda\nabla t) \tag{2.44}$$

where $h = c_p t$, while c_p is specific heat.

In Cartesian form, the energy Eq. (2.44) can be rewritten as

$$\begin{aligned}&\frac{\partial(\rho c_p t)}{\partial\tau} + w_x\frac{\partial(\rho c_p t)}{\partial x} + w_y\frac{\partial(\rho c_p t)}{\partial y} + w_z\frac{\partial(\rho c_p t)}{\partial z}\\ &= \frac{Dp}{D\tau} + \frac{\partial}{\partial x}(\lambda\frac{\partial t}{\partial x}) + \frac{\partial}{\partial y}(\lambda\frac{\partial t}{\partial y}) + \frac{\partial}{\partial z}(\lambda\frac{\partial t}{\partial z}) + \Phi\end{aligned} \tag{2.45}$$

For steady state and nearly constant pressure processes, the viscous dissipation can be ignored, and then the Cartesian form of the energy equation (2.45) is changed into

$$w_x\frac{\partial(\rho c_p t)}{\partial x} + w_y\frac{\partial(\rho c_p t)}{\partial y} + w_z\frac{\partial(\rho c_p t)}{\partial z} = \frac{\partial}{\partial x}(\lambda\frac{\partial t}{\partial x}) + \frac{\partial}{\partial y}(\lambda\frac{\partial t}{\partial y}) + \frac{\partial}{\partial z}(\lambda\frac{\partial t}{\partial z}) \tag{2.46}$$

Above equation is usually approximately rewritten as

$$\rho[w_x\frac{\partial(c_p t)}{\partial x} + w_y\frac{\partial(c_p t)}{\partial y} + w_z\frac{\partial(c_p t)}{\partial z}] = \frac{\partial}{\partial x}(\lambda\frac{\partial t}{\partial x}) + \frac{\partial}{\partial y}(\lambda\frac{\partial t}{\partial y}) + \frac{\partial}{\partial z}(\lambda\frac{\partial t}{\partial z}) \tag{2.46a}$$

or

$$\rho c_p[w_x\frac{\partial t}{\partial x} + w_y\frac{\partial t}{\partial y} + w_z\frac{\partial t}{\partial z}] = \frac{\partial}{\partial x}(\lambda\frac{\partial t}{\partial x}) + \frac{\partial}{\partial y}(\lambda\frac{\partial t}{\partial y}) + \frac{\partial}{\partial z}(\lambda\frac{\partial t}{\partial z}) \tag{2.46b}$$

In fact, in Eq. (2.46a) the temperature-dependent density is ignored, and in (2.46b) both the temperature-dependent density and specific heat are ignored.

2.4 Conservation Equations of Laminar Mixed Convection Boundary Layer

2.4.1 Continuity Equation

Based on the Eq. (2.7), the steady state three-dimensional continuity equation is given by

$$\frac{\partial}{\partial x}(\rho w_x) + \frac{\partial}{\partial y}(\rho w_y) + \frac{\partial}{\partial z}(\rho w_z) = 0. \tag{2.47}$$

While, the steady state two-dimensional continuity equation is given by

$$\frac{\partial}{\partial x}(\rho w_x) + \frac{\partial}{\partial y}(\rho w_y) = 0 \tag{2.48}$$

In Eqs. (2.47) and (2.48) variable fluid density with temperature is considered.

Before the quantitative grade analysis on the above equations, it is necessary to define its analytical standard. A normal quantitative grade is regarded as $\{1\}$, i.e. unit quantity grade, a very small quantitative grade is regarded as $\{\delta\}$, even very small quantitative grade is regarded as $\{\delta^2\}$, and so on. The ration of the quantities is easily defined, and some examples of ratios are introduced as follows:

$$\frac{\{1\}}{\{1\}} = \{1\}, \frac{\{\delta\}}{\{\delta\}} = \{1\}, \frac{\{1\}}{\{\delta\}} = \{\delta^{-1}\}, \frac{\{1\}}{\{\delta^2\}} = \{\delta^{-2}\}$$

According to the theory of laminar free boundary layer, the quantities of the velocity component w_x and the coordinate x can be regarded as unity, i.e. $\{w_x\} = \{1\}$ and $\{x\} = \{1\}$. However, the quantities of the velocity component w_y and the coordinate y should be regarded as δ, i.e. $\{w_y\} = \{\delta\}$ and $\{y\} = \{\delta\}$.

For the terms of Eq. (2.48) the following ratios of quantity grade are obtained: $\frac{\{\rho w_x\}}{\{x\}} = \frac{\{1\}}{\{1\}} = \{1\}$ and $\frac{\{\rho w_y\}}{\{y\}} = \frac{\{\delta\}}{\{\delta\}} = \{1\}$. Therefore both the two terms of Eq. (2.48) should be kept, and Eq. (2.48) can be regarded as the continuity equation of the steady state laminar two-dimensional boundary layers. Of course, Eq. (2.48) is also suitable for the steady state two-dimensional boundary layers with laminar free convection.

2.4.2 Momentum Equation (Navier-Stokes Equation)

According to Eqs. (2.23a) and (2.24a), the momentum equations for steady two-dimensional convection are

$$\rho(w_x\frac{\partial w_x}{\partial x}+w_y\frac{\partial w_x}{\partial y})$$
$$=-\frac{\partial p}{\partial x}+2\frac{\partial}{\partial x}(\mu\frac{\partial w_x}{\partial x})+\frac{\partial}{\partial y}[\mu(\frac{\partial w_x}{\partial y}+\frac{\partial w_y}{\partial x})]-\frac{\partial}{\partial x}[\frac{2}{3}\mu(\frac{\partial w_x}{\partial x}+\frac{\partial w_y}{\partial y}]+\rho g_x \tag{2.49}$$

$$\rho(w_x\frac{\partial w_y}{\partial x}+w_y\frac{\partial w_y}{\partial y})$$
$$=-\frac{\partial p}{\partial y}+\frac{\partial}{\partial x}[\mu(\frac{\partial w_x}{\partial y}+\frac{\partial w_y}{\partial x})]+2\frac{\partial}{\partial y}(\mu\frac{\partial w_y}{\partial y})-\frac{\partial}{\partial y}[\frac{2}{3}\mu(\frac{\partial w_x}{\partial x}+\frac{\partial w_y}{\partial y})]+\rho g_y \tag{2.50}$$

According to the theory of boundary layer, the quantity grade of the pressure gradient $\frac{\partial p}{\partial x}$ can be regarded as unity, i.e. $\{\frac{\partial p}{\partial x}\}=\{1\}$, but the quantity grade of the pressure gradient $\frac{\partial p}{\partial y}$ is only regarded as very small quantity grade, i.e. $\{\frac{\partial p}{\partial y}\}=\{\delta\}$.

The quantity grades of the terms of Eqs. (2.49) and (2.50) are expressed as follows respectively:

$$\rho(w_x\frac{\partial w_x}{\partial x}+w_y\frac{\partial w_x}{\partial y})=-\frac{\partial p}{\partial x}+2\frac{\partial}{\partial x}(\mu\frac{\partial w_x}{\partial x})$$
$$+\frac{\partial}{\partial y}[\mu(\frac{\partial w_x}{\partial y}+\frac{\partial w_y}{\partial x})]-\frac{\partial}{\partial x}[\frac{2}{3}\mu(\frac{\partial w_x}{\partial x}+\frac{\partial w_y}{\partial y})]+\rho g_x$$
$$\{1\}(\{1\}\frac{\{1\}}{\{1\}}+\{\delta\}\frac{\{1\}}{\{\delta\}})=-\{1\}+\frac{\{1\}}{\{1\}}\{\delta^2\}\frac{\{1\}}{\{1\}}+\frac{\{1\}}{\{\delta\}}\{\delta^2\}(\frac{\{1\}}{\{\delta\}}+\frac{\{\delta\}}{\{1\}})$$
$$-\frac{\{1\}}{\{1\}}\delta^2(\frac{\{1\}}{\{1\}}+\frac{\{\delta\}}{\{\delta\}})+\{1\}\{1\} \tag{2.49a}$$

$$\rho(w_x\frac{\partial w_y}{\partial x}+w_y\frac{\partial w_y}{\partial y})=-\frac{\partial p}{\partial y}+\frac{\partial}{\partial x}[\mu(\frac{\partial w_x}{\partial y}+\frac{\partial w_y}{\partial x})]$$
$$+2\frac{\partial}{\partial y}(\mu\frac{\partial w_y}{\partial y})-\frac{\partial}{\partial y}[\frac{2}{3}\mu(\frac{\partial w_x}{\partial x}+\frac{\partial w_y}{\partial y})]+\rho g_y$$
$$\{1\}(\{1\}\frac{\{\delta\}}{\{1\}}+\{\delta\}\frac{\{\delta\}}{\{\delta\}})=-\{\delta\}+\frac{\{1\}}{\{1\}}\{\delta^2\}\ (\frac{\{1\}}{\{\delta\}}+\frac{\{\delta\}}{\{1\}})+\frac{\{1\}}{\{\delta\}}\{\delta^2\}\frac{\{\delta\}}{\{\delta\}}$$
$$-\frac{\{1\}}{\{\delta\}}\{\delta^2\}(\frac{\{1\}}{\{1\}}+\frac{\{\delta\}}{\{\delta\}})+\{1\}\{\delta\} \tag{2.50a}$$

The quantity grades of Eqs. (2.49a) and (2.50a) are simplified as follows respectively:

$$\begin{aligned}\rho(w_x\frac{\partial w_x}{\partial x}+w_y\frac{\partial w_x}{\partial y}) &= -\frac{\partial p}{\partial x}+2\frac{\partial}{\partial x}(\mu\frac{\partial w_x}{\partial x})\\ &\quad+\frac{\partial}{\partial y}[\mu(\frac{\partial w_x}{\partial y}+\frac{\partial w_y}{\partial x})]-\frac{\partial}{\partial x}[\frac{2}{3}\mu(\frac{\partial w_x}{\partial x}+\frac{\partial w_y}{\partial y})]+\rho g_x\\ \{1\}(\{1\}+\{1\}) &= -\{1\}+\{\delta^2\}+\{1\}+\{\delta^2\}\\ &\quad-(\{\delta^2\}+\{\delta^2\})+\{1\}\end{aligned} \tag{2.49b}$$

$$\begin{aligned}\rho(w_x\frac{\partial w_y}{\partial x}+w_y\frac{\partial w_y}{\partial y}) &= -\frac{\partial p}{\partial y}+\frac{\partial}{\partial x}[\mu(\frac{\partial w_x}{\partial y}+\frac{\partial w_y}{\partial x})]\\ &\quad+2\frac{\partial}{\partial y}(\mu\frac{\partial w_y}{\partial y})-\frac{\partial}{\partial y}[\frac{2}{3}\mu(\frac{\partial w_x}{\partial x}+\frac{\partial w_y}{\partial y})]+\rho g_y\\ \{1\}(\{\delta\}+\{\delta\}) &= -\{\delta\}+(\{\delta\}+\{\delta^3\})+\{\delta\}\\ &\quad-(\{\delta\}(\{1\}+\{1\}))+\{\delta\}\end{aligned} \tag{2.50b}$$

Observing the quantity grades in Eq. (2.49b) it is found that the terms $2\frac{\partial}{\partial x}(\mu\frac{\partial w_x}{\partial x})$, and $\frac{\partial w_y}{\partial x}$ in term $\frac{\partial}{\partial y}[\mu(\frac{\partial w_x}{\partial y}+\frac{\partial w_y}{\partial x})]$, and $\frac{\partial}{\partial x}[\frac{2}{3}\mu(\frac{\partial w_x}{\partial x}+\frac{\partial w_y}{\partial y})]$ are very small and can be ignored from Eq. (2.49). Then, Eq. (2.49) is simplified as follows:

$$\rho(w_x\frac{\partial w_x}{\partial x}+w_y\frac{\partial w_x}{\partial y})=-\frac{\partial p}{\partial x}+\frac{\partial}{\partial y}(\mu\frac{\partial w_x}{\partial y})+\rho g_x \tag{2.51}$$

Comparing the quantity grades of Eq. (2.49b) with those of Eq. (2.50b), it is found that the quantity grades of Eq. (2.50b) are very small. Then, Eq. (2.50) can be ignored, and only Eq. (2.51) is taken as the momentum equation of two-dimensional boundary layer convection.

For consideration of the buoyancy term ρg_x, Eq. (2.51) actually the momentum equation of free convection. If free convection is located on inclined plate the gravity acceleration component g_x is expressed as

$$g_x=g\cdot\cos\alpha \tag{2.52}$$

where g is gravity acceleration and α is the inclined angle of the plate.

With Eq. (2.52), Eq. (2.51) is rewritten as

$$\rho(w_x\frac{\partial w_x}{\partial x}+w_y\frac{\partial w_x}{\partial y})=-\frac{\partial p}{\partial x}+\frac{\partial}{\partial y}(\mu\frac{\partial w_x}{\partial y})+\rho g\cdot\cos\alpha \tag{2.53}$$

Suppose the direction of $g \cdot \cos\alpha$ is reverse to that of the velocity component w_x, Eq. (2.53) can be rewritten as

$$\rho(w_x\frac{\partial w_x}{\partial x}+w_y\frac{\partial w_x}{\partial y})=-\frac{\partial p}{\partial x}+\frac{\partial}{\partial y}(\mu\frac{\partial w_x}{\partial y})-\rho g\cdot\cos\alpha \tag{2.54}$$

Beyond the boundary layer, where the effects of viscosity can be ignored, the momentum equation (2.54) is simplified into the following equation:

$$-\frac{dp}{dx}=\rho_\infty g\cdot\cos\alpha+\rho_\infty w_{x,\infty}\frac{dw_{x,\infty}}{dx} \tag{2.55}$$

where ρ_∞ and $w_{x,\infty}$ are fluid density and velocity component beyond the boundary layer.

With Eq. (2.55), Eq. (2.54) becomes

$$\rho(w_x\frac{\partial w_x}{\partial x}+w_y\frac{\partial w_x}{\partial y})=\frac{\partial}{\partial y}(\mu\frac{\partial w_x}{\partial y})+g(\rho_\infty-\rho)\cos\alpha+\rho_\infty w_{x,\infty}\frac{dw_{x,\infty}}{dx} \tag{2.56}$$

For constant $w_{x,\infty}$ the Eq. (2.56) transforms to

$$\rho(w_x\frac{\partial w_x}{\partial x}+w_y\frac{\partial w_x}{\partial y})=\frac{\partial}{\partial y}(\mu\frac{\partial w_x}{\partial y})+g(\rho_\infty-\rho)\cos\alpha \tag{2.57}$$

This is the momentum equation of two-dimensional boundary layer on an inclined plate with laminar convection.

Equation (2.57) can be rewritten as

$$\rho(w_x\frac{\partial w_x}{\partial x}+w_y\frac{\partial w_x}{\partial y})=\frac{\partial}{\partial y}(\mu\frac{\partial w_x}{\partial y})+g|\rho_\infty-\rho|\cos\alpha \tag{2.57a}$$

In (2.57a), the absolute value of buoyancy factor $|\rho_\infty-\rho|$ shows that the buoyancy term $g|\rho_\infty-\rho|\cos\alpha$ has always positive sign no matter which one is larger between ρ and ρ_∞. In this case, the buoyancy term $g|\rho_\infty-\rho|\cos\alpha$ and the velocity component w_x have same sign.

For the free convection of a perfect gas (ideal gas) the following simple power law can be used:

$\frac{\rho_\infty}{\rho}=\frac{T}{T_\infty}$ where T denotes absolute temperature. In fact, for general real gas, this relation is also available. Therefore,

$$|\rho_\infty-\rho|\cos\alpha=\rho\left|\frac{T}{T_\infty}-1\right|\cos\alpha \tag{2.58}$$

Thus, for the laminar free convection of a perfect gas, Eq. (2.57) can be changed into

$$\rho(w_x\frac{\partial w_x}{\partial x}+w_y\frac{\partial w_x}{\partial y})=\frac{\partial}{\partial y}(\mu\frac{\partial w_x}{\partial y})+g\rho\left|\frac{T}{T_\infty}-1\right|\cos\alpha \tag{2.59}$$

If the temperature difference $|T_w - T_\infty|$ is very small, which will lead to a very small density difference $|\rho_\infty - \rho_w|$, the Boussinesq approximation can be applied. In this case, buoyancy factor in Eq. (2.57a) becomes $|\rho_\infty - \rho| = \rho\beta|T - T_\infty|$, and then, Eq. (2.57a) is changed to

$$w_x\frac{\partial w_x}{\partial x}+w_y\frac{\partial w_x}{\partial y}=v\frac{\partial^2 w_x}{\partial y^2}+g\beta|T-T_\infty|\cos\alpha \tag{2.57b}$$

2.4.3 Energy Equation

According to Eq. (2.46a), the energy equation for steady two-dimensional convection is shown as follows:

$$\rho[w_x\frac{\partial(c_pt)}{\partial x}+w_y\frac{\partial(c_pt)}{\partial y}]=\frac{\partial}{\partial x}(\lambda\frac{\partial t}{\partial x})+\frac{\partial}{\partial y}(\lambda\frac{\partial t}{\partial y}) \tag{2.60}$$

With the quantity grade analysis similar to that mentioned above, Eq. (2.60) can be changed into the following form for energy equation of two-dimensional boundary layer convection.

$$\rho[w_x\frac{\partial(c_pt)}{\partial x}+w_y\frac{\partial(c_pt)}{\partial y}]=\frac{\partial}{\partial y}(\lambda\frac{\partial t}{\partial y}) \tag{2.61}$$

Up to now it is the time to summarize the basic governing equations for description of mass, momentum, and energy conservation of two-dimensional boundary layers with laminar steady state mixed free and forced convection as follows:

$$\frac{\partial}{\partial x}(\rho w_x)+\frac{\partial}{\partial y}(\rho w_y)=0 \tag{2.48}$$

$$\rho(w_x\frac{\partial w_x}{\partial x}+w_y\frac{\partial w_x}{\partial y})=\frac{\partial}{\partial y}(\mu\frac{\partial w_x}{\partial y})+g(\rho_\infty-\rho)\cos\alpha \tag{2.57}$$

$$\rho[w_x\frac{\partial(c_pt)}{\partial x}+w_y\frac{\partial(c_pt)}{\partial y}]=\frac{\partial}{\partial y}(\lambda\frac{\partial t}{\partial y}) \tag{2.61}$$

with convection boundary condition equations

$$y = 0 : w_x = 0, w_y = 0, t = t_w \tag{2.62}$$

$$y \to \infty : w_x = w_{x,\infty}, t = t_\infty \tag{2.63}$$

For rigorous solutions of the governing equations, the fluid temperature-dependent properties, such as density ρ in mass equation and in buoyancy factor of momentum equation, absolute viscosity μ, specific heat c_p, and thermal conductivity λ will be considered in the successive chapters of this book. In addition, t_w is plate temperature, t_∞ is the fluid temperature beyond the boundary layer, and $w_{x,\infty}$ denotes the fluid velocity component in x-direction beyond the boundary layer. Here, the boundary conditions are the isothermal plate boundary conditions.

It is known from the above governing equations and boundary conditions that the laminar mixed convection with two-dimensional boundary layer belongs to two-point boundary value problem.

2.5 Summary

Up to now the related governing partial differential conservation equations can be summarized as follows:

2.5.1 Governing Partial Differential Conservation Equations of Laminar Convection with Consideration of Variable Physical Properties

Governing partial differential conservation equations in rectangular coordinate system for laminar convection with consideration of variable physical properties are

Mass equation:

$$\frac{\partial}{\partial x}(\rho w_x) + \frac{\partial}{\partial y}(\rho w_y) + \frac{\partial}{\partial z}(\rho w_z) = 0$$

Momentum equation:

$$\begin{aligned}
&\rho\left(\frac{\partial w_x}{\partial x}w_x + \frac{\partial w_x}{\partial y}w_y + \frac{\partial w_x}{\partial z}w_z\right) \\
&= -\frac{\partial p}{\partial x} + 2\frac{\partial}{\partial x}\left(\mu\frac{\partial w_x}{\partial x}\right) + \frac{\partial}{\partial y}\left[\mu\left(\frac{\partial w_x}{\partial y} + \frac{\partial w_y}{\partial x}\right)\right] + \frac{\partial}{\partial z}\left[\mu\left(\frac{\partial w_x}{\partial z} + \frac{\partial w_z}{\partial x}\right)\right] \\
&\quad - \frac{\partial}{\partial x}\left[\frac{2}{3}\mu\left(\frac{\partial w_x}{\partial x} + \frac{\partial w_y}{\partial y} + \frac{\partial w_z}{\partial z}\right)\right] + \rho g_x
\end{aligned}$$

$$\rho(\frac{\partial w_y}{\partial x}w_x+\frac{\partial w_y}{\partial y}w_y+\frac{\partial w_y}{\partial z}w_z)$$
$$=-\frac{\partial p}{\partial y}+\frac{\partial}{\partial x}[\mu(\frac{\partial w_x}{\partial y}+\frac{\partial w_y}{\partial x})]+2\frac{\partial}{\partial y}(\mu\frac{\partial w_y}{\partial y})+\frac{\partial}{\partial z}[\mu(\frac{\partial w_y}{\partial z}+\frac{\partial w_z}{\partial y})]$$
$$-\frac{\partial}{\partial y}[\frac{2}{3}\mu(\frac{\partial w_x}{\partial x}+\frac{\partial w_y}{\partial y}+\frac{\partial w_z}{\partial z})]+\rho g_y$$

$$\rho(\frac{\partial w_z}{\partial x}w_x+\frac{\partial w_z}{\partial y}w_y+\frac{\partial w_z}{\partial z}w_z)$$
$$=-\frac{\partial p}{\partial z}+\frac{\partial}{\partial x}[\mu(\frac{\partial w_x}{\partial z}+\frac{\partial w_z}{\partial x})]+\frac{\partial}{\partial y}[\mu(\frac{\partial w_y}{\partial z}+\frac{\partial w_z}{\partial y})]+2\frac{\partial}{\partial z}(\mu\frac{\partial w_z}{\partial z})$$
$$-\frac{\partial}{\partial z}[\frac{2}{3}\mu(\frac{\partial w_x}{\partial x}+\frac{\partial w_y}{\partial y}+\frac{\partial w_z}{\partial z})]+\rho g_z$$

Energy equation:

$$\rho[w_x\frac{\partial(c_p\cdot t)}{\partial x}+w_y\frac{\partial(c_p\cdot t)}{\partial y}+w_z\frac{\partial(c_p\cdot t)}{\partial z}]=\frac{\partial}{\partial x}(\lambda\frac{\partial t}{\partial x})+\frac{\partial}{\partial y}(\lambda\frac{\partial t}{\partial y})+\frac{\partial}{\partial z}(\lambda\frac{\partial t}{\partial z})+\Phi$$

$$\Phi=\mu\{2(\frac{\partial w_x}{\partial x})^2+2(\frac{\partial w_y}{\partial y})^2+2(\frac{\partial w_z}{\partial z})^2+(\frac{\partial w_x}{\partial y}+\frac{\partial w_y}{\partial x})^2$$
$$+(\frac{\partial w_y}{\partial z}+\frac{\partial w_z}{\partial y})^2+(\frac{\partial w_z}{\partial x}+\frac{\partial w_x}{\partial z})^2]-\frac{2}{3}[div(\vec{W})]^2\}$$

2.5.2 *Governing Partial Differential Equations of Laminar Mixed Convection Boundary Layer with Consideration of Variable Physical Properties*

Governing partial differential equations in rectangular coordinate system for two-dimensional laminar mixed convection boundary layer with consideration of variable physical properties are

Mass equation:

$$\frac{\partial}{\partial x}(\rho w_x)+\frac{\partial}{\partial y}(\rho w_y)=0$$

Momentum equation:

$$\rho(w_x\frac{\partial w_x}{\partial x}+w_y\frac{\partial w_x}{\partial y})=\frac{\partial}{\partial y}(\mu\frac{\partial w_x}{\partial y})+g|\rho_\infty-\rho|\cos\alpha$$

Energy equation:

$$\rho[w_x\frac{\partial(c_pt)}{\partial x}+w_y\frac{\partial(c_pt)}{\partial y}]=\frac{\partial}{\partial y}(\lambda\frac{\partial t}{\partial y})$$

Boundary conditions:

$$y=0:w_x=0,w_y=0,t=t_w$$

$$y\to\infty:w_x=w_{x,\infty},t=t_\infty$$

2.5.3 *Governing Partial Differential Equations of Laminar Mixed Convection Boundary Layer for Boussinesq Approximation*

Governing partial differential equations in rectangular coordinate system for two-dimensional laminar mixed convection boundary layer for Boussinesq approximation are

Mass equation:

$$\frac{\partial w_x}{\partial x}+\frac{\partial w_y}{\partial y}=0$$

Momentum equation:

$$w_x\frac{\partial w_x}{\partial x}+w_y\frac{\partial w_x}{\partial y}=v\frac{\partial^2 w_x}{\partial y^2})+g\beta|T-T_\infty|\cos\alpha$$

Energy equation:

$$w_x\frac{\partial t}{\partial x}+w_y\frac{\partial t}{\partial y}=\frac{v}{\mathrm{Pr}}\frac{\partial^2 t}{\partial y^2}$$

Boundary conditions:

$$y=0:w_x=0,w_y=0,t=t_w$$

$$y\to\infty:w_x=w_{x,\infty},t=t_\infty$$

2.6 Remarks

In this chapter, the theoretical foundation of conservation equations on laminar mixed convection are introduced. For this purpose, first, the conservation equations of general laminar convection on continuity, momentum and energy are derived with a series of theoretical and mathematical approaches. On this basis, the corresponding conservation equations of mass, momentum, and energy for laminar mixed convection boundary layer are obtained by the quantity grade analysis. In these derived conservation equations, variable physical properties are fully taken into account. These equations are important theoretical foundation of the study for this book.

Chapter 3
Our Innovative Similarity Transformation Models of Convection Velocity Field

Abstract Our innovative similarity transformation models for in-depth research of convection heat and mass transfer are presented in this Chapter. For demonstration of the theoretical rationality on these similarity transformation models, the related theoretical derivations are performed. For solving convection heat and mass transfer issues, the boundary layer analysis method is always used. There could be different similarity transformation models which are related to different study levels on convection heat transfer. For example, Falkner-Skan transformation is currently still popularly used to treat the similarity transformation of core similarity variables of velocity field. In fact this type of transformation is inconvenient to do this core work for similarity transformation of velocity field, because it is necessary to first induce flow function and group theory to derive an intermediate function for an indirect similarity transformation of the velocity field. This case also causes a difficult situation on consideration of variable physical properties. However, our innovative similarity transformation models are based on the laws of physics and the analysis of convection partial differential equations. Thus, the above difficult situation caused by derivation of the Falkner-Skan transformation model could be resolved. Furthermore, with our innovative similarity transformation models, the velocity components can be directly transformed to the related dimensionless similarity ones. Then, the similarity analysis and transformation of the convection governing partial differential equations can have obvious physical significance. Moreover, our innovative similarity transformation models can conveniently treat variable physical properties and their coupled effect on convection heat and mass transfer for enhancement of the theoretical and practical value of the related study.

Keywords Free convection · Forced convection · Mixed convection · Innovative similarity transformation models · Laws of physics · Analysis of convection partial differential equations · Similarity variable · Falkner-Skan transformation · Flow function · Group theory

D.-Y. Shang and L.-C. Zhong, *Heat Transfer of Laminar Mixed Convection of Liquid*, Heat and Mass Transfer, DOI 10.1007/978-3-319-27959-6_3

3.1 Introduction

3.1.1 Development Background of the Innovative Similarity Transformation

Since Prandtl proposed his famous boundary layer theory [1], many complex issues on convective hydrodynamics and heat and mass transfer could be solved more conveniently. Meanwhile, the similar analysis method is usually used to transform the dimensional physical variables into the dimensionless physical parameters, and then the governing partial differential equations are transformed equivalently into the governing ordinary ones. Since the transformed dimensionless parameter is the group of the dimensional physical variables, the transformed governing ordinary differential equations will be greatly simplified. This is the reason why the boundary layer theory greatly accelerated the development of the research of convection heat and mass transfer.

Actually, the transformation for velocity field is the core work for similarity transformation of the governing partial differential equations. However, currently popular Falkner-Skan transformation [2] is difficult to do this job, especially with consideration of variable physical properties, because it is necessary to first induce flow function and group theory to derive an intermediate function for an indirect transformation of the velocity field. It is a complicated process, and allows a more complicated issue for consideration of coupled effect of variable physical properties, which is necessary for assurance of practical value of theoretical study on convection heat transfer. It is the reason that most of the related traditional theoretical research on convection heat and mass transfer by using the traditional Falkner-Skan transformation did not consider or did not consider well the coupled effect of variable physical properties. It leads to that a series of traditional related researches lack practical application value on convection heat and mass transfer, for a simple example, a lot of reported correlations on convection heat and mass transfer application are empirical or semi-empirical obtained from experiment. Therefore, a big challenge is to develop innovative similarity transformation for enhancement of the practical application value of convection heat and mass transfer. It is the background for development of the innovative similarity transformation.

3.1.2 Successful Application of the Innovative Similarity Transformation in Our In-depth Studies on Convection Heat and Mass Transfer

The innovative similarity transformation for in-depth research on convection hydrodynamics and heat and mass transfer is divided to two models. The first model is for similarity transformation of governing partial differential equations of free

convection [3], while the second model is for that of forced convection. In this Chapter, we will give rigorous theoretical and mathematical derivation for demonstration of their theoretical rationality. So far, the innovative similarity transformation models have been applied in our investigation of convection hydrodynamics and heat and mass transfer both without and with phase change, for instance of the following topics [4–15]:

- Free/forced convection;
- Free film boiling convection;
- Free/forced film condensation convection of pure vapour;
- Free/forced film condensation convection of vapour-gas mixture;
- Accelerating falling film flows of non-Newtonian power law fluids.

3.1.3 The Extended Application of the Innovative Similarity Transformation in the International Academic Community

The innovative similarity transformation has also got its wide application in the international academic community, for example as below:

Studies applied our formulization equations on heat transfer coefficient of free convection [5, 7] were applied in the studies [16, 17] for temperature distribution assessment during radiofrequency ablation related to surgical medical treatment. It is seen that even for the lead phantom close to the edges, for the maximal discrepancy from their test data, a satisfactory agreement (2 %) was achieved. Our formulization equations on heat transfer coefficient were just obtained by using the present innovative similarity transformation.

Our innovative similarity transformation was applied for study on deposition of SiO_2 nanoparticles in heat exchanger during combustion of biogas [18]. In this study, our set of dimensionless similarity physical parameters with their formulae including our innovative core similarity variables for similarity transformation of velocity field [4] were applied for similarity transformation of the governing partial differential equations of a laminar forced convection. Based on our innovative similarity transformation, the governing ordinary differential equations were obtained for numerical solution.

Ref. [19] successfully applied our heat transfer equations of free convection of gas with consideration of variable physical properties [5, 6] for analytical and experimental study on multiple fire sources in a kitchen. It follows that our formulization equation of Nusselt number combined with the gaseous temperature parameter has wide application value for evaluation of heat transfer with large temperature differences. Our formulization equations on heat transfer coefficient were just obtained by using the present innovative similarity transformation.

The above examples also reflect that our innovative method has special theoretical and practical value and broad application prospects in more industrial departments.

3.2 Basis Models of the Innovative Similarity Transformation for Free Convection Boundary Layer

3.2.1 Physical and Mathematical Derivation of the Similarity Transformation Model

To conduct the derivation of basis model of the innovative similarity transformation of velocity field for free convection boundary layer, it is suitable to use simple and typical governing partial differential equations of laminar free convection boundary layer as below with consideration of variable physical properties:

$$\frac{\partial}{\partial x}(\rho w_x) + \frac{\partial}{\partial y}(\rho w_y) = 0 \tag{3.1}$$

$$\rho(w_x \frac{\partial w_x}{\partial x} + w_y \frac{\partial w_x}{\partial y}) = \frac{\partial}{\partial y}(\mu \frac{\partial w_x}{\partial y}) + g|\rho_\infty - \rho| \cos \alpha \tag{3.2}$$

$$\rho c_p(w_x \frac{\partial t}{\partial x} + w_y \frac{\partial t}{\partial y}) = \frac{\partial}{\partial y}(\lambda \frac{\partial t}{\partial y}) \tag{3.3}$$

For derivation of the basis model of the innovative similarity transformation for free convection, first, we assume the following form for expression of similarity coordinate variable η. Because η is a function of the coordinate variables x and y, and then, it can be given as the following form:

$$\eta = \frac{y}{Kx^n} = \frac{y}{x}\frac{1}{K}x^{-n+1} \tag{3.4}$$

where K is undetermined coefficient, index n is a dimensionless exponent, and factor $\frac{1}{K}x^{-n+1}$ are dimensionless.

Now, we take a control volume with volume V in the boundary layer, and set the fluid density in it for ρ and the fluid density in the fluid bulk for ρ_∞. For steady state, the kinetic energy $\frac{1}{2}Gw_x{}^2$ of the control volume is balanced to its potential energy $Vgx|\rho_\infty - \rho| \cos \alpha$ caused by the buoyancy force, where α is the inclined angle of the plate. Thus,

$$\frac{1}{2}Gw_x^2 = Vgx|\rho_\infty - \rho|\cos\alpha$$

where G is mass of the control volume, and can be expressed as $G = \rho \cdot V$. Then, the above equation is changed to

$$\frac{1}{2}\rho \cdot Vw_x^2 = Vgx|\rho_\infty - \rho|\cos\alpha$$

i.e.

$$1 = \frac{w_x^2}{2gx\left|\frac{\rho_\infty - \rho}{\rho}\right|\cos\alpha}$$

Taking ρ_w to replace ρ, the above equation can be written as

$$A = \frac{{w_x}^2}{2gx\left|\frac{\rho_\infty - \rho_w}{\rho_w}\right|\cos\alpha}$$

where A is dimensionless variable. Then,

$$\sqrt{A} = \frac{w_x}{\sqrt{2gx\left|\frac{\rho_\infty - \rho_w}{\rho_w}\right|\cos\alpha}}$$

It is seen that the dimensionless variable $\sqrt{A}$ depends on the velocity component w_x and the coordinate variable x. It means that it can be regarded as the representative of the velocity component w_x. Then, it is reasonable to assume a dimensionless variable W_x as the representative of the dimensionless variable $\sqrt{A}$ for description of the velocity component w_x, i.e.

$$W_x = \frac{w_x}{\sqrt{2gx\left|\frac{\rho_\infty - \rho_w}{\rho_w}\right|\cos\alpha}} \tag{3.5}$$

where W_x is defined as the similarity velocity component W_x, dependent on velocity component w_x, coordinate variable x, and buoyancy force factor $\left|\frac{\rho_\infty - \rho_w}{\rho_w}\right|\cos\alpha$. Obviously, W_x is ideal similarity variable theoretically related to the velocity component w_x.

Now, let us derive the expression of the similarity variable W_y related to velocity component w_y:Consulting Eq. (3.5), we can reasoning that W_y depends on the factor $\sqrt{2gx\left|\frac{\rho_\infty-\rho_w}{\rho_w}\right|\cos\alpha}$ too. Then, we can set the following form to describe the velocity component w_y:

$$w_y = \sqrt{2gx\left|\frac{\rho_\infty-\rho_w}{\rho_w}\right|\cos\alpha}\cdot Bx^p\cdot W_y \tag{3.6}$$

where W_y is dimensionless variable, B is a coefficient, exponent p is dimensionless undetermined exponent, and factor Bx^p should be dimensionless.

The next work is to investigate the coefficient B and indexes p and n of Eqs. (3.4) and (3.6) by analysis of the momentum Eq. (3.2):

From Eq. (3.4), we have

$$\frac{\partial\eta}{\partial x} = -n\frac{y}{Kx^{n+1}} = -n\eta x^{-1}$$

From Eq. (3.5), we have

$$\begin{aligned}\frac{\partial w_x}{\partial x} &= \frac{1}{2}x^{-\frac{1}{2}}left(2g\left|\frac{\rho_\infty-\rho_w}{\rho_w}\right|\cos\alpha)^{\frac{1}{2}}\cdot W_x + left(2gx\left|\frac{\rho_\infty-\rho_w}{\rho_w}\right|\cos\alpha)^{\frac{1}{2}}\cdot\frac{dW_x}{d\eta}left(-n\eta x^{-1}\right)\\ &= \frac{1}{2}x^{-\frac{1}{2}}(2g\left|\frac{\rho_\infty-\rho_w}{\rho_w}\right|\cos\alpha)^{\frac{1}{2}}\cdot W_x + (2gx\left|\frac{\rho_\infty-\rho_w}{\rho_w}\right|\cos\alpha)^{\frac{1}{2}}\cdot\frac{dW_x}{d\eta}(-n\eta\frac{1}{x})\end{aligned}$$

While,

$$\frac{\partial\rho}{\partial x} = \frac{\partial\rho}{\partial\eta}\frac{\partial\eta}{\partial x} = \frac{\partial\rho}{\partial\eta}(-n\eta x^{-1})$$

From Eq. (3.6), we have

$$\frac{\partial w_y}{\partial y} = (2gx\left|\frac{\rho_\infty-\rho_w}{\rho_w}\right|\cos\alpha)^{\frac{1}{2}}\cdot Bx^p\frac{dW_y}{d\eta}\frac{\partial\eta}{\partial y}$$

Since

$$\frac{\partial\eta}{\partial y} = \frac{1}{Kx^n},$$

$$\begin{aligned}\frac{\partial w_y}{\partial y} &= \frac{\partial w_y}{\partial \eta}\frac{d\eta}{dy} \\ &= (\sqrt{2g\left|\frac{\rho_\infty - \rho_w}{\rho_w}\right|\cos\alpha}\cdot Bx^{p+\frac{1}{2}}\frac{dW_y}{d\eta}\frac{1}{Kx^n} \\ &= x^{\frac{1}{2}+p-n}(2g\left|\frac{\rho_\infty - \rho_w}{\rho_w}\right|\cos\alpha))^{\frac{1}{2}}\cdot B\frac{dW_y}{d\eta}\frac{1}{K}\end{aligned}$$

and

$$\begin{aligned}\frac{\partial \rho}{\partial y} &= \frac{\partial \rho}{\partial \eta}\frac{\partial \eta}{\partial y} = \frac{\partial \rho}{\partial \eta}\frac{1}{Kx^n} \\ \frac{\partial \mu}{\partial y} &= \frac{\partial \mu}{\partial \eta}\frac{\partial \eta}{\partial y} = \frac{\partial \mu}{\partial \eta}\frac{1}{Kx^n}\end{aligned}$$

With Eq. (3.5) we have

$$\frac{\partial w_x}{\partial y} = \sqrt{2gx\left|\frac{\rho_\infty - \rho_w}{\rho_w}\right|\cos\alpha}\frac{dW_x}{d\eta}\frac{\partial \eta}{\partial y} = \sqrt{2gx\left|\frac{\rho_\infty - \rho_w}{\rho_w}\right|\cos\alpha}\frac{dW_x}{d\eta}\frac{1}{Kx^n}$$

Then,

$$\frac{\partial^2 w_x}{\partial y^2} = \sqrt{2gx\left|\frac{\rho_\infty - \rho_w}{\rho_w}\right|\cos\alpha}\frac{1}{K^2x^{2n}}\frac{d^2W_x}{d\eta^2}$$

Equation (3.2) is changed to

$$\rho w_x\frac{\partial w_x}{\partial x} + \rho w_y\frac{\partial w_x}{\partial y} = \frac{\partial \mu}{\partial y}\frac{\partial w_x}{\partial y} + \mu\frac{\partial^2 w_x}{\partial y^2} + g|\rho_\infty - \rho|\cos\alpha \tag{3.2a}$$

With above equations, we further have

$$\begin{aligned}\rho w_x\frac{\partial w_x}{\partial x} &= \rho\sqrt{2gx\left|\frac{\rho_\infty - \rho_w}{\rho_w}\right|\cos\alpha}W_x[\frac{1}{2}x^{-\frac{1}{2}}(2g\left|\frac{\rho_\infty - \rho_w}{\rho_w}\right|\cos\alpha)^{\frac{1}{2}}\cdot W_x + (2gx\left|\frac{\rho_\infty - \rho_w}{\rho_w}\right|\cos\alpha)^{\frac{1}{2}}\cdot\frac{dW_x}{d\eta}(-n\eta\frac{1}{x})] \\ &= \rho x^{\frac{1}{2}}2g\left|\frac{\rho_\infty - \rho_w}{\rho_w}\right|\cos\alpha)W_x[\frac{1}{2}x^{-\frac{1}{2}}(\cdot W_x + x^{-\frac{1}{2}}\cdot\frac{dW_x}{d\eta}(-n\eta)]\end{aligned}$$

$$\begin{aligned}\rho w_y\frac{\partial w_x}{\partial y} &= \rho\sqrt{2gx\left|\frac{\rho_\infty - \rho_w}{\rho_w}\right|\cos\alpha}\cdot Bx^pW_y\sqrt{2gx\left|\frac{\rho_\infty - \rho_w}{\rho_w}\right|\cos\alpha}\frac{dW_x}{d\eta}\frac{1}{Kx^n} \\ &= \rho x^{1-n+p}\sqrt{2g\left|\frac{\rho_\infty - \rho_w}{\rho_w}\right|\cos\alpha}\cdot BW_y\sqrt{2g\left|\frac{\rho_\infty - \rho_w}{\rho_w}\right|\cos\alpha}\frac{dW_x}{d\eta}\frac{1}{K}\end{aligned}$$

$$\frac{\partial \mu}{\partial y}\frac{\partial w_x}{\partial y} = \frac{\partial \mu}{\partial \eta}\frac{1}{Kx^n}\sqrt{2gx\left|\frac{\rho_\infty - \rho_w}{\rho_w}\right|\cos\alpha}\frac{dW_x}{d\eta}\frac{1}{Kx^n}$$
$$= x^{\frac{1}{2}-2n}\frac{\partial \mu}{\partial \eta}\frac{1}{K}\sqrt{2g\left|\frac{\rho_\infty - \rho_w}{\rho_w}\right|\cos\alpha}\frac{dW_x}{d\eta}\frac{1}{K}$$

$$\mu\frac{\partial^2 w_x}{\partial y^2} = \mu\sqrt{2gx\left|\frac{\rho_\infty - \rho_w}{\rho_w}\right|\cos\alpha}\frac{1}{K^2x^{2n}}\frac{d^2W_x}{d\eta^2}$$
$$= \mu x^{\frac{1}{2}-2n}\sqrt{2gx\left|\frac{\rho_\infty - \rho_w}{\rho_w}\right|\cos\alpha}\frac{1}{K^2}\frac{d^2W_x}{d\eta^2}$$

Then, Eq. (3.2a) is changed to

$$\rho x^{\frac{1}{2}}2g\left|\frac{\rho_\infty - \rho_w}{\rho_w}\right|\cos\alpha)W_x[\frac{1}{2}x^{-\frac{1}{2}}(\cdot W_x + x^{-\frac{1}{2}}\cdot\frac{dW_x}{d\eta}(-n\eta)]$$
$$+\rho x^{1-n+p}\sqrt{2g\left|\frac{\rho_\infty - \rho_w}{\rho_w}\right|\cos\alpha}\cdot BW_y\sqrt{2g\left|\frac{\rho_\infty - \rho_w}{\rho_w}\right|\cos\alpha}\frac{dW_x}{d\eta}\frac{1}{K}$$
$$= x^{\frac{1}{2}-2n}\frac{\partial \mu}{\partial \eta}\frac{1}{K}\sqrt{2g\left|\frac{\rho_\infty - \rho_w}{\rho_w}\right|\cos\alpha}\frac{dW_x}{d\eta}\frac{1}{K}$$
$$+\mu x^{\frac{1}{2}-2n}\sqrt{2gx\left|\frac{\rho_\infty - \rho_w}{\rho_w}\right|\cos\alpha}\frac{1}{K^2}\frac{d^2W_x}{d\eta^2} + g|\rho_\infty - \rho|\cos\alpha$$

i.e.

$$\rho 2g\left|\frac{\rho_\infty - \rho}{\rho}\right|\cos\alpha)W_x[\frac{1}{2}(\cdot W_x + \frac{dW_x}{d\eta}(-n\eta)]$$
$$+\rho x^{1-n+p}\sqrt{2g\left|\frac{\rho_\infty - \rho_w}{\rho_w}\right|\cos\alpha}\cdot BW_y\sqrt{2g\left|\frac{\rho_\infty - \rho_w}{\rho_w}\right|\cos\alpha}\frac{dW_x}{d\eta}\frac{1}{K}$$
$$= x^{\frac{1}{2}-2n}\frac{\partial \mu}{\partial \eta}\frac{1}{K}\sqrt{2g\left|\frac{\rho_\infty - \rho_w}{\rho_w}\right|\cos\alpha}\frac{dW_x}{d\eta}\frac{1}{K}$$
$$+\mu x^{\frac{1}{2}-2n}\sqrt{2gx\left|\frac{\rho_\infty - \rho_w}{\rho_w}\right|\cos\alpha}\frac{1}{K^2}\frac{d^2W_x}{d\eta^2} + g|\rho_\infty - \rho|\cos\alpha$$

We compare the exponent of coordinate x among the terms of the above equation, and have the following equations:

$$1 - n + p = 0$$
$$\frac{1}{2} - 2n = 0$$

The solutions of the above set of equations are $n = \frac{1}{4}$ and $p = -\frac{3}{4}$.

Then, the similarity coordinate variable is expressed as

$$\eta = \frac{y}{Kx^n} = \frac{y}{Kx^{1/4}} = \frac{y}{x}\frac{1}{K}x^{\frac{3}{4}}$$

Since factor $\frac{1}{K}x^{3/4}$ should be dimensional and contains $x^{3/4}$, and then, we can induce the local Grashof number

$$Gr_{x,\infty} = \frac{g\left|\frac{\rho_\infty - \rho_w}{\rho_w}\right|x^3 \cos\alpha}{v_\infty^2} \tag{3.7}$$

and reasonably set

$$\frac{1}{K}x^{3/4} = (\frac{1}{4}Gr_{x,\infty})^{1/4}$$

for coincidence of the exponent of the coordinate variable x. Then, we have

$$\eta = \frac{y}{x}(\frac{1}{4}Gr_{x,\infty})^{1/4} \tag{3.8}$$

It is the expression of the similarity coordinate variable to equivalently represent the coordinate variables x and y.

With $p = -\frac{3}{4}$, we further have

$$w_y = \sqrt{2gx\left|\frac{\rho_\infty - \rho_w}{\rho_w}\right|\cos\alpha} \cdot Bx^{-\frac{3}{4}}W_y$$

Here, dimensionless factor $Bx^{-3/4}$ contains $x^{-3/4}$. Then, we can induce the local Grashof number again as Eq. (3.7), and then, the factor $Bx^{-3/4}$ is reasonably set as

$$Bx^{-3/4} = (\frac{1}{4}Gr_{x,\infty})^{-1/4}$$

Then,

$$w_y = \sqrt{2gx\left|\frac{\rho_\infty - \rho_w}{\rho_w}\right|\cos\alpha} \cdot (\frac{1}{4}Gr_{x,\infty})^{-1/4}W_y$$

i.e.

$$W_y = \frac{w_y}{\sqrt{2gx\left|\frac{\rho_\infty - \rho_w}{\rho_w}\right| \cos\alpha}} \left(\frac{1}{4} Gr_{x,\infty}\right)^{1/4} \tag{3.9}$$

Here, W_y is defined as the similarity velocity component corresponding to velocity component w_y.

For summery, the derived similarity variables of velocity field of laminar free convection are

$$W_x = \frac{w_x}{\sqrt{2gx\left|\frac{\rho_\infty - \rho_w}{\rho_w}\right| \cos\alpha}} \tag{3.5}$$

$$W_y = \frac{w_y}{\sqrt{2gx\left|\frac{\rho_\infty - \rho_w}{\rho_w}\right| \cos\alpha}} \left(\frac{1}{4} Gr_{x,\infty}\right)^{1/4} \tag{3.9}$$

with the related coordinate similarity variable

$$\eta = \frac{y}{x} \left(\frac{1}{4} Gr_{x,\infty}\right)^{1/4} \tag{3.8}$$

where the local Grashof number $Gr_{x,\infty}$ is induced as

$$Gr_{x,\infty} = \frac{g\left|\frac{\rho_\infty - \rho_w}{\rho_w}\right| x^3 \cos\alpha}{v_\infty^2} \tag{3.7}$$

In addition, a similarity temperature is induced as

$$\theta = \frac{t - t_\infty}{t_w - t_\infty} \tag{3.10}$$

for transformation of temperature variable t.

3.2.2 *An Application Example of the Innovative Similarity Transformation*

Equations (3.1)–(3.3) can be taken as the most typical and simple governing partial differential equations of laminar free convection for an application example of the innovative similarity transformation.

By using the above Eqs. (3.5), (3.7)–(3.10), governing partial differential equations of laminar free convection, Eqs. (3.1)–(3.3) are equivalently transformed into the following related ordinary differential equations respectively:

$$2W_x - \eta\frac{dW_x}{d\eta} + 4\frac{dW_y}{d\eta} - \frac{1}{\rho}\frac{d\rho}{d\eta}(\eta W_x - 4W_y) = 0 \tag{3.11}$$

$$\frac{v_\infty}{v}(W_x(2W_x - \eta\frac{dW_x}{d\eta}) + 4W_y\frac{dW_x}{d\eta}) = \frac{d^2W_x}{d\eta^2} + \frac{1}{\mu}\frac{d\mu}{d\eta}\frac{dW_x}{d\eta} + \frac{v_\infty}{v}\frac{\frac{\rho_\infty}{\rho} - 1}{\frac{\rho_\infty}{\rho_w} - 1} \tag{3.12}$$

$$\mathrm{Pr}\frac{v_\infty}{v}(-\eta W_x + 4W_y)\frac{d\theta}{d\eta} = \frac{1}{\lambda}\frac{d\lambda}{d\eta}\frac{d\theta}{d\eta} + \frac{d^2\theta}{d\eta^2} \tag{3.13}$$

It is indicated that the related transformation processes are omitted for saving space. Readers interested in the related transformation process can refer to ref. [5].

3.3 Basis Models of the Innovative Similarity Transformation for Forced Convection Boundary Layer

3.3.1 Physical and Mathematical Derivation of the Similarity Transformation Model

To conduct the derivation of basis models of the innovative similarity transformation for forced convection boundary layer, it is suitable to use typical governing partial differential equations of laminar forced convection boundary layer as below with consideration of variable physical properties:

$$\frac{\partial}{\partial x}(\rho w_x) + \frac{\partial}{\partial y}(\rho w_y) = 0 \tag{3.14}$$

$$\rho(w_x\frac{\partial w_x}{\partial x} + w_y\frac{\partial w_x}{\partial y}) = -\frac{1}{\rho}\frac{dp}{dx} + \frac{\partial}{\partial y}(\mu\frac{\partial w_x}{\partial y}) \tag{3.15}$$

$-\frac{1}{\rho}\frac{dp}{dx} = w_{x,\infty}\frac{\partial w_{x,\infty}}{\partial x}$ (Now, $w_{x,\infty}$ is supposed as constant)

$$\rho c_p(w_x\frac{\partial t}{\partial x} + w_y\frac{\partial t}{\partial y}) = \frac{\partial}{\partial y}(\lambda\frac{\partial t}{\partial y}) \tag{3.16}$$

According to the boundary layer theory, the velocity component w_x can be regarded to have a quantitative grade equivalent to that of the main stream velocity $w_{x,\infty}$, i.e.

$$w_x \propto w_{x,\infty}$$

Again, According to the boundary layer theory, the ratio $\frac{w_{x,\infty}}{x}$ can be regarded to have a quantitative grade equivalent to the ratio $\frac{w_y}{y}$, i.e.

$$\frac{w_{x,\infty}}{x} \propto \frac{w_y}{y} \text{ or } w_y \propto \frac{w_{x,\infty} \cdot y}{x}$$

With above equations, the momentum Eq. (3.15) can be approximately expressed as

$$w_{x,\infty}\frac{w_{x,\infty}}{x} + \frac{w_{x,\infty}}{x} \cdot w_{x,\infty} \propto v_\infty \frac{w_{x,\infty}}{y^2}$$

Then, we have

$$y^2 \propto \frac{v_\infty \cdot x}{w_{x,\infty}} \text{ or } y \propto \sqrt{\frac{v_\infty \cdot x}{w_{x,\infty}}}$$

Inducing the local Reynolds number

$$Re_{x,\infty} = \frac{w_{x,\infty}x}{v_\infty} \tag{3.17}$$

we will have

$$y \propto \sqrt{\frac{x^2}{Re_{x,\infty}}}$$

Inducing an undetermined similarity coordinate variable η, the above equation becomes

$$y = \eta\sqrt{\frac{x^2}{Re_{x,\infty}}}$$

or

$$\eta = \frac{y}{x}(\frac{1}{2}Re_{x,\infty})^{1/2} \tag{3.18}$$

It is seen that the induced similarity dimensionless coordinate variable η depends on the coordinate variables x and y, and then, and then, η is defined as a similarity coordinate variable. On this basis, we will focus on derivation for core similarity variables of velocity field as below:

First, set W_x and W_y to be the core similarity variables to respectively represent velocity components w_x and w_y. Since the velocity component w_x can be regarded

to have a quantitative grade equivalent to that of the main stream velocity $w_{x,\infty}$, we have

$$w_x \propto w_{x,\infty}$$

Inducing the local Reynolds number of Eq. (3.17), the velocity component w_x can be regarded as

$$w_x \propto w_{x,\infty} \cdot (\frac{1}{2} Re_{x,\infty})^p$$

where p is undetermined dimensionless exponent.

Inducing dimensionless variable C, the above formula is expressed as an equation

$$w_x = C w_{x,\infty} \cdot \left(\frac{1}{2} Re_{x,\infty}\right)^p$$

or

$$C = \frac{w_x}{w_{x,\infty}} \cdot \left(\frac{1}{2} Re_{x,\infty}\right)^{-p}$$

where dimensionless variable C is function of the velocity component w_x, and then, can be regarded as similarity variable for it. Then, C can be replaced by the assumed similarity velocity component W_x, and the above equation becomes

$$W_x = \frac{w_x}{w_{x,\infty}} \cdot (\frac{1}{2} Re_{x,\infty})^{-p} \tag{3.19}$$

Consulting Eq. (3.18), we can set another similarity variable W_y to describe the velocity component w_y as below:

$$W_y = \frac{w_y}{w_{x,\infty}} (\frac{1}{2} Re_{x,\infty})^{-q} \tag{3.20}$$

The following work is to determine the constants p and q.

From Eqs. (3.14) we have

$$\begin{aligned} \frac{\partial \eta}{\partial x} &= -\frac{1}{2} x^{-3/2} y (\frac{1}{2} \frac{w_{x,\infty}}{v_\infty})^{1/2} \\ &= -\frac{1}{2} x^{-1} \frac{y}{x} (\frac{1}{2} \frac{w_{x,\infty} x}{v_\infty})^{1/2} \\ &= -\frac{1}{2} x^{-1} \eta \end{aligned}$$

$$\frac{\partial \eta}{\partial y} = \frac{1}{x}\left(\frac{1}{2}Re_{x,\infty}\right)^{1/2}$$

$$\begin{aligned}
\frac{\partial w_x}{\partial x} &= \frac{\partial[W_x \cdot w_{x,\infty} \cdot (\frac{1}{2}Re_{x,\infty})^p]}{\partial x} \\
&= w_{x,\infty} \cdot p\left(\frac{1}{2}Re_{x,\infty}\right)^{p-1}\left(\frac{1}{2}\frac{w_{x,\infty}}{v_\infty}\right)W_x(\eta) + w_{x,\infty}\left(\frac{1}{2}Re_{x,\infty}\right)^p \frac{dW_x(\eta)}{d\eta} \cdot \frac{\partial \eta}{\partial x} \\
&= x^{-1}w_{x,\infty} \cdot p\left(\frac{1}{2}\frac{w_{x,\infty}x}{v_\infty}\right)^{p-1}\left(\frac{1}{2}\frac{w_{x,\infty}x}{v_\infty}\right) \cdot W_x(\eta) + w_{x,\infty}\left(\frac{1}{2}Re_{x,\infty}\right)^p \frac{dW_x(\eta)}{d\eta} \cdot \left(-\frac{1}{2}x^{-1}\eta\right) \\
&= x^{-1}w_{x,\infty} \cdot p\left(\frac{1}{2}Re_{x,\infty}\right)^p \cdot W_x(\eta) + w_{x,\infty}\left(\frac{1}{2}Re_{x,\infty}\right)^p \frac{dW_x(\eta)}{d\eta} \cdot \left(-\frac{1}{2}x^{-1}\eta\right) \\
&= x^{-1}w_{x,\infty} \cdot p\left(\frac{1}{2}Re_{x,\infty}\right)^p \cdot W_x(\eta) - \frac{1}{2}x^{-1}\eta \cdot w_{x,\infty}\left(\frac{1}{2}Re_{x,\infty}\right)^p \frac{dW_x(\eta)}{d\eta}
\end{aligned}$$

Then,

$$\frac{\partial w_x}{\partial x} = x^{-1}\left(\frac{1}{2}Re_{x,\infty}\right)^p \cdot w_{x,\infty}\left[p \cdot W_x(\eta) - \frac{1}{2}\eta\frac{dW_x(\eta)}{d\eta}\right]$$

With Eq. (3.19) we have

$$\begin{aligned}
\frac{\partial w_x}{\partial y} &= \frac{\partial[w_{x,\infty}(\frac{1}{2}Re_{x,\infty})^p W_x]}{\partial y} \\
&= \left(\frac{1}{2}Re_{x,\infty}\right)^p w_{x,\infty}\frac{dW_x(\eta)}{d\eta} \cdot \frac{1}{x}\left(\frac{1}{2}Re_{x,\infty}\right)^{1/2} \\
&= \frac{1}{x}\left(\frac{1}{2}Re_{x,\infty}\right)^{p+1/2} w_{x,\infty}\frac{dW_x(\eta)}{d\eta}
\end{aligned}$$

$$\begin{aligned}
\frac{\partial^2 w_x}{\partial y^2} &= \frac{1}{x}\left(\frac{1}{2}Re_{x,\infty}\right)^{p+1/2} w_{x,\infty}\frac{d^2W_x(\eta)}{d\eta^2} \cdot \frac{\partial \eta}{\partial y} \\
&= \frac{1}{x}\left(\frac{1}{2}Re_{x,\infty}\right)^{p+1/2} w_{x,\infty}\frac{d^2W_x(\eta)}{d\eta^2} \cdot \frac{1}{x}\left(\frac{1}{2}Re_{x,\infty}\right)^{1/2} \\
&= \frac{1}{x^2}\left(\frac{1}{2}Re_{x,\infty}\right)^{p+1} w_{x,\infty}\frac{d^2W_x(\eta)}{d\eta^2}
\end{aligned}$$

$$\frac{\partial \mu}{\partial y} = \frac{d\mu}{d\eta} \cdot \frac{\partial \eta}{\partial y} = \frac{1}{x}\left(\frac{1}{2}Re_{x,\infty}\right)^{1/2}\frac{d\mu}{d\eta}$$

Then, the momentum Eq. (3.12) is transformed to

$$\begin{aligned}
&\rho w_{x,\infty}\left(\frac{1}{2}Re_{x,\infty}\right)^{p} W_x x^{-1}\left(\frac{1}{2}Re_{x,\infty}\right)^{p}\cdot w_{x,\infty}\left[p\cdot W_x(\eta)-\frac{1}{2}\eta\frac{dW_x(\eta)}{d\eta}\right]\\
&\quad+\rho w_{x,\infty}\left(\frac{1}{2}Re_{x,\infty}\right)^{q} W_y\frac{1}{x}\left(\frac{1}{2}Re_{x,\infty}\right)^{p+1/2} w_{x,\infty}\frac{dW_x(\eta)}{d\eta}\\
&=\frac{1}{x}\left(\frac{1}{2}Re_{x,\infty}\right)^{1/2}\frac{d\mu}{d\eta}\cdot\frac{1}{x}\left(\frac{1}{2}Re_{x,\infty}\right)^{p+1/2} w_{x,\infty}\frac{dW_x(\eta)}{d\eta}\\
&\quad+\mu\frac{1}{x^2}\left(\frac{1}{2}Re_{x,\infty}\right)^{p+1} w_{x,\infty}\frac{d^2W_x(\eta)}{d\eta^2}
\end{aligned}$$

i.e.

$$\begin{aligned}
&\rho w_{x,\infty}\left(\frac{1}{2}Re_{x,\infty}\right)^{2p} W_x x^{-1}\cdot w_{x,\infty}\left[p\cdot W_x(\eta)-\frac{1}{2}\eta\frac{dW_x(\eta)}{d\eta}\right]\\
&\quad+\rho w_{x,\infty}\left(\frac{1}{2}Re_{x,\infty}\right)^{q+p+1/2} W_y\frac{1}{x} w_{x,\infty}\frac{dW_x(\eta)}{d\eta}\\
&=\frac{1}{x^2}\frac{d\mu}{d\eta}\cdot\left(\frac{1}{2}Re_{x,\infty}\right)^{p+1} w_{x,\infty}\frac{dW_x(\eta)}{d\eta}\\
&\quad+\mu\frac{1}{x^2}\left(\frac{1}{2}Re_{x,\infty}\right)^{p+1} w_{x,\infty}\frac{d^2W_x(\eta)}{d\eta^2}
\end{aligned}$$

Comparing the exponents of x in different term, we find

$$\begin{aligned}
2p-1&=p-1\\
p+q+\frac{1}{2}&=p-1
\end{aligned}$$

The solution of the above two equations are $p=0$ and $q=-\frac{1}{2}$.
In this case, Eqs. (3.19) and (3.20) become

$$W_x=\frac{w_x}{w_{x,\infty}} \tag{3.21}$$

$$W_y=\frac{w_y}{w_{x,\infty}}\left(\frac{1}{2}Re_{x,\infty}\right)^{\frac{1}{2}} \tag{3.22}$$

For summery, the derived similarity variables of velocity field of laminar forced convection boundary layer are

$$W_x=\frac{w_x}{w_{x,\infty}} \tag{3.21}$$

$$W_y=\frac{w_y}{w_{x,\infty}}\left(\frac{1}{2}Re_{x,\infty}\right)^{\frac{1}{2}} \tag{3.22}$$

with the related similarity coordinate variable

$$\eta = \frac{y}{x}\left(\frac{1}{2}Re_{x,\infty}\right)^{1/2} \tag{3.18}$$

where the Reynolds number $\mathrm{Re}_{x,\infty}$ is induced as

$$Re_{x,\infty} = \frac{w_{x,\infty}x}{v_\infty} \tag{3.17}$$

In addition, a similarity temperature variable is induced as

$$\theta = \frac{t - t_\infty}{t_w - t_\infty} \tag{3.10}$$

for transformation of temperature variable t.

3.3.2 An Application Example of the Innovative Similarity Transformation Model

Equations (3.14)–(3.16) can be taken as the most typical governing partial differential equations of laminar forced convection for the application example of the innovative similarity transformation.

By using the above Eqs. (3.10), (3.17), (3.18), (3.21) and (3.22), the governing partial differential equations of laminar forced convection, Eqs. (3.14)–(3.16) are equivalently transformed into the following ordinary differential equations respectively:

$$-\eta\frac{dW_x(\eta)}{d\eta} + 2\frac{dW_y(\eta)}{d\eta} + \frac{1}{\rho}\frac{d\rho}{d\eta}[-\eta \cdot W_x(\eta) + 2W_y(\eta)] = 0 \tag{3.23}$$

$$\frac{v_\infty}{v}(-\eta W_x(\eta) + 2W_y(\eta))\frac{dW_x(\eta)}{d\eta} = \frac{d^2W_x(\eta)}{d\eta^2} + \frac{1}{\mu}\frac{d\mu}{d\eta}\frac{dW_x(\eta)}{d\eta} \tag{3.24}$$

$$Pr\frac{v_\infty}{v}[(-\eta W_x(\eta) + 2W_y(\eta))\frac{d\theta(\eta)}{d\eta}] = \frac{d^2\theta(\eta)}{d\eta^2} + \frac{1}{\lambda}\frac{\partial\lambda}{\partial\eta}\frac{d\theta(\eta)}{d\eta} \tag{3.25}$$

It is indicated that the detailed transformation processes for the governing ordinary differential equations of laminar forced convection are omitted for saving space. The readers interested in the detailed processes can refer to [4].

Through the above theoretical derivations, we have obtained all of similarity variables both for free and forced convection. These similarity variables constitute the main body of the innovative similarity transformation models. So far, combined with the novel models of variable physical properties, the innovative similarity

transformation models have been used in our series of extensive studies on convection heat and mass transfer [4–15], and accepted by the international scientists for their different fields of study, such as [16–19] and more. While, the innovative similarity transformation model of velocity field on forced convection will be further applied for extensive study of this present on mixed convection heat transfer.

3.4 Remarks

For solving convection governing partial differential equations, the similarity transformation approach is usually performed. Meanwhile, some dimensionless similarity variables (or parameters) are formed, which as the groups of the dimensional physical variables reduce the number of the independent variables so that simplifies the mathematical description of the physical phenomena. Then, these similarity variables (or parameters) will simplify the convection governing partial differential equations for getting the solutions more easily. These innovative similarity transformation models were developed for in-depth research on convection hydrodynamics and heat and mass transfer both without and with phase change, and will be further applied for extensive study in this book on mixed convection heat transfer.

Currently popular Fakner-Skan transformation on convection heat transfer has some inconvenience for similarity transformation of the core variables of velocity field. By using this transformation, it is necessary to first induce flow function and group theory to derive an intermediate function for an indirect similarity transformation of the velocity field. It is a complicated process and also causes difficult consideration of variable physical properties, and then confines the theoretical and practical value of research results on convection heat and mass transfer.

Compared the Falkner-Skan transformation, a big advantage of our innovative similarity transformation models lie that the velocity variables can be directly transformed to the corresponding similarity velocity variables. Then, all inconvenient issues caused by using Falkner-Skan transformation can be avoided. In addition, our innovative similarity transformation can transform the variable physical properties into the physical property factors, organically combined with the transformed governing ordinary differential equations for convenience of treatment of variable physical properties and getting solution, so that it will be possible to focus on investigation of more and more complicated and difficult issues on convection heat and mass transfer.

References

1. Prandtl, L.: Über Die Flussigkeitsbewegung bei Sehr Kleiner Reibung. In: Proc. 3d Intern. Math. Koug. Heidelberg (1904)
2. Falkner, V.M., Skan, S.W.: Some approximate solutions of the boundary layer equations. Phil. Mag. **12**, pp. 865 (1931)
3. Shang, D.Y., Zhong, L.C.: A similarity transformation of velocity field and its application for an in-depth study on laminar free convection heat transfer of gases, Int. J. Therm. Sci. **101**, 106–115 (2016)
4. Shang, D.Y.: Theory of heat transfer with forced convection film flows. In: Series (Book) of Heat and Mass Transfer, 1st edn, p. 346. Springer, Berlin (2011)
5. Shang, D.Y.: Free convection film flows and heat transfer-models of laminar free convection with phase change for heat and mass transfer. In: Series (Book) of Heat and Mass Transfer, 2nd edn., p. 535. Springer, Berlin (2013)
6. Shang, D.Y., Wang, B.X.: Effect of variable thermophysical properties on laminar free convection of gas. Int. J. Heat Mass Transfer **33**(7), 1387–1395 (1990)
7. Shang, D.Y., Wang, B.X.: Effect of variable thermophysical properties on laminar free convection of polyatomic gas. Int. J. Heat Mass Transfer **34**(3), 749–755 (1991)
8. Shang, D.Y., Wang, B.X., Wang, Y., Quan, Y.: Study on liquid laminar free convection with consideration of variable thermophysical properties. Int. J. Heat Mass Transfer **36**(14), 3411–3419 (1993)
9. Shang, D.Y., Wang, B.X., Zhong, L.C.: A study on laminar film boiling of liquid along an sothermal vertical plate in a pool with consideration of variable thermophysical properties. Int. J. Heat Mass Transfer **37**(5), 819–828 (1994)
10. Shang, D.Y., Adamek, T.: Study on laminar film condensation of saturated steam on a vertical flat plate for consideration of various physical factors including variable thermophysical properties. Warme-und Stoffübertragung **30**, 89–100 (1994)
11. Shang, D.Y., Wang, B.X.: An extended study on steady state laminar film condensation of a superheated vapor on an isothermal vertical plate. Int. J. Heat Mass Transfer **40**(4), 931–941 (1997)
12. Shang, D.Y., Zhong, L.C.: Extensive study on laminar free film condensation from vapor gas mixture. Int. J. Heat Mass Transfer **51**, 4300–4314 (2008)
13. Andersson, H., Shang, D.Y.: An extended study of hydrodynamics of gravity-driven film flow of power-law fluids. Fluid Dyn. Res. pp. 345–357 (1998)
14. Shang, D.Y., Andersson, H.I.: Heat transfer in gravity driven film flow of power-law fluids. Int. J. Heat Mass Transfer **42**(11), 2085–2099 (1999)
15. Shang, D.Y., Gu, J.: Analyses of pseudo-similarity and boundary layer thickness for non-Newtonian falling film flow. Heat Mass Transfer **41**(1), 44–50 (2004)
16. Taton, G., Rok, T., Rokita, E.: Temperature distribution assessment during radiofrequency ablation. IFMBE Proc. **22**, 2672–2676 (2008)
17. Taton, G., Rok, T., Rokita, E.: Estimation of temperature distribution with the use of a thermo-camera. Pol. J. Med. Phys. Eng. **14**(1), 47–61 (2008)
18. Turkin, A.A., Dutka, M., Vainchtein, D., Gersen, S., et al.: Deposition of SiO_2 nanoparticles in heat exchanger during combustion of biogas. Appl. Energy **113**, 1141–1148 (2014)
19. Gao, Y., Liu, Q.K., Chow, W.K., Wu, M.: Analytical and experimental study on multiple fire sources in a kitchen. Fire Saf. J. **63**, 101–112 (2014)

Part II
Hydrodynamics and Heat Transfer with Consideration of Boussinesq Approximation

Chapter 4
Pseudo-Similarity Transformation of Governing Partial Differential Equations

Abstract With our innovative similarity transformation model on forced convection, the advanced governing ordinary differential equations of laminar mixed convection are obtained from the related governing partial differential equations by using a pseudo-similarity transformation. Here, it contains the following research investigations: (i) pseudo-similarity analysis and transformation based on our innovative similarity transformation replacing the traditional Falkner-Skan type transformation; (ii) delivery of new governing pseudo-similarity mathematical model, which is first applied in study of laminar mixed convection. This new model can be more conveniently applied compared with that based on the Falkner-Skan type transformation for investigation of hydrodynamics and heat transfer of mixed convection.

Keywords Pseudo-similarity transformation · Similarity transformation variables · Governing similarity model · Mixed convection parameter · Boussinesq approximation

4.1 Introduction

The presentation of this book for laminar free and forced mixed convection (For short, hereinafter referred to as mixed convection) hydrodynamics and heat transfer is divided to two parts, which are respectively with consideration of variable physical properties and Boussinesq approximation. In this Part of the book, the presentation will focus on hydrodynamics and heat transfer with Boussinesq approximation. In this Chapter, we will present the related process of transformation of the governing partial differential equations to their ordinary ones. In the successive chapters of this part, we will continue to present the related hydrodynamics and heat transfer issues.

D.-Y. Shang and L.-C. Zhong, *Heat Transfer of Laminar Mixed Convection of Liquid*, Heat and Mass Transfer, DOI 10.1007/978-3-319-27959-6_4

4.2 Governing Partial Differential Equations

In Fig. 4.1 the physical model and co-ordinate system of boundary layer with two-dimensional mixed convection are shown schematically. A flat plate is vertically located in parallel fluid flow with its main stream velocity $w_{x,\infty}$. The plate surface temperature is t_w and the fluid bulk temperature is t_∞. Then, a coupled velocity boundary layer is formed near the plate. According to Chap. 2, governing partial differential Eqs. (4.1)–(4.3) can express the laminar mixed convection boundary layer with Boussinesq approximation and without viscous thermal dissipation:

$$\frac{\partial}{\partial x}(w_x) + \frac{\partial}{\partial y}(w_y) = 0 \tag{4.1}$$

$$w_x \frac{\partial w_x}{\partial x} + w_y \frac{\partial w_x}{\partial y} = v_f \frac{\partial^2 w_x}{\partial y^2} + g\beta(t - t_\infty) \tag{4.2}$$

$$w_x \frac{\partial t}{\partial x} + w_y \frac{\partial t}{\partial y} = \frac{v_f}{Pr_f} \frac{\partial^2 t}{\partial y^2} \tag{4.3}$$

with the boundary condition equations

$$y = 0: \quad w_x = 0,\ w_y = 0,\ t = t_w \tag{4.4}$$

$$y \to \infty: \quad w_x = w_{x,\infty},\ t = t_\infty \tag{4.5}$$

where Eqs. (4.1)–(4.3) are continuity, momentum, and energy equations respectively, and the subscript f denotes that the related reference temperature is the average temperature $t_f = \frac{t_w + t_\infty}{2}$. It shows that so-called combined free and forced convection is formed by the interaction between free and forced convections.

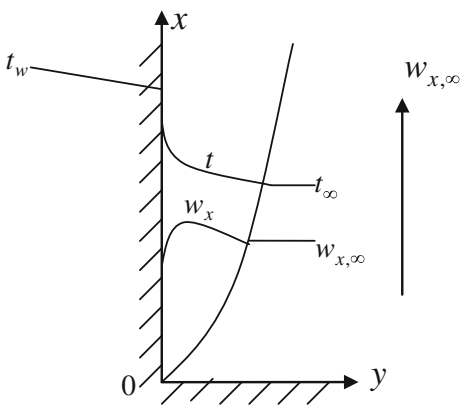

Fig. 4.1 Physical model and coordinate system of boundary layer for laminar mixed convection on a vertical flat plate

4.3 Similarity Variables for Pseudo-Similarity Transformation

As a partial-similarity issue, the governing partial differential equations of laminar mixed convection do not meet the full similarity. However, according to our studies in [1, 2], the heat transfer coefficient calculated by using partial-similarity transformation is very coincident to that evaluated by using pseudo-similarity transformation for Newtonian fluid. Therefore, the pseudo-similarity transformation is here used for transformation of the governing partial differential equations of laminar mixed convection. It is seen from the governing partial differential equations (4.1)–(4.5) that the boundary condition Eqs. (4.4) and (4.5) belong to the forced convection boundary conditions, and the conservation Eqs. (4.1)–(4.3) belong to the free convection boundary layer ones. In this case, the core similarity variables for similarity transformation of velocity field should be formation of forced convection in order for coincidence with the boundary conditions. Consulting the innovative similarity transformation proposed in [3] and Chap. 3 for forced convection boundary layer equations, the core similarity variables and their formulae are induced as below:

For pseudo-similarity transformation of the velocity components w_x and w_y, the following forced convection similarity velocity component $W_x(\eta)$ and $W_y(\eta)$ are induced

$$w_x = w_{x,\infty} W_x(\eta) \tag{4.6}$$

$$w_y = w_{x,\infty} \left(\frac{1}{2} Re_{x,f}\right)^{-1/2} W_y(\eta) \tag{4.7}$$

Here, $W_x(\eta)$ and $W_y(\eta)$ are core similarity variables denoting the similarity transformation of velocity field, namely similarity velocity variables. It is expected that the core similarity variables $W_x(\eta, x)$ and $W_y(\eta, x)$ will dominate the transformed governing ordinary differential equations, while w_x and w_y are velocity components in x and y directions respectively.

The similarity coordinate variable η, the local Reynolds number $Re_{x,f}$ and local mixed convection parameter $Mc_{x,f}$ with consideration of Boussinesq approximation are respectively induced as

$$Re_{x,f} = \frac{w_{x,\infty} x}{\nu_f} \tag{4.8}$$

$$\eta = \frac{y}{x} \left(\frac{1}{2} Re_{x,f}\right)^{1/2} \tag{4.9}$$

In addition, for the local-similarity analysis of the buoyancy term, with consideration of Boussinesq approximation, the local Grashof number will be set as follow:

$$Gr_{x,f} = \frac{g\beta(t_w - t_\infty)x^3}{v_f^2} \tag{4.10}$$

With consideration of Boussinesq approximation, local mixed convection parameter for consideration of variable physical properties is set up as

$$Mc_{x,f} = Gr_{x,f}Re_{x,f}^{-2} \tag{4.11}$$

The similarity temperature variable $\theta(\eta, x)$ is induced as

$$\theta(\eta, x) = \frac{t - t_\infty}{t_w - t_\infty} \tag{4.12}$$

4.4 Performance of the Pseudo-Similarity Transformation

For similarity analysis on the supposed dimensionless coordinate variable η for the governing partial differential Eqs. (4.1)–(4.3) of combined laminar free and forced convection, the following transformation will be done.

4.4.1 Transformation of Eq. (4.1)

With Eqs. (4.6), (4.8) and (4.9) we have

$$\frac{\partial w_x}{\partial x} = w_{x,\infty}\left(\frac{\partial W_x(\eta)}{\partial \eta}\frac{\partial \eta}{\partial x}\right)$$

where

$$\frac{\partial \eta}{\partial x} = -\frac{1}{2}y\left(\frac{1}{2}\frac{w_{x,\infty}}{v_f}\right)^{1/2}x^{-3/2} = -\frac{1}{2}\eta x^{-1}$$

Then,

$$\frac{\partial w_x}{\partial x} = -\frac{1}{2}w_{x,\infty}\eta x^{-1}\frac{\partial W_x(\eta)}{\partial \eta}$$

With Eqs. (4.7)–(4.9) we have

$$\frac{\partial w_y}{\partial y} = w_{x,\infty}\left(\frac{1}{2}Re_{x,f}\right)^{-1/2}\left(\frac{\partial W_y(\eta)}{\partial \eta}\frac{\partial \eta}{\partial y}\right)$$

where

$$\frac{\partial \eta}{\partial y} = x^{-1}\left(\frac{1}{2}Re_{x,f}\right)^{1/2}$$

$$\frac{\partial w_y}{\partial y} = w_{x,\infty}\left(\frac{1}{2}Re_{x,f}\right)^{-1/2}\frac{\partial W_y(\eta)}{\partial \eta}x^{-1}\left(\frac{1}{2}Re_{x,f}\right)^{1/2}$$

i.e.

$$\frac{\partial w_y}{\partial y} = w_{x,\infty}\frac{\partial W_y(\eta)}{\partial \eta}x^{-1}$$

Then, Eq. (4.1) is transformed to

$$-\frac{1}{2}w_{x,\infty}\eta x^{-1}\frac{\partial W_x(\eta)}{\partial \eta} + w_{x,\infty}\frac{\partial W_y(\eta)}{\partial \eta}x^{-1} = 0$$

i.e.

$$-\eta\frac{\partial W_x(\eta)}{\partial \eta} + 2\frac{\partial W_y(\eta)}{\partial \eta} = 0 \tag{4.13}$$

4.4.2 Transformation of Eq. (4.2)

With Eqs. (4.6) and (4.9) we have

$$\frac{\partial w_x}{\partial y} = w_{x,\infty}\left[\frac{\partial W_x(\eta)}{\partial \eta}\frac{\partial \eta}{\partial y}\right] = w_{x,\infty}\frac{\partial W_x(\eta)}{\partial \eta}x^{-1}\left(\frac{1}{2}Re_{x,f}\right)^{1/2}$$

$$\frac{\partial^2 w_x}{\partial y^2} = w_{x,\infty}\frac{\partial^2 W_x(\eta)}{\partial \eta^2}x^{-1}\left(\frac{1}{2}Re_{x,f}\right)^{1/2}\frac{\partial \eta}{\partial y}$$

$$= w_{x,\infty}\frac{\partial^2 W_x(\eta)}{\partial \eta^2}x^{-2}\left(\frac{1}{2}Re_{x,f}\right)$$

Then, Eq. (4.2) is changed to

$$
\begin{aligned}
&w_{x,\infty} W_x(\eta)[-\frac{1}{2} w_{x,\infty} \eta x^{-1} \frac{\partial W_x(\eta)}{\partial \eta}] \\
&\quad + w_{x,\infty} \left(\frac{1}{2} Re_{x,f}\right)^{-1/2} W_y(\eta) w_{x,\infty} \frac{\partial W_x(\eta)}{\partial \eta} x^{-1} \left(\frac{1}{2} Re_{x,f}\right)^{1/2} \\
&= v_f w_{x,\infty} \frac{\partial^2 W_x(\eta)}{\partial \eta^2} x^{-2} \left(\frac{1}{2} Re_{x,f}\right) + g\beta(t - t_\infty)
\end{aligned}
$$

The above equation should be

$$
\begin{aligned}
&w_{x,\infty} W_x(\eta)[-\frac{1}{2} w_{x,\infty} \eta x^{-1} \frac{\partial W_x(\eta)}{\partial \eta}] \\
&\quad + w_{x,\infty} W_y(\eta, x) w_{x,\infty} \frac{\partial W_x(\eta)}{\partial \eta} x^{-1} \\
&= v_f w_{x,\infty} \frac{\partial^2 W_x(\eta)}{\partial \eta^2} x^{-2} \left(\frac{1}{2} Re_{x,f}\right) + g\beta(t - t_\infty)
\end{aligned}
$$

The above equation is divided by $\frac{1}{2} x^{-1} w_{x,\infty}^2$, and changed to

$$
W_x(\eta)[-\eta \frac{\partial W_x(\eta)}{\partial \eta}] + 2W_y(\eta) \frac{\partial W_x(\eta)}{\partial \eta} = v_f \frac{\partial^2 W_x(\eta)}{\partial \eta^2} (\frac{1}{v_f}) + 2g\beta(t - t_\infty) \frac{x}{w_{x,\infty}^2}
$$

The above equation is changed equivalently to

$$
W_x(\eta)(-\eta \frac{\partial W_x(\eta)}{\partial \eta}) + 2W_y(\eta) \frac{\partial W_x(\eta)}{\partial \eta} = \frac{\partial^2 W_x(\eta)}{\partial \eta^2} + 2 \frac{g\beta(t - t_\infty) x^3}{v_f^2} \frac{v_f^2}{w_{x,\infty}^2 x^2}
$$

The above equation is further equivalently changed to

$$
W_x(\eta) \left(-\eta \frac{\partial W_x(\eta)}{\partial \eta}\right) + 2W_y(\eta) \frac{dW_x(\eta)}{\partial \eta} = \frac{\partial^2 W_x(\eta)}{\partial \eta^2} + \frac{t - t_\infty}{t_w - t_\infty} 2 \frac{g\beta(t_w - t_\infty) x^3}{v_f^2} Re_{x,f}^{-2}
$$

i.e.

$$
W_x(\eta) \left(-\eta \frac{\partial W_x(\eta)}{\partial \eta}\right) + 2W_y(\eta) \frac{\partial W_x(\eta)}{\partial \eta} = \frac{\partial^2 W_x(\eta)}{\partial \eta^2} + 2\theta(\eta) \cdot Gr_{x,f} Re_{x,f}^{-2}
$$

or

$$
[-\eta W_x(\eta) + 2W_y(\eta)] \frac{\partial W_x(\eta)}{\partial \eta} = \frac{\partial^2 W_x(\eta)}{\partial \eta^2} + 2\theta(\eta) \cdot Mc_{x,f} \tag{4.14}
$$

where

$$Mc_{x,f} = Gr_{x,f}Re_{x,f}^{-2}$$

is Richardson number or here called local mixed convection parameter with consideration of Boussinesq approximation. It demonstrates the effective rate of the free convection in the mixed convection. Theoretically, the value for the mixed convection parameter $Mc_{x,f}$ can be in a large range $-\infty < Mc_{x,f} < +\infty$. The free/forced mixed convection can be divided to three types, respectively for $Mc > 0$(adding flow), $Mc_{x,f} = 0$ (forced convection) and $Mc_{x,f} < 0$ (opposing flow). In this sense, forced convection can be regarded a special case of free and forced convection.

4.4.3 Transformation of Eq. (4.3)

With Eq. (4.11) we have

$$\frac{\partial t}{\partial x} = (t_w - t_\infty)\frac{\partial \theta(\eta)}{\partial \eta}\frac{\partial \eta}{\partial x}$$

Therefore,

$$\begin{aligned}\frac{\partial t}{\partial x} &= (t_w - t_\infty)\frac{\partial \theta(\eta)}{\partial \eta}\left(-\frac{1}{2}\eta x^{-1}\right) \\ &= (t_w - t_\infty)\left(-\frac{1}{2}\eta x^{-1}\right)\frac{\partial \theta(\eta)}{\partial \eta}\end{aligned}$$

With Eq. (4.11) we have

$$\frac{\partial t}{\partial y} = (t_w - t_\infty)\frac{\partial \theta(\eta)}{\partial \eta}\frac{\partial \eta}{\partial y}$$

Therefore,

$$\frac{\partial t}{\partial y} = (t_w - t_\infty)\frac{\partial \theta(\eta)}{\partial \eta}x^{-1}(\frac{1}{2}Re_{x,f})^{1/2}$$

$$\frac{\partial^2 t}{\partial y^2} = x^{-2}(\frac{1}{2}Re_{x,f})(t_w - t_\infty)\frac{\partial \theta^2(\eta)}{\partial \eta^2}$$

Then, Eq. (4.3) is changed to

$$w_{x,\infty}W_x(\eta)(t_w - t_\infty)[-\frac{1}{2}\eta x^{-1}\frac{\partial\theta(\eta)}{\partial\eta}]$$
$$+ w_{x,\infty}(\frac{1}{2}Re_{x,f})^{-1/2}W_y(\eta)(t_w - t_\infty)\frac{\partial\theta(\eta)}{\partial\eta}x^{-1}(\frac{1}{2}Re_{x,f})^{1/2}$$
$$= \frac{v_f}{Pr_f}x^{-2}(\frac{1}{2}Re_{x,f})(t_w - t_\infty)\frac{\partial^2\theta(\eta)}{\partial\eta^2}$$

i.e.

$$w_{x,\infty}W_x(\eta)(t_w - t_\infty)[-\eta x^{-1}\frac{\partial\theta(\eta)}{\partial\eta}]$$
$$+ 2w_{x,\infty}W_y(\eta)(t_w - t_\infty)\frac{\partial\theta(\eta)}{\partial\eta}x^{-1}$$
$$= \frac{v_f}{Pr_f}x^{-2}(\frac{xw_{x,\infty}}{v_f})(t_w - t_\infty)\frac{\partial^2\theta(\eta)}{\partial\eta^2}$$

The above equation is divided by $x^{-1}w_{x,\infty}(t_w - t_\infty)$, and transformed to

$$W_x(\eta)[-\eta\frac{\partial\theta(\eta)}{\partial\eta}] + 2W_y(\eta)\frac{\partial\theta(\eta)}{\partial\eta} = \frac{1}{Pr_f}\frac{\partial^2\theta(\eta)}{\partial\eta^2}$$

or

$$[-\eta W_x(\eta) + 2W_y(\eta)]\frac{\partial\theta(\eta)}{\partial\eta} = \frac{1}{Pr_f}\frac{\partial^2\theta(\eta)}{\partial\eta^2} \tag{4.15}$$

Then, for the similarity analysis, Eqs. (4.1)–(4.3) are transformed to the following equivalent governing dimensionless differential equations:

$$-\eta\frac{\partial W_x(\eta)}{\partial\eta} + 2\frac{\partial W_y(\eta)}{\partial\eta} = 0 \tag{4.13}$$

$$[-\eta W_x(\eta) + 2W_y(\eta)]\frac{\partial W_x(\eta)}{\partial\eta} = \frac{\partial^2 W_x(\eta)}{\partial\eta^2} + 2\theta(\eta)\cdot Mc_{x,f} \tag{4.14}$$

$$[-\eta W_x(\eta) + 2W_y(\eta, x)]\frac{\partial\theta(\eta)}{\partial\eta} = \frac{1}{Pr_f}\frac{\partial^2\theta(\eta)}{\partial\eta^2} \tag{4.15}$$

with the following dimensionless equations on the boundary layer conditions:

$$\eta = 0: \quad W_x(\eta) = 0,\ W_y(\eta) = 0,\ \theta(\eta) = 1 \tag{4.16}$$

$$\eta \to \infty : \quad W_x(\eta) = 1,\ \theta(\eta) = 0 \tag{4.17}$$

4.5 Rewriting the Governing Ordinary Differential Equations

From the defined equation of the mixed convection parameter, it is seen that the independent coordinate variable x is included in local mixed convection parameter $Mc_{x,f}$. Then, the local mixed parameter $Mc_{x,f}$ is reasonably taken as the second independent coordinate variable. In this case, the governing partial differential Eqs. (4.13)–(4.15) are equivalently become the following rewriting governing partial differential equations respectively

$$-\eta \frac{\partial W_x(\eta, Mc_{x,f})}{\partial \eta} + 2\frac{\partial W_y(\eta, Mc_{x,f})}{\partial \eta} = 0 \tag{4.13*}$$

$$\begin{aligned}&[-\eta W_x(\eta, Mc_{x,f}) + 2W_y(\eta, Mc_{x,f})]\frac{\partial W_x(\eta, Mc_{x,f})}{\partial \eta} \\ &= \frac{\partial^2 W_x(\eta, Mc_{x,f})}{\partial \eta^2} + 2\theta(\eta, Mc_{x,f}) \cdot Mc_{x,f}\end{aligned} \tag{4.14*}$$

$$[-\eta W_x(\eta, Mc_{x,f}) + 2W_y(\eta, Mc_{x,f})]\frac{\partial \theta(\eta, Mc_{x,f})}{\partial \eta} = \frac{1}{Pr_f}\frac{\partial^2 \theta(\eta, Mc_{x,f})}{\partial \eta^2} \tag{4.15*}$$

with the following equivalent dimensionless equations on the boundary conditions

$$\eta = 0 : \quad W_x(\eta, Mc_{x,f}) = 0,\ W_y(\eta, Mc_{x,f}) = 0,\ \theta(\eta, Mc_{x,f}) = 1 \tag{4.16*}$$

$$\eta \to \infty : \quad W_x(\eta, Mc_{x,f}) = 1,\ \theta(\eta, Mc_{x,f}) = 0 \tag{4.17*}$$

In this case, Eqs. (4.6), (4.7) and (4.12) should be equivalently rewritten as below respectively:

$$w_x = w_{x,\infty} W_x(\eta, Mc_{x,f}) \tag{4.6*}$$

$$w_y = w_{x,\infty}\left(\frac{1}{2}Re_{x,f}\right)^{-1/2} W_y(\eta, Mc_{x,f}) \tag{4.7*}$$

$$\theta(\eta, Mc_{x,f}) = \frac{t - t_\infty}{t_w - t_\infty} \tag{4.12*}$$

4.6 Summary

It is the time to summarize the governing similarity equations of combined free and forced convection with Boussinesq approximation in Table 4.1.

Table 4.1 Summary of the governing differential equations of laminar mixed convection boundary layer with consideration of Boussinesq approximation

Term	Equation
Governing partial differential equations	
Mass equation	$\frac{\partial w_x}{\partial x}+\frac{\partial w_y}{\partial y}=0$
Momentum equation	$w_x\frac{\partial w_x}{\partial x}+w_y\frac{\partial w_x}{\partial y}=\nu\frac{\partial^2 w_x}{\partial y^2}+g\beta\lvert t-t_\infty\rvert$
Energy equation	$w_x\frac{\partial t}{\partial x}+w_y\frac{\partial t}{\partial y}=\frac{\nu}{Pr}\frac{\partial^2 t}{\partial y^2}$
Boundary conditions	$y=0:\ \mathrm{w}_x=0,\ \mathrm{w}_y=0,\ t=t_w$ $y\to\infty:\ w_x=w_{x,\infty},\ t=t_\infty$
Induced similarity variables	
Core similarity variable $W_x(\eta)$	$w_x=w_{x,\infty}W_x(\eta)$
Core similarity variable $W(\eta)$	$w_y=w_{x,\infty}\left(\frac{1}{2}Re_{x,f}\right)^{-1/2}W_y(\eta)$
Dimensionless coordinate variable	$\eta=\frac{y}{x}\left(\frac{1}{2}Re_{x,f}\right)^{1/2}$
Local Reynolds number $Re_{x,f}$	$Re_{x,f}=\frac{w_{x,\infty}x}{\nu_f}$
Local Grashof number $Gr_{x,f}$	$Gr_{x,f}=\frac{g\beta(t_w-t_\infty)x^3}{\nu_f^2}$
Local mixed convection parameter $Mc_{x,f}$	$Mc_{x,f}=Gr_{x,f}Re_{x,f}^{-2}$
Dimensionless temperature $\theta(\eta)$	$\theta(\eta)=\frac{t-t_\infty}{t_w-t_\infty}$
Governing ordinary differential equations	
Mass equation	$-\eta\frac{\partial W_x(\eta)}{\partial\eta}+2\frac{\partial W_y(\eta)}{\partial\eta}=0$
Momentum equation	$[-\eta W_x(\eta)+2W_y(\eta)]\frac{\partial W_x(\eta)}{\partial\eta}=\frac{\partial^2 W_x(\eta)}{\partial\eta^2}+2\theta(\eta)\cdot Mc_{x,f}$
Energy equation	$[-\eta W_x(\eta)+2W_y(\eta)]\frac{\partial\theta(\eta)}{\partial\eta}=\frac{1}{\mathrm{Pr}_f}\frac{\partial^2\theta(\eta)}{\partial\eta^2}$
Boundary conditions	$\eta=0:\quad W_x(\eta)=0,\ W_y(\eta)=0,\ \theta(\eta)=1$ $\eta\to\infty:\quad W_x(\eta)=1,\ \theta(\eta)=0$
Equivalent governing ordinary differential equations	
Mass equation	$-\eta\frac{\partial W_x(\eta,Mc_{x,f})}{\partial\eta}+2\frac{\partial W_y(\eta,Mc_{x,f})}{\partial\eta}=0$

(continued)

Table 4.1 (continued)

Term	Equation
Momentum equation	$[-\eta W_x(\eta, Mc_{x,f}) + 2W_y(\eta, Mc_{x,f})]\frac{\partial W_x(\eta, Mc_{x,f})}{\partial \eta} = \frac{\partial^2 W_x(\eta, Mc_{x,f})}{\partial \eta^2} + 2\theta(\eta, Mc_{x,f}) \cdot Mc_{x,f}$
Energy equation	$[-\eta W_x(\eta, Mc_{x,f}) + 2W_y(\eta, Mc_{x,f})]\frac{\partial \theta(\eta, Mc_{x,f})}{\partial \eta} = \frac{1}{Pr_f}\frac{\partial^2 \theta(\eta, Mc_{x,f})}{\partial \eta^2}$
Boundary conditions	$y = 0:\ W_x(\eta, Mc_{x,f}) = 0,\ W_y(\eta, Mc_{x,f}) = 0,\ \theta(\eta, Mc_{x,f}) = 1$ $y \to \infty:\ W_x(\eta, Mc_{x,f}) = 1,\ \theta(\eta, Mc_{x,f}) = 0$
Core similarity variable $W_x(\eta, Mc_{x,f})$	$w_x = w_{x,\infty} W_x(\eta, Mc_{x,f})$
Core similarity variable $W_x(\eta, Mc_{x,f})$	$w_y = w_{x,\infty}(\frac{1}{2}Re_{x,f})^{-1/2} W_y(\eta, Mc_{x,f})$
Dimensionless coordinate variable	$\eta = \frac{y}{x}(\frac{1}{2}Re_{x,f})^{1/2}$
Local Reynolds number $Re_{x,f}$	$Re_{x,f} = \frac{w_{x,\infty} x}{\nu_f}$
Local Grashof number $Gr_{x,f}$	$Gr_{x,f} = \frac{g\beta(t_w - t_\infty)x^3}{\nu_f^2}$
Local mixed convection parameter $Mc_{x,f}$	$Mc_{x,f} = Gr_{x,f} Re_{x,f}^{-2}$
Dimensionless temperature $\theta(\eta, Mc_{x,f})$	$\theta(\eta, Mc_{x,f}) = \frac{t - t_\infty}{t_w - t_\infty}$

4.7 Remarks

The governing similarity models of laminar mixed convection with consideration of Boussinesq approximation are obtained in this Chapter by using the innovative similarity transformation model for velocity field on forced convection. Meanwhile, a pseudo-similarity transformation is performed for the transformation. Although the governing partial differential equations of mixed convection do not meet the complete similarity transformation, based on our previous studies on Newtonian fluid's convection heat transfer, the convection heat transfer coefficient calculated by using pseudo-similarity transformation is very coincident to that evaluated by using partial-similarity transformation.

For description of the characteristics of forced convection, except Grashof number, all proposed similarity variables are based on treatment of the similarity analysis of forced convection. While, for treatment of the characteristics of free convection, the Grashof number is induced.

The velocity components are described by the related similarity velocity variables W_x and W_y, which have definite physical meanings.

In this Chapter, our work focuses on constitution of similarity mathematical models of laminar mixed convection. The derived similarity mathematical models are simple in form and can be conveniently used for investigation of hydrodynamics and heat transfer of mixed convection with Boussinesq approximation.

References

1. Shang, D.Y., Gu, J.: Analyses of pseudo-similarity and boundary layer thickness for non-Newtonian falling film flow. Heat Mass Transf. **41**(1), 44–50 (2004)
2. Shang, D.Y.: Free Convection Film Flows and Heat Transfer—Models of Laminar Free Convection with Phase Change for Heat and Mass Transfer Analysis. Springer, Berlin, 487–516, (2013)
3. Shang, D.Y.: Theory of Heat Transfer with Forced Convection Film Flows. Springer, Berlin (2011)

Chapter 5
Hydrodynamics

Abstract In Chap. 4, the complete governing partial differential equations of laminar mixed convection were transformed equivalently to the corresponding similarity governing partial differential ones, where the Boussinesq approximation is considered. On this basis, in this Chapter, the similarity governing partial differential equations with the boundary conditions will be solved in the wide range of averages Prandtl number and local mixed convection parameter with consideration of Boussinesq approximation. Moreover, the velocity fields and Skin-friction coefficient will be analyzed and calculated numerically.

Keywords Similarity velocity variables · Similarity governing model · Boussinesq approximation · Mixed convection · Mixed convection parameter · Numerical solutions · Skin-friction coefficient · Wall similarity velocity gradient

5.1 Similarity Governing Partial Differential Equations

In Fig. 5.1 the physical model and co-ordinate system of boundary layer with two-dimensional combined laminar free and forced mixed convection are shown schematically. A flat plate is vertically located in parallel fluid flow with its main stream velocity $w_{x,\infty}$. The plate surface temperature is t_w and the fluid bulk temperature is t_∞. Then, a velocity boundary layer will occur near the plate. According to Chap. 4, governing partial differential equations of the laminar mixed convection boundary layer with Boussinesq approximation are as follows:

$$\frac{\partial}{\partial x}(w_x) + \frac{\partial}{\partial y}(w_y) = 0 \tag{4.1}$$

$$w_x \frac{\partial w_x}{\partial x} + w_y \frac{\partial w_x}{\partial y} = v_f \frac{\partial^2 w_x}{\partial y^2} + g\beta(t - t_\infty) \tag{4.2}$$

$$w_x \frac{\partial t}{\partial x} + w_y \frac{\partial t}{\partial y} = \frac{v_f}{Pr_f} \frac{\partial^2 t}{\partial y^2} \tag{4.3}$$

D.-Y. Shang and L.-C. Zhong, *Heat Transfer of Laminar Mixed Convection of Liquid*, Heat and Mass Transfer, DOI 10.1007/978-3-319-27959-6_5

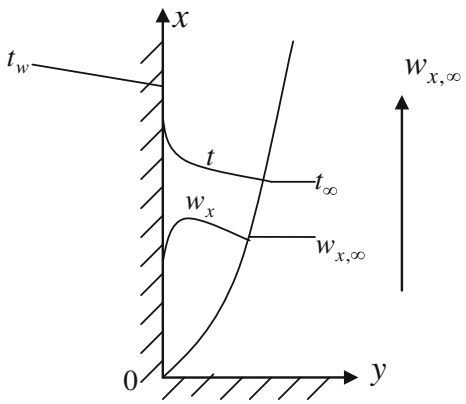

Fig. 5.1 Physical model and coordinate system of boundary layer for combined laminar free and forced convection on a vertical flat plate

with the boundary condition equations

$$y = 0: \quad w_x = 0, \quad w_y = 0, \quad t = t_w \tag{4.4}$$

$$y \to \infty: w_x = w_{x,\infty} \text{ (constant)}, \; t = t_\infty \tag{4.5}$$

According to Chap. 4, governing similarity differential equations of the laminar mixed convection boundary layer with Boussinesq approximation are obtained equivalently as follows:

$$-\eta \frac{\partial W_x(\eta, Mc_{x,f})}{\partial \eta} + 2\frac{\partial W_y(\eta, Mc_{x,f})}{\partial \eta} = 0 \tag{4.13*}$$

$$\begin{aligned}&[-\eta W_x(\eta, Mc_{x,f}) + 2W_y(\eta, Mc_{x,f})]\frac{\partial W_x(\eta, Mc_{x,f})}{\partial \eta} \\ &= \frac{\partial^2 W_x(\eta, Mc_{x,f})}{\partial \eta^2} + 2\theta(\eta, Mc_{x,f}) \cdot Mc_{x,f}\end{aligned} \tag{4.14*}$$

$$[-\eta W_x(\eta, Mc_{x,f}) + 2W_y(\eta, Mc_{x,f})]\frac{\partial \theta(\eta, Mc_{x,f})}{\partial \eta} = \frac{1}{Pr_f}\frac{\partial^2 \theta(\eta, Mc_{x,f})}{\partial \eta^2} \tag{4.15*}$$

with the following equivalent dimensionless equations on the boundary conditions

$$\eta = 0: \quad W_x(\eta, Mc_{x,f}) = 0, \quad W_y(\eta, Mc_{x,f}) = 0, \quad \theta(\eta, Mc_{x,f}) = 1 \tag{4.16*}$$

$$\eta \to \infty: \quad W_x(\eta, Mc_{x,f}) = 1, \quad \theta(\eta, Mc_{x,f}) = 0 \tag{4.17*}$$

where core similarity variables $W_x(\eta, Mc_{x,f})$ and $W_y(\eta, Mc_{x,f})$ of velocity field are defined as

$$w_x = w_{x,\infty} W_x(\eta, Mc_{x,f}) \tag{4.6*}$$

$$w_y = w_{x,\infty} (\frac{1}{2} Re_{x,f})^{-1/2} W_y(\eta, Mc_{x,f}) \tag{4.7*}$$

The similarity temperature variable $\theta(\eta, Mc_{x,f})$ is induced as

$$\theta(\eta, Mc_{x,f}) = \frac{t - t_\infty}{t_w - t_\infty} \tag{4.12*}$$

The included dimensionless coordinate variable η is shown as

$$\eta = \frac{y}{x} (\frac{1}{2} Re_{x,f})^{1/2} \tag{4.9}$$

Local Reynolds number $Re_{x,f}$, local Grashof number $Gr_{x,f}$, and local mixed convection parameter $Mc_{x,f}$ are defined as respectively

$$Re_{x,f} = \frac{w_{x,\infty} x}{\nu_f} \tag{4.8}$$

$$Gr_{x,f} = \frac{g\beta(t_w - t_\infty)x^3}{\nu_f^2} \tag{4.10}$$

$$Mc_{x,f} = Gr_{x,f} Re_{x,f}^{-2} \tag{4.11}$$

Here, it is indicated that the subscript f denotes the reference temperature by using an average temperature $t_f = \frac{t_w + t_\infty}{2}$.

5.2 Ranges of the Numerical Calculation

The similarity governing partial differential Eqs. (4.13*) to (4.15*) with their boundary condition Eqs. (4.16*) and (4.17*) are solved by a shooting method with fifth-order Runge-Kutta integration. For solving the nonlinear problem, a variable mesh approach is applied to the numerical calculation programs. It can be seen that for Boussinesq approximation, the solutions of the core similarity variables $W_x(\eta, Mc_{x,f})$ and $W_y(\eta, Mc_{x,f})$ for similarity transformation of the velocity field and the dimensionless temperature $\theta(\eta, Mc_{x,f})$ are dependent on Prandtl number Pr_f and mixed convection parameter $Mc_{x,f}$. Then, the accurate numerical results are

obtained in the wide ranges of Prandtl number Pr_f $(0.3 \leq Pr_f \leq 20)$ and mixed parameter $Mc_{x,f}$ $(0 \leq Mc_{x,f} \leq 10)$.

5.3 Velocity Fields

From the selected numerical solutions, the similarity velocity field is plotted in Figs. 5.2, 5.3, 5.4, 5.5, 5.6 and 5.7 for different Prandtl number Pr_f and mixed convection parameter Mc with variation of the dimensionless coordinate variable η.

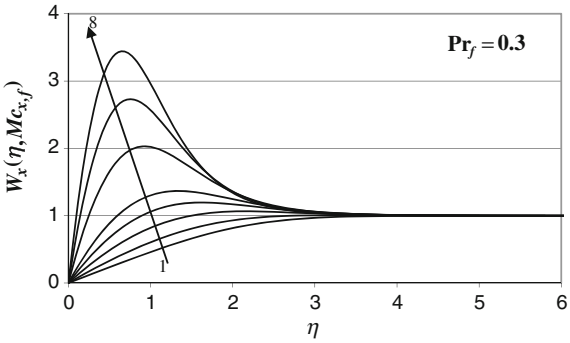

Fig. 5.2 Numerical results of similarity velocity field $W_x(\eta, Mc_{x,f})$ for laminar water fixed convection on a vertical flat plate at $Pr_f = 0.3$ and different $Mc_{x,f}$ (Lines *1* to *8* denote $Mc_{x,f} = 0, 0.1, 0.3, 0.6, 1, 3, 6$ and 10 respectively)

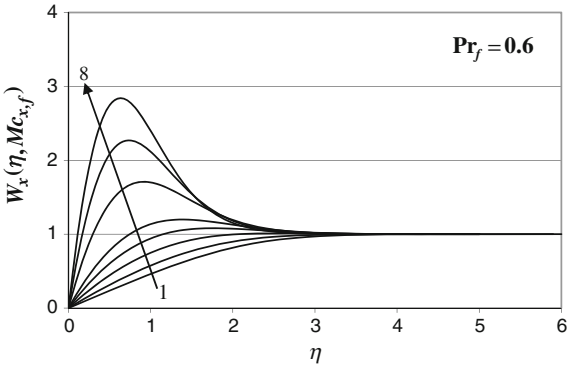

Fig. 5.3 Numerical results of similarity velocity field $W_x(\eta, Mc_{x,f})$ for laminar water fixed convection on a vertical flat plate at $Pr_f = 0.6$ and different $Mc_{x,f}$ (Lines *1* to *8* denote $Mc_{x,f} = 0, 0.1, 0.3, 0.6, 1, 3, 6$ and 10 respectively)

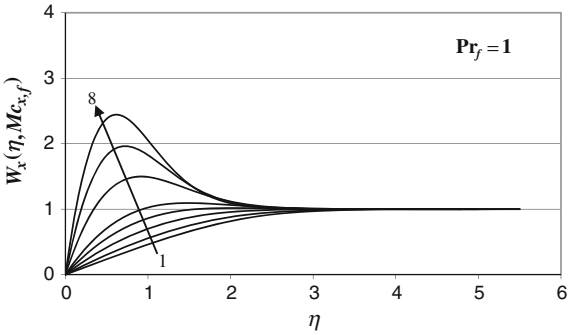

Fig. 5.4 Numerical results of similarity velocity field $W_x(\eta, Mc_{x,f})$ for laminar water fixed convection on a vertical flat plate at $Pr_f = 1$ and different $Mc_{x,f}$ (Lines *1* to *8* denote $Mc_{x,f} = 0, 0.1, 0.3, 0.6, 1, 3, 6$ and 10 respectively)

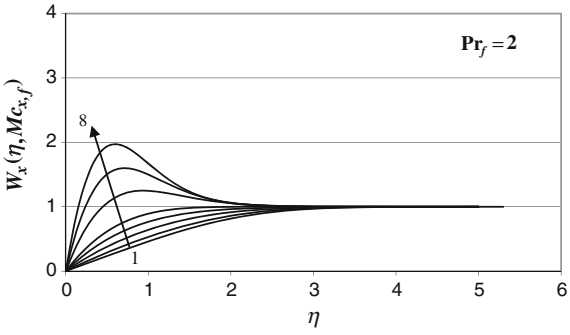

Fig. 5.5 Numerical results of similarity velocity field $W_x(\eta, Mc_{x,f})$ for laminar water fixed convection on a vertical flat plate at $Pr_f = 2$ and different $Mc_{x,f}$ (Lines *1* to *8* denote $Mc_{x,f} = 0, 0.1, 0.3, 0.6, 1, 3, 6$ and 10 respectively)

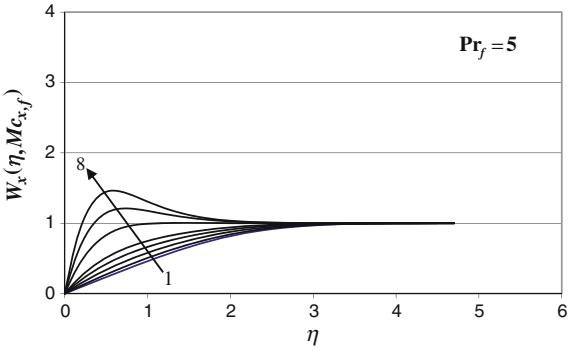

Fig. 5.6 Numerical results of similarity velocity field $W_x(\eta, Mc_{x,f})$ for laminar water fixed convection on a vertical flat plate at $Pr_f = 5$ and different $Mc_{x,f}$ (Lines *1* to *8* denote $Mc_{x,f} = 0, 0.1, 0.3, 0.6, 1, 3, 6$ and 10 respectively)

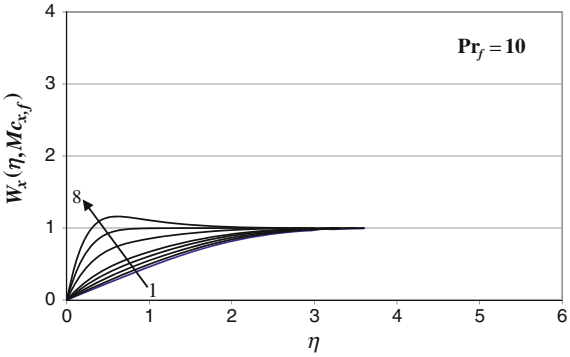

Fig. 5.7 Numerical results of similarity velocity field $W_x(\eta, Mc_{x,f})$ for laminar water fixed convection on a vertical flat plate at $Pr_f = 10$ and different $Mc_{x,f}$ (Lines *1* to *8* denote $Mc_{x,f} = 0, 0.1, 0.3, 0.6, 1, 3, 6$ and 10 respectively)

It is seen that with increasing the average Prandtl number, the velocity and its boundary layer thickness will decrease monotonically. It shows the effect of average physical properties. However, with increasing the mixed convection parameter $Mc_{x,f}$, the velocity and its boundary layer thickness will increase monotonically, which demonstrates the effect of buoyancy force.

5.4 Skin-Friction Coefficient

So far, the skin friction coefficient has been analyzed by means of Falkner-Skan type transformation for laminar mixed convection. In this book, we will analyze it based on our new similarity transformation system. For this analysis, the velocity gradient at the wall is an important characteristic of the solution, and the local skin-friction coefficient $C_{x,f}$ is a dimensionless measure of the shear stress at the wall, i.e.

$$C_{x,f} = \frac{\tau_{w,x}}{\frac{1}{2}\rho_f w_{x,\infty}^2} = \frac{\mu_f (\frac{\partial w_x}{\partial y})_{y=0}}{\frac{1}{2}\rho_f w_{x,\infty}^2} \tag{5.1}$$

According to the related derivation in Chap. 4, we have

$$(\frac{\partial w_x}{\partial y})_{y=0} = x^{-1}(\frac{1}{2}Re_{x,f})^{1/2} w_{x,\infty} (\frac{\partial W_x(\eta, Mc_{x,f})}{\partial \eta})_{\eta=0}$$

Therefore, the local skin-friction coefficient $C_{f,x}$ is expressed as

$$C_{x,f} = \frac{\mu_f x^{-1}(\frac{1}{2}Re_{x,f})^{1/2} w_{x,\infty}(\frac{\partial W_x(\eta, Mc_{x,f})}{\partial \eta})_{\eta=0}}{\frac{1}{2}\rho_f w_{x,\infty}^2}$$
$$= \sqrt{2}\frac{v_f}{x w_{x,\infty}}(Re_{x,f})^{1/2}(\frac{\partial W_x(\eta, Mc_{x,f})}{\partial \eta})_{\eta=0}$$

i.e.

$$C_{x,f} = \sqrt{2}(\mathrm{Re}_{x,f})^{-1/2}(\frac{\partial W_x(\eta, Mc_{x,f})}{\partial \eta})_{\eta=0} \tag{5.2}$$

The average skin friction coefficient $\overline{C}_{x,f}$ from $x = 0$ to x is described as

$$\overline{C}_{x,f} = \frac{1}{x}\int_0^x C_{x,f}dx = \frac{1}{x}\int_0^x \sqrt{2}(Re_{x,f})^{-1/2}(\frac{\partial W_x(\eta, Mc_{x,f})}{\partial \eta})_{\eta=0}dx$$

i.e.

$$\overline{C}_{x,f} = \sqrt{2}(\frac{\partial W_x(\eta, Mc_{x,f})}{\partial \eta})_{\eta=0}\frac{1}{x}\int_0^x (Re_{x,f})^{-1/2}dx$$

With definition of Eq. (4.8) for local Reynolds number we have the expression on the average skin friction coefficient $\overline{C}_{x,f}$:

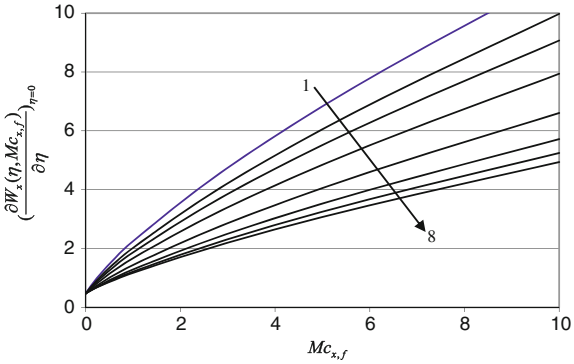

Fig. 5.8 Numerical solutions of wall velocity gradient $(\frac{\partial W_x(\eta, Mc_{x,f})}{\partial \eta})_{\eta=0}$ varying with local mixed convection parameter $Mc_{x,f}$ at different mean Prandtl number Pr_f (Lines *1* to *8* denote Pr_f = 0.3, 0.6, 1, 2, 5, 10, 15 and 20 respectively)

Table 5.1 Numerical solutions of wall similarity velocity gradient $(\frac{\partial W_x(\eta,Mc_{x,f})}{\partial \eta})_{\eta=0}$ varying with local mixed convection parameter $Mc_{x,f}$ at different mean Prandtl number Pr_f

Pr_f	$Mc_{x,f}$							
	0	0.1	0.3	0.6	1	3	6	10
	$(\frac{\partial W_x(\eta,Mc_{x,f})}{\partial \eta})_{\eta=0}$							
0.3	0.4696	0.710069	1.116442	1.638457	2.251451	4.746438	7.790528	11.29826
0.6	0.4696	0.675936	1.029251	1.486558	2.024951	4.218962	6.895673	9.979574
1	0.4696	0.652596	0.96972	1.382153	1.868958	3.855735	6.280259	9.073102
2	0.4696	0.623616	0.894704	1.250539	1.672377	3.399484	5.509253	7.939596
5	0.4696	0.590353	0.807129	1.095825	1.440521	2.861203	4.60151	6.607166
10	0.4696	0.572616	0.75227	0.99557	1.288912	2.503249	3.996003	5.719424
15	0.4696	0.571656	0.733078	0.949119	1.21391	2.315243	3.677123	5.247122
20	0.4696	0.571181	0.726757	0.92476	1.170915	2.198377	3.468757	4.937554

$$\overline{C}_{x,f} = 2\sqrt{2}(Re_{x,f})^{-1/2}(\frac{\partial W_x(\eta, Mc_{x,f})}{\partial \eta})_{\eta=0} \tag{5.3}$$

Equations (5.2) and (5.3) show that the skin friction coefficient increases with increasing the wall velocity gradient $(\frac{\partial W_x(\eta,Mc_{x,f})}{\partial \eta})_{\eta=0}$. A system of the rigorous numerical solutions on the wall velocity gradient $(\frac{\partial W_x(\eta,Mc_{x,f})}{\partial \eta})_{\eta=0}$ has been obtained, and the selected solutions of them are plotted in Fig. 5.8 and listed in Table 5.1 with variation of Prandtl number Pr_f and mixed convection parameter $Mc_{x,f}$. Then, it is seen that wall velocity gradient $(\frac{\partial W_x(\eta,Mc_{x,f})}{\partial \eta})_{\eta=0}$ increases with increasing the mixed convection parameter $Mc_{x,f}$, and decreases in an accelerative pace. It shows the effects of buoyancy force. With increasing Prandtl number Pr_f, the wall velocity gradient $(\frac{\partial W_x(\eta,Mc_{x,f})}{\partial \eta})_{\eta=0}$ will decrease. It demonstrates the effect of the average physical properties. As a result, the skin-friction coefficient will decrease with increase in average Prandtl number Pr_f and increase with increase in mixed convection parameter $Mc_{x,f}$.

If we set $Mc_{x,f} = 0$, the flow is corresponding to net forced convection, and the wall velocity gradient will be $(\frac{\partial W_x(\eta,Mc_{x,f})}{\partial \eta})_{\eta=0} = 0.4696$ according to the rigorous numerical results listed in Table 5.1. Then, we have $C_{x,f} = 0.664(Re_{x,f})^{-1/2}$ and $\overline{C}_{x,f} = 1.328(Re_{x,f})^{-1/2}$, according with the related derivation in [1] for net forced convection. Logically, these demonstrate that net forced convection is only the special case of mixed convection when the mixed convection parameter $Mc_{x,f}$ is equal to zero.

From Eqs. (5.2) and (5.3) it is seen that the wall velocity gradient $(\frac{\partial W_x(\eta,Mc_{x,f})}{\partial \eta})_{\eta=0}$ is the only one unknown variable for evaluation of the skin-friction coefficient.

Then, the selected values listed in Table 5.1 can be used for evaluation of the skin-friction coefficient by using the interpolation of the wall velocity gradient $(\frac{\partial W_x(\eta,Mc_{x,f})}{\partial \eta})_{\eta=0}$.

5.5 Remarks

The equations for skin-friction coefficient are derived out based on our innovative similarity transformation model. It is found that the wall velocity gradient $(\frac{\partial W_x(\eta,Mc_{x,f})}{\partial \eta})_{\eta=0}$ is only one unknown variable for evaluation of the skin-friction coefficient. A system of rigorous numerical solutions of the wall velocity gradient $(\frac{\partial W_x(\eta,Mc_{x,f})}{\partial \eta})_{\eta=0}$ are obtained and provided in wide ranges of average Prandtl number $(0.3 \leq Pr_f \leq 20)$ and local mixed parameter $(0 \leq Mc_{x,f} \leq 10)$. It is seen that wall velocity gradient $(\frac{\partial W_x(\eta,Mc_{x,f})}{\partial \eta})_{\eta=0}$ increases with increasing the average mixed convection parameter $Mc_{x,f}$, and decreases with increasing Prandtl number Pr_{f}. Meanwhile, with increasing the average Prandtl number Pr_f, the wall velocity gradient $(\frac{\partial W_x(\eta,Mc_{x,f})}{\partial \eta})_{\eta=0}$ will decrease slowly. As a result, the skin-friction coefficient will increase with decreasing the average Prandtl number Pr_{f}. Meanwhile, the skin-friction coefficient will increase with increasing the mixed convection parameter $Mc_{x,f}$ due to increase of the buoyancy force.

Reference

1. Shang, D.Y.: Theory of Heat Transfer with Forced Convection Film Flows, p. 82. Springer, Berlin (2011)

Chapter 6
Heat Transfer

Abstract Through the series of studies, the optimal formalization of Nusselt number for laminar mixed convection on a vertical flat plate is obtained for consideration of Boussinesq approximation. It contains the following research investigations: (i) pseudo-similarity analysis and transformation based on our developed innovative similarity transformation replacing the traditional Falkner-Skan type transformation; (ii) new governing similarity mathematical model, which is first applied in study of laminar free/forced mixed convection, and is more conveniently derived and applied compared with that based on the Falkner-Skan type transformation for investigation of mixed convection heat transfer; (iii) the system of numerical solutions of wall similarity temperature gradient; and (iv) optimal formalized equations of Nusselt number of mixed convection are derived by using a curve-fitting method for multiple variables. The optimal formalized equations are very coincident to those calculated based on the numerical solutions. The optimal formalized equations of Nusselt number are suitable for wide coverage of Prandtl number and mixed convection parameter, and can be used for calculation of heat transfer coefficient of laminar mixed convection with consideration of Boussinesq approximation.

Keywords Nusselt number · Theoretical equation · Optimal formalized equation · Wall similarity temperature gradient · Curve-fitting method · Average Prandtl number · Local mixed convection parameter · Boussinesq approximation

6.1 Introduction

In Chap. 5, the mathematical model with the similarity governing partial differential equations and the boundary conditions are solved by a successively iterative procedure in the wide range of average Prandtl number and mixed convection parameter. Meanwhile, the Skin-friction coefficient fields are analysed and a system of its results are provided. In this Chapter, we will further present heat transfer of mixed convection. First, the system of temperature fields will be obtained. Moreover, the theoretical heat transfer equations will be derived by means of heat transfer theoretical analysis based on our new similarity transformation model. It is seen that in the theoretical heat transfer equations the wall similarity temperature gradient is only

D.-Y. Shang and L.-C. Zhong, *Heat Transfer of Laminar Mixed Convection of Liquid*, Heat and Mass Transfer, DOI 10.1007/978-3-319-27959-6_6

one un-known variable for evaluation of Nusselt number, which is dependent on the mixed convection parameter and average Prandtl number. Based on the system of the numerical solutions, the optimal formalized equations of Nusselt number are developed by using a curve-fitting method with multiple variables. Furthermore, some calculation examples are given for demonstration of heat transfer application of the developed optimal formalized equations of Nusselt number.

6.2 Temperature Field

With the numerical calculation for laminar mixed convection for consideration of Boussinesq approximation, the similarity temperature field is obtained together with the similarity velocity field, and a system of the numerical solutions of similarity temperature field are plotted in Figs. 6.1, 6.2, 6.3, 6.4, 6.5 and 6.6 with variation of average Prandtl number and mixed convection parameter.

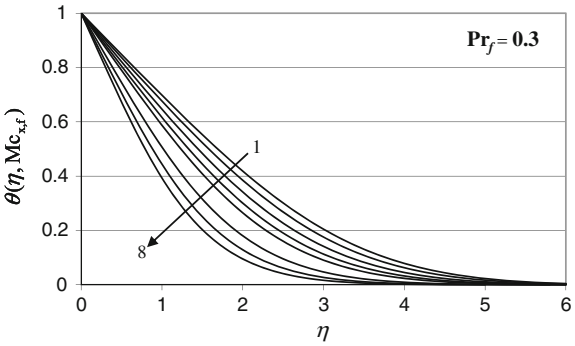

Fig. 6.1 Numerical results of similarity temperature $\theta(\eta, Mc_{x,f})$ profiles for laminar water mixed convection on a vertical flat plate at fluid average Prandtl number $Pr_f = 0.3$ and different local mixed convection parameter $Mc_{x,f}$ (Lines *1* to *8* denote $Mc_{x,f} = 0, 0.1, 0.3, 0.6, 1, 3, 6$ and 10 respectively)

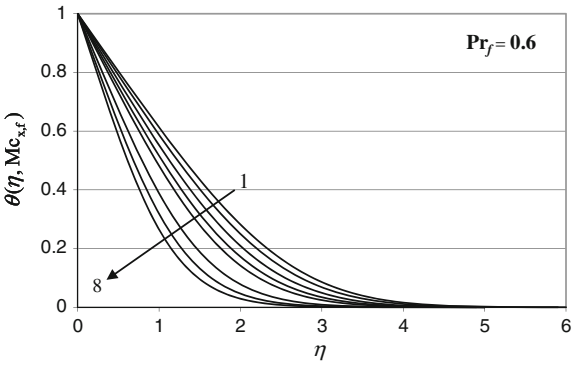

Fig. 6.2 Numerical results of similarity temperature $\theta(\eta, Mc_{x,f})$ profiles for laminar water mixed convection on a vertical flat plate at fluid average Prandtl number $Pr_f = 0.6$ and different local mixed convection parameter $Mc_{x,f}$ (Lines *1* to *8* denote $Mc_{x,f} = 0, 0.1, 0.3, 0.6, 1, 3, 6$ and 10 respectively)

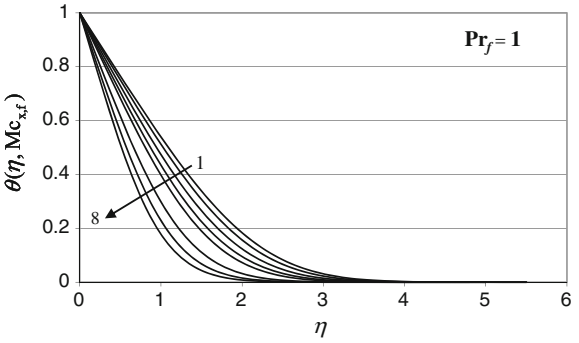

Fig. 6.3 Numerical results of similarity temperature $\theta(\eta, Mc_{x,f})$ profiles for laminar water mixed convection on a vertical flat plate at fluid average Prandtl number $Pr_f = 1$ and different local mixed convection parameter $Mc_{x,f}$ (Lines *1* to *8* denote $Mc_{x,f} = 0, 0.1, 0.3, 0.6, 1, 3, 6$ and 10 respectively)

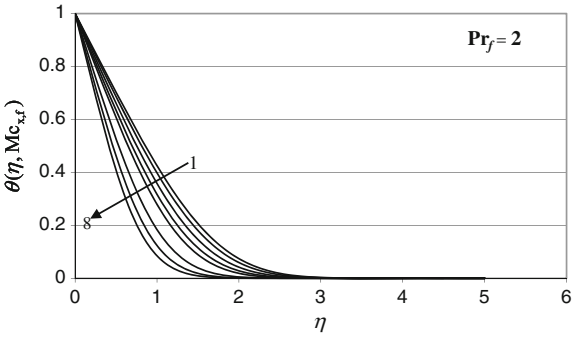

Fig. 6.4 Numerical results of similarity temperature $\theta(\eta, Mc_{x,f})$ profiles for laminar water mixed convection on a vertical flat plate at fluid average Prandtl number $Pr_f = 2$ and different local mixed convection parameter $Mc_{x,f}$ (Lines *1* to *8* denote $Mc_{x,f} = 0, 0.1, 0.3, 0.6, 1, 3, 6$ and 10 respectively)

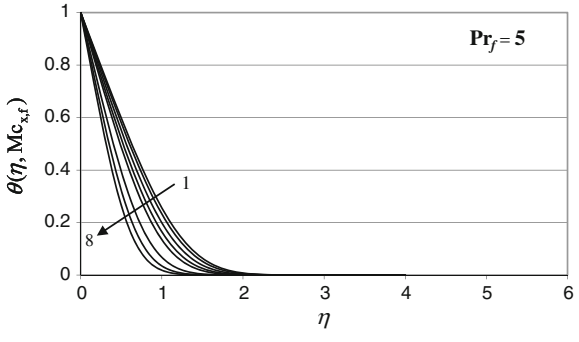

Fig. 6.5 Numerical results of similarity temperature $\theta(\eta, Mc_{x,f})$ profiles for laminar water mixed convection on a vertical flat plate at fluid average Prandtl number $Pr_f = 5$ and different local mixed convection parameter $Mc_{x,f}$ (Lines *1* to *8* denote $Mc_{x,f} = 0, 0.1, 0.3, 0.6, 1, 3, 6$ and 10 respectively)

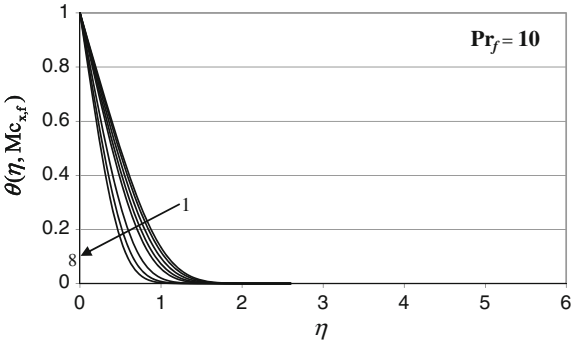

Fig. 6.6 Numerical results of similarity temperature $\theta(\eta, Mc_{x,f})$ profiles for laminar water mixed convection on a vertical flat plate at fluid average Prandtl number $Pr_f = 10$ and different local mixed convection parameter $Mc_{x,f}$ (Lines *1* to *8* denote $Mc_{x,f} = 0, 0.1, 0.3, 0.6, 1, 3, 6$ and 10 respectively)

It is seen that with increasing the average Prandtl number, the temperature profiles will be steeper and steeper, and the temperature boundary layer thickness will decrease monotonically. Meanwhile, with increasing the mixed convection parameter, the temperature profiles will be steeper and steeper too, due to increase of the buoyancy force. However, the steepening trend of temperature profiles will be weaker and weaker with increasing the Prandtl number.

6.3 Theoretical Equations of Nusselt Number

6.3.1 Theoretical Equations of Nusselt Number

The local heat transfer rate $q_{x,f}$ at position x per unit area from the surface of the plate without consideration of variable physical properties can be calculated by Fourier's law as $q_{x,f} = -\lambda_f(\frac{\partial t}{\partial y})_{y=0}$. The subscript f denotes the case that the boundary layer average temperature $t_f = \frac{t_w + t_\infty}{2}$ is taken as the reference temperature with with consideration of Boussinesq approximation.

With Eqs. (4.9) and (4.11) we have

$$q_{x,f} = -\lambda_f(t_w - t_\infty)(\frac{\partial\theta(\eta, Mc_{x,f})}{\partial\eta})_{\eta=0}\frac{\partial\eta}{\partial y}$$

where

$$\frac{\partial\eta}{\partial y} = x^{-1}(\frac{1}{2}Re_{x,f})^{1/2}$$

Then,

$$q_{x,f} = \lambda_f (t_w - t_\infty)(\frac{1}{2} Re_{x,f})^{1/2} x^{-1} (-\frac{\partial \theta(\eta, Mc_{x,f})}{\partial \eta})_{\eta=0}$$

The local heat transfer coefficient $\alpha_{x,f}$, defined as $q_{x,f} = \alpha_{x,f}(t_w - t_\infty)$, will be given by

$$\alpha_{x,f} = \lambda_f (\frac{1}{2} Re_{x,f})^{1/2} x^{-1} (-\frac{\partial \theta(\eta, Mc_{x,f})}{\partial \eta})_{\eta=0}$$

The local Nusselt number, defined by $Nu_{x,f} = \frac{\alpha_{x,f} \cdot x}{\lambda_f}$, will be

$$Nu_{x,f} = (\frac{1}{2} Re_{x,f})^{1/2} (-\frac{\partial \theta(\eta, Mc_{x,f})}{\partial \eta})_{\eta=0} \tag{6.1}$$

Equation (6.1) is the theoretical equation of local Nusselt number for consideration of Boussinesq approximation.

Total heat transfer rate $Q_{x,f}$ from position $x = 0$ to x with width of s on the plate for consideration of Boussinesq approximation

$$Q_{x,f} = \iint_A q_{x,f} dA = \int_0^x q_{x,f} s \cdot dx$$

and hence

$$Q_{x,f} = \lambda_f \cdot s(t_w - t_\infty)(-\frac{\partial \theta(\eta, Mc_{x,f})}{\partial \eta})_{\eta=0} \int_0^x (\frac{1}{2} Re_{x,f})^{1/2} x^{-1} dx$$

With Eq. (4.8) for definition of the local Reynolds number $Re_{x,f}$ we obtain

$$Q_{x,f} = 2s\lambda_f (t_w - t_\infty)(\frac{1}{2} Re_{x,f})^{1/2} (-\frac{\partial \theta(\eta, Mc_{x,f})}{\partial \eta})_{\eta=0}$$

The average heat transfer rate $\overline{Q}_{x,f}$ from the per unit plate area related to the plate area $A = x \cdot s$ is expressed as

$$\overline{Q}_{x,f} = \frac{Q_{x,f}}{x \cdot s} = 2x^{-1} \lambda_f (t_w - t_\infty)(\frac{1}{2} Re_{x,f})^{1/2} (-\frac{\partial \theta(\eta, Mc_{x,f})}{\partial \eta})_{\eta=0}$$

The average heat transfer coefficient $\overline{\alpha}_{x,f}$, defined as $\overline{Q}_{x,f} = \overline{\alpha}_{x,f}(t_w - t_\infty)$ is expressed as

$$\overline{\alpha}_{x,f} = 2x^{-1}\lambda_f(\frac{1}{2}Re_{x,f})^{1/2}(-\frac{\partial\theta(\eta, Mc_{x,f})}{\partial\eta})_{\eta=0}$$

The average Nussel number defined as $\overline{Nu}_{x,f} = \frac{\overline{\alpha}_{x,f}\cdot x}{\lambda_f}$ will be

$$\overline{Nu}_{x,f} = 2(\frac{1}{2}Re_{x,f})^{1/2}(-\frac{\partial\theta(\eta, Mc_{x,f})}{\partial\eta})_{\eta=0} \tag{6.2}$$

Equation (6.2) is theoretical equation of average Nusselt number for consideration of Boussinesq approximation.

It is seen from the Nusselt number theoretical Eqs. (6.1) and (6.2) that the wall similarity temperature gradient $(-\frac{\partial\theta(\eta,Mc_{x,f})}{\partial\eta})_{\eta=0}$ is the only unknown variable dominating prediction of Nusselt number of laminar mixed convection. Then, evaluation of the Nusselt number is attributed to evaluate the wall similarity temperature gradient. This work will be performed in next section.

6.3.2 *Optimal Formalization of Wall Similarity Temperature Gradient*

It is seen from the Nusselt number theoretical Eqs. (6.1) and (6.2) that the wall similarity temperature gradient as the only one unknown variable for prediction of heat dominates the prediction of mixed convection heat transfer. Here, it is necessary to find the prediction equation of wall similarity temperature gradient.

In this present work, a system of rigorous solutions on the wall similarity temperature gradient have been obtained numerically, and their selected values are plotted in Fig. 6.7, and listed in Table 6.1, respectively. It is seen that the wall similarity temperature gradient increases with increasing the mixed parameter $Mc_{x,f}$, and increases with increasing the Prandtl number Pr_f.

The system of rigorous numerical solutions of the wall similarity temperature gradient are formulated by means of an optimal curve-fitting approach for consideration of two variables, and the obtained formulized correlations are shown as follows with the ranges of Prandtl number between 0.3 and 20 and the mixed convection parameter between 0 and 10:

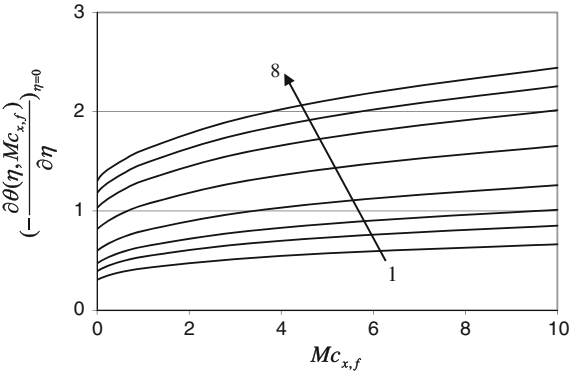

Fig. 6.7 Numerical solutions of wall similarity temperature gradient on the vertical flat plate surface, varying with average Prandtl number Pr_f and mixed convection parameter Mc (Lines *1* to *8* denote $Pr_f = 0.3$, 0.6, 1, 2, 5, 10, 15 and 20 respectively)

Table 6.1 Numerical solutions of wall similarity temperature gradient on the vertical plat surface, varying with average Prandtl number and mixed convection parameter

Pr_f	$Mc_{x,f}$							
	0	0.1	0.3	0.6	1	3	6	10
	$(-\frac{\partial\theta(\eta,Mc_{x,f})}{\partial\eta})_{\eta=0}$							
0.3	0.304010	0.326674	0.357910	0.390368	0.421909	0.514989	0.594022	0.663901
0.6	0.391718	0.419017	0.458042	0.499082	0.539374	0.659147	0.761145	0.851321
1	0.469601	0.500094	0.544658	0.592619	0.640063	0.782055	0.903412	1.010804
2	0.597234	0.631660	0.683822	0.741380	0.799155	0.974363	1.125256	1.259114
5	0.815561	0.854542	0.915958	0.986399	1.058680	1.283084	1.479155	1.653815
10	1.029735	1.073799	1.140716	1.220468	1.304086	1.568637	1.803302	2.014039
15	1.179622	1.233357	1.303399	1.385543	1.474928	1.762639	2.021957	2.255761
20	1.298817	1.336533	1.437139	1.520671	1.613732	1.917488	2.192537	2.442278

Table 6.2 Values of wall similarity temperature gradient on the vertical flat plate, predicted by using Eq. (6.3)

Pr_f	$Mc_{x,f}$							
	0	0.1	0.3	0.6	1	3	6	10
	$(-\frac{\partial\theta(\eta,Mc_{x,f})}{\partial\eta})_{\eta=0}$							
0.3	0.310814	0.329603	0.3610318	0.397437	0.4334	0.530043	0.611347	0.672561
0.6	0.394316	0.416442	0.4534434	0.496433	0.539229	0.657003	0.757442	0.836109
1	0.4699	0.49477	0.536372	0.584852	0.633431	0.76965	0.887019	0.981589
2	0.596141	0.625125	0.6736645	0.73053	0.788104	0.954002	1.098992	1.220285
5	0.816511	0.851581	0.9105103	0.980226	1.051995	1.267147	1.458866	1.627141
10	1.03587	1.075944	1.143569	1.224386	1.308874	1.570662	1.807496	2.022818
15	1.190577	1.233674	1.3066538	1.394509	1.48731	1.780877	2.048873	2.297494
20	1.314162	1.359418	1.4362827	1.529363	1.628479	1.946877	2.239438	2.514713

Table 6.3 Deviation of predicted values of the wall similarity temperature gradient to the related Numerical solutions

Pr_f	$Mc_{x,f}$							
	0	0.1	0.3	0.6	1	3	6	10
	$\left(-\frac{\partial\theta(\eta,Mc_{x,f})}{\partial\eta}\right)_{\eta=0}$							
0.3	0.022382	0.008965	0.008722	0.01811	0.027236	0.029232	0.029165	0.013044
0.6	0.006633	−0.00615	−0.01004	−0.00531	−0.00027	−0.00325	−0.00486	−0.01787
1	0.000637	−0.01065	−0.01521	−0.01311	−0.01036	−0.01586	−0.01815	−0.0289
2	−0.00183	−0.01035	−0.01485	−0.01463	−0.01383	−0.0209	−0.02334	−0.03084
5	0.001164	−0.00346	−0.00595	−0.00626	−0.00631	−0.01242	−0.01372	−0.01613
10	0.005958	0.001998	0.002501	0.003211	0.003672	0.001291	0.002326	0.004359
15	0.009287	0.000257	0.002497	0.006471	0.008395	0.010347	0.013312	0.018501
20	0.011815	0.017123	−0.0006	0.005716	0.009138	0.015327	0.021391	0.029659

$$\left(-\frac{\partial\theta(\eta, Mc_{x,f})}{\partial\eta}\right)_{\eta=0} = aPr_f^b \quad (0.3 \le Pr_f \le 20) \tag{6.3}$$

where

$$a = \frac{(-0.0002Mc_{x,f}^4 + 0.0039Mc_{x,f}^3 - 0.0262Mc_{x,f}^2 + 0.6179Mc_{x,f} + 0.4699)}{(1 + Mc_{x,f})^{0.75}}$$
$$(0 \le Mc \le 10)$$

$$b = \frac{(0.00009\mathrm{Mc}_{x,f}^4 - 0.0018Mc_{x,f}^3 + 0.0117Mc_{x,f}^2 + 0.2771Mc_{x,f} + 0.3433)}{1 + Mc_{x,f}}$$
$$(0 \le Mc_{x,f} \le 10)$$

If $Mc_{x,f} = 0$, Eq. (6.3) will become the following related equation corresponding to laminar forced convection:

$$\left(-\frac{\partial\theta(\eta, Mc_{x,f} = 0)}{\partial\eta}\right)_{\eta=0} = 0.4699Pr_f^{0.3433} \tag{6.4}$$

It is interesting that Eq. (6.4) is equivalent to Eq. (5.12) in Ref. [1] for laminar forced convection, corresponding to well-known Pohlhausen equation [2] for consideration of Boussinesq approximation. Therefore, the well-known Pohlhausen equation can be regarded as the special case of Eq. (6.3) when the local mixed convection number tends to zero.

With Eq. (6.3), a system of the similarity temperature gradient is obtained, and plotted in Table 6.2 with variation of average Prandtl number and local mixed convection parameter. Furthermore, the deviations of the predicted values in Table 6.2 to the related numerical solutions of the similarity temperature gradient in Table 6.1 are plotted in Table 6.3. It is seen that the maximal deviation is about 3 % in the range of average Prandtl number from 0.3 to 20 and the local mixed convection number from 0 to 10. However, as high as 84 % possibility is located under the deviation value of 2 %.

6.4 Optimal Formalized Equations of Nusselt Number

Obviously, the optimal formalized equations of Nusselt number of laminar mixed convection on a vertical flat plate with consideration of Boussinesq approximation consist of the follows:

1. Theoretical equations of Nusselt number

(1) Theoretical equation of local Nusselt number

$$Nu_{x,f} = (\frac{1}{2}Re_{x,f})^{1/2}(-\frac{\partial\theta(\eta, Mc_{x,f})}{\partial\eta})_{\eta=0} \tag{6.1}$$

where the local Nusselt number is defined as $Nu_{x,f} = \frac{\alpha_{x,f}\cdot x}{\lambda_f}$

(2) Theoretical equation of average Nusselt number

$$\overline{Nu}_{x,f} = 2(\frac{1}{2}Re_{x,f})^{1/2}(-\frac{\partial\theta(\eta, Mc_{x,f})}{\partial\eta})_{\eta=0} \tag{6.2}$$

where the average Nusselt number is defined as $\overline{Nu}_{x,f} = \frac{\overline{\alpha}_{x,f}\cdot x}{\lambda_f}$

2. Formalized equations of the wall similarity temperature gradient for water laminar mixed convection on a vertical flat plate

$$(-\frac{\partial\theta(\eta, Mc_{x,f})}{\partial\eta})_{\eta=0} = aPr_f^b \quad (0.3 \le Pr_f \le 20) \tag{6.3}$$

where

$$a = \frac{(-0.0002Mc_{x,f}^4 + 0.0039Mc_{x,f}^3 - 0.0262Mc_{x,f}^2 + 0.6179Mc_{x,f} + 0.4699)}{(1 + Mc_{x,f})^{0.75}}$$
$$(0 \le Mc_{x,f} \le 10)$$

$$b = \frac{(0.00009Mc_{x,f}^4 - 0.0018Mc_{x,f}^3 + 0.0117Mc_{x,f}^2 + 0.2771Mc_{x,f} + 0.3433)}{1 + Mc_{x,f}}$$
$$(0 \le Mc_{x,f} \le 10)$$

Then, Eqs. (6.1) to (6.3) are regarded as the optimal formalized equations of Nusselt number of laminar mixed convection on a vertical flat plate with consideration of Boussinesq approximation.

6.5 Calculation Examples

6.5.1 Question 1

A flat plate with $s = 0.1$ m in width and $x = 0.10$ m in length is suspended vertically in the space of water. The bulk velocity is 0.1 m/s parallel to plate (see Fig. 4.1). The bulk temperature is 0 °C, and the plate temperature is $t_w = 20$ °C.

Suppose the mixed convection is laminar, please calculate the mixed convection heat transfer on the plate.

Solution:

(1) Heat transfer analysis

From Sect. 6.3.1, the correlations of mixed convection heat transfer on a flat plate are

$$\overline{Nu}_{x,f} = 2\left(\frac{1}{2}Re_{x,f}\right)^{1/2}\left(-\frac{\partial\theta(\eta, Mc_{x,f})}{\partial\eta}\right)_{\eta=0} \tag{6.2}$$

where

$$\left(-\frac{\partial\theta(\eta, Mc_{x,f})}{\partial\eta}\right)_{\eta=0} = aPr_f^b \quad (0.3 \le Pr_f \le 20) \tag{6.3}$$

$$a = \frac{(-0.0002Mc_{x,f}^4 + 0.0039Mc_{x,f}^3 - 0.0262Mc_{x,f}^2 + 0.6179Mc_{x,f} + 0.4699)}{(1 + Mc_{x,f})^{0.75}}$$
$$(0 \le Mc_{x,f} \le 10)$$

$$b = \frac{(0.00009Mc_{x,f}^4 - 0.0018Mc_{x,f}^3 + 0.0117Mc_{x,f}^2 + 0.2771Mc_{x,f} + 0.3433)}{1 + Mc_{x,f}}$$
$$(0 \le Mc_{x,f} \le 10)$$

Obviously, for evaluation of heat transfer, first, it is necessary to evaluate average Reynolds number $Re_{x,f}$ and wall similarity temperature gradient $\left(-\frac{\partial\theta(\eta,Mc_{x,f})}{\partial\eta}\right)_{\eta=0}$. While the latter is decided by the average Prandtl number Pr_f, and the coefficient a and exponent b. Here, the coefficient a and exponent b are dependent on mixed convection parameter $Mc_{x,f}$. While Mc is dependent on average Reynolds number $Re_{x,f}$, and average Grashof number $Gr_{x,f}$.

(2) Data of the related water's physical properties

The average temperature $t_f = (0 + 20)/2 = 10\,^\circ\text{C}$.

From appendix, the related physical properties of water can be obtained as below:

$v_f = 1.2996 \times 10^{-6}\ \mathrm{m^2/s}$, $Pr_f = 9.30$ and $\rho_\infty = 999.9\,\mathrm{kg/m^3}$ at t_∞ = 0 °C; λ_f = 0.586 W/(m °C), $\beta_f = 0.87 \times 10^{-4}/\mathrm{K}$ and $\rho_w = 998.2\,\mathrm{kg/m^3}$ at $t_w = 20$ °C.

(3) Evaluation of the physical parameters $Re_{x,f}$, $Gr_{x,f}$ and $Mc_{x,f}$

$$Re_{x,f} = \frac{w_{x,\infty}x}{v_f} = 0.1\,\mathrm{m/s} \times 0.10\,\mathrm{m}/(1.2996 \times 10^{-6}\,\mathrm{m^2/s}) = 7694.7$$

$$Gr_{x,f} = \frac{g\beta(t_w - t_\infty)x^3}{v_f^2} = \frac{9.8 \times (0.87 \times 10^{-4})(20-0) \times 0.1^3}{(1.2996 \times 10^{-6})^2} = 10096153$$

$$Mc_{x,f} = Gr_{x,f}Re_{x,f}^{-2} = 10096153/(7694.7)^2 = 0.170519$$

(4) Evaluation of a and b

$$\begin{aligned} a &= \frac{(-0.0002Mc^4 + 0.0039Mc^3 - 0.0262Mc^2 + 0.6179Mc + 0.4699)}{(1+Mc)^{0.75}} \\ &= \frac{(-0.0002 \times 0.170519^4 + 0.0039 \times 0.170519^3 - 0.0262 \times 0.170519^2 + 0.6179 \times 0.170519 + 0.4699)}{(1+0.170519)^{0.75}} \\ &= 0.510531 \end{aligned}$$

$$\begin{aligned} b &= \frac{(0.00009Mc^4 - 0.0018Mc^3 + 0.0117Mc^2 + 0.2771Mc + 0.3433)}{1+Mc} \\ &= \frac{(0.00009 \times 0.170519^4 - 0.0018 \times 0.170519^3 + 0.0117 \times 0.170519^2 + 0.2771 \times 0.170519 + 0.3433)}{1+0.170519} \\ &= 0.333939 \end{aligned}$$

(5) Evaluation of the wall similarity temperature gradient

$$\left(-\frac{\partial\theta(\eta, Mc_{x,f})}{\partial\eta}\right)_{\eta=0} = aPr_f^b = 0.510531 \times 9.3^{0.333685} = 1.074460$$

(6) Evaluation of average Nusselt number (defined by $\overline{Nu}_{x,f} = \frac{\overline{\alpha}_{x,f} \cdot x}{\lambda_f}$)

$$\begin{aligned}\overline{Nu}_{x,f} &= 2\left(\frac{1}{2}Re_{x,f}\right)^{1/2}\left(-\frac{\partial\theta(\eta, Mc_{x,f})}{\partial\eta}\right)_{\eta=0} \\ &= 2\left(\frac{1}{2}\times 7694.7\right)^{1/2}\times 1.074460 \\ &= 133.29\end{aligned}$$

Then,

$$\begin{aligned}Q_x &= \overline{\alpha}_x(t_w - t_\infty)\times x \times s \\ &= \overline{Nu}_{x,f}\frac{\lambda_f}{x}(t_w - t_\infty)\times x \times s \\ &= \overline{Nu}_{x,f}\cdot\lambda_f(t_w - t_\infty)\times s \\ &= 133.29\times 0.586\times(20-0)\times 0.1 \\ &= 156.2\,\mathrm{W}\end{aligned}$$

6.5.2 Question 2

All geometric and physical conditions in Question 1 are kept except t_w = 40 °C. Suppose the mixed convection is laminar, please calculate the mixed convection heat transfer on the plate.

Solution:

(1) Heat transfer analysis is the same as that in the above solution.
(2) Data of some water's physical properties

The average temperature $t_f = (0+40)/2 = 20\ ^\circ\mathrm{C}$.

From appendix, the related physical properties of water can be obtained as below:

$$\begin{aligned}&\nu_f = 1.0033\times 10^{-6}\,\mathrm{m^2/s}, \quad Pr_f = 6.96, \quad \lambda_f = 0.602\,\mathrm{W/(m\ ^\circ C)}, \\ &\beta_f = 2.09\times 10^{-4}/\mathrm{K}\end{aligned}$$

(3) Evaluation of the physical parameters $Re_{x,f}$, $Gr_{x,f}$ and $Mc_{x,f}$

$$Re_{x,f} = \frac{w_{x,\infty}x}{v_f} = 0.1\,\text{m/s} \times 0.10\,\text{m}/(1.0033 \times 10^{-6}\,\text{m}^2/\text{s}) = 9967.1$$

$$Gr_{x,f} = \frac{g\beta(t_w - t_\infty)x^3}{v_f^2} = \frac{9.8 \times (2.09 \times 10^{-4})(40-0) \times 0.1^3}{(1.0033 \times 10^{-6})^2} = 81389940$$

$$Mc_{x,f} = Gr_{x,f}Re_{x,f}^{-2} = 81389940/(9967.1)^2 = 0.819281$$

(4) Evaluation of a and b

$$\begin{aligned} a &= \frac{(-0.0002Mc^4 + 0.0039Mc^3 - 0.0262Mc^2 + 0.6179Mc + 0.4699)}{(1+Mc)^{0.75}} \\ &= \frac{(-0.0002 \times 0.819281^4 + 0.0039 \times 0.819281^3 - 0.0262 \times 0.819281^2 + 0.6179 \times 0.819281 + 0.4699)}{(1+0.819281)^{0.75}} \\ &= 0.614165 \end{aligned}$$

$$\begin{aligned} b &= \frac{(0.00009Mc^4 - 0.0018Mc^3 + 0.0117Mc^2 + 0.2771Mc + 0.3433)}{1+Mc} \\ &= \frac{(0.00009 \times 0.819281^4 - 0.0018 \times 0.819281^3 + 0.0117 \times 0.819281^2 + 0.2771 \times 0.819281 + 0.3433)}{1+0.819281} \\ &= 0.317283 \end{aligned}$$

(5) Evaluation of the wall similarity temperature gradient

$$\left(-\frac{\partial\theta(\eta, Mc_{x,f})}{\partial\eta}\right)_{\eta=0} = aPr_f^b = 0.614165 \times 6.96^{0.317283} = 1.136660$$

(6) Evaluation of average Nusselt number (defined by $\overline{Nu}_{x,f} = \frac{\overline{\alpha}_{x,f} \cdot x}{\lambda_f}$)

$$\begin{aligned}\overline{Nu}_{x,f} &= 2\left(\frac{1}{2}Re_{x,f}\right)^{1/2}\left(-\frac{\partial\theta(\eta, Mc_{x,f})}{\partial\eta}\right)_{\eta=0} \\ &= 2\left(\frac{1}{2}\times 9967.1\right)^{1/2}\times 1.136660 \\ &= 160.48\end{aligned}$$

Then,

$$\begin{aligned}Q_x &= \overline{\alpha}_x(t_w - t_\infty)\times x \times s \\ &= \overline{Nu}_{x,f}\frac{\lambda_f}{x}(t_w - t_\infty)\times x \times s \\ &= \overline{Nu}_{x,f}\cdot\lambda_f(t_w - t_\infty)\times s \\ &= 160.48\times 0.602\times(40-0)\times 0.1 \\ &= 386.4W\end{aligned}$$

6.5.3 Question 3

All geometric and physical conditions in Question 1 are kept except t_w = 40 °C and t_∞ = 20 °C. Suppose the mixed convection is laminar, please calculate the mixed convection heat transfer on the plate.

Solution:

(1) Heat transfer analysis is same as that in the above solution.
(2) Data of some water's physical properties.

The average temperature $t_f = (40+20)/2 = 30$ °C.

From appendix, the related physical properties of water can be obtained as below:

$$\begin{aligned}&v_f = 0.8004\times 10^{-6}\,\mathrm{m^2/s}, \quad Pr_f = 5.4, \quad \lambda_f = 0.617\ \mathrm{W/(m\,^\circ C)}, \\ &\beta_f = 3.05\times 10^{-4}/\mathrm{K}\end{aligned}$$

(3) Evaluation of the physical parameters $Re_{x,f}, Gr_{x,f}$ and $Mc_{x,f}$

$$Re_{x,f} = \frac{w_{x,\infty}x}{v_f} = 0.1\ \text{m/s} \times 0.10\ \text{m}/(0.8004 \times 10^{-6}\ \text{m}^2/\text{s}) = 12493.75$$

$$Gr_{x,f} = \frac{g\beta(t_w - t_\infty)x^3}{v_f^2} = \frac{9.8 \times (3.05 \times 10^{-4})(40 - 20) \times 0.1^3}{(0.8004 \times 10^{-6})^2} = 93312914$$

$$Mc_{x,f} = Gr_{x,f}Re_{x,f}^{-2} = 93312914/(12493.75)^2 = 0.5978$$

(4) Evaluation of a and b

$$\begin{aligned} a &= \frac{(-0.0002Mc^4 + 0.0039Mc^3 - 0.0262Mc^2 + 0.6179Mc + 0.4699)}{(1+Mc)^{0.75}} \\ &= \frac{(-0.0002 \times 0.5978^4 + 0.0039 \times 0.5978^3 - 0.0262 \times 0.5978^2 + 0.6179 \times 0.5978 + 0.4699)}{(1+0.5978)^{0.75}} \\ &= 0.5853 \end{aligned}$$

$$\begin{aligned} b &= \frac{(0.00009Mc^4 - 0.0018Mc^3 + 0.0117Mc^2 + 0.2771Mc + 0.3433)}{1+Mc} \\ &= \frac{(0.00009 \times 0.5978^4 - 0.0018 \times 0.5978^3 + 0.0117 \times 0.5978^2 + 0.2771 \times 0.5978 + 0.3433)}{1+0.5978} \\ &= 0.320915 \end{aligned}$$

(5) Evaluation of wall similarity temperature gradient

$$\left(-\frac{\partial\theta(\eta, Mc_{x,f})}{\partial\eta}\right)_{\eta=0} = aPr_f^b = 0.5853 \times 5.4^{0.320915} = 1.005575$$

(6) Evaluation of average Nusselt number (defined by $\overline{Nu}_{x,f} = \frac{\overline{\alpha}_{x,f} \cdot x}{\lambda_f}$)

$$\begin{aligned} \overline{Nu}_{x,f} &= 2\left(\frac{1}{2}Re_{x,f}\right)^{1/2}\left(-\frac{\partial\theta(\eta, Mc_{x,f})}{\partial\eta}\right)_{\eta=0} \\ &= 2\left(\frac{1}{2} \times 12493.75\right)^{1/2} \times 1.005575 \\ &= 158.96 \end{aligned}$$

Then,

$$\begin{aligned} Q_x &= \overline{\alpha}_x(t_w - t_\infty) \times x \times s \\ &= \overline{Nu}_{x,f}\frac{\lambda_f}{x}(t_w - t_\infty) \times x \times s \\ &= \overline{Nu}_{x,f} \cdot \lambda_f(t_w - t_\infty) \times s \\ &= 158.96 \times 0.617 \times (40 - 20) \times 0.1 \\ &= 196.16\,\mathrm{W} \end{aligned}$$

6.6 Remarks

In this work, the temperature fields of laminar mixed convection on a vertical flat plate are calculated in the wide range of average Prandtl number $(0.3 \leq Pr_f \leq 20)$ and mixed convection parameter $(0 \leq Mc_{x,f} \leq 10)$. It is seen that with increasing the average Prandtl number, the temperature profiles will be steeper and steeper, and the temperature boundary layer thickness will decrease monotonically. Meanwhile, with increasing the mixed convection parameter $Mc_{x,f}$, the temperature profiles will be steeper and steeper too, due to effect of increasing buoyancy force. However, the steepening trend of temperature profiles will be weaker and weaker with increasing the Prandtl number or mixed convection parameter.

The theoretical equations of Nusselt number are reported based on the innovative similarity transformation model. Since the wall similarity temperature gradient is the only one un-known variable of the Nusselt number theoretical equations, accurately prediction of the wall temperature gradient is the key work to achieve optimal prediction of Nusselt number. Then, optimal formulated equations of wall temperature gradient of laminar mixed convection on a vertical flat plate are obtained by using optimal curve-fitting approach based on the system of numerical solutions of the wall temperature gradient. The theoretical equations of Nusselt number of laminar mixed convection combined with the optimal formalized equations of the wall similarity temperature gradient become the optimal equations of Nusselt number of laminar mixed convection on a vertical flat plate.

References

1. Shang, D.Y.: Theory of Heat Transfer with Forced Convection Film Flows. Springer, Berlin (2011)
2. Pohlhausen, E.: Der Warmeaustausch zwischen festen Korpern und Flussigkeiten mit kleiner Reiburg und kleiner Warmeleitung. Z. Angew. Math. Mech. *1*, 115–121 (1921)

Part III
Heat Transfer for Consideration of Coupled Effect of Variable Physical Properties

Chapter 7
Pseudo-Similarity Transformation of Governing Partial Differential Equations

Abstract The governing partial differential equations of laminar mixed convection with consideration of variable physical properties are equivalently transformed into the similarity governing partial differential equations by our innovative similarity transformation model. Due to our previous study, the pseudo-similarity transformation will be very coincident to the related partial-similarity transformation for the calculation results of convection heat transfer. Therefore, a pseudo-similarity transformation can be performed for the similarity transformation of mixed convection. The similarity transformation model for forced convection is taken as main model for coincidence of forced boundary conditions. Meanwhile, Grashof number is induced for treatment of free convection characteristics. In this similarity transformation, the velocity similarity variables are taken as the core similarity variables. They have definite physical meanings, and can lead to a better advantage for treating the physical properties factors compared with those of Falkner-Skan transformation. In addition, by taking water mixed convection as an example, a polynomial model is induced for treatment of the coupled effect of liquid variable physical properties, so that the transformed governing similarity mathematical models have their theoretical and practical value.

Keywords Pseudo-similarity transformation · Innovative similarity transformation · Similarity variables · Polynomial model · Treatment of variable physical properties · Theoretical equation of physical property factor · Mixed convection

7.1 Introduction

In Part 1, we reported the pseudo-similarity model of laminar mathematical model of mixed convection with consideration of Boussinesq approximation. Although the mixed convection issue does not meet the complete similarity transformation, according to our study in [1, 2], the pseudo-similarity transformation is very well equivalent to the related partial-similarity transformation for convection heat transfer calculation of Newtonian fluids. It is the reason that we perform the pseudo-similarity transformation for similarity transformation of the governing partial differential equations of mixed convection, instead of the partial-similarity

D.-Y. Shang and L.-C. Zhong, *Heat Transfer of Laminar Mixed Convection of Liquid*, Heat and Mass Transfer, DOI 10.1007/978-3-319-27959-6_7

transformation for the similarity transformation. On this basis in this part, the hydrodynamics and heat transfer analysis and calculation with consideration of variable physical properties will be further conducted. At first in this present chapter, we will focus on derivation of the related mathematical similarity model with consideration of variable physical properties. Through the pseudo-similarity transformation, it can be seen that our similarity transformation model is very conveniently applied for similarity transformation of mixed convection issue with consideration of variable physical properties.

7.2 Governing Partial Differential Equations

According to Chap. 2, Eqs. (7.1)–(7.3) can be taken as governing partial differential equations of the laminar mixed convection boundary layer with consideration of variable physical properties:

$$\frac{\partial}{\partial x}(\rho w_x) + \frac{\partial}{\partial y}(\rho w_y) = 0 \tag{7.1}$$

$$\rho\left(w_x \frac{\partial w_x}{\partial x} + w_y \frac{\partial w_x}{\partial y}\right) = \frac{\partial}{\partial y}\left(\mu \frac{\partial w_x}{\partial y}\right) + g(\rho_\infty - \rho) \tag{7.2}$$

$$\rho\left[w_x \frac{\partial (c_p t)}{\partial x} + w_y \frac{\partial (c_p t)}{\partial y}\right] = \frac{\partial}{\partial y}\left(\lambda \frac{\partial t}{\partial y}\right) \tag{7.3}$$

with the boundary conditions

$$y = 0: \quad w_x = 0, \quad w_y = 0, \quad t = t_w, \tag{7.4}$$

$$y \to \infty: \quad w_x = w_{x,\infty}(\text{constant}), \quad t = t_\infty \tag{7.5}$$

Here, temperature-dependent physical properties density ρ, absolute viscosity μ, thermal conductivity λ, and specific heat c_p are taken into account.

7.3 Similarity Variables for Pseudo-Similarity Transformation

Because the boundary conditions are attributed to those of forced convection, we selected the similarity transformation model of forced convection [3] for coincidence of the forced convection boundary conditions. However, this similarity transformation model is not coincident to the transformation with buoyancy, i.e. the mixed convection issue does not meet the complete similarity transformation. According to our study in [1, 2] for heat transfer of Newtonian fluid convection

flow, the pseudo-similarity transformation is very well equivalent to the partial-similarity transformation. On the other hand, the core similarity variables will be always those for transformation of the velocity field, and are set up as below according to our innovative similarity transformation for forced convection [3] and model derived in Chap. 3.

$$W_x(\eta) = \frac{w_x}{w_{x,\infty}} \tag{7.6}$$

$$W_y(\eta) = \frac{w_y}{w_{x,\infty}} \left(\frac{1}{2} Re_{x,\infty}\right)^{1/2} \tag{7.7}$$

where similarity velocity variables $W_x(\eta)$ and $W_y(\eta)$ are defined as core similarity of velocity field. While, η and $Re_{x,\infty}$ are similarity coordinate variable and local Reynolds number respectively. They are defined as below respectively:

$$\eta = \frac{y}{x} \left(\frac{1}{2} Re_{x,\infty}\right)^{1/2} \tag{7.8}$$

$$Re_{x,\infty} = \frac{w_{x,\infty} x}{v_\infty} \tag{7.9}$$

where v_∞ is local kinetic viscosity. Meanwhile it is necessary to induce local Grashof number as below for description of buoyancy action:

$$Gr_{x,\infty} = \frac{g(\rho_\infty/\rho_w - 1)x^3}{v_\infty^2} \tag{7.10}$$

where ρ_∞ and ρ_w are local densities respectively.

Finally, the temperature similarity variable is induced as

$$\theta(\eta) = \frac{t - t_\infty}{t_w - t_\infty} \tag{7.11}$$

Here, it is seen that in the equations of above similarity variables, all variables of physical properties are local in order to consider variable physical properties.

It is emphasized that the similarity variables $W_x(\eta)$ and $W_y(\eta)$ are core similarity variables of the similarity transformation, responsible for the similarity transformation of velocity field. Then, it is expected that they will dominate the transformed governing ordinary differential equations.

7.4 Pseudo-Similarity Transformation of the Governing Partial Differential Equations

With Eqs. (7.6)–(7.11) with the dimensionless similarity variables η, $Re_{x,\infty}$, $W_x(\eta)$, $W_y(\eta)$, $Gr_{x,\infty}$ and $\theta(\eta, x)$, the governing partial differential equations (7.1)–(7.3) are transformed as below respectively.

7.4.1 Transformation of Eq. (7.1)

Equation (7.1) is changed to the following form

$$\rho\frac{\partial w_x}{\partial x}+\rho\frac{\partial w_y}{\partial y}+w_x\frac{\partial \rho}{\partial x}+w_y\frac{\partial \rho}{\partial y}=0 \tag{7.1a}$$

With Eq. (7.6) we have

$$\frac{\partial w_x}{\partial x}=w_{x,\infty}\frac{dW_x(\eta)}{d\eta}\frac{\partial \eta}{\partial x}$$

where with Eq. (7.8) we have

$$\frac{\partial \eta}{\partial x}=-\frac{1}{2}\eta x^{-1} \tag{a}$$

Then,

$$\frac{\partial w_x}{\partial x}=-\frac{1}{2}\eta x^{-1}w_{x,\infty}\frac{dW_x(\eta)}{d\eta} \tag{b}$$

With (7.7) we have

$$\frac{\partial w_y}{\partial y}=w_{x,\infty}\left(\frac{1}{2}Re_{x,\infty}\right)^{-1/2}\frac{dW_y(\eta)}{d\eta}\frac{\partial \eta}{\partial y}$$

where

$$\frac{\partial \eta}{\partial y}=x^{-1}\left(\frac{1}{2}Re_{x,\infty}\right)^{1/2} \tag{c}$$

Then,

$$\frac{\partial w_y}{\partial y} = w_{x,\infty} \frac{dW_y(\eta)}{d\eta} x^{-1} \tag{d}$$

In addition,

$$\frac{\partial \rho}{\partial x} = \frac{d\rho}{d\eta}\frac{\partial \eta}{\partial x} = -\frac{1}{2}\frac{d\rho}{d\eta}\eta x^{-1} \tag{e}$$

$$\frac{\partial \rho}{\partial y} = \frac{d\rho}{d\eta}\frac{\partial \eta}{\partial y} = \frac{d\rho}{d\eta} x^{-1}\left(\frac{1}{2}Re_{x,\infty}\right)^{1/2} \tag{f}$$

With Eqs.(a)–(f), Eq. (7.1a) is changed to

$$\rho\left[-\frac{1}{2}\eta x^{-1} w_{x,\infty}\frac{dW_x(\eta)}{d\eta} + w_{x,\infty}\frac{dW_y(\eta)}{d\eta}x^{-1}\right] - \frac{1}{2}\frac{d\rho}{d\eta}\eta x^{-1} w_{x,\infty} W_x(\eta) + \frac{d\rho}{d\eta}x^{-1}\left(\frac{1}{2}Re_{x,\infty}\right)^{1/2} w_{x,\infty}\left(\frac{1}{2}Re_{x,\infty}\right)^{-1/2} W_y(\eta) = 0$$

The above equation is divided by $\frac{1}{2}x^{-1}w_{x,\infty}$, and we have

$$\rho\left[-\eta\frac{dW_x(\eta)}{d\eta} + 2\frac{dW_y(\eta)}{d\eta}\right] - \frac{d\rho}{d\eta}\eta \cdot W_x(\eta, x) + 2\frac{d\rho}{d\eta}W_y(\eta) = 0$$

The above equation is simplified to

$$-\eta\frac{dW_x(\eta)}{d\eta} + 2\frac{dW_y(\eta)}{d\eta} + \frac{1}{\rho}\frac{d\rho}{d\eta}[-\eta \cdot W_x(\eta) + 2W_y(\eta)] = 0 \tag{7.11}$$

7.4.2 Transformation of Eq. (7.2)

Equation (7.2) is changed to

$$\rho\left(w_x\frac{\partial w_x}{\partial x} + w_y\frac{\partial w_x}{\partial y}\right) = \mu\frac{\partial^2 w_x}{\partial y^2} + \frac{\partial \mu}{\partial y}\frac{\partial w_x}{\partial y} + g(\rho_\infty - \rho) \tag{7.2a}$$

With Eq. (7.6) we have

$$\frac{\partial w_x}{\partial y} = w_{x,\infty}\frac{dW_x(\eta)}{d\eta}\frac{\partial \eta}{\partial y}$$

Then,

$$\frac{\partial w_x}{\partial y} = w_{x,\infty} \frac{dW_x(\eta)}{d\eta} x^{-1} \left(\frac{1}{2} Re_{x,\infty}\right)^{1/2} \tag{g}$$

and

$$\frac{\partial^2 w_x}{\partial y^2} = w_{x,\infty} \frac{d^2 W_x(\eta)}{d\eta^2} x^{-1} \left(\frac{1}{2} Re_{x,\infty}\right)^{1/2} \frac{\partial \eta}{\partial y}$$

i.e.

$$\frac{\partial^2 w_x}{\partial y^2} = w_{x,\infty} \frac{d^2 W_x(\eta)}{d\eta^2} x^{-2} \left(\frac{1}{2} Re_{x,\infty}\right) \tag{h}$$

Additionally,

$$\frac{\partial \mu}{\partial y} = \frac{d\mu}{d\eta} x^{-1} \left(\frac{1}{2} Re_{x,\infty}\right)^{1/2} \tag{i}$$

With Eqs. (g)–(i), Eq. (7.2a) is changed to

$$\begin{aligned}
&\rho \Bigg[-w_{x,\infty} W_x(\eta) \frac{1}{2} \eta x^{-1} w_{x,\infty} \frac{dW_x(\eta)}{d\eta} \\
&\quad + w_{x,\infty} \left(\frac{1}{2} Re_{x,\infty}\right)^{-1/2} W_y(\eta) \cdot w_{x,\infty} \frac{dW_x(\eta)}{d\eta} x^{-1} \left(\frac{1}{2} Re_{x,\infty}\right)^{1/2} \Bigg] \\
&\quad - g(\rho_\infty - \rho) = \mu w_{x,\infty} \frac{d^2 W_x(\eta)}{d\eta^2} x^{-2} \left(\frac{1}{2} Re_{x,\infty}\right) \\
&\quad + \frac{d\mu}{d\eta} x^{-1} \left(\frac{1}{2} Re_{x,\infty}\right)^{1/2} w_{x,\infty} \frac{dW_x(\eta)}{d\eta} x^{-1} \left(\frac{1}{2} Re_{x,\infty}\right)^{1/2}
\end{aligned}$$

The above equation is divided by $\frac{1}{2}$, and simplified to

$$\begin{aligned}
&\rho \Bigg[-w_{x,\infty} W_x(\eta) \cdot \eta x^{-1} w_{x,\infty} \frac{dW_x(\eta)}{d\eta} \\
&\quad + 2 w_{x,\infty} W_y(\eta) \cdot w_{x,\infty} \frac{dW_x(\eta)}{d\eta} x^{-1} \Bigg] \\
&\quad - 2g(\rho_\infty - \rho) = \mu w_{x,\infty} \frac{d^2 W_x(\eta)}{d\eta^2} x^{-2} (Re_{x,\infty}) \\
&\quad + \frac{\partial \mu}{d\eta} x^{-1} (Re_{x,\infty}) w_{x,\infty} \frac{dW_x(\eta)}{d\eta} x^{-1}
\end{aligned}$$

With definition of the local Reynolds number, the above equation is changed to

$$\begin{aligned}
&\rho\Bigg[-w_{x,\infty}W_x(\eta)\cdot\eta x^{-1}w_{x,\infty}\frac{dW_x(\eta)}{d\eta}\\
&\quad+2w_{x,\infty}W_y(\eta)\cdot w_{x,\infty}\frac{dW_x(\eta)}{d\eta}x^{-1}\Bigg]\\
&-2g(\rho_\infty-\rho)=\mu w_{x,\infty}\frac{d^2W_x(\eta)}{d\eta^2}x^{-2}\left(\frac{w_{x,\infty}x}{v_\infty}\right)\\
&+\frac{d\mu}{d\eta}x^{-1}\left(\frac{w_{x,\infty}x}{v_\infty}\right)w_{x,\infty}\frac{dW_x(\eta)}{d\eta}x^{-1}
\end{aligned}$$

The above equation is divided by $x^{-1}w_{x,\infty}^2\frac{\mu}{v_\infty}$, and simplified to

$$\begin{aligned}
&\frac{v_\infty}{v}\left(-\eta W_x(\eta)+2W_y(\eta)\right)\frac{dW_x(\eta)}{d\eta}\\
&\quad=\frac{d^2W_x(\eta)}{d\eta^2}+\frac{1}{\mu}\frac{d\mu}{d\eta}\frac{dW_x(\eta)}{d\eta}+\frac{v_\infty}{\mu}\frac{2g(\rho_\infty-\rho)x}{w_{x,\infty}^2}
\end{aligned}$$

i.e.

$$\begin{aligned}
&\frac{v_\infty}{v}\left(-\eta W_x(\eta)+2W_y(\eta)\right)\frac{dW_x(\eta)}{d\eta}\\
&\quad=\frac{d^2W_x(\eta)}{d\eta^2}+\frac{1}{\mu}\frac{d\mu}{d\eta}\frac{dW_x(\eta)}{d\eta}+2\frac{v_\infty}{v}\cdot\frac{\frac{\rho_\infty}{\rho}-1}{\frac{\rho_\infty}{\rho_w}-1}\cdot\frac{g\left(\frac{\rho_\infty-\rho_w}{\rho_w}\right)x^3}{v_\infty^2}\cdot\frac{v_\infty^2}{w_{x,\infty}^2x^2}
\end{aligned}$$

or

$$\begin{aligned}
&\frac{v_\infty}{v}\left(-\eta W_x(\eta)+2W_y(\eta)\right)\frac{dW_x(\eta)}{d\eta}\\
&\quad=\frac{d^2W_x(\eta)}{d\eta^2}+\frac{1}{\mu}\frac{d\mu}{d\eta}\frac{dW_x(\eta)}{d\eta}+2\frac{v_\infty}{v}\cdot\frac{\frac{\rho_\infty}{\rho}-1}{\frac{\rho_\infty}{\rho_w}-1}\cdot Gr_{x,\infty}\cdot Re_{x,\infty}^{-2}
\end{aligned}$$

The above equation can be rewritten as

$$\begin{aligned}
&\frac{v_\infty}{v}\left(-\eta W_x(\eta)+2W_y(\eta)\right)\frac{dW_x(\eta)}{d\eta}\\
&\quad=\frac{d^2W_x(\eta)}{d\eta^2}+\frac{1}{\mu}\frac{d\mu}{d\eta}\frac{dW_x(\eta)}{d\eta}+2\frac{v_\infty}{v}\cdot\frac{\frac{\rho_\infty}{\rho}-1}{\frac{\rho_\infty}{\rho_w}-1}\cdot Mc_{x,\infty}
\end{aligned}\tag{7.12}$$

where

$$Mc_{x,\infty} = Gr_{x,\infty} \cdot Re_{x,\infty}^{-2} \tag{j}$$

is defined as local mixed convection parameter.

7.4.3 Transformation of Eq. (7.3)

Equation (7.3) is changed to

$$\rho\left(w_x c_p \frac{\partial t}{\partial x} + w_x t \frac{\partial c_p}{\partial x} + w_y c_p \frac{\partial t}{\partial y} + w_y t \frac{\partial c_p}{\partial y}\right) = \lambda \frac{\partial^2 t}{\partial y^2} + \frac{\partial \lambda}{\partial y}\frac{\partial t}{\partial y} \tag{7.3a}$$

where

$$\begin{aligned} \frac{\partial t}{\partial x} &= (t_w - t_\infty)\frac{d\theta(\eta)}{d\eta}\frac{\partial \eta}{\partial x} \\ &= (t_w - t_\infty)\frac{d\theta(\eta)}{d\eta}\left(-\frac{1}{2}\eta x^{-1}\right) \\ &= -\frac{1}{2}\eta x^{-1}(t_w - t_\infty)\frac{d\theta(\eta)}{d\eta} \end{aligned} \tag{k}$$

While,

$$\begin{aligned} \frac{\partial t}{\partial y} &= (t_w - t_\infty)\frac{d\theta(\eta)}{d\eta}\frac{\partial \eta}{\partial y} \\ &= (t_w - t_\infty)\frac{d\theta(\eta)}{d\eta}x^{-1}\left(\frac{1}{2}Re_{x,\infty}\right)^{1/2} \\ &= x^{-1}\left(\frac{1}{2}Re_{x,\infty}\right)^{1/2}(t_w - t_\infty)\frac{d\theta(\eta)}{d\eta} \end{aligned} \tag{l}$$

$$\frac{\partial^2 t}{\partial y^2} = x^{-2}\left(\frac{1}{2}Re_{x,\infty}\right)(t_w - t_\infty)\frac{d^2\theta(\eta)}{d\eta^2} \tag{m}$$

In addition,

$$\frac{\partial c_p}{\partial x} = -\frac{1}{2}\frac{dc_p}{d\eta}\eta x^{-1} \tag{n}$$

Similar to Eq. (f), we have

$$\frac{\partial \lambda}{\partial y} = \frac{d\lambda}{d\eta} x^{-1} \left(\frac{1}{2} Re_{x,\infty}\right)^{1/2} \tag{o}$$

$$\frac{\partial c_p}{\partial y} = \frac{dc_p}{d\eta} x^{-1} \left(\frac{1}{2} Re_{x,\infty}\right)^{1/2} \tag{p}$$

With above equation, Eq. (7.3a) is changed to

$$\begin{aligned}
&\rho \left[w_{x,\infty} W_x(\eta) c_p \left(-\frac{1}{2} \eta x^{-1} (t_w - t_\infty) \frac{d\theta(\eta)}{d\eta} \right) + w_{x,\infty} W_x(\eta) t \left(-\frac{1}{2} \eta x^{-1} \frac{dc_p}{d\eta} \right) \right. \\
&\quad + w_{x,\infty} \left(\frac{1}{2} Re_{x,\infty}\right)^{-1/2} W_y(\eta) c_p x^{-1} \left(\frac{1}{2} Re_{x,\infty}\right)^{1/2} (t_w - t_\infty) \frac{d\theta(\eta)}{d\eta} \\
&\quad \left. + w_{x,\infty} \left(\frac{1}{2} Re_{x,\infty}\right)^{-1/2} W_y(\eta) t \frac{dc_p}{d\eta} x^{-1} \left(\frac{1}{2} Re_{x,\infty}\right)^{1/2} \right] \\
&= \lambda x^{-2} \left(\frac{1}{2} Re_{x,\infty}\right) (t_w - t_\infty) \frac{d^2\theta(\eta)}{d\eta^2} \\
&\quad + \frac{d\lambda}{d\eta} x^{-1} \left(\frac{1}{2} Re_{x,\infty}\right)^{1/2} x^{-1} \left(\frac{1}{2} Re_{x,\infty}\right)^{1/2} (t_w - t_\infty) \frac{d\theta(\eta)}{d\eta}
\end{aligned}$$

The above equation is simplified to

$$\begin{aligned}
&\rho \left[w_{x,\infty} W_x(\eta) c_p \left(-\frac{1}{2} \eta x^{-1} (t_w - t_\infty) \frac{d\theta(\eta)}{d\eta} \right) + w_{x,\infty} W_x(\eta) t \left(-\frac{1}{2} \eta x^{-1} \frac{dc_p}{d\eta} \right) \right. \\
&\quad \left. + w_{x,\infty} W_y(\eta) c_p x^{-1} (t_w - t_\infty) \frac{d\theta(\eta)}{d\eta} + w_{x,\infty} W_y(\eta) t \frac{dc_p}{d\eta} x^{-1} \right] \\
&= \lambda x^{-2} \left(\frac{1}{2} Re_{x,\infty}\right) (t_w - t_\infty) \frac{d^2\theta(\eta)}{d\eta^2} \\
&\quad + \frac{d\lambda}{d\eta} x^{-1} \left(\frac{1}{2} Re_{x,\infty}\right) x^{-1} (t_w - t_\infty) \frac{d\theta(\eta)}{d\eta}
\end{aligned}$$

With definition of $Re_{x,\infty}$, the above equation is changed to

$$\rho\left[w_{x,\infty}W_x(\eta)c_p\left(-\frac{1}{2}\eta x^{-1}(t_w-t_\infty)\frac{d\theta(\eta)}{d\eta}\right)+w_{x,\infty}W_x(\eta)t\left(-\frac{1}{2}\eta x^{-1}\frac{dc_p}{d\eta}\right)\right.$$
$$\left.+w_{x,\infty}W_y(\eta)c_p x^{-1}(t_w-t_\infty)\frac{d\theta(\eta)}{d\eta}+w_{x,\infty}W_y(\eta)t\frac{dc_p}{d\eta}x^{-1}\right]$$
$$=\lambda x^{-2}\left(\frac{1}{2}\frac{w_{x,\infty}x}{v_\infty}\right)(t_w-t_\infty)\frac{d^2\theta(\eta)}{d\eta^2}$$
$$+\frac{d\lambda}{d\eta}x^{-1}\left(\frac{1}{2}\frac{w_{x,\infty}x}{v_\infty}\right)x^{-1}(t_w-t_\infty)\frac{d\theta(\eta)}{d\eta}$$

The above equation is divided by $\frac{1}{2}(t_w-t_\infty)\frac{c_p w_{x,\infty}\lambda}{xv_\infty}$, and changed to

$$\frac{\rho v_\infty}{\lambda}\left[W_x(\eta)\left(-\eta\frac{d\theta(\eta)}{d\eta}\right)+W_x(\eta)\frac{t}{t_w-t_\infty}\left(-\eta\frac{1}{c_p}\frac{dc_p}{d\eta}\right)+2W_y(\eta)\frac{d\theta(\eta)}{d\eta}\right.$$
$$\left.+2W_y(\eta)\frac{t}{t_w-t_\infty}\frac{1}{c_p}\frac{dc_p}{d\eta}\right]=\frac{1}{c_p}\frac{d^2\theta(\eta)}{d\eta^2}+\frac{1}{c_p}\frac{1}{\lambda}\frac{d\lambda}{d\eta}\frac{d\theta(\eta)}{d\eta} \tag{7.3b}$$

where

$$\frac{t}{t_w-t_\infty}=\frac{t-t_\infty+t_\infty}{t_w-t_\infty}=\frac{t-t_\infty}{t_w-t_\infty}+\frac{t_\infty}{t_w-t_\infty}=\theta(\eta,x)+\frac{t_\infty}{t_w-t_\infty} \tag{q}$$

Then, Eq. (7.3b) is changed to

$$\frac{\rho v_\infty}{\lambda}\left[W_x(\eta)\left(-\eta\frac{d\theta(\eta)}{d\eta}\right)+W_x(\eta)\left(\theta+\frac{t_\infty}{t_w-t_\infty}\right)\left(-\eta\frac{1}{c_p}\frac{dc_p}{d\eta}\right)+2W_y(\eta)\frac{d\theta(\eta)}{d\eta}\right.$$
$$\left.+2W_y(\eta)\left(\theta+\frac{t_\infty}{t_w-t_\infty}\right)\frac{1}{c_p}\frac{dc_p}{d\eta}\right]=\frac{1}{c_p}\frac{d^2\theta(\eta)}{d\eta^2}+\frac{1}{c_p}\frac{1}{\lambda}\frac{d\lambda}{d\eta}\frac{d\theta(\eta)}{d\eta}$$

or

$$Pr\frac{\lambda}{\mu c_p}c_p\frac{\rho v_\infty}{\lambda}\left[-\eta W_x(\eta)\frac{d\theta(\eta)}{d\eta}-\eta W_x(\eta)\left(\theta(\eta)+\frac{t_\infty}{t_w-t_\infty}\right)\frac{1}{c_p}\frac{dc_p}{d\eta}\right.$$
$$\left.+2W_y(\eta)\frac{d\theta(\eta)}{d\eta}+2W_y(\eta)\left(\theta(\eta)+\frac{t_\infty}{t_w-t_\infty}\right)\frac{1}{c_p}\frac{dc_p}{d\eta}\right]$$
$$=\frac{d^2\theta(\eta)}{d\eta^2}+\frac{1}{\lambda}\frac{d\lambda}{d\eta}\frac{d\theta(\eta)}{d\eta}$$

The above equation is further changed to

$$Pr\frac{v_\infty}{v}\left[-\eta W_x(\eta)\frac{d\theta(\eta)}{d\eta}+2W_y(\eta)\frac{d\theta(\eta)}{d\eta}-\eta W_x(\eta)\left(\theta(\eta)+\frac{t_\infty}{t_w-t_\infty}\right)\frac{1}{c_p}\frac{dc_p}{d\eta}\right.$$
$$\left.+2W_y(\eta)\left(\theta(\eta)+\frac{t_\infty}{t_w-t_\infty}\right)\frac{1}{c_p}\frac{dc_p}{d\eta}\right]$$
$$=\frac{d^2\theta(\eta)}{d\eta^2}+\frac{1}{\lambda}\frac{d\lambda}{d\eta}\frac{d\theta(\eta)}{d\eta}$$

i.e.

$$Pr\frac{v_\infty}{v}\left[(-\eta W_x(\eta)+2W_y(\eta))\frac{d\theta(\eta)}{d\eta}+(-\eta W_x(\eta)+2W_y(\eta))(\theta(\eta)\right.$$
$$\left.+\frac{t_\infty}{t_w-t_\infty})\frac{1}{c_p}\frac{dc_p}{d\eta}\right]=\frac{d^2\theta(\eta)}{d\eta^2}+\frac{1}{\lambda}\frac{d\lambda}{d\eta}\frac{d\theta(\eta)}{d\eta} \tag{7.13}$$

For summary, governing partial differential equations (7.1)–(7.3) have been transformed to the following governing ordinary differential equations:

$$-\eta\frac{dW_x(\eta)}{d\eta}+2\frac{dW_y(\eta)}{d\eta}+\frac{1}{\rho}\frac{d\rho}{d\eta}[-\eta\cdot W_x(\eta)+2W_y(\eta)]=0 \tag{7.11}$$

$$\frac{v_\infty}{v}(-\eta W_x(\eta)+2W_y(\eta))\frac{dW_x(\eta)}{d\eta}$$
$$=\frac{d^2W_x(\eta)}{d\eta^2}+\frac{1}{\mu}\frac{d\mu}{d\eta}\frac{dW_x(\eta)}{d\eta}+2\frac{v_\infty}{v}\cdot\frac{\frac{\rho_\infty}{\rho}-1}{\frac{\rho_\infty}{\rho_w}-1}\cdot Mc_{x,\infty} \tag{7.12}$$

where

$$Mc_{x,\infty}=Gr_{x,\infty}\cdot Re_{x,\infty}^{-2} \tag{j}$$

$$Pr\frac{v_\infty}{v}\left[(-\eta W_x(\eta)+2W_y(\eta))\frac{d\theta(\eta)}{d\eta}+(-\eta W_x(\eta)+2W_y(\eta))(\theta(\eta)\right.$$
$$\left.+\frac{t_\infty}{t_w-t_\infty})\frac{1}{c_p}\frac{dc_p}{d\eta}\right]=\frac{d^2\theta(\eta)}{d\eta^2}+\frac{1}{\lambda}\frac{d\lambda}{d\eta}\frac{d\theta(\eta)}{d\eta} \tag{7.13}$$

with the boundary condition equations

$$\eta=0:\quad W_x(\eta)=0,\quad W_y(\eta)=0,\quad \theta(\eta)=1 \tag{7.14}$$

$$\eta\to\infty:\quad W_x(\eta)=1,\quad \theta(\eta)=0 \tag{7.15}$$

7.5 Equivalently Rewriting the Transformed Governing Ordinary Differential Equations

From the defined equation of the local mixed convection parameter $Mc_{x,\infty}$, it is seen that the independent coordinate variable x is included in it, which is caused by using the pseudo-similarity transformation. From the transformed governing Eqs. (7.11)–(7.15), it is found that the coordinate variable x exists in the transformed governing equations in form of the local mixed convection parameter $Mc_{x,\infty}$. Then, the local mixed parameter $Mc_{x,\infty}$ is reasonably taken as the second independent similarity coordinate variable. In this case, the transformed governing ordinary differential equations (7.11)–(7.15) are equivalent to the following ones respectively

$$\begin{aligned} &-\eta\frac{dW_x(\eta,Mc_{x,\infty})}{d\eta}+2\frac{dW_y(\eta,Mc_{x,\infty})}{d\eta}\\ &\quad+\frac{1}{\rho}\frac{d\rho}{d\eta}\left[-\eta\cdot W_x(\eta,Mc_{x,\infty})+2W_y(\eta,Mc_{x,\infty})\right]=0 \end{aligned} \tag{7.11*}$$

$$\begin{aligned} &\frac{v_\infty}{v}\left(-\eta W_x(\eta,Mc_{x,\infty})+2W_y(\eta,Mc_{x,\infty})\right)\frac{dW_x(\eta,Mc_{x,\infty})}{d\eta}\\ &=\frac{d^2W_x(\eta,Mc_{x,\infty})}{d\eta^2}+\frac{1}{\mu}\frac{d\mu}{d\eta}\frac{dW_x(\eta,Mc_{x,\infty})}{d\eta}+2\frac{v_\infty}{v}\cdot\frac{\frac{\rho_\infty}{\rho}-1}{\frac{\rho_\infty}{\rho_w}-1}\cdot Mc_{x,\infty} \end{aligned} \tag{7.12*}$$

$$\begin{aligned} &Pr\frac{v_\infty}{v}\left[\left(-\eta W_x(\eta,Mc_{x,\infty})+2W_y(\eta,Mc_{x,\infty})\right)\frac{d\theta(\eta,Mc_{x,\infty})}{d\eta}+\left(-\eta W_x(\eta,Mc_{x,\infty})\right.\right.\\ &\qquad\left.\left.+2W_y(\eta,Mc_{x,\infty})\right)\left(\theta(\eta,Mc_{x,\infty})+\frac{t_\infty}{t_w-t_\infty}\right)\frac{1}{c_p}\frac{dc_p}{d\eta}\right]\\ &=\frac{d^2\theta(\eta,Mc_{x,\infty})}{d\eta^2}+\frac{1}{\lambda}\frac{d\lambda}{d\eta}\frac{d\theta(\eta,Mc_{x,\infty})}{d\eta} \end{aligned} \tag{7.13*}$$

with the boundary condition equations

$$\eta=0:\quad W_x(\eta,Mc_{x,\infty})=0,\quad W_y(\eta,Mc_{x,\infty})=0,\quad \theta(\eta,Mc_{x,\infty})=1 \tag{7.14*}$$

$$\eta\to\infty:\quad W_x(\eta,Mc_{x,\infty})=1,\quad \theta(\eta,Mc_{x,\infty})=0 \tag{7.15*}$$

7.6 Physical Property Factors

It is found in the similarity governing partial differential equations (7.11*)–(7.13*) of laminar mixed convection that the fluid physical properties density ρ, absolute

viscosity μ, thermal conductivity λ and specific heat c_p exist in the form of the related physical property factors $\frac{1}{\rho}\frac{d\rho}{d\eta}$, $\frac{1}{\mu}\frac{d\mu}{d\eta}$, $\frac{1}{\lambda}\frac{d\lambda}{d\eta}$, $\frac{1}{c_p}\frac{dc_p}{d\eta}$ respectively. Since these physical properties are temperature-dependent, their physical property factors $\frac{1}{\rho}\frac{d\rho}{d\eta}$, $\frac{1}{\mu}\frac{d\mu}{d\eta}$, $\frac{1}{\lambda}\frac{d\lambda}{d\eta}$, $\frac{1}{c_p}\frac{dc_p}{d\eta}$ are temperature-dependent, too. For consideration of the coupled effect of variable physical properties on fluid flow and heat transfer of laminar mixed convection, we have to treat carefully temperature-dependence of these physical property factors. It is the necessary work to ensure the practical value of research result of fluid flow and heat transfer of laminar mixed convection.

7.7 Treatment of Variable Physical Properties

7.7.1 Models of Temperature-Dependent Properties of Water

Our treatment method of variable physical properties was already reported in [2, 3] for liquid, gas and vapour-gas mixture respectively. Here, we only introduce the treatment of liquid physical properties. Although there could be different models for consideration of liquid variable physical properties, according to our study, the polynomial model is more convenient one for treatment of the variable physical properties of liquids for extensive investigation of convection heat transfer. Take water for an example, the following polynomial equations are suggested for the temperature-dependent expressions of density and thermal conductivity with the temperature range between 0 and 100 °C:

$$\rho = -4.48 \times 10^{-3} t^2 + 999.9 \tag{7.16}$$

$$\lambda = -8.01 \times 10^{-6} t^2 + 1.94 \times 10^{-3} t + 0.563 \tag{7.17}$$

For the absolute viscosity of water, the following expression is applied:

$$\mu = 10^{-3} \exp\left[-1.6004 - \frac{1152.7}{T} + \left(\frac{689.58}{T}\right)^2\right] \tag{7.18}$$

It can be verified that the above correlations are coincident well to their typical experiment values for water physical properties.

In addition, for a lot of liquid including water, the specific heat varies very little with temperature, and can be regarded as constant with temperature.

7.7.2 Models of Physical Property Factors of Water

Taking water as an example, the above temperature-dependent *physical properties factors* are described as

Transformation for density factor $\frac{1}{\rho}\frac{d\rho}{d\eta}$

At first, the *density factor* $\frac{1}{\rho}\frac{d\rho}{d\eta}$ is expressed as

$$\frac{1}{\rho}\frac{d\rho}{d\eta} = \frac{1}{\rho}\frac{d\rho}{dt}\frac{dt}{d\eta}$$

With Eq. (7.16) the following equation is obtained

$$\frac{d\rho}{dt} = -2 \times 4.48 \times 10^{-3} t$$

With Eq. (7.11) we obtain

$$\frac{dt}{d\eta} = (t_s - t_\infty)\frac{d\theta}{d\eta}$$

Therefore,

$$\frac{1}{\rho}\frac{d\rho}{d\eta} = \frac{1}{\rho}(-2 \times 4.48 \times 10^{-3} t)(t_w - t_\infty)\frac{d\theta}{d\eta}$$

Then,

$$\frac{1}{\rho}\frac{d\rho}{d\eta} = \frac{(-2 \times 4.48 \times 10^{-3} t)(t_w - t_\infty)}{-4.48 \times 10^{-3} t^2 + 999.9} \cdot \frac{d\theta}{d\eta} \tag{7.19}$$

This is the theoretical equation of density factor for water.

Transformation for viscosity factor $\frac{1}{\mu}\frac{d\mu}{d\eta}$

With (7.18) the viscosity factor can be expressed as

$$\begin{aligned}\frac{1}{\mu}\frac{d\mu}{d\eta} &= \frac{1}{\mu}\frac{d}{d\eta}\left\{\exp\left[-1.6004 - \frac{1152.7}{T} + \left(\frac{689.58}{T}\right)^2\right] \times 10^{-3}\right\} \\ &= \frac{\mu}{\mu}\left[\frac{1152.7}{T^2} - 2 \times \frac{689.58^2}{T^3}\right]\frac{dT}{d\eta}\end{aligned}$$

where

$$\frac{dT}{d\eta} = (T_w - T_\infty)\frac{d\theta}{d\eta}$$

Then,

$$\frac{1}{\mu}\frac{d\mu}{d\eta} = \left(\frac{1152.7}{T^2} - 2 \times \frac{689.58^2}{T^3}\right)(T_w - T_\infty)\frac{d\theta}{d\eta} \tag{7.20}$$

This is the theoretical equation of viscosity factor for water.

Transformation for thermal conductivity factor $\frac{1}{\lambda}\frac{d\lambda}{d\eta}$

With Eq. (7.17) the thermal conductivity factor becomes

$$\frac{1}{\lambda}\frac{d\lambda}{d\eta} = \frac{1}{\lambda}\frac{d}{d\eta}(-8.01 \times 10^{-6}t^2 + 1.94 \times 10^{-3}t + 0.563)$$

i.e.

$$\frac{1}{\lambda}\frac{d\lambda}{d\eta} = \frac{1}{\lambda}(-8.01 \times 2 \times 10^{-6}t + 1.94 \times 10^{-3})\frac{dt}{d\eta}$$

where

$$\frac{dt}{d\eta} = (t_w - t_\infty)\frac{d\theta}{d\eta}$$

Then,

$$\frac{1}{\lambda}\frac{d\lambda}{d\eta} = \frac{(-8.01 \times 2 \times 10^{-6}t + 1.94 \times 10^{-3})(t_w - t_\infty)}{-8.01 \times 10^{-6}t^2 + 1.94 \times 10^{-3}t + 0.563}\frac{d\theta}{d\eta} \tag{7.21}$$

This is the theoretical equation of thermal conductivity for water.

It is indicated that the variation of water specific heat is very small with temperature. Then water specific heat factor $\frac{1}{c_p}\frac{dc_p}{d\eta}$ can be regards as zero, and the deviation caused by such treatment will tend to zero.

7.8 Summary

It is the time to summarize the governing similarity equations of laminar mixed convection with consideration of coupled effect of variable physical properties in Table 7.1.

Table 7.1 Summary of the governing differential equations of laminar mixed convection with consideration of coupled effect of variable physical properties

Governing partial differential equations	
Mass equation	$\frac{\partial}{\partial x}(\rho w_x) + \frac{\partial}{\partial y}(\rho w_y) = 0$
Momentum equation	$\rho\left(w_x \frac{\partial w_x}{\partial x} + w_y \frac{\partial w_x}{\partial y}\right) = \frac{\partial}{\partial y}\left(\mu \frac{\partial w_x}{\partial y}\right) + g(\rho_\infty - \rho)$
Energy equation	$\rho\left[w_x \frac{\partial (c_p t)}{\partial x} + w_y \frac{\partial (c_p t)}{\partial y}\right] = \frac{\partial}{\partial y}\left(\lambda \frac{\partial t}{\partial y}\right)$
Boundary conditions	$y = 0$: $w_x = 0,\ w_y = 0,\ t = t_w;\ y \to \infty$: $w_x = w_{x,\infty},\ t = t_\infty$
Assumed similarity variables for pseudo-similarity transformation	
Core similarity variable for velocity field similarity transformation, $W_x(\eta)$	$w_x = w_{x,\infty} W_x(\eta)$
Core similarity variable for velocity field similarity transformation, $W(\eta)$	$w_y = w_{x,\infty} W_y(\eta)\left(\frac{1}{2} Re_{x,\infty}\right)^{-1/2}$
Coordinate variable η	$\eta = \frac{y}{x}\left(\frac{1}{2} Re_{x,\infty}\right)^{1/2}$
Average Reynolds number $Re_{x,\infty}$	$Re_{x,\infty} = \frac{w_{x,\infty} x}{\nu_\infty}$
Average Grashof number $Gr_{x,\infty}$	$Gr_{x,\infty} = \frac{g(\rho_\infty/\rho_w - 1)x^3}{\nu_\infty^2}$
Local mixed convection parameter $Mc_{x,\infty}$	$Mc_{x,\infty} = Gr_{x,\infty} \cdot Re_{x,\infty}^{-2}$
Temperature similarity variable $\theta(\eta)$	$\theta(\eta) = \frac{t - t_\infty}{t_w - t_\infty}$
Equivalent governing similarity ordinary differential equations	
Mass equation	$-\eta \frac{dW_x(\eta, Mc_{x,\infty})}{d\eta} + 2\frac{dW_y(\eta, Mc_{x,\infty})}{d\eta} + \frac{1}{\rho}\frac{d\rho}{d\eta}[-\eta \cdot W_x(\eta, Mc_{x,\infty}) + 2W_y(\eta, Mc_{x,\infty})] = 0$

(continued)

Table 7.1 (continued)

Momentum equation	$\frac{v_\infty}{v}(-\eta W_x(\eta, Mc_{x,\infty}) + 2W_y(\eta, Mc_{x,\infty}))\frac{dW_x(\eta, Mc_{x,\infty})}{d\eta}$ $= \frac{d^2 W_x(\eta, Mc_{x,\infty})}{d\eta^2} + \frac{1}{\mu}\frac{d\mu}{d\eta}\frac{dW_x(\eta, Mc_{x,\infty})}{d\eta} + 2\frac{v_\infty}{v}\cdot\frac{\frac{\rho_\infty}{\rho} - 1}{\frac{\rho_\infty}{\rho_w} - 1}\cdot Mc_{x,\infty}$
Energy equation	$Pr\frac{v_\infty}{v}\left[(-\eta W_x(\eta, Mc_{x,\infty}) + 2W_y(\eta, Mc_{x,\infty}))\frac{d\theta(\eta, Mc_{x,\infty})}{d\eta} + (-\eta W_x(\eta, Mc_{x,\infty}) + 2W_y(\eta, Mc_{x,\infty}))(\theta(\eta, Mc_{x,\infty}) + \frac{t_\infty}{t_w - t_\infty})\frac{1}{c_p}\frac{dc_p}{d\eta}\right]$ $= \frac{d^2\theta(\eta, Mc_{x,\infty})}{d\eta^2} + \frac{1}{\lambda}\frac{d\lambda}{d\eta}\frac{d\theta(\eta, Mc_{x,\infty})}{d\eta}$
Boundary conditions	$\eta = 0$: $W_x(\eta, Mc_{x,\infty}) = 0,\ W_y(\eta, Mc_{x,\infty}) = 0, \theta(\eta, Mc_{x,\infty}) = 1$ $\eta \to \infty$: $W_x(\eta, Mc_{x,\infty}) = 1,\ \theta(\eta, Mc_{x,\infty}) = 0$

7.9 Remarks

The complete governing similarity mathematical models of mixed convection with consideration of variable physical properties are derived out based on our innovative similarity transformation for forced convection [3]. Although the governing partial differential equations of mixed convection does not meet complete similarity transformation, according to our studies in ref. [1, 2], the pseudo-similarity transformation is very much equivalent to the partial similarity transformation for convection heat transfer of Newtonian fluids. Then pseudo-similarity transformation is used to treat similarity transformation of the present governing partial differential equations of laminar mixed convection.

In this similarity transformation of mixed convection, the similarity transformation model for forced convection is taken as main model for coincidence of forced boundary conditions. While, for treatment of the characteristics of free convection, the Grashof number is induced.

In the present similarity transformation, the similarity velocity variables for similarity transformation of velocity field are taken as the core similarity variables. Such similarity velocity variables have definite physical meanings, which leads to that the similarity governing partial differential equations become intuitive physical models compared with those produced by Falkner-Skan transformation. Meanwhile, our innovative similarity transformation model leads to that the transformed governing similarity mathematical models are organically combined with the physical properties factors, and then, provide convenient condition for treatment of variable physical properties and for simultaneous solution.

At last, the temperature-dependent physical properties of liquid are treated by the polynomial model reported in refs. [1, 2]. Although there could be different models for consideration of liquid variable physical properties, according to our study, the polynomial model is more convenient one for treatment of the variable physical properties of liquids for extensive investigation of convection heat transfer. Such treatment model of liquid variable physical properties ensures that the governing similarity mathematical models have their theoretical and practical application value.

References

1. Shang, D.Y., Gu, J.: Analyses of pseudo-similarity and boundary layer thickness for non-Newtonian falling film flow. Heat Mass Transf. **41**(1), 44–50 (2004)
2. Shang, D.Y.: Free Convection Film Flows and Heat Transfer—Models of Laminar Free Convection with Phase Change for Heat and Mass Transfer Analysis. Springer, Berlin (2013)
3. Shang, D.Y.: Theory of Heat Transfer with Forced Convection Film Flows. Springer, Berlin (2011)

Chapter 8
Velocity Fields

Abstract System of rigorous numerical solutions on velocity fields of laminar water mixed convection are obtained with consideration of coupled effect of variable physical properties. The similarity velocity field is obviously effected by the boundary temperatures t_w and t_∞. It demonstrates clearly also the influence of the variable physical properties. With increasing the local mixed convection parameter $Mc_{x,\infty}$, the level of velocity field will increase, and gradually form the more and more obvious parabola. It reflects the effect of buoyancy force on mixed convection. Since the coupled effect of variable physical properties are well considered in the governing mathematical models, the calculated results of the velocity fields have theoretical and practical values.

Keywords Velocity field · Numerical solution · Local Prandtl number · Local mixed convection parameter · Variable physical properties

8.1 Introduction

In Chap. 4, a system of the velocity field of mixed convection was reported with consideration of Boussinesq approximation, where dependent physical conditions are treated by the related average physical properties. In this chapter, the aim is to obtain calculated results of mixed convection with consideration of variable physical properties, and meanwhile, the related dependent physical properties are treated by the local physical properties. Because liquid and gas have different regulation on their physical property variations, in this book, we only investigate liquid mixed convection for consideration of variable physical properties, and take water mixed convection flow as an example. By using the complete similarity mathematical model derived out in the last Chapter for laminar mixed convection, where the variable physical properties are taken into account, the governing similarity mathematical model with the partial differential equations and the boundary

D.-Y. Shang and L.-C. Zhong, *Heat Transfer of Laminar Mixed Convection of Liquid*, Heat and Mass Transfer, DOI 10.1007/978-3-319-27959-6_8

conditions are solved in this Chapter. Laminar water mixed convection is taken as an example, and a system of numerical solutions of velocity field are obtained.

8.2 Dependent Variables and Ranges of the Numerical Solutions

The similarity governing partial differential equations (7.11*)–(7.13*) with the boundary condition Eqs. (7.14*) and (7.15*) combined with the physical property factor Eqs. (7.19)–(7.21) are solved by a shooting method with fifth-order Runge-Kutta integration. For solving the nonlinear problem, a variable mesh approach is applied to the numerical calculation programs. It can be seen that with consideration of variable physical properties, the solutions of the similarity velocity variables $W_x(\eta, Mc_{x,\infty})$ and $W_y(\eta, Mc_{x,\infty})$ and the similarity temperature variable $\theta(\eta, Mc_{x,\infty})$ are dependent on local mixed convection parameter $Mc_{x,\infty}$, wall temperature t_w (or local Prandtl number Pr_w), and bulk temperature t_∞ (local Prandtl number Pr_∞) for laminar mixed convection of liquid. For laminar water mixed convection, these ranges can be taken as $0 \le t_\infty \le 100$, $0 \le t_w \le 100$ and $0 \le Mc_{x,\infty} \le 10$.

8.3 Velocity Fields with Variation of Wall Temperature t_w

8.3.1 *For* $\mathbf{Mc_{x,\infty}} = 0$

Figure 8.1 expresses numerical solutions of velocity fields $W_x(\eta, Mc_{x,\infty})$ with variation of wall temperature t_w at $Mc_{x,\infty} = 0$ and different t_∞.

8.3.2 *For* $\mathbf{Mc_{x,\infty}} = 0.3$

Figure 8.2 expresses numerical solutions of velocity fields $W_x(\eta, Mc_{x,\infty})$ with variation of wall temperature t_w at $Mc_{x,\infty} = 0.3$ and different t_∞.

8.3.3 *For* $\mathbf{Mc_{x,\infty}} = 1$

Figure 8.3 expresses numerical solutions of velocity fields $W_x(\eta, Mc_{x,\infty})$ with variation of wall temperature t_w at $Mc_{x,\infty} = 1$ and different t_∞.

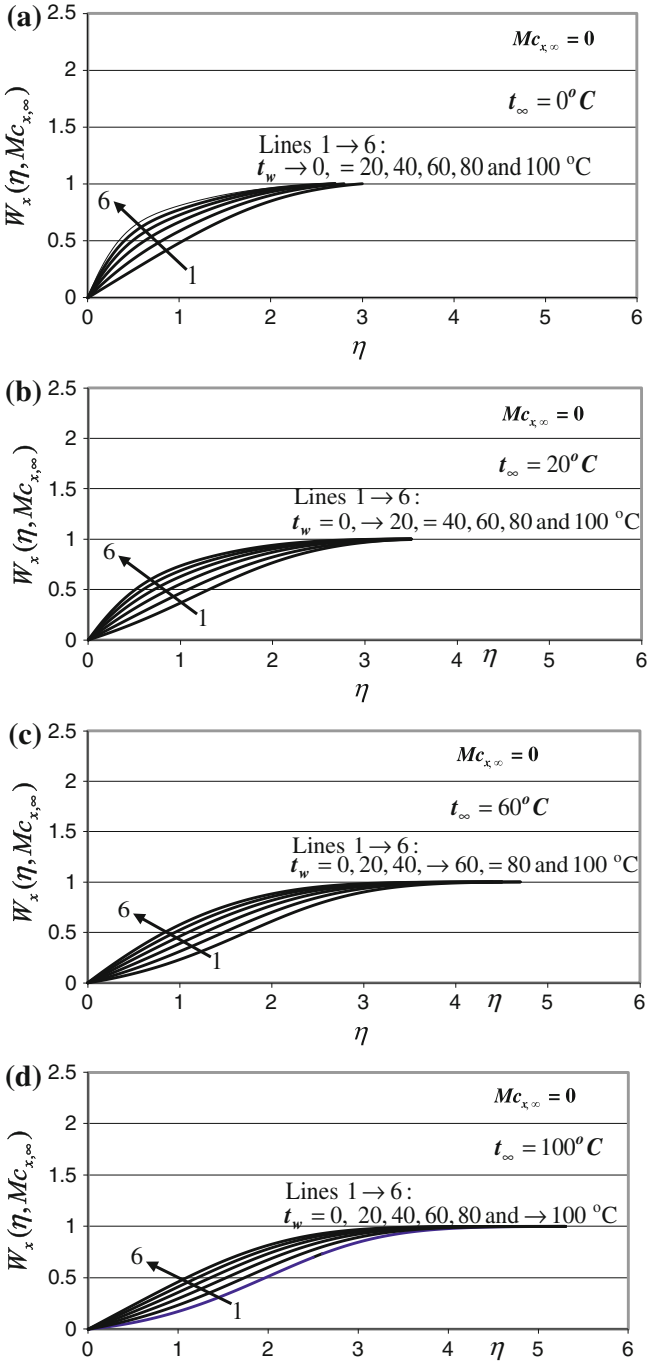

Fig. 8.1 Similarity velocity $W_x(\eta, Mc_{x,\infty})$ profiles of water mixed convection with variation of wall temperature t_w at $Mc_{x,\infty} = 0$ and different t_∞

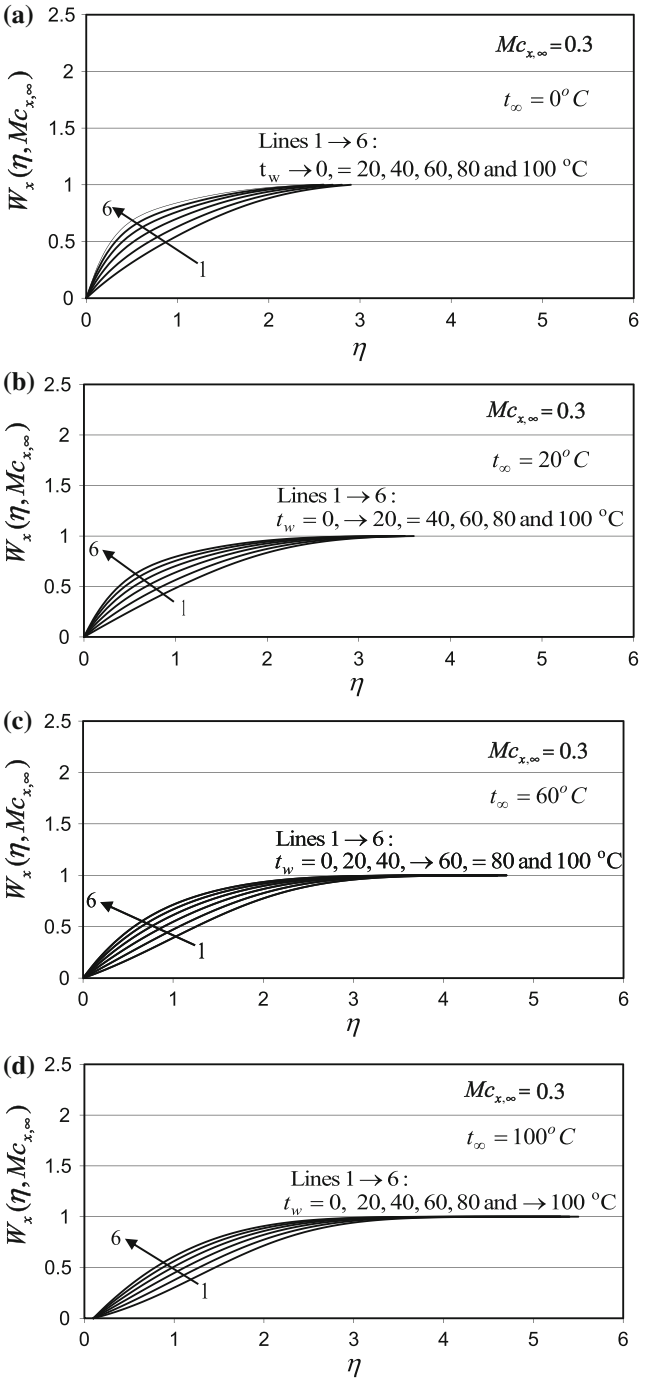

Fig. 8.2 Similarity velocity profiles of water mixed convection with variation of wall temperature t_w at $Mc_{x,\infty} = 0.3$ and different t_∞

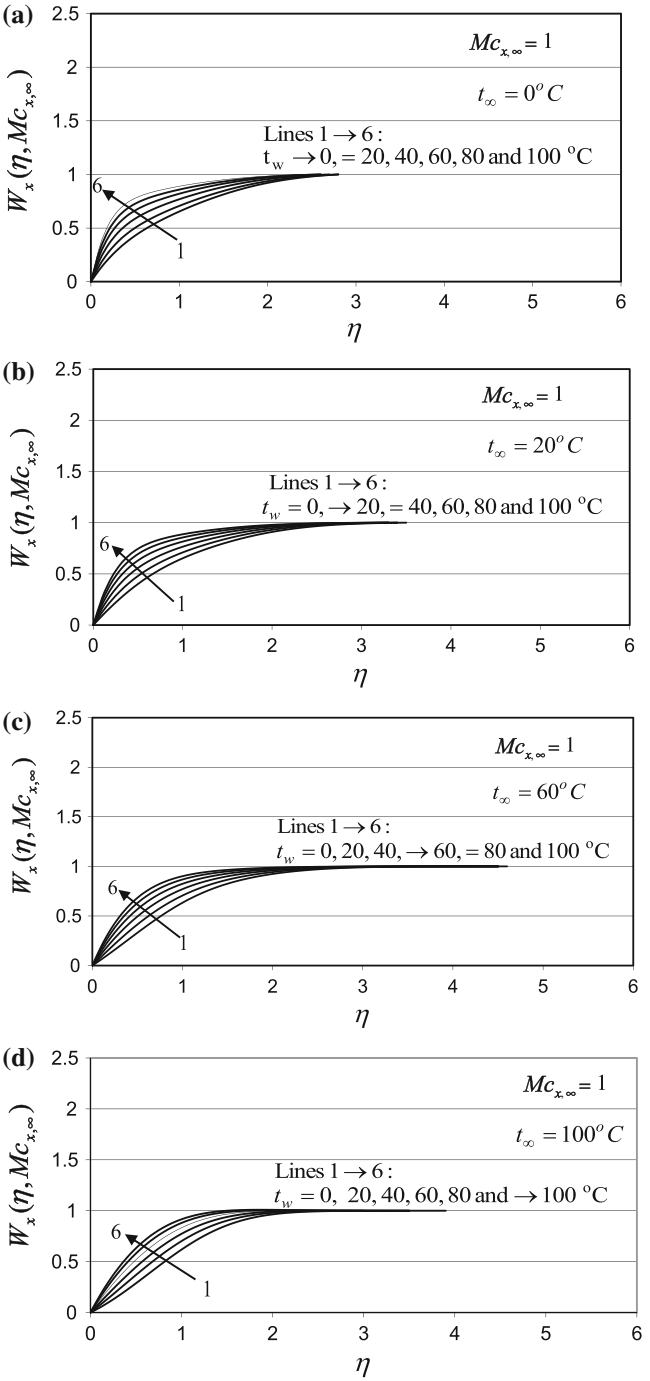

Fig. 8.3 Similarity velocity $W_x(\eta, Mc_{x,\infty})$ profiles of water mixed convection with variation of wall temperature t_w at $Mc_{x,\infty} = 1$ and different t_∞

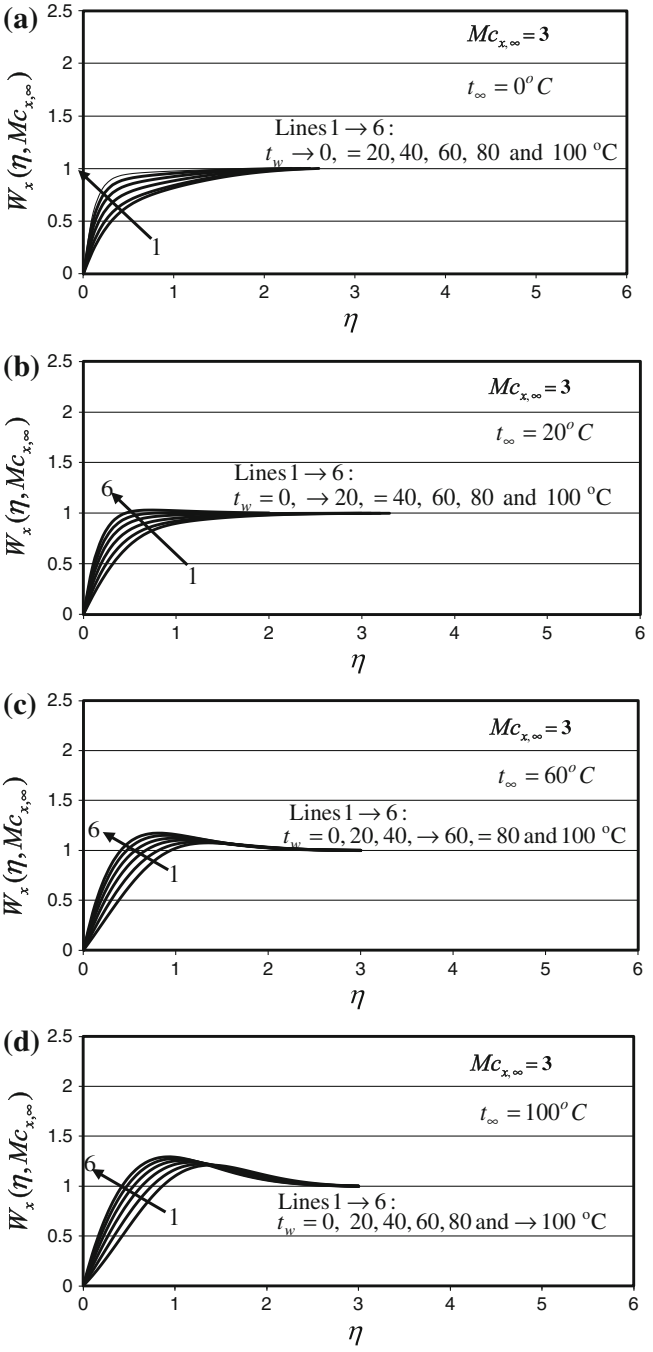

Fig. 8.4 Similarity velocity $W_x(\eta, Mc_{x,\infty})$ profiles of water mixed convection with variation of wall temperature t_w at $Mc_{x,\infty} = 3$ and different t_∞

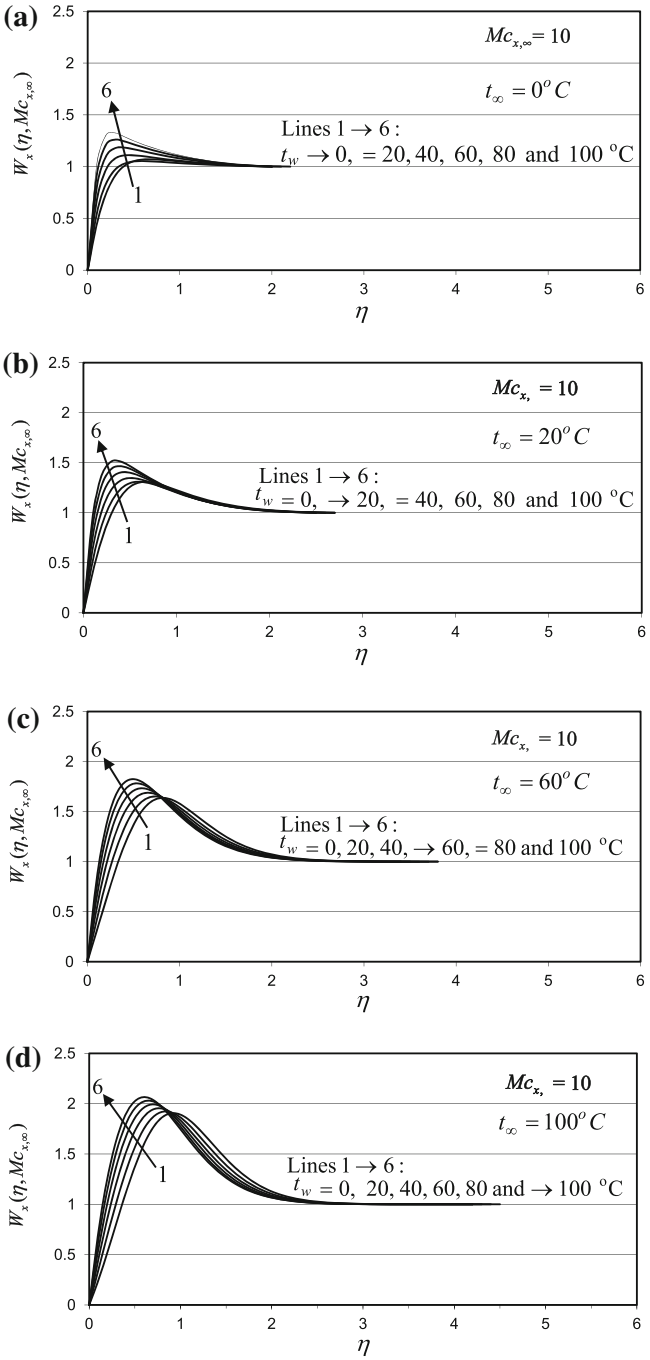

Fig. 8.5 Similarity velocity $W_x(\eta, Mc_{x,\infty})$ profiles of water mixed convection with variation of wall temperature t_w at $Mc_{x,\infty} = 10$ and different t_∞

8.3.4 *For* $\mathbf{Mc_{x,\infty}} = 3$

Figure 8.4 express numerical solutions of velocity fields $W_x(\eta, Mc_{x,\infty})$ with variation of wall temperature t_w at $Mc_{x,\infty}$ = 3 and different t_∞.

8.3.5 *For* $\mathbf{Mc_{x,\infty}} = 10$

Figure 8.5 expresses numerical solutions of velocity fields $W_x(\eta, Mc_{x,\infty})$ with variation of wall temperature t_w at $Mc_{x,\infty}$ = 10 and different t_∞.

8.4 Velocity Fields with Variation of Fluid Bulk Temperature

8.4.1 *For* $\mathbf{Mc_{x,\infty}} = 0$

Figure 8.6 expresses numerical solutions of velocity $W_x(\eta, Mc_{x,\infty})$ fields with variation of fluid bulk temperature t_∞ at $Mc_{x,\infty}$ = 0 and different t_w.

8.4.2 *For* $\mathbf{Mc_{x,\infty}} = 0.3$

Figure 8.7 expresses numerical solutions of velocity $W_x(\eta, Mc_{x,\infty})$ fields with variation of fluid bulk temperature t_∞ at $Mc_{x,\infty}$ = 0.3 and different t_w.

8.4.3 *For* $\mathbf{Mc_{x,\infty}} = 1$

Figure 8.8 expresses numerical solutions of velocity $W_x(\eta, Mc_{x,\infty})$ fields with variation of fluid bulk temperature t_∞ at $Mc_{x,\infty}$ = 1 and different t_w.

8.4.4 *For* $\mathbf{Mc_{x,\infty}} = 3$

Figure 8.9 expresses numerical solutions of velocity $W_x(\eta, Mc_{x,\infty})$ fields with variation of fluid bulk temperature t_∞ at $Mc_{x,\infty}$ = 3 and different t_w.

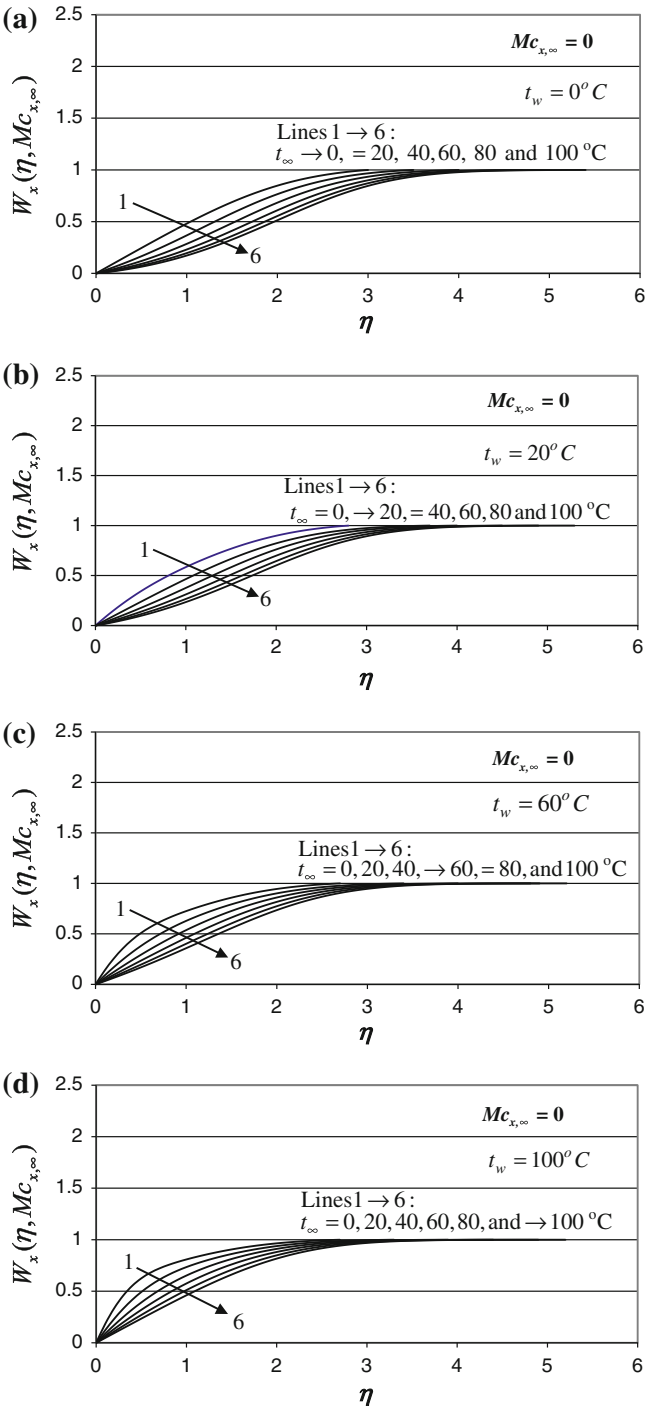

Fig. 8.6 Similarity velocity $W_x(\eta, Mc_{x,\infty})$ profiles of water mixed convection with variation of fluid bulk temperature t_∞ at $Mc_{x,\infty} = 0$ different t_w

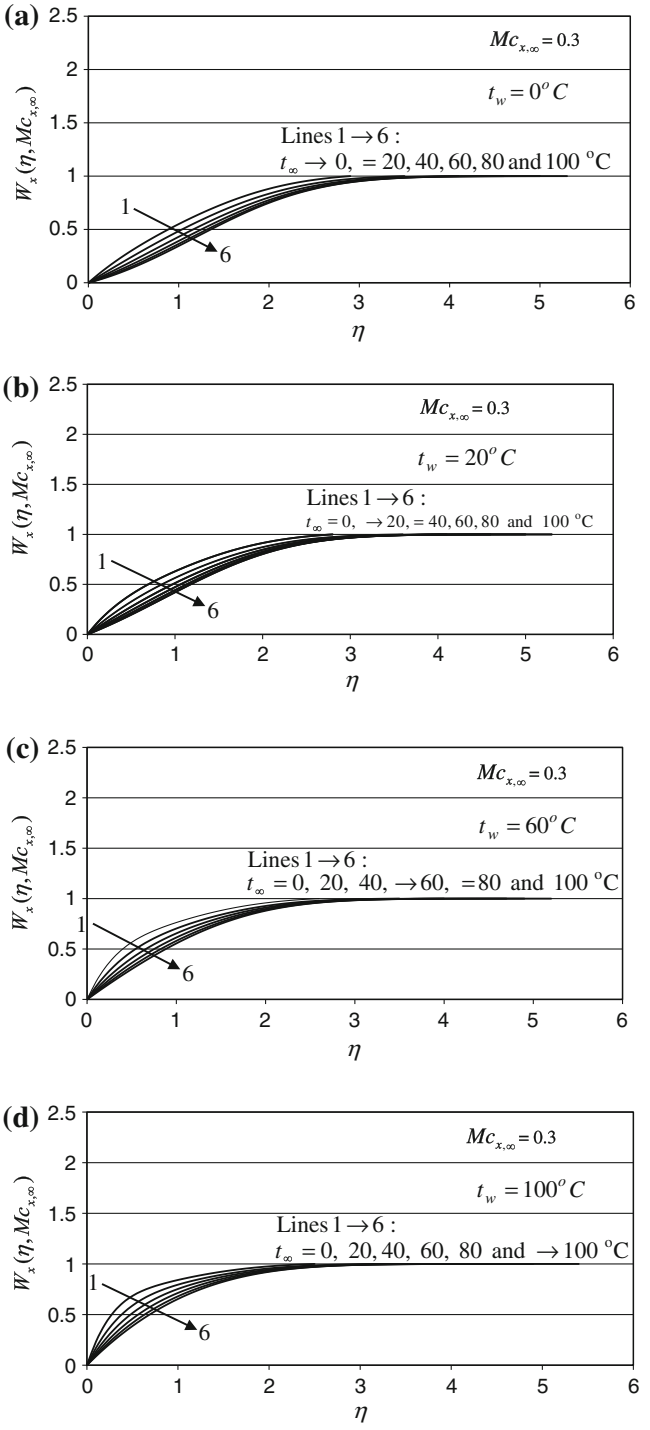

Fig. 8.7 Similarity velocity $W_x(\eta, Mc_{x,\infty})$ profiles of water mixed convection with variation of fluid bulk temperature t_∞ at $Mc_{x,\infty} = 0.3$ and different t_w

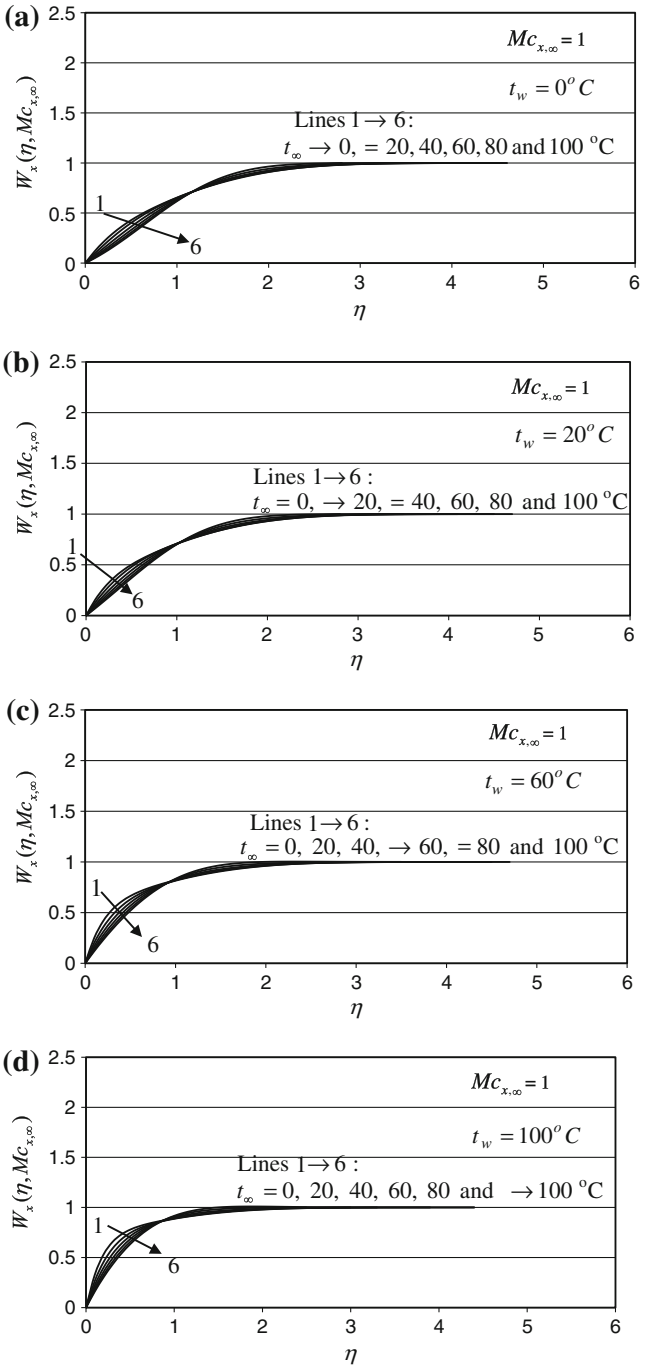

Fig. 8.8 Similarity velocity $W_x(\eta, Mc_{x,\infty})$ profiles of water mixed convection at with variation of fluid bulk temperature t_∞ $Mc_{x,\infty} = 1$ and different t_w

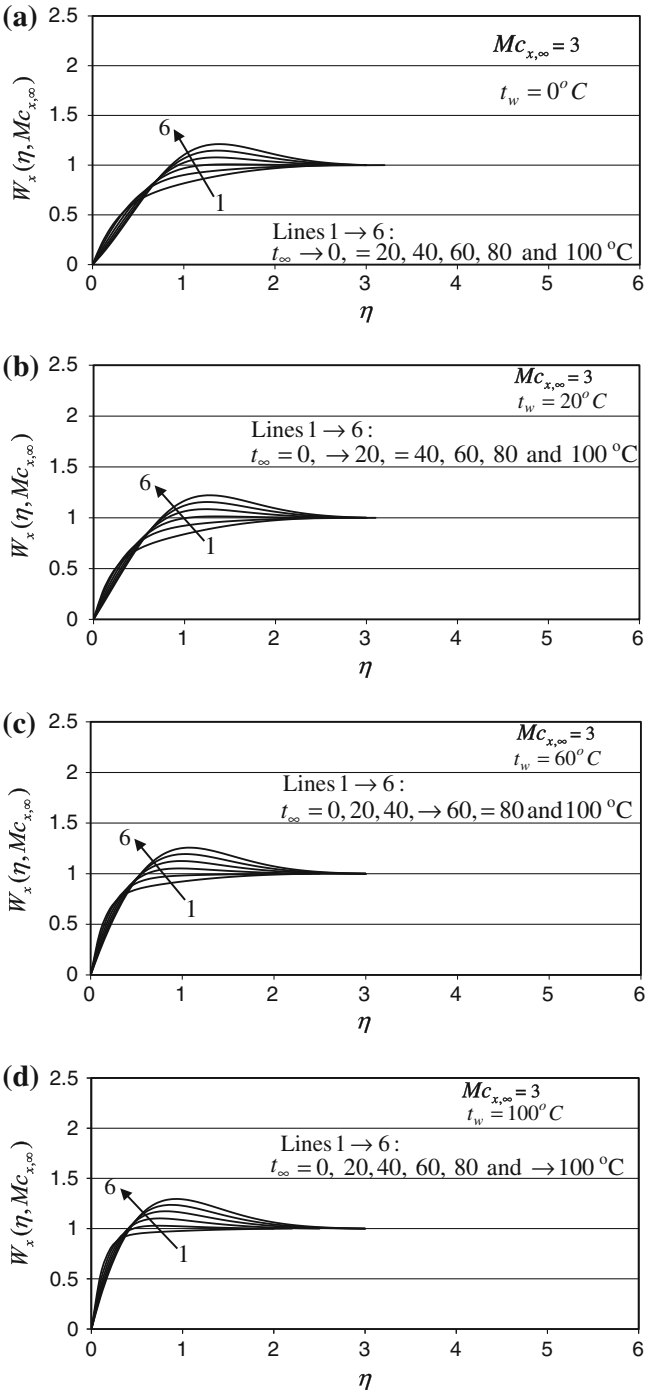

Fig. 8.9 Similarity velocity $W_x(\eta, Mc_{x,\infty})$ profiles of water mixed convection with variation of fluid bulk temperature t_∞ at $Mc_{x,\infty} = 3$ and different t_w

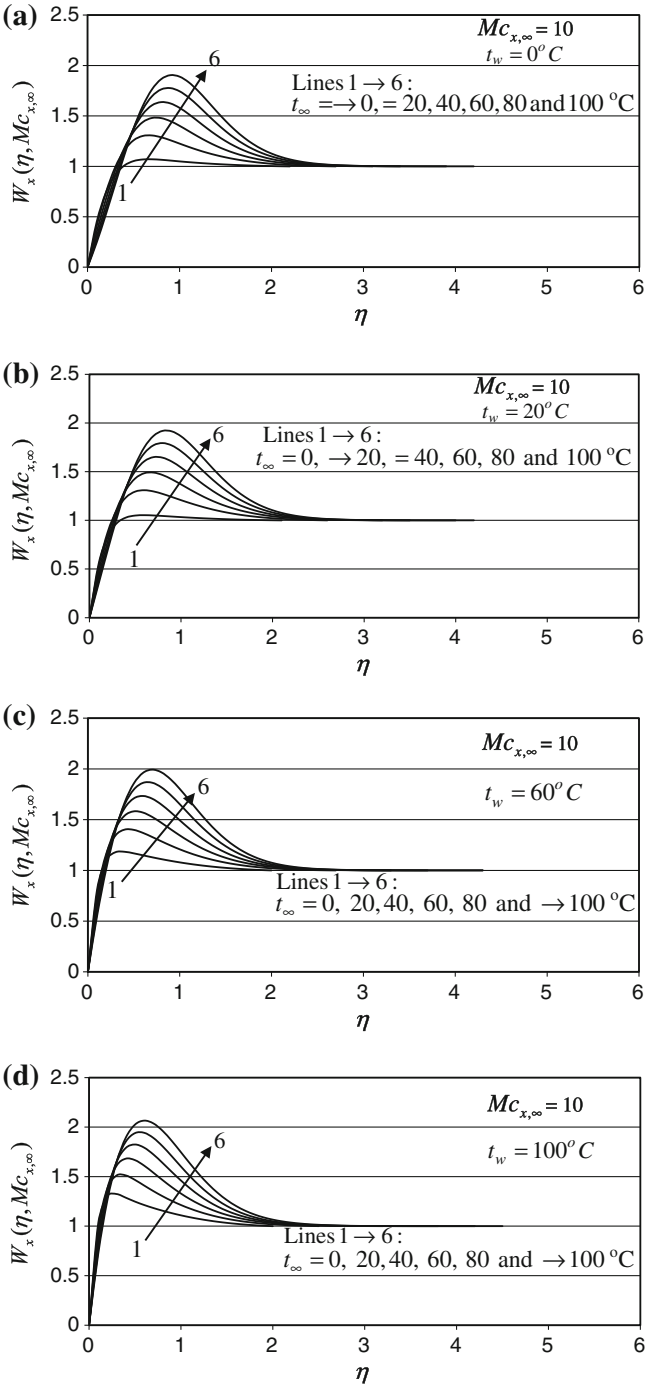

Fig. 8.10 Similarity velocity $W_x(\eta, Mc_{x,\infty})$ profiles of water mixed convection with variation of fluid bulk temperature t_∞ at $Mc_{x,\infty}$ = 10 and different t_w

8.4.5 *For* $\mathbf{Mc_{x,\infty}} = 10$

Figure 8.10 expresses numerical solutions of velocity $W_x(\eta, Mc_{x,\infty})$ fields with variation of fluid bulk temperature t_∞ at $Mc_{x,\infty}$ = 10 and different t_w.

From Figs. 8.1, 8.2, 8.3, 8.4, 8.5, 8.6, 8.7, 8.8, 8.9 and 8.10 on the variation of similarity velocity $W_x(\eta, Mc_{x,\infty})$ field, it is seen that with increasing the local mixed convection parameter $Mc_{x,\infty}$, the velocity profile will increase and gradually form a parabola, which reflects the increasing effect of free convection.

8.5 Remarks

In this chapter, a system of calculated results on similarity velocity fields of laminar water mixed convection are obtained with consideration of coupled effect of variable physical properties. The effect of the dependent physical variables on velocity fields is demonstrated clearly with variation of boundary temperature t_w and t_∞. Additionally, with increasing the local mixed convection parameter $Mc_{x,\infty}$, the level of velocity field will increase, and gradually form a parabola. It reflects the effect of buoyancy force. Since the coupled effect of variable physical properties are well considered in the governing mathematical models, the calculated results of the velocity fields have theoretical and practical values.

Chapter 9
Skin-Friction Coefficient

Abstract Skin-friction coefficient is analyzed with consideration of variable physical properties. The skin velocity gradient is the only one unknown variable for evaluation of the skin-friction coefficient. Systems of numerical solutions on the skin velocity gradient are obtained with consideration of variable physical properties. They have theoretical and practical value due to consideration of coupled effect of variable physical properties. The skin velocity gradient (or skin-friction coefficient) depends on local Prandtl numbers Pr_w and Pr_∞, as well as the local mixed convection parameter $Mc_{x,\infty}$. The former is used for demonstration of the effect of variable physical properties on velocity fields as well as skin-friction coefficient. The latter reflects the effect of buoyancy force. The skin velocity gradient will increase with increasing local Prandtl number Pr_∞ and will decrease with increasing local Prandtl number Pr_w. The skin velocity gradient will increase with increasing the local mixed convection parameter. On the other hand, with increasing the local mixed convection parameter, the effect of the local Prandtl numbers Pr_w and Pr_∞ on the skin velocity gradient will be stranger and stranger.

Keywords Skin velocity gradient · Skin-friction coefficient · Local Prandtl number · Local mixed convection parameter · Variable physical properties

9.1 Introduction

In Chap. 3 the skin friction coefficient under Boussinesq approximation has been analyzed by means of our innovative similarity transformation, and the following equations are obtained for expression of the local skin-friction coefficient $C_{f,x}$ and average skin friction coefficient $\overline{C}_{x,f}$:

D.-Y. Shang and L.-C. Zhong, *Heat Transfer of Laminar Mixed Convection of Liquid*, Heat and Mass Transfer, DOI 10.1007/978-3-319-27959-6_9

$$C_{x,f} = \sqrt{2}(Re_{x,f})^{-1/2}\left(\frac{\partial W_x(\eta, Mc_{x,f})}{\partial \eta}\right)_{\eta=0}$$
$$\overline{C}_{x,f} = 2\sqrt{2}(Re_{x,f})^{-1/2}\left(\frac{\partial W_x(\eta, Mc_{x,f})}{\partial \eta}\right)_{\eta=0}$$

Here, the mixed convection parameter $Mc_{x,f} = Gr_{x,f}Re_{x,f}^{-2}$, local Reynolds number $Re_{x,f} = \frac{w_{x,\infty}x}{v_f}$, and local Grashof number $Gr_{x,f} = \frac{g\beta(t_w - t_\infty)}{v_f^2}$ refer to the case with Boussinesq approximation, and therefore the physical property v_f has the mean value property. Then, the skin dimensionless velocity gradient (i.e. wall dimensionless velocity gradient) $\left(\frac{\partial W_x(\eta, Mc_{x,f})}{\partial \eta}\right)_{\eta=0}$ is dependent on average physical properties. In this chapter, we will further analyzed the skin-friction coefficient of mixed convection with the case of consideration of variable physical properties.

9.2 Skin-Friction Coefficient

In order to present the skin-friction coefficient on laminar mixed convection with consideration of variable physical properties, the skin velocity gradient is important, and the local skin-friction coefficient $C_{x,w}$ is a dimensionless measure of the shear stress at the wall, i.e.

$$C_{x,w} = \frac{\tau_{x,w}}{\frac{1}{2}\rho_w w_{x,\infty}^2} = \frac{\mu_w\left(\frac{\partial w_x}{\partial y}\right)_{y=0}}{\frac{1}{2}\rho_w w_{x,\infty}^2} \tag{9.1}$$

where variable physical properties are taken into account, and the skin velocity gradient is expressed as

$$\left(\frac{\partial w_x}{\partial y}\right)_{y=0} = w_{x,\infty}\left(\frac{\partial W_x(\eta, Mc_{x,\infty})}{\partial \eta}\right)_{\eta=0}\left(\frac{\partial \eta}{\partial y}\right)_{y=0}$$

where $Mc_{x,\infty}$ refers to the local mixed convection parameter for consideration of variable physical properties. While,

$$\left(\frac{\partial \eta}{\partial y}\right)_{y=0} = x^{-1}\left(\frac{1}{2}Re_{x,\infty}\right)^{1/2}$$

where $Re_{x,\infty}$ is local Reynolds number for consideration of variable physical properties. Then, the skin velocity gradient

$$\left(\frac{\partial w_x}{\partial y}\right)_{y=0} = x^{-1}\left(\frac{1}{2}Re_{x,\infty}\right)^{1/2} w_{x,\infty}\left(\frac{\partial W_x(\eta, Mc_{x,\infty})}{\partial \eta}\right)_{\eta=0}$$

Therefore, the local skin-friction coefficient $C_{x,m}$ with consideration of variable physical properties is expressed as

$$\begin{aligned} C_{x,w} &= \frac{\mu_w x^{-1}\left(\frac{1}{2}Re_{x,\infty}\right)^{1/2} w_{x,\infty}\left(\frac{\partial W_x(\eta, Mc_{x,\infty})}{\partial \eta}\right)_{\eta=0}}{\frac{1}{2}\rho_w w_{x,\infty}^2} \\ &= \sqrt{2}\frac{v_\infty}{v_\infty}\frac{v_w}{x w_{x,\infty}}(Re_{x,\infty})^{1/2}\left(\frac{\partial W_x(\eta, Mc_{x,\infty})}{\partial \eta}\right)_{\eta=0} \end{aligned}$$

i.e.

$$C_{x,w} = \sqrt{2}\frac{v_w}{v_\infty}(Re_{x,\infty})^{-1/2}\left(\frac{\partial W_x(\eta, Mc_{x,\infty})}{\partial \eta}\right)_{\eta=0} \tag{9.2}$$

It should be indicated that the value $\left(\frac{\partial W_x(\eta, Mc_{x,\infty})}{\partial \eta}\right)_{\eta=0}$ here for consideration of variable physical properties is different from that for consideration of Boussinesq approximation reported in Chap. 5. The former numerical solution $\left(\frac{\partial W_x(\eta, Mc_{x,\infty})}{\partial \eta}\right)_{\eta=0}$ is variable with the temperatures boundary conditions t_w and t_∞ (or Pr_w and Pr_∞), while the latter one is variable only with the average Prandtl number Pr_f.

The average skin friction coefficient for consideration of variable physical properties from $x = 0$ to x is described as

$$\begin{aligned} \overline{C}_{x,w} &= \frac{1}{x}\int_0^x C_{x,w}dx \\ &= \sqrt{2}\frac{1}{x}\int_0^x \frac{v_w}{v_\infty}(Re_{x,\infty})^{-1/2}\left(\frac{\partial W_x(\eta, Mc_{x,\infty})}{\partial \eta}\right)_{\eta=0} dx \end{aligned}$$

i.e.

$$\overline{C}_{x,w} = 2 \times \sqrt{2}\frac{v_w}{v_\infty}(Re_{x,\infty})^{-1/2}\left(\frac{\partial W_x(\eta, Mc_{x,\infty})}{\partial \eta}\right)_{\eta=0} \tag{9.3}$$

It is seen from Eq. (9.3) that the skin velocity gradient $\left(\frac{\partial W_x(\eta, Mc_{x,\infty})}{\partial \eta}\right)_{\eta=0}$ is only one unknown variable for evaluation of the Skin-friction coefficient with consideration of variable physical properties.

It is obvious from the governing equations that the skin-friction coefficient of mixed convection with consideration of variable physical properties depends on local mixed convection parameter $Mc_{x,\infty}$, wall temperature t_w and fluid bulk temperature t_∞ (or local Prandtl numbers Pr_w and Pr_∞). In the successive sections, a series of numerical solutions of the skin dimensionless velocity gradient will be presented in order for evaluation of the skin-friction coefficient.

9.3 Numerical Solutions on Skin Velocity Gradient

A system of numerical solutions on skin velocity gradient have been obtained and listed as in Tables 9.1, 9.2, 9.3, 9.4 and 9.5 with variation of wall temperature t_w and fluid bulk temperature t_∞ at different local mixed convection parameter $Mc_{x,\infty}$ for mixed convection of water.

Table 9.1 Numerical solutions on skin velocity gradient with variation of wall temperature t_w and fluid bulk temperature at local mixed convection parameter $Mc_{x,\infty} = 0$

t_∞	$Mc_{x,\infty} = 0$						
	t_w						
	0	10	20	40	60	80	100
	$\left(\frac{\partial W_x(\eta, Mc_{x,\infty})}{\partial \eta}\right)_{\eta=0}$						
0	0.491493	0.638057	0.799717	1.134992	1.454051	1.739215	1.978215
10	0.372249	0.47894	0.607259	0.866195	1.124216	1.363774	1.565907
20	0.290521	0.378691	0.474332	0.686552	0.901633	1.100245	1.275352
40	0.194	0.254637	0.322235	0.470967	0.62589	0.773801	0.906994
60	0.141192	0.186605	0.237293	0.350337	0.470296	0.586396	0.693227
80	0.11016	0.145795	0.186076	0.276621	0.373691	0.470134	0.55896
100	0.090137	0.119577	0.152935	0.228557	0.310496	0.392451	0.469981

Table 9.2 Numerical solutions on skin velocity gradient with variation of wall temperature t_w and fluid bulk temperature t_∞ at local mixed convection parameter $Mc_{x,\infty} = 0.3$

t_∞	$Mc_{x,\infty} = 0.3$						
	t_w						
	0	10	20	40	60	80	100
	$\left(\frac{\partial W_x(\eta, Mc_{x,\infty})}{\partial \eta}\right)_{\eta=0}$						
0	0.747656	0.91997	1.121138	1.550089	1.976968	2.359943	2.696265
10	0.617938	0.762741	0.925842	1.273549	1.625563	1.949049	2.23148
20	0.518919	0.643772	0.782665	1.076976	1.375898	1.656108	1.903322
40	0.386497	0.484397	0.591049	0.821769	1.052903	1.272833	1.469444
60	0.305976	0.38653	0.47418	0.662609	0.855855	1.038432	1.203647
80	0.25371	0.322517	0.39753	0.559358	0.725616	0.885765	1.029359
100	0.218089	0.278652	0.344873	0.48835	0.636575	0.77938	0.910294

Table 9.3 Numerical solutions on skin velocity gradient with variation of wall temperature t_w and fluid bulk temperature t_∞ at local mixed convection parameter $Mc_{x,\infty} = 1$

t_∞	$Mc_{x,\infty} = 1$						
	t_w						
	0	10	20	40	60	80	100
	$\left(\frac{\partial W_x(\eta, Mc_{x,\infty})}{\partial \eta}\right)_{\eta=0}$						
0	1.245402	1.485803	1.769547	2.394912	3.027138	3.612291	4.132077
10	1.089475	1.311718	1.550697	2.080188	2.615992	3.119707	3.56526
20	0.946723	1.146341	1.368903	1.831538	2.302984	2.745163	3.138656
40	0.738336	0.907666	1.089585	1.477484	1.859692	2.22197	2.545189
60	0.601489	0.747905	0.904783	1.235786	1.568961	1.880566	2.160029
80	0.508764	0.63808	0.776972	1.070944	1.367047	1.647848	1.897163
100	0.443797	0.560393	0.686011	0.953362	1.224018	1.480574	1.710954

Table 9.4 Numerical solutions on skin velocity gradient with variation of wall temperature t_w and fluid bulk temperature t_∞ at local mixed convection parameter $Mc_{x,\infty} = 3$

t_∞	$Mc_{x,\infty} = 3$						
	t_w						
	0	10	20	40	60	80	100
	$\left(\frac{\partial W_x(\eta, Mc_{x,\infty})}{\partial \eta}\right)_{\eta=0}$						
0	2.387813	2.795485	3.289471	4.385324	5.509233	6.57375	7.530324
10	2.149154	2.544042	2.978276	3.935274	4.909894	5.832577	6.661961
20	1.90465	2.275594	2.68943	3.545874	4.417435	5.238203	5.972324
40	1.517906	1.848389	2.200507	2.94487	3.67212	4.360674	4.975882
60	1.253153	1.54642	1.858043	2.509056	3.157984	3.762424	4.302864
80	1.069452	1.332783	1.613436	2.201673	2.788299	3.341401	3.829037
100	0.938765	1.178929	1.436068	1.977862	2.520898	3.031734	3.490211

Table 9.5 Numerical solutions on skin velocity gradient with variation of wall temperature t_w and fluid bulk temperature t_∞ at local mixed convection parameter $Mc_{x,\infty} = 10$

t_∞	$Mc_{x,\infty} = 10$						
	t_w						
	0	10	20	40	60	80	100
	$\left(\frac{\partial W_x(\eta, Mc_{x,\infty})}{\partial \eta}\right)_{\eta=0}$						
0	5.419557	6.282821	7.34707	9.725169	12.18231	14.53807	16.6858
10	4.953705	5.819287	6.768932	8.875782	11.02858	13.08402	14.94767
20	4.427082	5.256059	6.180774	8.086904	10.03059	11.86984	13.53374
40	3.566964	4.323198	5.125984	6.814147	8.463305	10.02342	11.42105
60	2.964837	3.644701	4.364065	5.859345	7.342989	8.723446	9.957432
80	2.542784	3.158446	3.811936	5.174677	6.527058	7.799583	8.917823
100	2.240694	2.805572	3.40806	4.67122	5.930805	7.111542	8.170737

It should be indicated that these system of numerical solutions have practical value because they are obtained with consideration of coupled effect of variable physical properties. In the successive sections, we will further demonstrate the variation of the skin velocity gradient with the local Prandtl numbers Pr_w and Pr_∞ as well as local mixed convection parameter $Mc_{x,\infty}$.

9.4 Variation of Skin Velocity Gradient with Local Prandtl Number Pr_w

With the above numerical solutions, the variation of skin velocity gradient with local Prandtl numbers Pr_w and Pr_∞ as well as local mixed convection parameter $Mc_{x,\infty}$ are plotted as Figs. 9.1, 9.2, 9.3, 9.4 and 9.5.

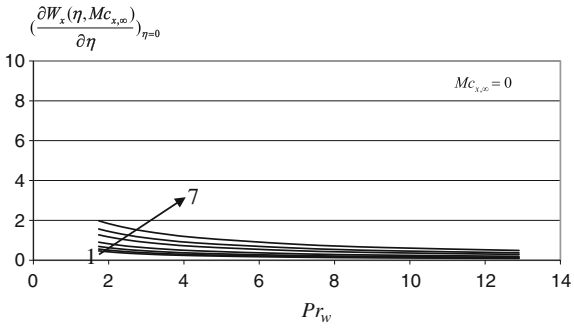

Fig. 9.1 Skin velocity gradient $\left(\frac{\partial W_x(\eta,Mc_{x,\infty})}{\partial \eta}\right)_{\eta=0}$ varying with Prandtl number Pr_w at different Prandtl number Pr_∞ and the local mixed convection parameter $Mc_{x,\infty} = 0$. *Note* lines *1* → *7* are related to Pr_∞ = 1.73, 2.2, 2.95, 4.32, 6.96, 9.46 and 13.39 respectively

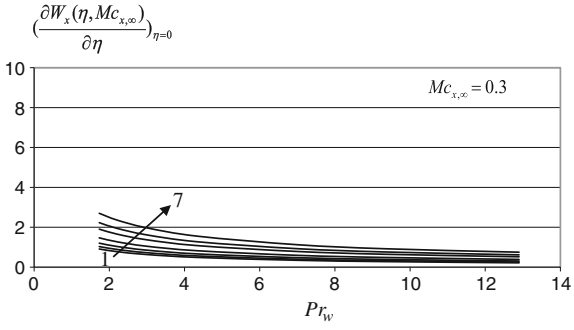

Fig. 9.2 Skin velocity gradient $\left(\frac{\partial W_x(\eta,Mc_{x,\infty})}{\partial \eta}\right)_{\eta=0}$ varying with Prandtl number Pr_w at different Prandtl number Pr_∞ and the local mixed convection parameter $Mc_{x,\infty} = 0.3$. *Note* lines *1* → *7* are related to Pr_∞ = 1.73, 2.2, 2.95, 4.32, 6.96, 9.3 and 12.99 respectively

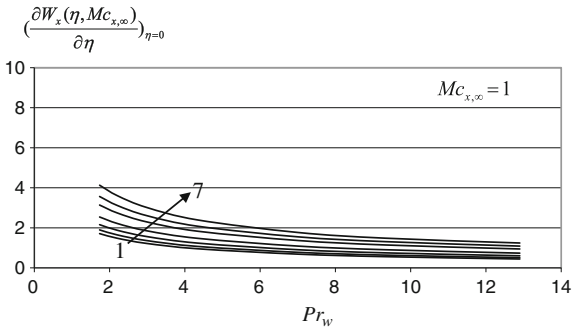

Fig. 9.3 Skin velocity gradient $\left(\frac{\partial W_x(\eta, Mc_{x,\infty})}{\partial \eta}\right)_{\eta=0}$ varying with Prandtl number Pr_w at different Prandtl number Pr_∞ and the local mixed convection parameter $Mc_{x,\infty} = 1$. *Note* lines *1* → *7* are related to Pr_∞ = 1.73, 2.2, 2.95, 4.32, 6.96, 9.3 and 12.99 respectively

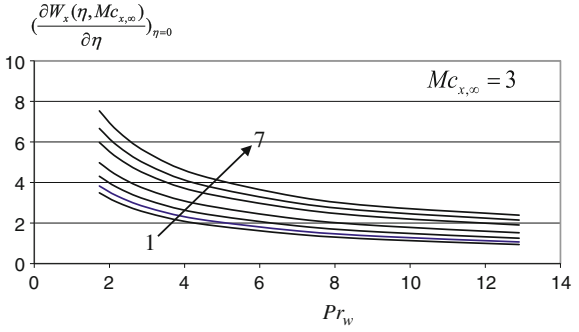

Fig. 9.4 Skin velocity gradient $\left(\frac{\partial W_x(\eta, Mc_{x,\infty})}{\partial \eta}\right)_{\eta=0}$ varying with Prandtl number Pr_w at different Prandtl number Pr_∞ and the local mixed convection parameter $Mc_{x,\infty} = 3$. *Note* lines *1* → *7* are related to Pr_∞ = 1.73, 2.2, 2.95, 4.32, 6.96, 9.3 and 12.99 respectively

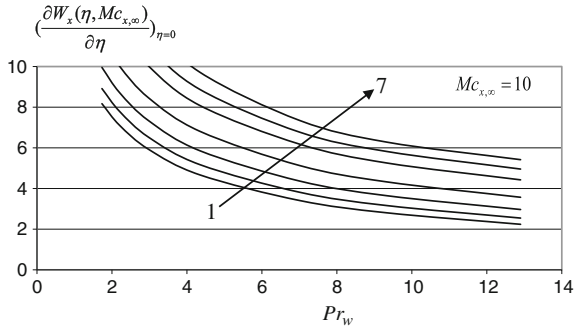

Fig. 9.5 Skin velocity gradient $\left(\frac{\partial W_x(\eta, Mc_{x,\infty})}{\partial \eta}\right)_{\eta=0}$ varying with Prandtl number Pr_w at different Prandtl number Pr_∞ and the local mixed convection parameter $Mc_{x,\infty} = 10$. *Note* lines *1* → *7* are related to Pr_∞ = 1.73, 2.2, 2.95, 4.32, 6.969.3 and 12.99 respectively

It is seen that the skin velocity gradient will increase with increasing Pr_∞ and decrease with increasing the local Prandtl number Pr_w. Meanwhile, the skin velocity gradient will increase with increasing the local mixed convection parameter due to the increase of buoyancy force. On the other hand, with increasing the local mixed convection parameter, the effect of the local Prandtl number Pr_w on the skin velocity gradient will be bigger and bigger.

9.5 Variation of Skin Velocity Gradient with Local Prandtl Number Pr_∞

With the above numerical solutions, the variation of skin velocity gradient with local Prandtl number Pr_∞ at different local Prandtl number Pr_w and local mixed convection parameter $Mc_{x,\infty}$ are plotted as Figs. 9.6, 9.7, 9.8, 9.9 and 9.10.

It is seen from the above figures that the skin velocity gradient will increase with increasing local Prandtl number Pr_∞ and decrease with increasing local Prandtl number Pr_w. Meanwhile, the skin velocity gradient will increase with increasing the local mixed convection parameter due to the effect of stronger and stronger free convection. On the other hand, with increasing the local mixed convection parameter, the effect of the local Prandtl number Pr_∞ on the skin velocity gradient will be stronger and stronger.

9.6 Remarks

In this chapter, skin-friction coefficient is analyzed for consideration of variable physical properties. It is found that the skin velocity gradient is the only one unknown variable for evaluation of the skin-friction coefficient. Systems of

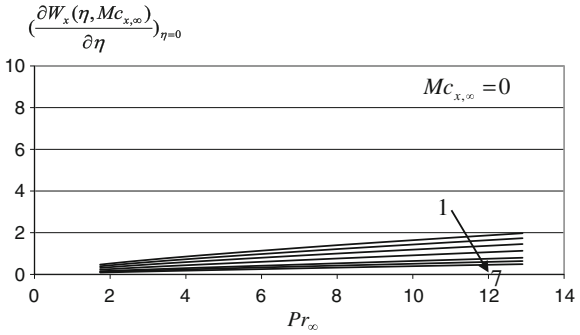

Fig. 9.6 Skin velocity gradient $\left(\frac{\partial W_x(\eta, Mc_{x,\infty})}{\partial \eta}\right)_{\eta=0}$ varying with Prandtl number Pr_∞ at different Prandtl number Pr_w at the local mixed convection parameter $Mc_{x,\infty} = 0$. *Note* lines *1* → *7* are related to Pr_w = 1.73, 2.2, 2.95, 4.32, 6.96, 9.3 and 12.99 respectively

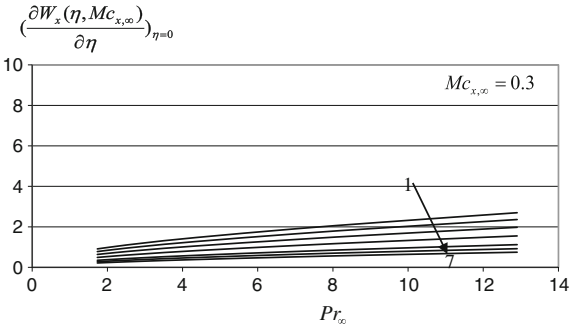

Fig. 9.7 Skin velocity gradient $\left(\frac{\partial W_x(\eta, Mc_{x,\infty})}{\partial \eta}\right)_{\eta=0}$ varying with Prandtl number Pr_∞ at different Prandtl number Pr_w at the local mixed convection parameter $Mc_{x,\infty} = 0.3$. *Note* lines *1* → *7* are related to Pr_w = 1.73, 2.2, 2.95, 4.32, 6.96, 9.3 and 12.99 respectively

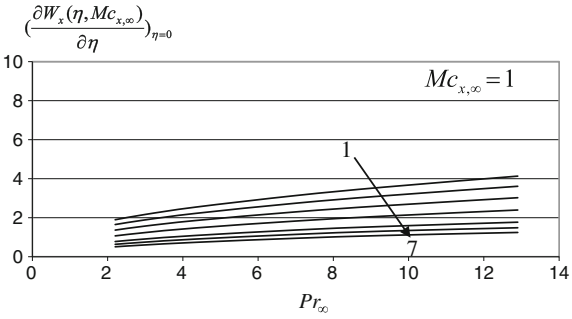

Fig. 9.8 Skin velocity gradient $\left(\frac{\partial W_x(\eta, Mc_{x,\infty})}{\partial \eta}\right)_{\eta=0}$ varying with Prandtl number Pr_∞ at different Prandtl number Pr_w at the local mixed convection parameter $Mc_{x,\infty} = 1$. *Note* lines *1* → *7* are related to Pr_w = 1.73, 2.2, 2.95, 4.32, 6.96, 9.3 and 12.99 respectively

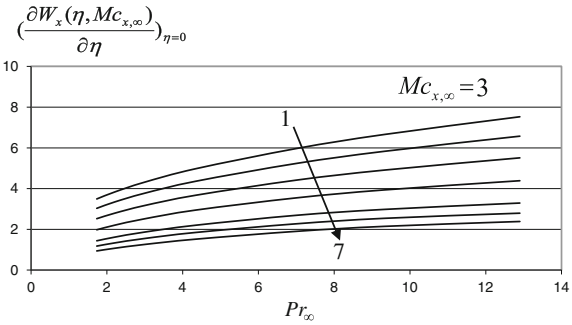

Fig. 9.9 Skin velocity gradient $\left(\frac{\partial W_x(\eta, Mc_{x,\infty})}{\partial \eta}\right)_{\eta=0}$ varying with Prandtl number Pr_∞ at different Prandtl number Pr_w at the local mixed convection parameter $Mc_{x,\infty} = 3$. *Note* lines *1* → *7* are related to Pr_w = 1.73, 2.2, 2.95, 4.32, 6.96, 9.3 and 12.99 respectively

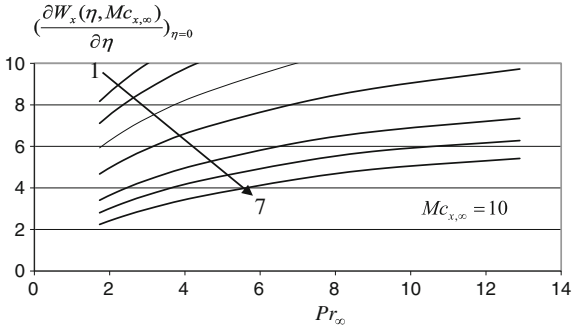

Fig. 9.10 Skin velocity gradient $\left(\frac{\partial W_x(\eta, Mc_{x,\infty})}{\partial \eta}\right)_{\eta=0}$ varying with Prandtl number Pr_∞ at different Prandtl number Pr_w at the local mixed convection parameter $Mc_{x,\infty} = 10$. *Note* lines *1* → *7* are related to Pr_w = 1.73, 2.2, 2.95, 4.32, 6.96, 9.3 and 12.99 respectively

numerical solutions on the skin velocity gradient are obtained based on consideration of variable physical properties. These numerical solutions have practical value because they are obtained with consideration of coupled effect of variable physical properties.

It is seen that the skin velocity gradient (or skin-friction coefficient) depends on local Prandtl numbers Pr_w and Pr_∞, as well as the local mixed convection parameter $Mc_{x,\infty}$ for consideration of variable physical properties, while, the skin velocity gradient depends on average Prandtl numbers Pr_f and the local mixed convection parameter $Mc_{x,f}$ due to consideration of Boussinesq approximation.

The skin velocity gradient will increase with increasing local Prandtl number Pr_∞ and will decrease with increasing local Prandtl number Pr_w. The skin velocity gradient will increase with increasing the local mixed convection parameter due to the effect of buoyancy force. On the other hand, with increasing the local mixed convection parameter, the effect of the local Prandtl numbers Pr_w and Pr_∞ on the skin velocity gradient will be bigger and bigger.

Chapter 10
Temperature Fields

Abstract A system of rigorous numerical solutions of the temperature fields of laminar water mixed convection on a vertical flat plate is obtained with variation of the local mixed convection parameter $Mc_{x,\infty}$, fluid bulk temperature t_∞ and wall temperature t_w for consideration of variable physical properties. On this basis, a analysis is done for the effect of the fluid bulk temperature t_∞ (or Pr_∞), wall temperature t_w (or Pr_w), and local mixed convection parameter $Mc_{x,\infty}$ on the temperature field. It is seen that although both fluid bulk temperature t_∞ (i.e. decreasing Pr_∞) and the wall temperature t_w (i.e. decreasing Pr_w) influence the temperature field, the effect of the fluid bulk temperature t_∞ is much stronger than that of the wall temperature t_w. It demonstrates the effect characteristics of variable physical properties on the temperature fields of mixed convection. In addition, with increasing the local mixed convection parameter $Mc_{x,\infty}$, the temperature gradient will increase due to the increase of the buoyancy force. It reflects the effect of buoyancy force on temperature fields and heat transfer of mixed convection. Since the coupled effect of variable physical properties is well considered and treated, the obtained temperature fields have theoretical and practical value for mixed convection.

Keywords Temperature field · Numerical solution · Variable physical properties · Local Prandtl number · Local mixed convection parameter

10.1 Introduction

Following the velocity fields reported in Chap. 8 with consideration of coupled effect of variable physical properties, the related temperature fields will be provided in this chapter for water laminar mixed convection with consideration of variable physical properties.

The numerical calculation is done under the regions of wall temperature $0\,^\circ\mathrm{C} \le t_w \le 100\,^\circ\mathrm{C}$, bulk temperature $0\,^\circ\mathrm{C} \le t_\infty \le 100\,^\circ\mathrm{C}$, and local mixed convection parameter $0 \le Mc_{x,\infty} \le 10$ respectively. Then, the variation of temperature

D.-Y. Shang and L.-C. Zhong, *Heat Transfer of Laminar Mixed Convection of Liquid*, Heat and Mass Transfer, DOI 10.1007/978-3-319-27959-6_10

fields will be investigated with variations of wall temperature t_w (or local Prandtl number Pr_w), fluid bulk temperature t_∞ (or local Prandtl number Pr_∞), and local mixed convection parameter $Mc_{x,\infty}$. These numerical solutions are obtained with consideration of coupled effect of variable physical properties for laminar water mixed convection on the isothermal vertical plate flat.

The numerical calculation is done by a shooting method with fifth-order Runge-Kutta integration. For solving the nonlinear problem, a variable mesh approach is applied to the numerical calculation programs. A system of numerical solutions of similarity governing partial differential equations for laminar mixed convection combined with physical property factors of water are solved and shown as below.

10.2 Temperature Field with Variation of Wall Temperature t_w

10.2.1 For $\mathbf{Mc_{x,\infty} = 0}$

Figure 10.1 expresses numerical solutions of temperature fields of water laminar mixed convection with variation of wall temperature t_w at the local mixed convection parameter $Mc_{x,\infty} = 0$ and different fluid bulk temperatures t_∞.

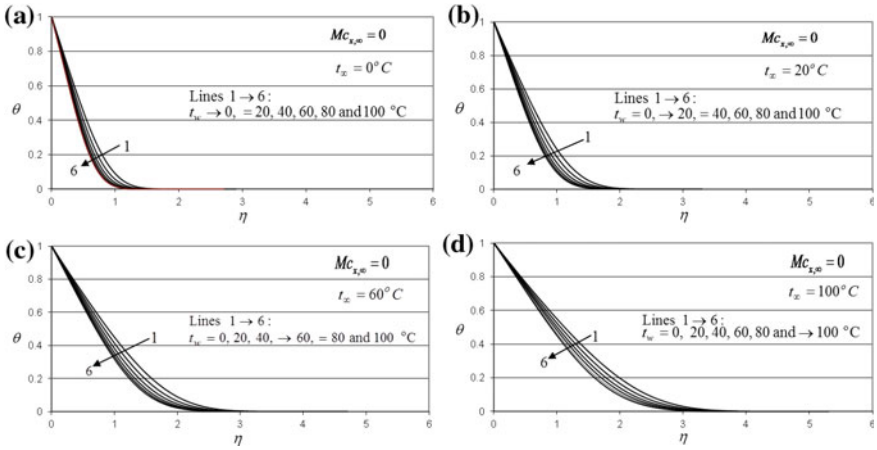

Fig. 10.1 Temperature profiles of water laminar mixed convection with variation of wall temperature t_w at $Mc_{x,\infty} = 0$ and different t_∞

10.2.2 For $\mathbf{Mc_{x,\infty}} = 0.3$

Figure 10.2 expresses numerical solutions of temperature fields of water laminar mixed convection with variation of wall temperature t_w at the local mixed convection parameter $Mc_{x,\infty}$ = 0.3 and different fluid bulk temperature t_∞.

10.2.3 For $\mathbf{Mc_{x,\infty}} = 1$

Figure 10.3 expresses numerical solutions of temperature fields of water laminar mixed convection with variation of wall temperature t_w at the local mixed convection parameter $Mc_{x,\infty}$ = 1 and different fluid bulk temperature t_∞.

10.2.4 For $\mathbf{Mc_{x,\infty}} = 3$

Figure 10.4 expresses numerical solutions of temperature fields of water laminar mixed convection with variation of wall temperature t_w at the local mixed convection parameter $Mc_{x,\infty} = 3$ and at different fluid bulk temperature t_∞.

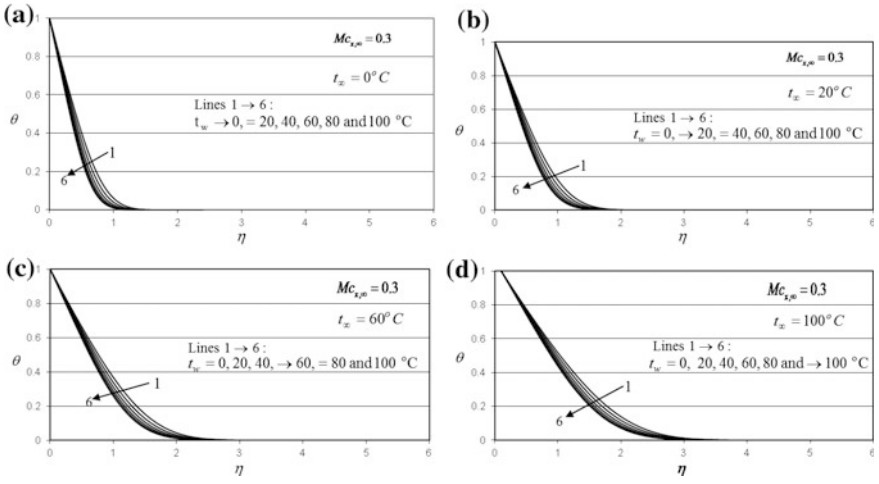

Fig. 10.2 Temperature profiles of water laminar mixed convection with variation of wall temperature t_w at $Mc_{x,\infty} = 0.3$ and different t_∞

10.2.5 *For* $\mathbf{Mc_{x,\infty}} = 10$

Figure 10.5 expresses numerical solutions of temperature fields of water laminar mixed convection with variation of wall temperature t_w under the local mixed convection parameter $Mc_{x,\infty} = 0$ and at different fluid bulk temperature t_∞.

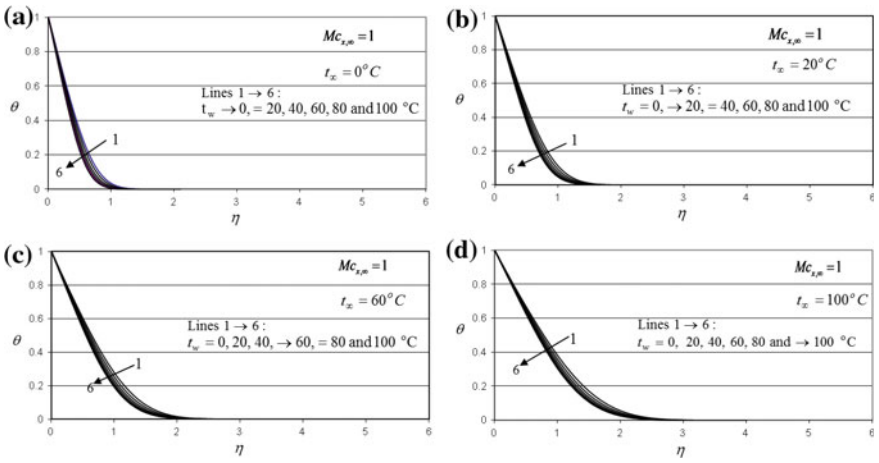

Fig. 10.3 Temperature profiles of water laminar mixed convection with variation of wall temperature t_w at $Mc_{x,\infty} = 1$ and different t_∞

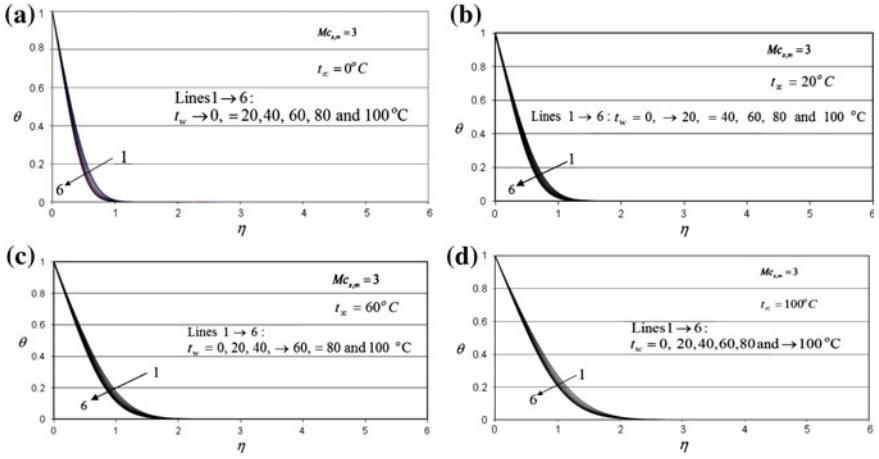

Fig. 10.4 Temperature profiles $Mc_{x,\infty} = 3$ of water laminar mixed convection with variation of wall temperature at $Mc_{x,\infty} = 3$ and different t_∞

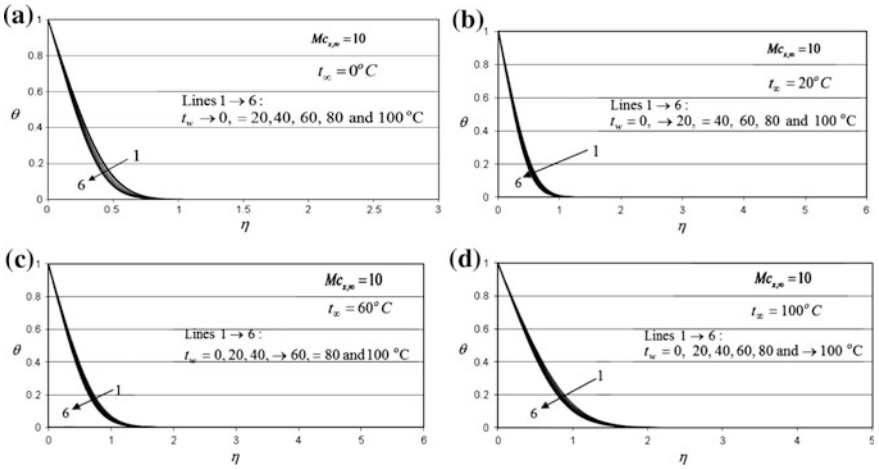

Fig. 10.5 Temperature profiles of water laminar mixed convection with variation of wall temperature t_w at $Mc_{x,\infty} = 10$ and different t_∞

10.3 Temperature Fields with Variation of Fluid Bulk Temperature t_∞

10.3.1 For $\mathbf{Mc_{x,\infty}} = 0$

Figure 10.6 expresses numerical solutions of temperature fields of water laminar mixed convection with variation of fluid bulk temperature t_∞ at the local mixed convection parameter $Mc_{x,\infty} = 0$ and different wall temperature t_w.

10.3.2 For $\mathbf{Mc_{x,\infty}} = 0.3$

Figure 10.7 expresses numerical solutions of temperature fields of water laminar mixed convection with variation of fluid bulk temperature t_∞ at the local mixed convection parameter $Mc_{x,\infty} = 0.3$ and different wall temperature t_w.

10.3.3 For $\mathbf{Mc_{x,\infty}} = 1$

Figure 10.8 expresses numerical solutions of temperature fields of water laminar mixed convection with variation of fluid bulk temperature t_∞ at the local mixed convection parameter $Mc_{x,\infty} = 1$ and different wall temperature t_w.

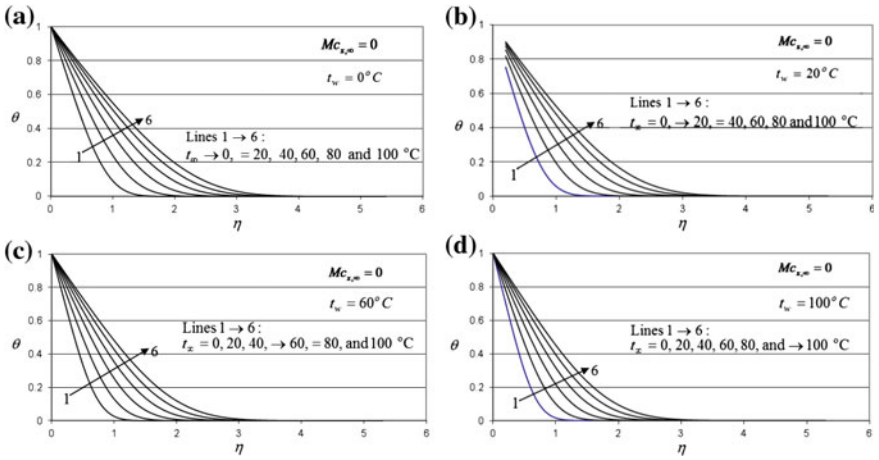

Fig. 10.6 Temperature profiles of laminar water mixed convection with variation of fluid bulk temperature t_∞ at $Mc_{x,\infty} = 0$ and different wall temperature t_w

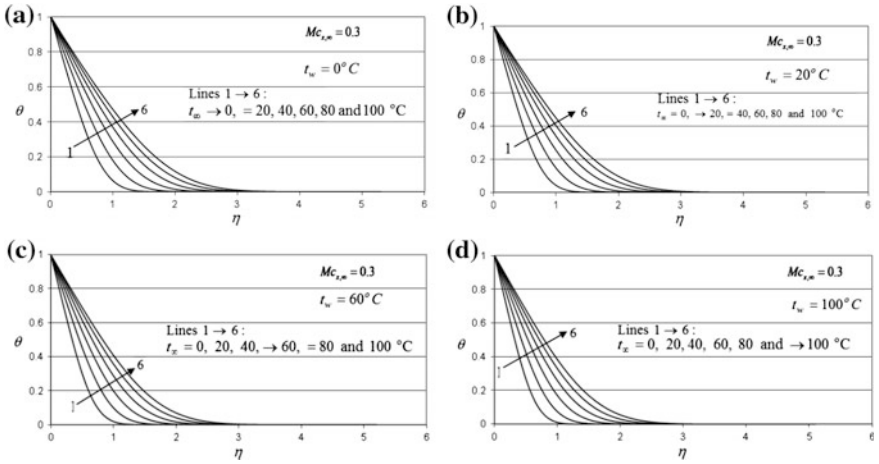

Fig. 10.7 Temperature profiles of laminar water mixed convection with variation of fluid bulk temperature t_∞ at $Mc_{x,\infty} = 0.3$ and different wall temperature t_w

10.3.4 For $\mathbf{Mc_{x,\infty}} = 3$

Figure 10.9 expresses numerical solutions of temperature fields of water laminar mixed convection with variation of fluid bulk temperature t_∞ at the local mixed convection parameter $Mc_{x,\infty} = 3$ and different wall temperature t_w.

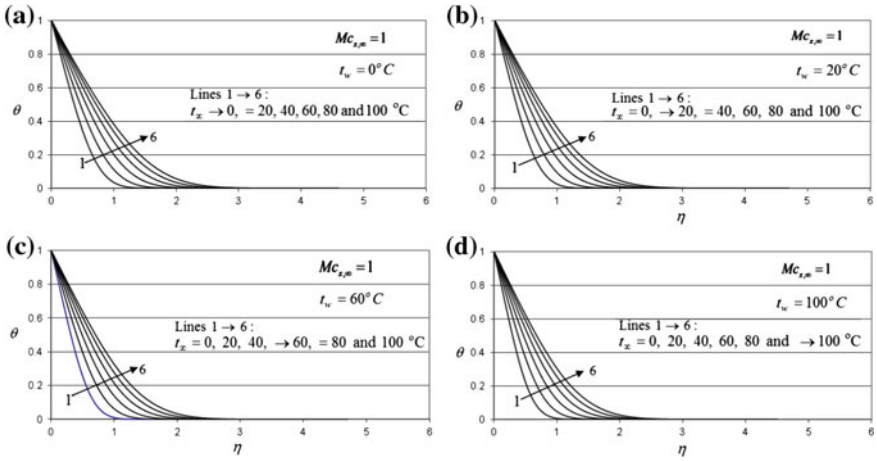

Fig. 10.8 Temperature profiles of laminar water mixed convection with variation of fluid bulk temperature t_∞ at $Mc_{x,\infty} = 1$ and different wall temperature t_w

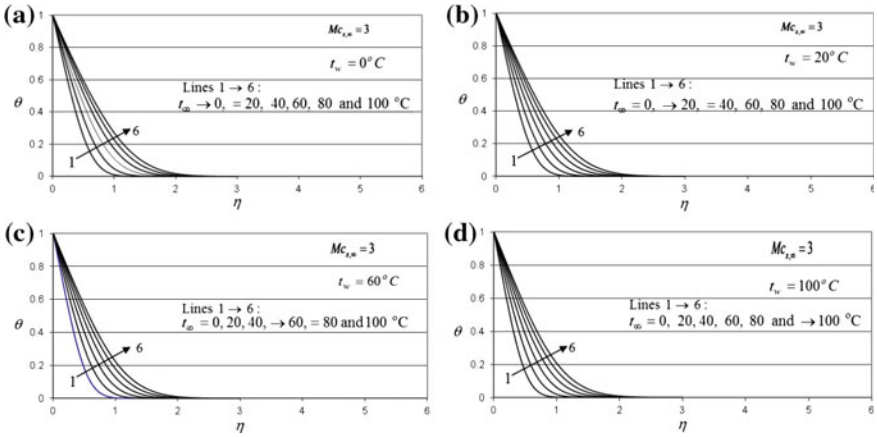

Fig. 10.9 Temperature profiles of laminar water mixed convection with variation of fluid bulk temperature t_∞ at $Mc_{x,\infty} = 3$ and different wall temperature t_w

10.3.5 For $\mathbf{Mc_{x,\infty} = 10}$

Figure 10.10 expresses numerical solutions of temperature fields of water laminar mixed convection with variation of fluid bulk temperature t_∞ at the local mixed convection parameter $Mc_{x,\infty}$ = 10 and different wall temperature t_w.

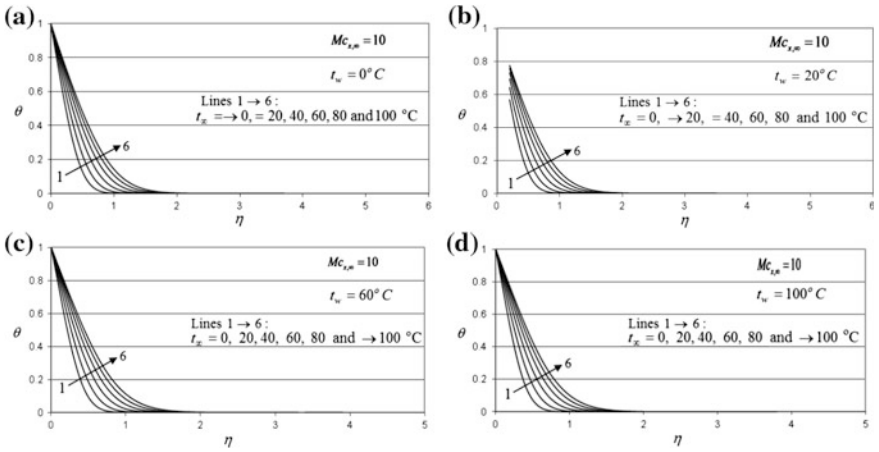

Fig. 10.10 Temperature profiles of laminar water mixed convection with variation of fluid bulk temperature t_∞ at $Mc_{x,\infty} = 10$ and different wall temperature t_w

From Figs. 10.1, 10.2, 10.3, 10.4, 10.5, 10.6, 10.7, 10.8, 10.9 and 10.10 it is seen that the fluid bulk temperature t_∞ (i.e. decreasing Pr_∞), the wall temperature t_w (i.e. decreasing Pr_w), and local mixed convection parameter $Mc_{x,\infty}$ influence the temperature field of laminar mixed convection for consideration of variable physical properties. However, with increasing the local mixed convection parameter $Mc_{x,\infty}$, the effect of the fluid bulk temperature t_∞ is much stronger and stronger than that of the wall temperature t_w on the temperature gradient. In addition, with increasing the local mixed convection parameter $Mc_{x,\infty}$, the temperature gradient will increase due to the effect of stronger buoyancy force.

10.4 Remarks

In this chapter, a system of numerical solutions of the temperature fields is described with variation of the local mixed convection parameter $Mc_{x,\infty}$, fluid bulk temperature t_∞ and wall temperature t_w for consideration of variable physical properties. On this basis, a analysis is done for the effect of the fluid bulk temperature t_∞ (or Pr_∞), wall temperature t_w (or Pr_w), and local mixed convection parameter $Mc_{x,\infty}$ on the temperature field. It is seen that although both fluid bulk temperature t_∞ (i.e. decreasing Pr_∞) and the wall temperature t_w (i.e. decreasing Pr_w) influence the temperature field, the effect of the fluid bulk temperature t_∞ is much stronger than that of the wall temperature t_w. In addition, with increasing the local mixed convection parameter $Mc_{x,\infty}$, the temperature gradient will increase due to the increase of buoyancy force.

Since the coupled effect of variable physical properties is well considered, and simulated for solution of laminar water mixed convection, the numerical solutions for velocity and temperature fields have practical value.

Chapter 11
Procedure for Optimal Formalization of Nusselt Number

Abstract Theoretical equations of Nusselt number are derived out based on our innovative similarity transformation model. Such theoretical equations show that the wall similarity temperature gradient is the only one unknown variable dominating the evaluation of the Nusselt number. Then, it is key work to develop optimal formalization of the wall similarity temperature gradient for reliable formulaic calculation of the Nusselt number of mixed convection. To this end, a procedure for investigation of optimal formalization of wall similarity temperature gradient is planned in this chapter for complete optimal formalization of Nusselt number. Such formalized equations contain the independent physical variables such as the local Prandtl numbers Pr_w and Pr_∞ and the local mixed convection parameter $Mc_{x,\infty}$ for description of effect of fluid variable physical properties and buoyancy force on mixed convection heat transfer.

Keywords Nusselt number · Theoretical equations · Optimal equations · Wall similarity temperature gradient · Heat transfer analysis · Local Prandtl number · Local mixed convection parameter

11.1 Introduction

Based on the calculation of the temperature fields, from the last chapter on, we will investigate the issue for available prediction of heat transfer of laminar mixed convection. To this end, the theoretical equation of heat transfer will be set up in this chapter, where we can find the wall temperature gradient is the only one unknown variable for heat transfer. Then, investigation of the prediction correlation equations on the wall temperature gradient is the only one duty for available prediction of heat transfer of laminar mixed convection.

It can be found from the heat transfer analysis that the wall temperature gradient of laminar mixed convection depends on local mixed convection parameter $Mc_{x,\infty}$, local Prandtl number Pr_w (or t_w) and local Prandtl number Pr_∞ (or t_∞). Then, in this work, it is important to decide the dependent correlation between these

D.-Y. Shang and L.-C. Zhong, *Heat Transfer of Laminar Mixed Convection of Liquid*, Heat and Mass Transfer, DOI 10.1007/978-3-319-27959-6_11

variables according to the systems of numerical solutions. From now on, this work will be completed successively.

11.2 Theoretical Equation of Nusselt Number

Derivation of the theoretical equation of Nusselt number is the first step of investigation of reliable prediction of heat transfer coefficient of mixed convection. Its derivation is as follows.

Here, the analysis will be conducted for heat transfer of laminar mixed convection for consideration of coupled effect of variable physical properties.

The local heat transfer rate $q_{x,w}$ at position x per unit area from the surface of the plate to the fluid with consideration of variable physical properties is calculated by Fourier's law as $q_{x,w} = -\lambda_w \left(\frac{\partial t}{\partial y}\right)_{y=0}$

While, with our innovative similarly tansformation model we have

$$-\left(\frac{\partial t}{\partial y}\right)_{y=0} = x^{-1}\left(\frac{1}{2}Re_{x,\infty}\right)^{1/2}(t_w - t_\infty)\left(-\frac{\partial\theta(\eta, Mc_{x,\infty})}{\partial\eta}\right)_{\eta=0}$$

Then,

$$q_{x,w} = \lambda_w(t_w - t_\infty)\left(\frac{1}{2}Re_{x,\infty}\right)^{1/2}x^{-1}\left(-\frac{\partial\theta(\eta, Mc_{x,\infty})}{\partial\eta}\right)_{\eta=0}$$

where $\left(-\frac{\partial\theta(\eta,Mc)}{\partial\eta}\right)_{\eta=0}$ is wall similarity temperature gradient for consideration of variable physical properties.

The local heat transfer coefficient $\alpha_{x,w}$, defined as $q_{x,w} = \alpha_{x,w}(t_w - t_\infty)$, will be given by

$$\alpha_{x,w} = \lambda_w\left(\frac{1}{2}Re_{x,\infty}\right)^{1/2}x^{-1}\left(-\frac{\partial\theta(\eta, Mc_{x,\infty})}{\partial\eta}\right)_{\eta=0}$$

The local Nusselt number defined by $Nu_{x,w} = \frac{\alpha_{x,w}\cdot x}{\lambda_w}$ will be

$$Nu_{x,w} = \left(\frac{1}{2}Re_{x,\infty}\right)^{1/2}\left(-\frac{\partial\theta(\eta, Mc_{x,\infty})}{\partial\eta}\right)_{\eta=0} \tag{11.1}$$

This is the theoretical equation of local Nusselt number.

Total theoretical heat transfer rate for position $x = 0$ to x with width of b on the plate is a integration $Q_{x,w} = \iint_A q_{x,w}dA = \int_0^x q_{x,w}bdx$, and hence

$$Q_{x,w} = \int_0^x \lambda_w (t_w - t_\infty) \left(\frac{1}{2} Re_{x,\infty}\right)^{1/2} x^{-1} \left(-\frac{\partial\theta(\eta, Mc_{x,\infty})}{\partial\eta}\right)_{\eta=0} bdx$$

$$Q_{x,w} = 2b\lambda_w (t_w - t_\infty) \left(\frac{1}{2} Re_{x,\infty}\right)^{1/2} \left(-\frac{\partial\theta(\eta, Mc_{x,\infty})}{\partial\eta}\right)_{\eta=0}$$

The average heat transfer rate defined as $\overline{Q}_{x,w} = \frac{Q_{x,w}}{b\times x}$ is

$$\overline{Q}_{x,w} = 2x^{-1}\lambda_w (t_w - t_\infty) \left(\frac{1}{2} Re_{x,\infty}\right)^{1/2} \left(-\frac{\partial\theta(\eta, Mc_{x,\infty})}{\partial\eta}\right)_{\eta=0}$$

i.e.

$$\overline{Q}_{x,w} = \sqrt{2}x^{-1}\lambda_w (t_w - t_\infty) Re_{x,\infty}^{1/2} \left(-\frac{\partial\theta(\eta, Mc_{x,\infty})}{\partial\eta}\right)_{\eta=0}$$

The average heat transfer coefficient $\overline{\alpha}_{x,w}$ defined as $\overline{Q}_{x,w} = \overline{\alpha}_{x,w}(t_w - t_\infty)$ is expressed as

$$\overline{\alpha}_{x,w} = \sqrt{2}\lambda_w Re_{x,\infty}^{1/2} x^{-1} \left(-\frac{\partial\theta(\eta, Mc_{x,\infty})}{\partial\eta}\right)_{\eta=0}$$

The average Nusselt number is defined as $\overline{Nu}_{x,w} = \frac{\overline{\alpha}_{x,w}\cdot x}{\lambda_w}$, and hence

$$\overline{Nu}_{x,w} = 2\left(\frac{1}{2} Re_{x,\infty}\right)^{1/2} \left(-\frac{\partial\theta(\eta, Mc_{x,\infty})}{\partial\eta}\right)_{\eta=0} \tag{11.2}$$

This is the theoretical equation of average Nusselt number.

11.3 Procedure for Optimal Formalization of Nusselt Number

From the above theoretical heat transfer Eqs. (11.1)–(11.3), it is seen that the temperature gradient on the wall $\left(-\frac{\partial\theta(\eta,Mc)}{\partial\eta}\right)_{\eta=0}$ (for short, wall similarity temperature gradient) is the only one unknown variable dominating the heat transfer. Then, it is necessary to investigate the convenient and reliable formulation equations that predict the wall temperature gradient for heat transfer application of the laminar mixed convection.

It is clear that the wall similarity temperature gradient $\left(-\frac{\partial\theta(\eta,Mc)}{\partial\eta}\right)_{\eta=0}$ of mixed convection depends on the physical and boundary conditions, i.e. the local mixed convection parameter $Mc_{x,\infty}$, as well as the boundary temperatures t_w and t_∞(or Pr_w and Pr_∞) shown as

$$\left(-\frac{\partial\theta(\eta,Mc)}{\partial\eta}\right)_{\eta=0}=f(Mc_{x,\infty},Pr_w\cdot Pr_\infty)$$

In this analysis, it is seen that a key work is to investigate the correlation equations on prediction of the wall temperature gradient, in order for heat transfer formulization with theoretical and practical value. Obviously, such heat transfer formulization should be based on a system of reliable numerical solutions with consideration of coupled effect of variable physical properties.

In order to decide the dependent correlation among the wall temperature gradient, local mixed convection parameter $Mc_{x,\infty}$, local Prandtl number Pr_w (or t_w) and local Prandtl number Pr_∞ (or t_∞), the mathematical model should be selected at first. To this end, first, the following model is set up for description of the relation of the wall temperature gradient $\left(-\frac{\partial\theta(\eta,Mc)}{\partial\eta}\right)_{\eta=0}$ with local Prandtl number Pr_w:

$$\left(-\frac{\partial\theta(\eta,Mc)}{\partial\eta}\right)_{\eta=0}=a\frac{{Pr_w}^b}{Pr_w} \tag{11.3}$$

where the coefficient a and exponent b are respectively assumed with relation to local Prandtl number Pr_∞ as

$$a=a_1{Pr_\infty}^{a_2} \tag{11.4}$$

$$b=b_1\frac{{Pr_\infty}^{b_2}}{Pr_\infty} \tag{11.5}$$

where the coefficients and exponents a_1, a_2, b_1 and b_2 can be regarded as those only depend on the local mixed convection parameter $Mc_{x,\infty}$, i.e.

$$\begin{aligned}a_1&=f_{a_1}(Mc_{x,\infty})\\ b_1&=f_{b_1}(Mc_{x,\infty})\\ a_2&=f_{a_2}(Mc_{x,\infty})\\ b_2&=f_{b_2}(Mc_{x,\infty})\end{aligned}$$

From the theoretical equation of Nusselt number it is seen that investigation of optimal formalization of Nusselt number for accurate heat transfer evaluation is attributed to creation of optimal formalized equation for the wall similarity

temperature gradient. To this end, our work will be divided into the following three steps:

In step 1, the work is to investigate the effect of the local Prandtl number Pr_∞ on the wall similarity temperature gradient by means of Eq. (11.3). Then, the coefficient a and exponent b should be determined with variation of the local Prandtl number Pr_∞ at different values of the local mixed convection parameter $Mc_{x,\infty}$.

In step 2, the work is to investigate the effect of the local Prandtl number Pr_∞ on the coefficient a and exponent b by means of Eqs. (11.4) and (11.5) at different values of the local mixed convection parameter $Mc_{x,\infty}$.

In step 3, the work will focus on decision of correlation equations of the coefficients and exponents a_1, a_2, b_1 and b_2 with the local mixed convection parameter $Mc_{x,\infty}$.

The work of the above steps will be performed in the successive chapters.

11.4 Remarks

In this chapter, theoretical equations of Nussel number are derived out through heat transfer analysis. Such theoretical equations are based on our innovative similarity transformation model. From the theoretical equations of Nussel number it is shown that the wall similarity temperature gradient is the only one unknown variable dominating prediction of the Nusselt number. Then, it is key work to develop optimal formalized equations of wall similarity temperature gradient for formulaic calculation of Nusselt number of mixed convection, To this end, a procedure is planned for creation of the optimal formalized equations of the wall similarity temperature gradient in this chapter. The work of such formalization is to investigate the relation of the wall similarity temperature gradient to local Prandtl numbers Pr_w and Pr_∞ and the local mixed convection parameter $Mc_{x,\infty}$, which demonstrate the effect of fluid variable physical properties and buoyancy force on heat transfer of mixed convection.

Chapter 12
A System of Numerical Solutions of Wall Similarity Temperature Gradient

Abstract A system of numerical solutions of wall similarity temperature gradient $\left(-\frac{\partial\theta(\eta,Mc_{x,\infty})}{\partial\eta}\right)_{\eta=0}$ is obtained and shown for creation of the optimal formalization of the wall similarity temperature gradient. It is seen that with increasing local mixed convection parameter $Mc_{x,\infty}$, the wall temperature gradient $\left(-\frac{\partial\theta(\eta,Mc_{x,\infty})}{\partial\eta}\right)_{\eta=0}$ will increase obviously. It demonstrates the coupled effect of Buoyancy force on heat transfer coefficient. Meanwhile, both of the local Prandtl numbers Pr_w and Pr_∞ influence the wall similarity temperature gradient, although the effect of local Prandtl number Pr_∞ is stronger than that of the local Prandtl number Pr_w. It reflects the effect of fluid's variable physical properties on heat transfer of mixed convection. The work of the present chapter has completed the first step for creation of Nusselt number formalization. According to the numerical solutions of the wall similarity temperature gradient $\left(-\frac{\partial\theta(\eta,Mc_{x,\infty})}{\partial\eta}\right)_{\eta=0}$, effect of the local Prandtl number Pr_w was first considered. Then, a system of optimal formalized equations are obtained where the coefficient a and exponent b are regarded as the functions of local Prandtl number Pr_∞ at local mixed convection parameter $Mc_{x,\infty}$. In next chapter, the optimal equations of the coefficient a and exponent b will be obtained with variation of Prandtl number Pr_∞ at the mixed convection parameter $Mc_{x,\infty}$.

Keywords Numerical solution · Wall similarity temperature gradient · Local Prandtl number · Local mixed convection parameter

12.1 Introduction

In Chap. 11 the theoretical heat transfer equations were reported, where it is seen that the wall similarity temperature gradient $\left(-\frac{\partial\theta(\eta,Mc_{x,\infty})}{\partial\eta}\right)_{\eta=0}$ is the only unknown variable for prediction of heat transfer of laminar mixed convection. In this present

D.-Y. Shang and L.-C. Zhong, *Heat Transfer of Laminar Mixed Convection of Liquid*, Heat and Mass Transfer, DOI 10.1007/978-3-319-27959-6_12

chapter, a system of numerical solutions of wall similarity temperature gradient are obtained for laminar water mixed convection on a vertical flat plate with consideration of coupled effect of variable physical properties. It is seen that with increasing local mixed convection parameter $Mc_{x,\infty}$, the wall temperature gradient $\left(-\frac{\partial\theta(\eta,Mc_{x,\infty})}{\partial\eta}\right)_{\eta=0}$ will increase obviously. Meanwhile, both of the local Prandtl numbers Pr_w and Pr_∞ influence the wall similarity temperature gradient. However, the effect of local Prandtl number Pr_∞ on the wall temperature gradient is stronger than that of the local Prandtl number Pr_w.

The work in the present chapter will be completed as the first step for creation of the correlation equations of heat transfer for water laminar mixed convection on a vertical flat plate. This work is described as below.

The systems of numerical solutions on the wall similarity temperature gradient $\left(-\frac{\partial\theta(\eta,Mc_{x,\infty})}{\partial\eta}\right)_{\eta=0}$ will be provided in the present chapter. Then, the effect of the local Prandtl number Pr_w on the wall similarity temperature gradient will be investigated and the related correlations will be formulated with a system of exponent functions, where the coefficients and exponents will be regarded as the functions of local Prandtl number Pr_∞ and local mixed convection parameter $Mc_{x,\infty}$. In the successive Chapters, the relationship of the system of coefficients and exponents to local Prandtl number Pr_∞ and mixed convection parameter $Mc_{x,\infty}$ will be further investigated.

12.2 Numerical Solutions of Wall Similarity Temperature Gradient at $Mc_{x,\infty} = 0$

Table 12.1 expresses the system of numerical solutions on the wall temperature gradient $\left(-\frac{\partial\theta(\eta,Mc_{x,\infty})}{\partial\eta}\right)_{\eta=0}$ of water laminar mixed convection with variation of local Prandtl numbers Pr_w and Pr_∞, and at local mixed convection parameter $Mc_{x,\infty} = 0$.

For convenient analysis of effect of the local Prandtl number Pr_w on the wall temperature gradient, the numerical solutions in Table 12.1 are plotted to Fig. 12.1.

With a curve-fitting method, the data of coefficient a and exponent b for the formulated equations $\left(-\frac{\partial\theta(\eta,Mc_{x,\infty})}{\partial\eta}\right)_{\eta=0} = a\frac{Pr_w}{Pr_w}^b$ are obtained and shown in Table 12.2 to describe the effect of local Prandtl number Pr_w on the wall similarity temperature gradient $\left(-\frac{\partial\theta(\eta,Mc_{x,\infty})}{\partial\eta}\right)_{\eta=0}$ at $Mc_{x,\infty} = 0$ with different local Prandtl number Pr_∞ for water laminar mixed convection on a vertical flat plate.

Table 12.1 Numerical solutions of wall similarity temperature gradient $\left(-\frac{\partial\theta(\eta,Mc_{x,\infty})}{\partial\eta}\right)_{\eta=0}$ of water laminar mixed convection with variation of local Prandtl numbers Pr_w and Pr_∞ at local mixed convection parameter $Mc_{x,\infty} = 0$

t_∞ (°C)	Pr_∞	$Mc_{x,\infty} = 0$						
		Pr_w						
		12.99	9.3	6.96	4.32	2.97	2.2	1.73
		t_w (°C)						
		0	10	20	40	60	80	100
		$\left(-\frac{\partial\theta(\eta,Mc_{x,\infty})}{\partial\eta}\right)_{\eta=0}$						
0	12.99	1.138156	1.189996	1.238782	1.321261	1.386246	1.439942	1.485546
10	9.3	0.975751	1.012365	1.054936	1.121192	1.176783	1.224346	1.263996
20	6.96	0.853798	0.886771	0.916650	0.974311	1.022599	1.062722	1.097854
40	4.32	0.691774	0.715126	0.737547	0.778212	0.814021	0.844545	0.871452
60	2.97	0.591948	0.609447	0.626077	0.656926	0.684133	0.707876	0.729085
80	2.2	0.527981	0.540749	0.553387	0.577076	0.598323	0.617327	0.634314
100	1.73	0.484708	0.494315	0.503927	0.522399	0.539293	0.554553	0.568601

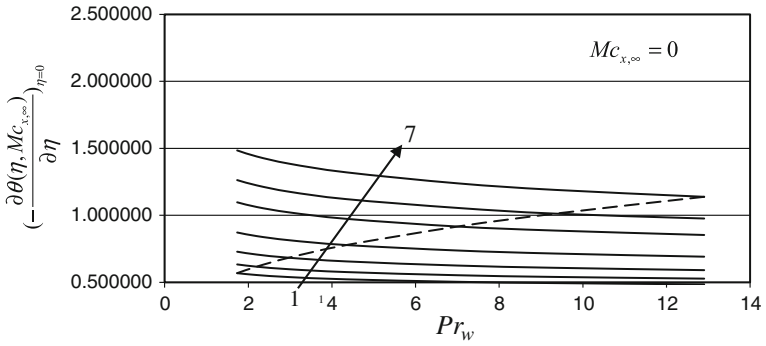

Fig. 12.1 Wall similarity temperature gradient $\left(-\frac{\partial\theta(\eta,Mc_{x,\infty})}{\partial\eta}\right)_{\eta=0}$ with variation of local Prandtl numbers Pr_w and Pr_∞ at local mixed convection parameter $Mc_{x,\infty} = 0$. *Note* Lines 1 to 7 are corresponding for Pr_∞ = 1.73, 2.20, 2.97, 4.32, 6.96, 9.3 and 12.99 respectively

12.3 Numerical Solutions of Wall Similarity Temperature Gradient at $Mc_{x,\infty} = 0.3$

In order to investigate the effect of local Prandtl number Pr_w on wall similarity temperature gradient $(-\frac{\partial\theta(\eta,Mc_{x,\infty})}{\partial\eta})_{\eta=0}$ at $Mc_{x,\infty} = 0.3$ and with variation of local Prandtl number Pr_∞, a system of numerical solutions $\left(-\frac{\partial\theta(\eta,Mc_{x,\infty})}{\partial\eta}\right)_{\eta=0}$ for the wall similarity temperature gradient is listed in Table 12.3 corresponding to the laminar water mixed convection on a vertical flat plate.

Table 12.2 Coefficient a and exponent b of the formulated correlations $\left(-\frac{\partial\theta(\eta,Mc_{x,\infty})}{\partial\eta}\right)_{\eta=0} = a\frac{Pr_w{}^b}{Pr_w}$ for the wall similarity temperature gradient with different local Prandtl numbers Pr_∞ at local mixed convection parameter $Mc_{x,\infty} = 0$

For $Mc_{x,\infty} = 0$		
Formulation equation $(-\frac{\partial\theta(\eta,Mc_{x,\infty})}{\partial\eta})_{\eta=0} = a\frac{Pr_W{}^b}{Pr_w}$		
Pr_∞	a	b
1.73	0.5901	0.9207
2.2	0.6631	0.9087
2.97	0.768	0.8964
4.32	0.9246	0.8851
6.96	1.1734	0.8746
9.3	1.3562	0.8704
12.99	1.6002	0.8676

Table 12.3 Numerical solutions of the wall similarity temperature gradient $\left(-\frac{\partial\theta(\eta,Mc_{x,\infty})}{\partial\eta}\right)_{\eta=0}$ at local mixed convection parameter $Mc_{x,\infty} = 0.3$ and with variation of local Prandtl numbers Pr_w and Pr_∞

t_w (°C)	Pr_∞	$Mc_{x,\infty} = 0.3$						
		Pr_w						
		12.99	9.3	6.96	4.32	2.97	2.2	1.73
		t_w (°C)						
		0	10	20	40	60	80	100
		$\left(-\frac{\partial\theta(\eta,Mc_{x,\infty})}{\partial\eta}\right)_{\eta=0}$						
0	13.39	1.245278	1.282377	1.325292	1.403844	1.470944	1.525295	1.573716
10	9.46	1.089597	1.118682	1.152112	1.212847	1.266958	1.312429	1.352090
20	6.96	0.969594	0.994532	1.020738	1.070514	1.114789	1.153357	1.187269
40	4.32	0.803851	0.822172	0.840743	0.876616	0.908015	0.935894	0.960833
60	2.97	0.699321	0.712991	0.726756	0.753051	0.776779	0.797807	0.816843
80	2.2	0.630252	0.640499	0.650883	0.670842	0.689018	0.705396	0.720205
100	1.73	0.583201	0.590836	0.598709	0.614023	0.628158	0.640978	0.652915

For convenient analysis of effect of local Prandtl number Pr_w on the wall temperature gradient $\left(-\frac{\partial\theta(\eta,Mc_{x,\infty})}{\partial\eta}\right)_{\eta=0}$, the numerical solutions in Table 12.3 are plotted in Fig. 12.2.

With a curve-fitting method, the data of coefficient a and exponent b for the formulated equations $\left(-\frac{\partial\theta(\eta,Mc_{x,\infty})}{\partial\eta}\right)_{\eta=0} = a\frac{Pr_w{}^b}{Pr_w}$ are obtained and shown in Table 12.4 to describe the effect of local Prandtl number Pr_w on the wall temperature gradient $\left(-\frac{\partial\theta(\eta,Mc_{x,\infty})}{\partial\eta}\right)_{\eta=0}$ at $Mc_{x,\infty} = 0.3$ with different local Prandtl number Pr_∞ for water laminar mixed convection on a vertical flat plate.

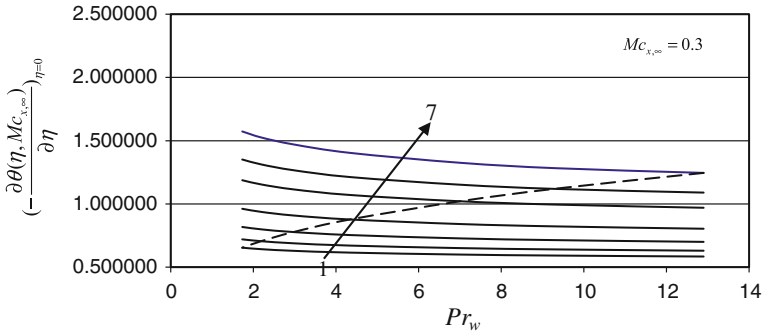

Fig. 12.2 Numerical solutions of wall similarity temperature gradient $\left(-\frac{\partial\theta(\eta,Mc_{x,\infty})}{\partial\eta}\right)_{\eta=0}$ at local mixed convection parameter $Mc_{x,\infty} = 0.3$ and with variation of local Prandtl numbers Pr_w and Pr_∞. *Note* Lines 1–7 denote Pr_∞ = 1.73, 2.20, 2.97, 4.32, 6.96, 9.3 and 12.99 respectively

Table 12.4 Coefficient a and exponent b of the formulated correlations $\left(-\frac{\partial\theta(\eta,Mc_{x,\infty})}{\partial\eta}\right)_{\eta=0} = a\frac{Pr_W}{Pr_w}^b$ for the wall temperature gradient with different local Prandtl numbers Pr_∞ at local mixed convection parameter $Mc_{x,\infty} = 0.3$

$Mc_{x,\infty} = 0.3$		
Formulation equation $\left(-\frac{\partial\theta(\eta,Mc_{x,\infty})}{\partial\eta}\right)_{\eta=0} = a\frac{Pr_W}{Pr_w}^b$		
Pr_∞	a	b
1.73	0.6698	0.9439
2.2	0.7430	0.9336
2.97	0.8477	0.9226
4.32	1.0036	0.911
6.96	1.2485	0.8986
9.3	1.4288	0.8914
12.99	1.6739	0.8819

12.4 Numerical Solutions of Wall Similarity Temperature Gradient at $Mc_{x,\infty} = 0.6$

In order to investigate of the effect of local Prandtl number Pr_w on wall similarity temperature gradient $\left(-\frac{\partial\theta(\eta,Mc_{x,\infty})}{\partial\eta}\right)_{\eta=0}$ at local mixed convection parameter $Mc_{x,\infty} = 0.6$ with different local Prandtl number Pr_∞, a system of numerical solutions of wall similarity temperature gradient $\left(-\frac{\partial\theta(\eta,Mc_{x,\infty})}{\partial\eta}\right)_{\eta=0}$ is listed in Table 12.5 corresponding to the laminar water mixed convection.

Table 12.5 Numerical solutions of the temperature gradient on the wall $\left(-\frac{\partial\theta(\eta,Mc_{x,\infty})}{\partial\eta}\right)_{\eta=0}$ at local mixed convection parameter $Mc_{x,\infty} = 0.6$ with variation of local Pranstl numbers Pr_w and Pr_∞

t_w (°C)	Pr_∞	$Mc_{x,\infty} = 0.6$						
		Pr_w						
		12.99	9.3	6.96	4.32	2.97	2.2	1.73
		t_w (°C)						
		0	10	20	40	60	80	100
		$\left(-\frac{\partial\theta(\eta,Mc_{x,\infty})}{\partial\eta}\right)_{\eta=0}$						
0	12.99	1.324697	1.357077	1.394806	1.471306	1.536780	1.593853	1.643213
10	9.3	1.172831	1.197755	1.225978	1.283964	1.336823	1.382704	1.422534
20	6.96	1.049989	1.071250	1.095464	1.142251	1.185019	1.222765	1.256127
40	4.32	0.877660	0.894116	0.911169	0.945431	0.974910	1.001844	1.026065
60	2.97	0.767034	0.779605	0.792464	0.817310	0.840093	0.860016	0.878295
80	2.2	0.693268	0.702813	0.712591	0.731492	0.748744	0.764271	0.778384
100	1.73	0.642774	0.649904	0.657325	0.671802	0.685151	0.697227	0.708492

For convenient analysis of effect of local Prandtl number Pr_w on the wall similarity temperature gradient $\left(-\frac{\partial\theta(\eta,Mc_{x,\infty})}{\partial\eta}\right)_{\eta=0}$, the numerical solutions in Table 12.5 are plotted to Fig. 12.3.

With a curve-fitting method, the data of coefficient a and exponent b for the formulated equations $\left(-\frac{\partial\theta(\eta,Mc_{x,\infty})}{\partial\eta}\right)_{\eta=0} = a\frac{Pr_W{}^b}{Pr_w}$ are obtained and shown in Table 12.6 to describe the effect of local Prandtl number Pr_w on the wall similarity temperature gradient $\left(-\frac{\partial\theta(\eta,Mc_{x,\infty})}{\partial\eta}\right)_{\eta=0}$ at $Mc_{x,\infty} = 0.6$ with different local Prandtl number Pr_∞ for water laminar mixed convection on a vertical flat plate.

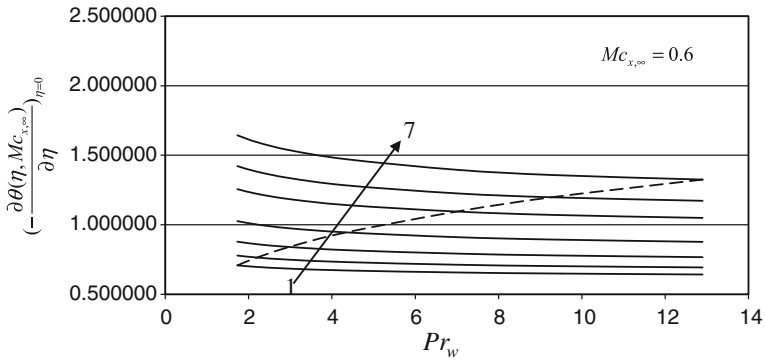

Fig. 12.3 Numerical solutions of the wall similarity temperature gradient $\left(-\frac{\partial\theta(\eta,Mc_{x,\infty})}{\partial\eta}\right)_{\eta=0}$ at local mixed convection parameter $Mc_{x,\infty} = 0.6$ with variation of local Prandtl numbers Pr_w and Pr_∞. *Note* Lines 1–7 denote Pr_∞ = 1.73, 2.20, 2.97, 4.32, 6.96, 9.3 and 12.99 respectively

Table 12.6 Coefficient a and exponent b of the formulated correlations $\left(-\frac{\partial\theta(\eta,Mc_{x,\infty})}{\partial\eta}\right)_{\eta=0} = a\frac{Pr_W}{Pr_w}^b$ for the wall similarity temperature gradient with different local Prandtl numbers Pr_∞ at local mixed convection parameter $Mc_{x,\infty} = 0.6$

$Mc_{x,\infty} = 0.6$		
Formulation equation $\left(-\frac{\partial\theta(\eta,Mc_{x,\infty})}{\partial\eta}\right)_{\eta=0} = a\frac{Pr_W}{Pr_w}^b$		
Pr_∞	a	b
1.73	0.7242	0.9516
2.2	0.7995	0.9424
2.97	0.9067	0.9325
4.32	1.0650	0.922
6.96	1.3115	0.91
9.3	1.4910	0.9026
12.99	1.7329	0.8911

12.5 Numerical Solutions of Wall Similarity Temperature Gradient at $Mc_{x,\infty} = 1$

In order to investigate the effect of local Prandtl number Pr_w on wall similarity temperature gradient at $Mc_{x,\infty} = 1$ with variation of Pr_∞, a system of numerical solutions of wall similarity temperature gradient is listed in Table 12.7 corresponding to the water laminar mixed convection.

For convenient analysis of effect of local Prandtl number Pr_w on the wall similarity temperature gradient $\left(-\frac{\partial\theta(\eta,Mc_{x,\infty})}{\partial\eta}\right)_{\eta=0}$, the numerical solutions in Table 12.7 can be plotted to Fig. 12.4.

Table 12.7 Numerical solutions of wall similarity temperature gradient $\left(-\frac{\partial\theta(\eta,Mc_{x,\infty})}{\partial\eta}\right)_{\eta=0}$ with local mixed convection parameter $Mc_{x,\infty} = 1$ and different local Prandtl numbers Pr_w and Pr_∞

t_∞ (°C)	Pr_∞	$Mc_{x,\infty} = 1$						
		Pr_w						
		13.39	9.46	6.96	4.32	2.97	2.2	1.73
		t_w (°C)						
		0	10	20	40	60	80	100
		$\left(-\frac{\partial\theta(\eta,Mc_{x,\infty})}{\partial\eta}\right)_{\eta=0}$						
0	12.99	1.411392	1.436096	1.471559	1.546635	1.613940	1.670774	1.721265
10	9.3	1.258770	1.280533	1.305437	1.361296	1.412980	1.458847	1.499218
20	6.96	1.131936	1.150628	1.173549	1.217622	1.259709	1.296912	1.330407
40	4.32	0.951124	0.966240	0.982416	1.015251	1.044104	1.070502	1.094392
60	2.97	0.833557	0.845477	0.857826	0.881887	0.903746	0.923487	0.941365
80	2.2	0.754669	0.763840	0.773306	0.791676	0.808447	0.823479	0.837236
100	1.73	0.700488	0.707357	0.714555	0.728617	0.741553	0.753213	0.764037

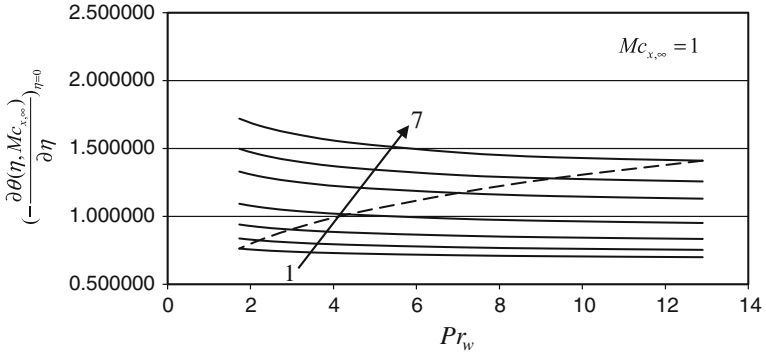

Fig. 12.4 Numerical solutions of the wall similarity temperature gradient $\left(-\frac{\partial\theta(\eta,Mc_{x,\infty})}{\partial\eta}\right)_{\eta=0}$ at local mixed convection parameter $Mc_{x,\infty} = 1$ with variation of local Prandtl numbers Pr_w and Pr_∞. *Note* Lines 1–7 denote Pr_∞ = 1.73, 2.20, 2.97, 4.32, 6.96, 9.3 and 12.99 respectively

Table 12.8 Coefficient a and exponent b of the formulated correlations $\left(-\frac{\partial\theta(\eta,Mc_{x,\infty})}{\partial\eta}\right)_{\eta=0} = a\frac{Pr_w}{Pr_w}^b$ for the wall similarity temperature gradient with variation of local Prandtl numbers Pr_∞ at local mixed convection parameter $Mc_{x,\infty} = 1$

$Mc_{x,\infty} = 1$		
Formulation equation $\left(-\frac{\partial\theta(\eta,Mc_{x,\infty})}{\partial\eta}\right)_{\eta=0} = a\frac{Pr_w}{Pr_w}^b$		
Pr_∞	a	b
1.73	0.7791	0.9568
2.2	0.8575	0.9483
2.97	0.9683	0.9394
4.32	1.1308	0.9299
6.96	1.3811	0.9189
9.3	1.5616	0.9117
12.99	1.8070	0.8987

With a curve-fitting method, the data of coefficient a and exponent b for the formulated equations $\left(-\frac{\partial\theta(\eta,Mc_{x,\infty})}{\partial\eta}\right)_{\eta=0} = a\frac{Pr_w}{Pr_w}^b$ are obtained and shown in Table 12.8 to describe the effect of local Prandtl number Pr_w on the wall similarity temperature gradient $\left(-\frac{\partial\theta(\eta,Mc_{x,\infty})}{\partial\eta}\right)_{\eta=0}$ at $Mc_{x,\infty} = 1$ with variation of the local Prandtl number Pr_∞ for water laminar mixed convection on a vertical flat plate.

12.6 Numerical Solutions of Wall Similarity Temperature Gradient at $Mc_{x,\infty} = 3$

In order to investigate the effect of local Prandtl number Pr_w on the wall similarity temperature gradient $\left(-\frac{\partial\theta(\eta,Mc_{x,\infty})}{\partial\eta}\right)_{\eta=0}$ at local mixed convection parameter

Table 12.9 Numerical solutions of wall similarity temperature gradient with $Mc_{x,\infty} = 3$ and variation of Pr_w and Pr_∞

t_∞ (°C)	Pr_∞	$Mc_{x,\infty} = 3$						
		Pr_w						
		13.39	9.46	6.96	4.32	2.97	2.2	1.73
		t_w (°C)						
		0	10	20	40	60	80	100
		$\left(-\frac{\partial\theta(\eta,Mc_{x,\infty})}{\partial\eta}\right)_{\eta=0}$						
0	12.99	1.689363	1.701487	1.732472	1.805956	1.876759	1.938181	1.993063
10	9.3	1.526040	1.538685	1.560539	1.613947	1.666495	1.714052	1.757043
20	6.96	1.383498	1.396828	1.417259	1.458756	1.500655	1.538772	1.573565
40	4.32	1.171466	1.184569	1.199826	1.231601	1.260278	1.286671	1.310911
60	2.97	1.030731	1.041781	1.054023	1.077783	1.099158	1.119203	1.137099
80	2.2	0.935332	0.943883	0.953678	0.971998	0.988683	1.003294	1.017149
100	1.73	0.869444	0.875656	0.883361	0.897379	0.910168	0.921572	0.931840

$Mc_{x,\infty} = 3$ with variation of local Prandtl number Pr_∞, a system of numerical solutions of wall similarity temperature gradient is listed in Table 12.9 corresponding to the water laminar mixed convection.

For convenient analysis of effect of local Prandtl number Pr_w on the wall similarity temperature gradient $\left(-\frac{\partial\theta(\eta,Mc_{x,\infty})}{\partial\eta}\right)_{\eta=0}$, the numerical solutions in Table 12.9 can be plotted to Fig. 12.5.

With a curve-fitting method, the data of coefficient a and exponent b for the formulated equations $\left(-\frac{\partial\theta(\eta,Mc_{x,\infty})}{\partial\eta}\right)_{\eta=0} = a\frac{Pr_w}{Pr_w}^b$ are obtained and shown in Table 12.10 to describe the effect of local Prandtl number Pr_w on the wall similarity temperature gradient $\left(-\frac{\partial\theta(\eta,Mc_{x,\infty})}{\partial\eta}\right)_{\eta=0}$ at $Mc_{x,\infty} = 3$ with variation of the local Prandtl number Pr_∞ for water laminar mixed convection on a vertical flat plate.

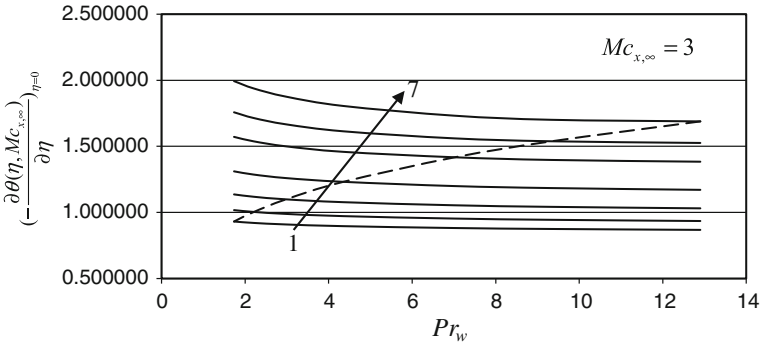

Fig. 12.5 Numerical solutions of wall similarity temperature gradient $\left(-\frac{\partial\theta(\eta,Mc_{x,\infty})}{\partial\eta}\right)_{\eta=0}$ at local mixed convection parameter $Mc_{x,\infty} = 3$ with variation of local Prandtl number Pr_w and Pr_∞. *Note* Lines 1–7 denote Pr_∞ = 1.73, 2.20, 2.97, 4.32, 6.96, 9.3 and 12.99 respectively

Table 12.10 Coefficient a and exponent b of the formulated correlations $\left(-\frac{\partial\theta(\eta,Mc_{x,\infty})}{\partial\eta}\right)_{\eta=0} = a\frac{Pr_w}{Pr_w}^b$ for wall similarity temperature gradient with variation of local Prandtl numbers Pr_∞ at local mixed convection parameter $Mc_{x,\infty} = 3$

$Mc_{x,\infty} = 3$		
Formulation equation $\left(-\frac{\partial\theta(\eta,Mc_{x,\infty})}{\partial\eta}\right)_{\eta=0} = a\frac{Pr_w}{Pr_w}^b$		
Pr_∞	a	b
1.73	0.9467	0.9651
2.2	1.0367	0.9582
2.97	1.1626	0.951
4.32	1.3437	0.9437
6.96	1.6170	0.935
9.3	1.8105	0.9281
12.99	2.0680	0.9145

12.7 Numerical Solutions of Wall Similarity Temperature Gradient at $Mc_{x,\infty} = 6$

In order to investigate the effect of local Prandtl number Pr_w on the wall similarity temperature gradient $\left(-\frac{\partial\theta(\eta,Mc_{x,\infty})}{\partial\eta}\right)_{\eta=0}$ at local mixed convection parameter $Mc_{x,\infty} = 6$ and with variation of local Prandtl number Pr_∞, a system of numerical solutions of wall similarity temperature gradient is listed in Table 12.11 corresponding to the water laminar mixed convection.

For convenient analysis of effect of local Prandtl number Pr_w on wall similarity temperature gradient, the numerical solutions in Table 12.11 can be plotted to Fig. 12.6.

With a curve-fitting method, the data of coefficient a and exponent b for the formulated equations $\left(-\frac{\partial\theta(\eta,Mc_{x,\infty})}{\partial\eta}\right)_{\eta=0} = a\frac{Pr_w}{Pr_w}^b$ are obtained and shown in Table 12.12 to describe the effect of local Prandtl number Pr_w on the wall similarity

Table 12.11 Numerical solutions of wall similarity temperature gradient with local mixed convection parameter $Mc_{x,\infty} = 6$ and with variation of local Prandtl numbers Pr_w and Pr_∞

t_∞ (°C)	Pr_∞	$Mc_{x,\infty} = 6$						
		Pr_w						
		13.39	9.46	6.96	4.32	2.97	2.2	1.73
		t_w (°C)						
		0	10	20	40	60	80	100
		$\left(-\frac{\partial\theta(\eta,Mc_{x,\infty})}{\partial\eta}\right)_{\eta=0}$						
0	12.99	1.938635	1.942276	1.971920	2.048034	2.122693	2.189365	2.249323
10	9.3	1.761284	1.769569	1.789273	1.843362	1.898253	1.948682	**1.994996**
20	6.96	1.601050	1.612009	1.632205	1.673618	1.717207	1.757250	1.794318
40	4.32	1.359453	1.372332	1.387534	1.420909	1.450005	1.477742	1.503249
60	2.97	1.197727	1.209234	1.221610	1.246339	1.268849	1.289587	1.308310
80	2.2	1.087681	1.096989	1.106759	1.125930	1.143351	1.158834	1.172946
100	1.73	1.011472	1.018527	1.025976	1.040637	1.053941	1.065724	1.076720

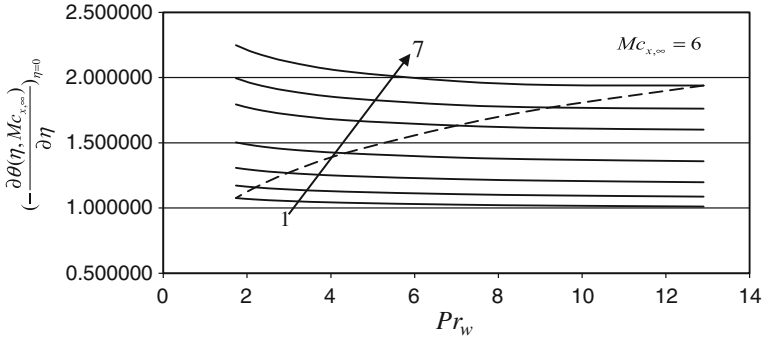

Fig. 12.6 Numerical solutions of wall similarity temperature gradient $\left(-\frac{\partial\theta(\eta,Mc_{x,\infty})}{\partial\eta}\right)_{\eta=0}$ at $Mc_{x,\infty} = 6$ and with variation of Pr_w and Pr_∞. *Note* Lines 1 to 7 denote Pr_∞ = 1.73, 2.20, 2.97, 4.32, 6.96, 9.3 and 12.99 respectively

Table 12.12 Coefficient a and exponent b of the formulated correlations $\left(-\frac{\partial\theta(\eta,Mc_{x,\infty})}{\partial\eta}\right)_{\eta=0} = a\frac{Pr_{\mathbf{W}}}{Pr_w}^b$ for wall similarity temperature gradient with variation of local Prandtl numbers Pr_∞ at local mixed convection parameter $Mc_{x,\infty} = 6$

$Mc_{x,\infty} = 6$		
Formulation equation $\left(-\frac{\partial\theta(\eta,Mc_{x,\infty})}{\partial\eta}\right)_{\eta=0} = a\frac{Pr_{\mathbf{W}}}{Pr_w}^b$		
Pr_∞	a	b
1.73	1.0921	0.9689
2.2	1.1934	0.9624
2.97	1.3346	0.956
4.32	1.5368	0.9496
6.96	1.8367	0.9424
9.3	2.0450	0.9362
12.99	2.3208	0.9225

temperature gradient $\left(-\frac{\partial\theta(\eta,Mc_{x,\infty})}{\partial\eta}\right)_{\eta=0}$ at $Mc_{x,\infty} = 6$ together with variation of the local Prandtl number Pr_∞ for water laminar mixed convection on a vertical flat plate.

12.8 Numerical Solutions of Wall Similarity Temperature Gradient at $Mc_{x,\infty} = 10$

In order to investigate the effect of local Prandtl number Pr_w on the wall similarity temperature gradient $\left(-\frac{\partial\theta(\eta,Mc_{x,\infty})}{\partial\eta}\right)_{\eta=0}$ at local mixed convection parameter $Mc_{x,\infty} = 10$ with variation of local Prandtl number Pr_∞, a system of numerical solutions of the wall similarity temperature gradient is listed in Table 12.13 corresponding to the water laminar mixed convection.

Table 12.13 Numerical solutions of wall similarity temperature gradient with local mixed convection parameter $Mc_{x,\infty} = 10$ and with variation of local Prandtl numbers Pr_w and Pr_∞

t_∞ (°C)	Pr_∞	$Mc_{x,\infty} = 10$						
		Pr_w						
		13.39	9.46	6.96	4.32	2.97	2.2	1.73
		t_w (°C)						
		0	10	20	40	60	80	100
		$\left(-\frac{\partial\theta(\eta,Mc_{x,\infty})}{\partial\eta}\right)_{\eta=0}$						
0	12.99	2.162470	2.161279	2.190115	2.269429	2.349104	2.421264	2.486405
10	9.3	1.970982	1.976324	1.995383	2.051343	2.109247	2.163301	2.212687
20	6.96	1.794022	1.803662	1.823833	1.866800	1.912610	1.954919	1.994458
40	4.32	1.525487	1.538481	1.554106	1.588478	1.619660	1.648960	1.676034
60	2.97	1.344910	1.356893	1.369831	1.395861	1.419450	1.441429	1.461163
80	2.2	1.221738	1.231550	1.241809	1.262047	1.280401	1.296648	1.311470
100	1.73	1.136342	1.143815	1.151612	1.167074	1.181052	1.193372	1.205014

For convenient analysis of effect of the local Prandtl number Pr_w on wall similarity temperature gradient $\left(-\frac{\partial\theta(\eta,Mc_{x,\infty})}{\partial\eta}\right)_{\eta=0}$, the numerical solutions in Table 12.13 can be plotted to Fig. 12.7.

With a curve-fitting method, the data of coefficient a and exponent b for the formulated equations $\left(-\frac{\partial\theta(\eta,Mc_{x,\infty})}{\partial\eta}\right)_{\eta=0} = a\frac{Pr_w{}^b}{Pr_w}$ are obtained and shown in Table 12.14 to describe the effect of local Prandtl number Pr_w on the wall similarity temperature gradient $\left(-\frac{\partial\theta(\eta,Mc_{x,\infty})}{\partial\eta}\right)_{\eta=0}$ at $Mc_{x,\infty} = 10$ together with variation of the local Prandtl number Pr_∞ for water laminar mixed convection on a vertical flat plate.

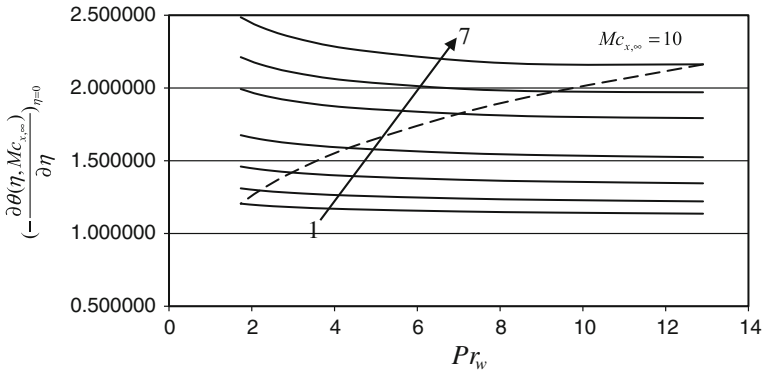

Fig. 12.7 Numerical solutions of wall similarity temperature gradient $\left(-\frac{\partial\theta(\eta,Mc_{x,\infty})}{\partial\eta}\right)_{\eta=0}$ at local mixed convection parameter $Mc_{x,\infty} = 10$ and with variation of local Prandtl numbers Pr_w and Pr_∞. *Note* Lines 1 to 7 denote Pr_∞ = 1.73, 2.20, 2.97, 4.32, 6.96, 9.3 and 12.99 respectively

Table 12.14 Coefficient a and exponent b of the correlated correlations $\left(-\frac{\partial\theta(\eta,Mc_{x,\infty})}{\partial\eta}\right)_{\eta=0} = a\frac{Pr_W}{Pr_w}^b$ of wall temperature gradient for $Mc_{x,\infty} = 10$ and different Prandtl numbers Pr_∞

$Mc_{x,\infty} = 10$		
Formulation equation $\left(-\frac{\partial\theta(\eta,Mc_{x,\infty})}{\partial\eta}\right)_{\eta=0} = a\frac{Pr_W}{Pr_w}^b$		
Pr_∞	a	b
1.73	1.2211	0.9708
2.2	1.3330	0.9647
2.97	1.4885	0.9587
4.32	1.7105	0.9528
6.96	2.0367	0.9464
9.3	2.2622	0.9405
12.99	2.5571	0.9269

It is seen from Figs. 12.1, 12.2, 12.3, 12.4, 12.5, 12.6 and 12.7 that with local mixed convection parameter $Mc_{x,\infty}$, the wall temperature gradient $\left(-\frac{\partial\theta(\eta,Mc_{x,\infty})}{\partial\eta}\right)_{\eta=0}$ will increase obviously. Meanwhile, both of the local Prandtl numbers Pr_w and Pr_∞ influence the wall temperature gradient. However, the effect of local Prandtl number Pr_∞ is stronger than that of the local Prandtl number Pr_w.

12.9 Remarks

A system of numerical solutions of wall similarity temperature gradient is obtained through the numerical calculation. It is seen that with increasing local mixed convection parameter, the wall temperature gradient will increase obviously. Meanwhile, both of the local Prandtl numbers under the boundary temperature conditions influence the wall similarity temperature gradient. However, the effect of local Prandtl number at the fluid bulk temperature is stronger than that at the wall temperature.

The work of the present chapter has completed the first step for formalization for water laminar mixed convection on a vertical flat plate. According to the system of rigorous numerical solutions of the wall similarity temperature gradient, effect of the local Prandtl number Pr_w was first investigated for formalization of the wall similarity temperature gradient. Then, a system of the optimal formalized equations are obtained where the coefficient a and exponent b are regarded as the functions of local Prandtl number Pr_∞ at the local mixed convection parameter $Mc_{x,\infty}$. It is verified that the obtained present correlation equations of the wall similarity temperature gradient are reliable.

In next chapter, the optimal formalization of the coefficient a and exponent b with Prandtl number Pr_∞ at the mixed convection parameter $Mc_{x,\infty}$ will be investigated.

Chapter 13
Effect of Local Prandtl Numbers on Wall Temperature Gradient

Abstract For investigation of effect of local Prandtl numbers on wall similarity gradient, in this chapter the work on step 2 is performed for obtaining the system of data on coefficients and exponents a_1, b_1, a_2 and b_2 respectively at different value of local mixed convection parameter $Mc_{x,\infty}$. The coefficients and exponents a_1, b_1, a_2 and b_2 are rigorously obtained with the optimal curve-fitting approach based on the system of the data on coefficient a and exponent b. On this basis, the coefficients and exponents a_1, b_1, a_2 and b_2 are attributed to the function of the local mixed convection parameter $Mc_{x,\infty}$ respectively. In the next Chapter, our work will focus on investigation of correlation equations of the coefficients and exponents a_1, b_1, a_2 and b_2 with variation of the local mixed convection parameter $Mc_{x,\infty}$ respectively.

Keywords Curve-fitting method · Wall similarity temperature gradient · Local Prandtl number · Local mixed convection parameter

13.1 Introduction

For clarification of effect of local Prandtl numbers on wall similarity gradient, in Chap. 12, we obtained the systems of data on the coefficients a and b corresponding to the assumed correlation equation $\left(-\frac{\partial\theta\left(\eta, Mc_{x,\infty}\right)}{\partial\eta}\right)_{\eta=0} = a\frac{Pr_w^b}{Pr_w}$ for description of effect of local Prandtl number Pr_w on the wall temperature gradient of water laminar mixed convection. While, the coefficient a and exponent b are respectively assumed with correlation equations $a = a_1 Pr_\infty^{a_2}$ and $b = b_1\frac{Pr_\infty^{b_2}}{Pr_\infty}$ regarded as the function of local Prandtl number Pr_∞ at the special values of local mixed convection parameter $Mc_{x,\infty}$. In this present chapter, the work will focus on determination of the system of data a_1, b_1, a_2 and b_2. On this basis, the coefficients and exponents a_1, b_1, a_2 and b_2 will be attributed to the functions of the local mixed convection parameter $Mc_{x,\infty}$ respectively.

D.-Y. Shang and L.-C. Zhong, *Heat Transfer of Laminar Mixed Convection of Liquid*, Heat and Mass Transfer, DOI 10.1007/978-3-319-27959-6_13

13.2 Correlation Equations for the Coefficient *a* and Exponent *b*

In this section, we will investigate the correlation equations for the coefficient a and exponent b with variation of local Prandtl number Pr_∞ at different values of local mixed convection parameter $Mc_{x,\infty}$. To this end, we assume the models $a = a_1 Pr_\infty^{a_2}$ and $b = b_1 \frac{Pr_\infty^{b_2}}{Pr_\infty}$. On this basis, the coefficients a_1 and b_1, as well as exponents a_2 and b_2 will be regarded as functions of local mixed convection parameter $Mc_{x,\infty}$ respectively.

13.2.1 For $\mathbf{Mc_{x,\infty} = 0}$

For convenient analysis of the correlation equations, the relationship of coefficient a and exponent b with variation of local Prandtl number Pr_∞ at local mixed convection parameter $Mc_{x,\infty} = 0$ in Table 12.2 is plotted in Figs. 13.1 and 13.2 respectively.

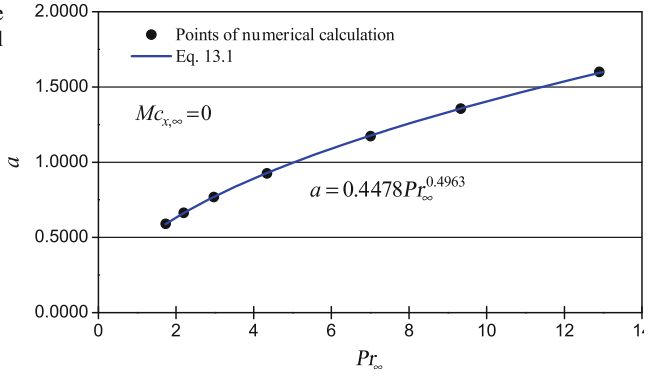

Fig. 13.1 Variation of the coefficient a with the local Prandtl number Pr_∞ at $Mc_{x,\infty} = 0$

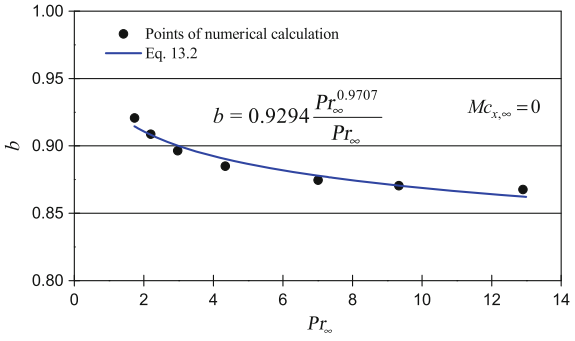

Fig. 13.2 Variation of the exponent b with the local Prandtl number Pr_∞ at $Mc_{x,\infty} = 0$

By using a curve-fitting method, we have the following equations respectively for expression of the relations of local Prandtl number Pr_∞ to coefficient a and exponent b respectively at local mixed convection parameter $Mc_{x,\infty} = 0$.

$$a = 0.4478 Pr_\infty^{0.4963} \tag{13.1}$$

$$b = 0.9294 \frac{Pr_\infty^{0.9707}}{Pr_\infty} \tag{13.2}$$

13.2.2 *For* $\mathbf{Mc_{x,\infty}} = 0.3$

For convenient analysis of the correlation, the relationship of coefficient a and exponent b with variation of local Prandtl number Pr_∞ at local mixed convection parameter $Mc_{x,\infty} = 0.3$ in Table 12.4 is plotted in Figs. 13.3 and 13.4 respectively.

By using a curve-fitting method, we have the following equations respectively for expression of the relations of local Prandtl number Pr_∞ to coefficient a and exponent b respectively at local mixed convection parameter $Mc_{x,\infty} = 0.3$.

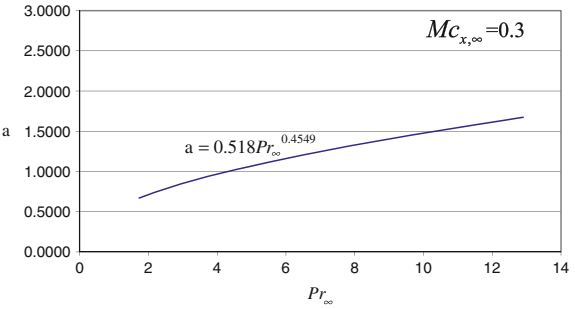

Fig. 13.3 Variation of the coefficient a with the local Prandtl number at $Mc_{x,\infty} = 0.3$

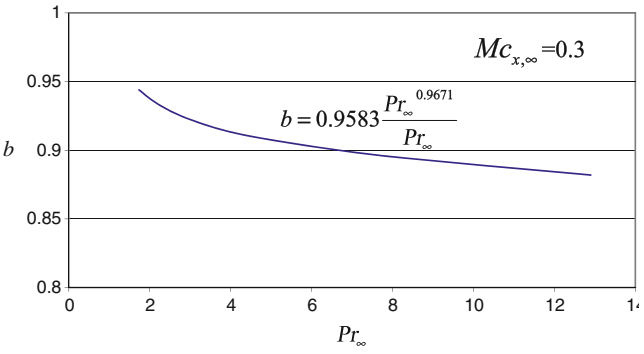

Fig. 13.4 Variation of the exponent b with the local Prandtl number Pr_∞ at $Mc_{x,\infty} = 0.3$

$$a = 0.518 Pr_{\infty}^{0.4549} \tag{13.3}$$

$$b = 0.9583 \frac{Pr_{\infty}^{0.9671}}{Pr_{\infty}} \tag{13.4}$$

13.2.3 *For* $\mathbf{Mc_{x,\infty}} = 0.6$

For convenient analysis of the correlation, the relationship of coefficient a and exponent b with variation of local Prandtl number Pr_{∞} at local mixed convection parameter $Mc_{x,\infty} = 0.6$ in Table 12.6 is plotted in Figs. 13.5 and 13.6 respectively.

By using a curve-fitting method, we have the following equations respectively for expression of the relations of local Prandtl number Pr_{∞} to coefficient a and exponent b respectively at local mixed convection parameter $Mc_{x,\infty} = 0.6$.

$$a = 0.5671 Pr_{\infty}^{0.4334} \tag{13.5}$$

$$b = 0.9663 \frac{Pr_{\infty}^{0.9688}}{Pr_{\infty}} \tag{13.6}$$

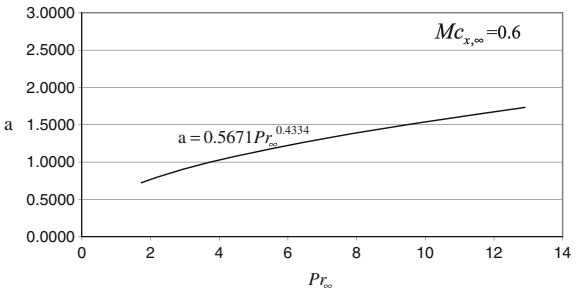

Fig. 13.5 Variation of the coefficient a with the local Prandtl number Pr_{∞} at $Mc_{x,\infty} = 0.6$

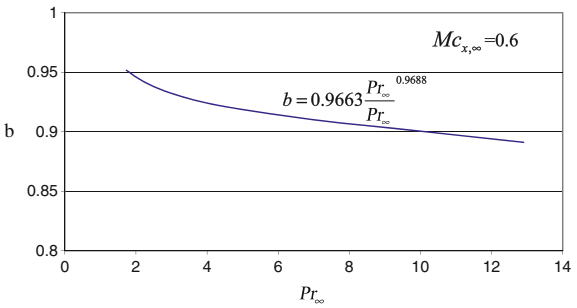

Fig. 13.6 Variation of the exponent b with the local Prandtl number Pr_{∞} at $Mc_{x,\infty} = 0.6$

13.2.4 *For* $\mathbf{Mc_{x,\infty} = 1}$

For convenient analysis of the correlation, the relationship of coefficient a and exponent b with variation of local Prandtl number Pr_∞ at local mixed convection parameter $Mc_{x,\infty} = 1$ in Table 12.8 is plotted in Figs. 13.7 and 13.8 respectively.

By using a curve-fitting method, we have the following equations respectively for expression of the relations of local Prandtl number Pr_∞ to coefficient a and exponent b respectively at local mixed convection parameter $Mc_{x,\infty} = 1$.

$$a = 0.6159 Pr_\infty^{0.4175} \tag{13.7}$$

$$b = 0.9714 \frac{Pr_\infty^{0.9706}}{Pr_\infty} \tag{13.8}$$

13.2.5 *For* $\mathbf{Mc_{x,\infty} = 3}$

For convenient analysis of the correlation, the relationship of coefficient a and exponent b with variation of local Prandtl number Pr_∞ at local mixed convection parameter $Mc_{x,\infty} = 3$ in Table 12.10 is plotted in Figs. 13.9 and 13.10 respectively.

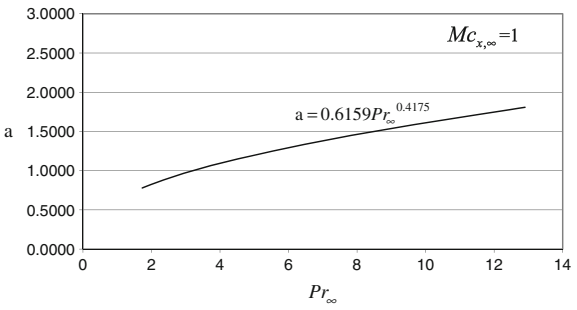

Fig. 13.7 Variation of coefficient a to the local Prandtl number Pr_∞ at $Mc_{x,\infty} = 1$

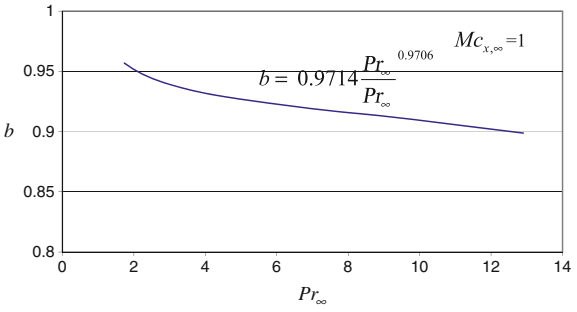

Fig. 13.8 Variation of the exponent b to the Prandtl number Pr_∞ at $Mc_{x,\infty} = 1$

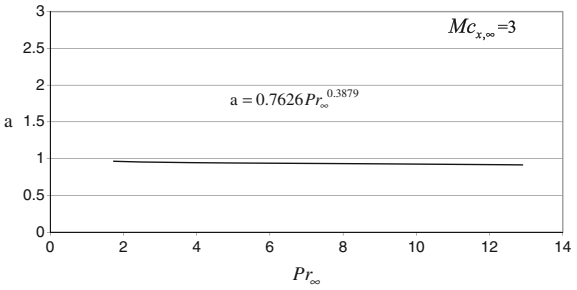

Fig. 13.9 Variation of coefficient a with the local Prandtl number Pr_∞ at $Mc_{x,\infty} = 3$

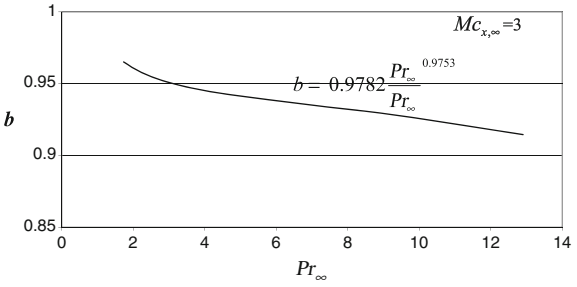

Fig. 13.10 Variation of the exponent b with the local Prandtl number Pr_∞ at $Mc_{x,\infty} = 3$

By using a curve-fitting method, we have the following equations respectively for expression of the relations of local Prandtl number Pr_∞ to coefficient a and exponent b respectively at local mixed convection parameter $Mc_{x,\infty} = 3$.

$$a = 0.7626 Pr_\infty^{0.3879} \tag{13.9}$$

$$b = 0.9782 \frac{Pr_\infty^{0.9753}}{Pr_\infty} \tag{13.10}$$

13.2.6 For $\mathbf{Mc_{x,\infty} = 6}$

For convenient analysis of the correlation, the relationship of coefficient a and exponent b with variation of local Prandtl number Pr_∞ at local mixed convection parameter $Mc_{x,\infty} = 6$ in Table 12.12 is plotted in Figs. 13.11 and 13.12 respectively.

By using a curve-fitting method, we have the following equations respectively for expression of the relations of local Prandtl number Pr_∞ to coefficient a and exponent b respectively at local mixed convection parameter $Mc_{x,\infty} = 6$:

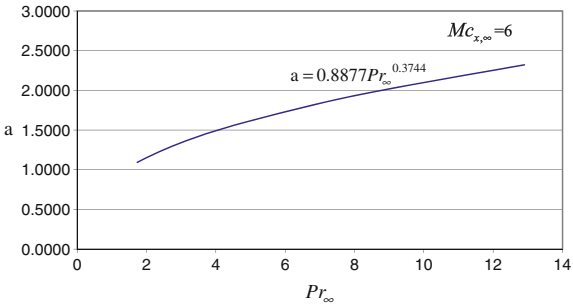

Fig. 13.11 Variation of coefficient a to the local Prandtl number Pr_∞ at $Mc_{x,\infty} = 6$

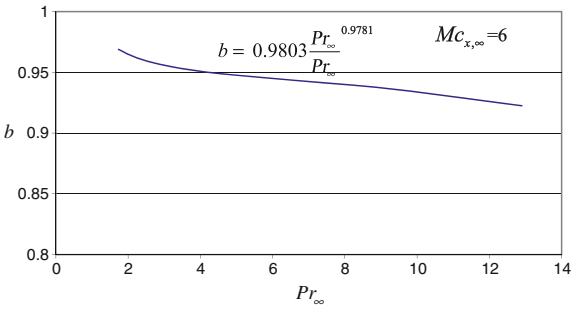

Fig. 13.12 Variation of exponent b to the local Prandtl number Pr_∞ at $Mc_{x,\infty} = 6$

$$a = 0.8877Pr_\infty^{0.3744} \tag{13.11}$$

$$b = 0.9803\frac{Pr_\infty}{Pr_\infty}^{0.9781} \tag{13.12}$$

13.2.7 For $\mathbf{Mc_{x,\infty}} = 10$

For convenient analysis of the correlation, the relationship of coefficient a and exponent b with variation of local Prandtl number Pr_∞ at local mixed convection parameter $Mc_{x,\infty} = 10$ in Table 12.14 is plotted in Figs. 13.13 and 13.14 respectively.

By using a curve-fitting method, we have the following equations respectively for expression of the relations of local Prandtl number Pr_∞ to coefficient a and exponent b respectively at local mixed convection parameter $Mc_{x,\infty} = 10$.

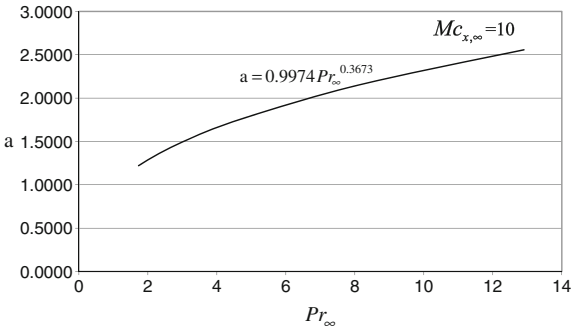

Fig. 13.13 Variation of coefficient a to the local Prandtl number Pr_∞ at $Mc_{x,\infty} = 10$

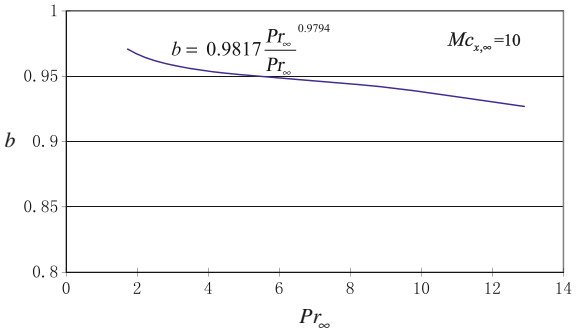

Fig. 13.14 Variation of exponent b with the local Prandtl number Pr_∞ at $Mc_{x,\infty} = 10$

$$a = 0.9974 Pr_\infty^{0.3673} \tag{13.13}$$

$$b = 0.9817 \frac{Pr_\infty^{0.9794}}{Pr_\infty} \tag{13.14}$$

13.3 Remarks

In this chapter the work on step 2 is completed for obtaining the system of data on coefficients and exponents a_1, b_1, a_2 and b_2 respectively with variation of local Prandtl number Pr_∞ at different value of local mixed convection parameter $Mc_{x,\infty}$. The coefficients and exponents a_1, b_1, a_2 and b_2 are rigorously obtained with the curve-fitting approach based on the system of the data on coefficient a and exponent b. On this basis, the coefficients and exponents a_1, b_1, a_2 and b_2 are attributed to the function of the local mixed convection parameter $Mc_{x,\infty}$ respectively. In the next Chapter, our work will focus on investigation of correlation equations of the coefficients and exponents a_1, b_1, a_2 and b_2 with variation of the local mixed convection parameter $Mc_{x,\infty}$ respectively.

Chapter 14
Formalized Equations

Abstract By using the data obtained in the last chapter for the coefficients a_1 and b_1 as well as exponents a_2 and b_2, only dependent on the local mixed convection parameter, in this present chapter, the optimal formalization of the coefficients a_1 and b_1 as well as exponents a_2 and b_2 is investigated with variation of the local mixed convection parameter. On this basis, complete optimal formalized equations are created for the wall similarity temperature gradient, and for Nusselt number of laminar water mixed convection on a vertical flat plate. Such complete optimal formalized equations depend on three physical variables, namely local Prandtl numbers at the boundary temperatures as well as local mixed convection parameter, where all fluid's variable physical properties and physical conditions are included. On the other hand, since the coupled effect of variable physical properties on mixed convection and its heat transfer is well taken into account, such optimal formalized equations not only have theoretical value, but also application value for heat transfer application of laminar mixed convection.

Keywords Nusselt number · Theoretical equation · Formalized equation · Curve-fitting method · Local Prandtl number · Local mixed convection parameter

14.1 Introduction

In the previous chapters, we investigated correlation equations for coefficient a and exponent b with variation of the local Prandtl number Pr_∞ at different local convection parameter $Mc_{x,\infty}$, according to the assumed correlation equations $a = a_1 Pr_\infty^{a_2}$ and $b = b_1 \frac{Pr_\infty^{b_2}}{Pr_\infty}$. Meanwhile, we obtained the system of data for the coefficients a_1 and b_1 as well as exponents a_2 and b_2, which depend on the local mixed convection parameter $Mc_{x,\infty}$ respectively. In this present chapter, we will investigate the correlation equations for the coefficients a_1 and b_1 as well as exponents a_2 and b_2 with variation of the local mixed convection parameter $Mc_{x,\infty}$ for completing the derivation of the formulized correlation equations for practical prediction of the wall temperature gradient.

D.-Y. Shang and L.-C. Zhong, *Heat Transfer of Laminar Mixed Convection of Liquid*, Heat and Mass Transfer, DOI 10.1007/978-3-319-27959-6_14

Table 14.1 Summary the correlation equations obtained in Chap. 13 for coefficient a and exponent b with variation of the local Prandtl number Pr_∞ at different local mixed convection parameter

Coefficients a_1 and b_1 as well as exponents a_2 and b_2		
$Mc_{x,\infty}$	$a = a_1 Pr_\infty^{a_2}$	$b = b_1 \frac{Pr_\infty{}^{b_2}}{Pr_\infty}$
0	$a = 0.4478 Pr_\infty^{0.4963}$	$b = 0.9294 \frac{Pr_\infty^{0.9707}}{Pr_\infty}$
0.3	$a = 0.518 Pr_\infty^{0.4549}$	$b = 0.9583 \frac{Pr_\infty^{0.9671}}{Pr_\infty}$
0.6	$a = 0.5671 Pr_\infty^{0.4334}$	$b = 0.9663 \frac{Pr_\infty^{0.9688}}{Pr_\infty}$
1	$a = 0.6159 Pr_\infty^{0.4175}$	$b = 0.9714 \frac{Pr_\infty^{0.9706}}{Pr_\infty}$
3	$a = 0.7626 Pr_\infty^{0.3879}$	$b = 0.9782 \frac{Pr_\infty^{0.9753}}{Pr_\infty}$
6	$a = 0.8877 Pr_\infty^{0.3744}$	$b = 0.9803 \frac{Pr_\infty^{0.9781}}{Pr_\infty}$
10	$a = 0.9974 Pr_\infty^{0.3673}$	$b = 0.9817 \frac{Pr_\infty^{0.9794}}{Pr_\infty}$

14.2 Summary of Data for Coefficients a_1 and b_1 as Well as Exponents a_2 and b_2

Now it is necessary to summarize as below the correlation equations obtained in Chap. 12 for coefficient a and exponent b, which vary with local Prandtl number Pr_∞ at different local mixed convection parameter $Mc_{x,\infty}$. With the assumed correlation equations

$$a = a_1 Pr_\infty^{a_2} \tag{11.4}$$

$$b = b_1 \frac{Pr_\infty{}^{b_2}}{Pr_\infty} \tag{11.5}$$

The coefficients a_1 and b_1 as well as exponents a_2 and b_2 with variation of different local mixed convection parameters $Mc_{x,\infty}$ are summarized in Table 14.2 according to Table 14.1. While, the data in Table 14.1 came from those in Chap. 13.

14.3 Correlation Equations for Coefficients a_1 and b_1 as Well as Exponents a_2 and b_2 with Local Mixed Convection Parameter $Mc_{x,\infty}$

14.3.1 For Coefficient a_1

For convenient analysis of relation of coefficient a_1 with variation of the local mixed convection parameter $Mc_{x,\infty}$, the data on the coefficient a_1 in Table 14.2 is plotted as curve in Fig. 14.1.

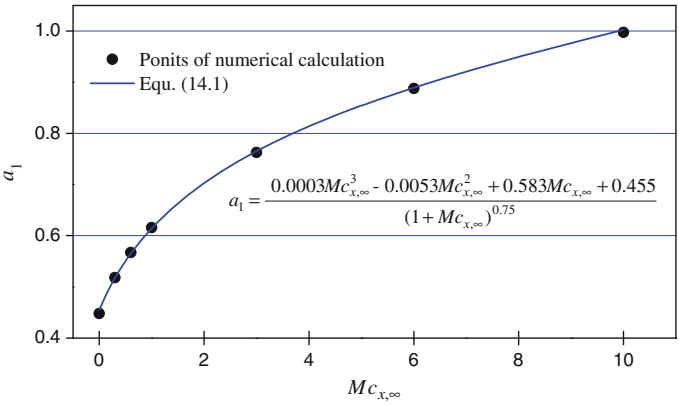

Fig. 14.1 Variation of coefficient a_1 with the local mixed convection parameter $Mc_{x,\infty}$

By using a curve-fitting method, we have the following equation for expression of coefficient a_1 with the local mixed convection parameter $Mc_{x,\infty}$.

$$a_1 = \frac{0.0003Mc_{x,\infty}^3 - 0.0053Mc_{x,\infty}^2 + 0.583Mc_{x,\infty} + 0.455}{(1+Mc_{x,\infty})^{0.75}} \tag{14.1}$$

14.3.2 For Exponent $\mathbf{a_2}$

For convenient analysis of relation of exponent a_2 with variation of the local mixed convection parameter $Mc_{x,\infty}$, the data on the coefficient a_2 in Table 14.2 is plotted as curve in Fig. 14.2.

Table 14.2 Coefficients a_1 and b_1 as well as exponents a_2 and b_2 at different local mixed convection parameters $Mc_{x,\infty}$

$a = a_1 Pr_\infty^{a_2}$ and $b = b_1 \frac{Pr_\infty^{b_2}}{Pr_\infty}$							
$Mc_{x,\infty}$	0	0.3	0.6	1	3	6	10
a_1	0.4478	0.518	0.5671	0.6159	0.7626	0.8877	0.9974
a_2	0.4963	0.4549	0.4334	0.4175	0.3879	0.6344	0.3673
b_1	0.9294	0.9583	0.9663	0.9714	0.9782	0.9803	0.9817
b_2	0.9707	0.9671	0.9688	0.9706	0.9753	0.9781	0.9794

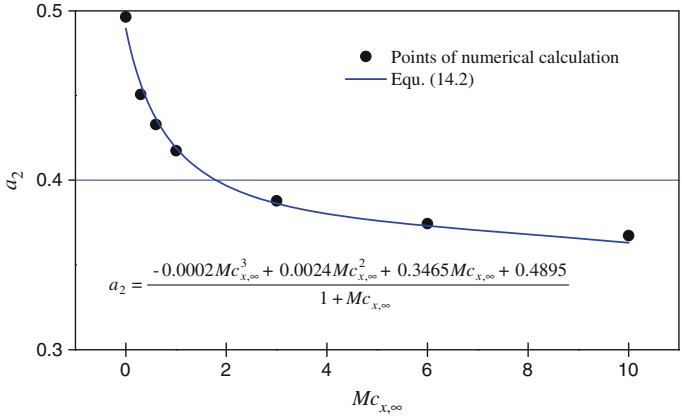

Fig. 14.2 Variation of exponent a_2 with the local mixed convection parameter $Mc_{x,\infty}$

By using a curve-fitting method, we have the following equation for expression of exponent a_2 with variation of the local mixed convection parameter $Mc_{x,\infty}$.

$$a_2 = \frac{-0.0002Mc_{x,\infty}^3 + 0.0024Mc_{x,\infty}^2 + 0.3465Mc_{x,\infty} + 0.4895}{1 + Mc_{x,\infty}} \tag{14.2}$$

14.3.3 For Coefficient $\mathbf{b_1}$

For convenient analysis of the variation of coefficient b_1 with the local mixed convection parameter $Mc_{x,\infty}$, the coefficient b_1 with different local mixed convection parameter in Table 14.2 is plotted as curve in Fig. 14.3.

By using a curve-fitting method, we have the following equation for expression of exponent b_1 with variation of the local mixed convection parameter $Mc_{x,\infty}$.

$$b_1 = \frac{0.0003Mc_{x,\infty}^3 - 0.0047Mc_{x,\infty}^2 + 1.005Mc_{x,\infty} + 0.9392}{1 + Mc_{x,\infty}} \tag{14.3}$$

14.3.4 For Exponent $\mathbf{b_2}$

For convenient analysis of the variation of exponent b_2 with the local mixed convection parameter $Mc_{x,\infty}$, the data of exponent b_2 with variation of the local mixed convection parameter in Table 14.2 is plotted as curve in Fig. 14.4.

By using a curve-fitting method, we have the following equation for expression of exponent b_2 with variation of the local mixed convection parameter $Mc_{x,\infty}$.

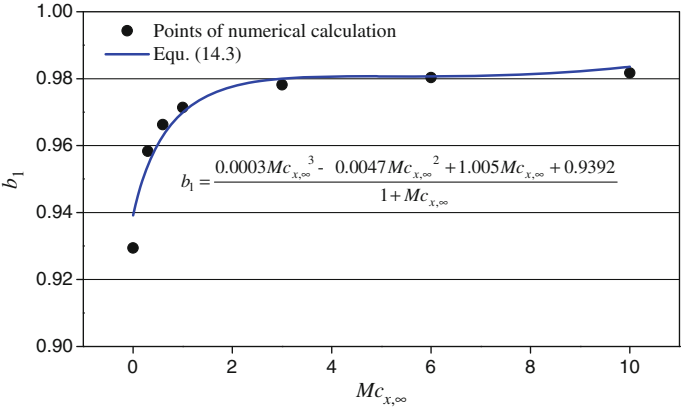

Fig. 14.3 Variation of coefficient b_1 with the local mixed convection parameter $Mc_{x,\infty}$

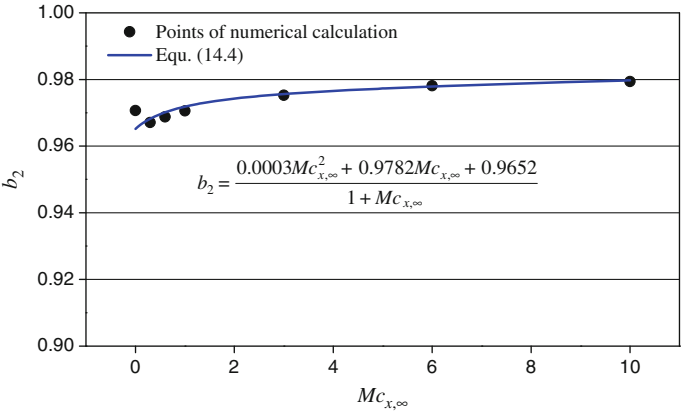

Fig. 14.4 Variation of exponent b_2 with the local mixed convection parameter $Mc_{x,\infty}$

$$b_2 = \frac{0.0003Mc_{x,\infty}^2 + 0.9782Mc_{x,\infty} + 0.9652}{1 + Mc_{x,\infty}} \tag{14.4}$$

14.4 Summary for Optimal Formalization of Nusselt Number

The optimal formalized equations of Nusselt number of laminar mixed convection on a vertical flat plate with consideration of variable physical properties are summarized as below:

1. Theoretical equations of Nusselt number of laminar mixed convection

   (a) Theoretical equation of local Nusselt number

$$Nu_{x,w} = \left(\frac{1}{2}Re_{x,\infty}\right)^{1/2}\left(-\frac{\partial\theta(\eta, Mc_{x,\infty})}{\partial\eta}\right)_{\eta=0} \tag{11.1}$$

   where the local Nusselt number is defined as $Nu_{x,w} = \frac{\alpha_{x,w}\cdot x}{\lambda_w}$

   (b) Theoretical equation of average Nusselt number

$$\overline{Nu}_{x,w} = \sqrt{2}(Re_{x,\infty})^{1/2}\left(-\frac{\partial\theta(\eta, Mc_{x,\infty})}{\partial\eta}\right)_{\eta=0} \tag{11.2}$$

   where the average Nusselt number is defined as $\overline{Nu}_{x,w} = \frac{\overline{\alpha}_{x,w}\cdot x}{\lambda_w}$

2. Optimal formalized equations of the wall similarity temperature gradient $\left(-\frac{\partial\theta(\eta,Mc_{x,\infty})}{\partial\eta}\right)_{\eta=0}$ for water laminar mixed convection on a vertical flat plate

$$\left(-\frac{\partial\theta(\eta, Mc_{x,\infty})}{\partial\eta}\right)_{\eta=0} = aPr_{\mathrm{w}}^{b-1} \tag{11.3}$$

   where

$$a = a_1 Pr_{\infty}^{a_2} \tag{11.4}$$

$$b = b_1 Pr_{\infty}^{b_2-1} \tag{11.5}$$

where the coefficients a_1 and b_1 as well as exponents a_2 and b_2 are evaluated by the following equations respectively:

$$a_1 = \frac{0.0003Mc_{x,\infty}^3 - 0.0053Mc_{x,\infty}^2 + 0.583Mc_{x,\infty} + 0.455}{(1 + Mc_{x,\infty})^{0.75}} \tag{14.1}$$

$$a_2 = \frac{-0.0002Mc_{x,\infty}^3 + 0.0024Mc_{x,\infty}^2 + 0.3465Mc_{x,\infty} + 0.4895}{1 + Mc_{x,\infty}} \tag{14.2}$$

$$b_1 = \frac{0.0003Mc_{x,\infty}{}^3 - 0.0047Mc_{x,\infty}^2 + 1.005Mc_{x,\infty} + 0.9392}{1 + Mc_{x,\infty}} \tag{14.3}$$

$$b_2 = \frac{0.0003Mc_{x,\infty}^2 + 0.9782Mc_{x,\infty} + 0.9652}{1 + Mc_{x,\infty}} \tag{14.4}$$

The theoretical Eqs. (11.1) and (11.2) of laminar mixed convection combined with the optimal formalized Eqs. (11.3)–(11.5) and (14.1) to (14.4) consist of the

complete optimal formulated equations of Nusselt number for evaluation of heat transfer for water laminar mixed convection on a vertical flat plane. These formalized equations are optimal, and have theoretical and practical application value, because they are obtained by means of a system of rigorous numerical solutions, optical curve-fitting method, better similarity transformation model, consideration of coupled effect of variable physical properties.

14.5 Remarks

The data obtained in last chapter are used for creation of optimal formalization of the coefficients a_1 and b_1 as well as exponents a_2 and b_2 for the third step of the formalization of the Nusselt number. The coefficients a_1 and b_1 as well as exponents a_2 and b_2 only depend on the local mixed convection parameter $Mc_{x,\infty}$ respectively. On this basis, the work in this present chapter is to investigate the optimal formalized equations of coefficients a_1 and b_1 as well as exponents a_2 and b_2 with variation of the local mixed convection parameter $Mc_{x,\infty}$. The complete optimal equations for Nusselt number of laminar mixed convection on a vertical flat plate are created by combination of the optimal formalization of the wall similarity temperature gradient of laminar mixed water convection on a vertical flat plate with the theoretical equations on Nusselt number. It is seen that the Nussel number depends on the three physical variable, namely local Prandtl numbers Pr_∞ and Pr_w as well as local mixed convection parameter $Mc_{x,\infty}$. While, all variable physical properties and physical conditions are involved in the three physical variables. The formalized equations are optimal, and have theoretical and practical application value, because they are obtained by means of a system of rigorous numerical solutions, optical curve-fitting method, better similarity transformation model, consideration of coupled effect of variable physical properties. Although the present provided formalized equations of Nusselt number are only suitable for water laminar mixed convection on vertical plate, we are sure, all corresponding study methods and investigating procedure in this book will be benefit to the whole research field of laminar mixed convection.

Chapter 15
Verification and Application of Optimal Formalized Equations

Abstract A series of calculations are performed for verification of the optimal formalized equations of Nusselt number. While, such optimal formalized equations are based on the rigorous numerical solutions of the wall similarity temperature gradient. The calculated results are very well coincident to the related numerical solutions on the wall similarity temperature gradient. Then, the optimal formalized equations of Nusselt number, which are based on consideration of coupled effect of variable physical properties have solid theoretical and practical value. Three calculation examples are given for evaluation of water mixed convection heat transfer, and demonstrate that the deviations of heat transfer rate with consideration of Boussinesq approximation is up to over 8.4 % to that with consideration of coupled effect of variable physical properties.

Keywords Verification · Formalized equation · Nusselt number · Calculation examples · Wall similarity temperature gradient · Heat transfer · Mixed convection · Variable physical properties

15.1 Introduction

In the previous chapters, we have done two works: First, the theoretical equations of Nusselt number are derived out, for heat transfer application where the wall temperature gradient is only one unknown variable for prediction of heat transfer coefficient. Second, according to the systems of numerical solutions, the correlation equations for the wall temperature gradient of laminar water mixed convection on a flat plate are created by means of a series of processes based on the curve-fitting approach. Then, it is realized to achieve optimal equations of Nusselt number for practical calculation of heat transfer coefficient of laminar water mixed convection by combination of the theoretical equations of Nusselt number with the correlation equations of the wall similarity temperature gradient. Since the numerical solutions for the wall similarity temperature gradient are obtained with consideration of coupled effect of variable physical properties, the complete optimal equations of

D.-Y. Shang and L.-C. Zhong, *Heat Transfer of Laminar Mixed Convection of Liquid*, Heat and Mass Transfer, DOI 10.1007/978-3-319-27959-6_15

Nusselt number on laminar mixed convection have theoretical and practical value on heat transfer application. In this chapter, we further verify the accuracy of the formulated correlation equations on the temperature equations in order to confirm the practical value of the optimal equations of Nusselt number of laminar mixed convection. At the end of this chapter, some practical calculation examples by using the optimal formalized equations of Nusselt number of laminar water mixed convection are applied for the practical calculation of heat transfer of laminar water mixed convection. On the other hand, these calculation examples also proved the importance of consideration of variable physical properties for enhancement of theoretical and practical value on in-depth study of convection heat transfer.

15.2 Verification Steps of the Formalized Equations

For verification of the formulated equations on wall similarity temperature gradient, the following steps of work will be processed:

Step 1: To evaluate a_1, a_2, b_1, and b_2 by using Eqs. (14.1)–(14.4), i.e.

$$a_1 = \frac{0.0003Mc_{x,\infty}^3 - 0.0053Mc_{x,\infty}^2 + 0.583Mc_{x,\infty} + 0.455}{(1+Mc_{x,\infty})^{0.75}} = 0.455 \quad (14.1)$$

$$a_2 = \frac{-0.0002Mc_{x,\infty}^3 + 0.0024Mc_{x,\infty}^2 + 0.3465Mc_{x,\infty} + 0.4895}{1+Mc_{x,\infty}} = 0.4895 \quad (14.2)$$

$$b_1 = \frac{0.0003Mc_{x,\infty}^3 - 0.0047Mc_{x,\infty}^2 + 1.005Mc_{x,\infty} + 0.9392}{1+Mc_{x,\infty}} = 0.9392 \quad (14.3)$$

$$b_2 = \frac{0.0003Mc_{x,\infty}^2 + 0.9782Mc_{x,\infty} + 0.9652}{1+Mc_{x,\infty}} = 0.9652 \quad (14.4)$$

Step 2: To evaluate a and b by using Eqs. (11.4) and (11.5), i.e.

$$a = a_1 Pr_\infty^{a_2} \quad (11.4)$$

$$b = b_1 Pr_\infty^{b_2-1} \quad (11.5)$$

Step 3: To evaluate the wall similarity temperature gradient by using Eq. (11.3), i.e.

$$\left(-\frac{\partial\theta(\eta, Mc_{x,\infty})}{\partial\eta}\right)_{\eta=0} = aPr_w^{b-1} \quad (0.3 \le Pr_w \le 20) \quad (11.3)$$

Step 4: Compare the evaluated results on the wall similarity temperature gradient with the related numerical solutions.

Here, the work for steps 1–3 is for evaluation of the wall similarity temperature gradient actually.

15.3 Verification

By using formalized equations in above steps 1–3, the prediction and verification results are obtained for the wall similarity temperature gradient, and listed in the following tables respectively for $Mc_{x,\infty}$ = 0, 0.3, 0.6, 1, 3, 6 and 10, with variation of local Prandtl numbers Pr_w and Pr_∞.

15.3.1 For $\mathbf{Mc_{x,\infty} = 0}$

For $Mc_{x,\infty} = 0$, the calculation results for coefficients and exponents a_1, a_2, b_1 and b_2 as well as for the wall similarity temperature gradient are listed in Table 15.1.

Compared with the corresponding numerical solutions at $Mc_{x,\infty} = 0$ reported in Chap. 12, the deviations of the predicted data in Table 15.1 for the wall similarity temperature gradient of laminar mixed convection of water on a vertical flat plate are predicted, and the prediction deviations are shown in Table 15.2.

It is seen from Table 15.2 that the maximum predicted deviation by using the present correlation equations for laminar mixed convection of water on a vertical flat plate is less than 2.76 % at $Mc_{x,\infty} = 0$.

15.3.2 For $\mathbf{Mc_{x,\infty} = 0.3}$

For $Mc_{x,\infty} = 0.3$, the coefficients and exponents a_1, a_2, b_1 and b_2 as well as the calculation results for the wall similarity temperature gradient are listed in Table 15.3.

Compared with the corresponding numerical solutions at $Mc_{x,\infty} = 0.3$ reported in Chap. 12, the deviations of the predicted data in Table 15.3 for the wall similarity temperature gradient of laminar mixed convection of water on a vertical flat plate are evaluated, and shown in Table 15.4.

It is seen from Table 15.4 that the maximum predicted deviation by using the present correlation equations for laminar mixed convection of water on a vertical flat plate is less than 2.98 % at $Mc_{x,\infty} = 0.3$.

Table 15.1 Predicted results of the wall similarity temperature gradient

Pr_∞	$a = 0.455\, Pr_\infty^{0.4895}$	$b = 0.9392 \frac{Pr_\infty^{0.9652}}{Pr_\infty}$	$Mc_{x,\infty} = 0$						
			a_1 = 0.455, a_2 = 0.4895, b_1 = 0.9392, b_2 = 0.9652						
			Pr_w						
			12.99	9.3	6.96	4.32	2.97	2.2	1.73
			$\left(-\frac{\partial\theta(\eta,Mc_{x,\infty})}{\partial\eta}\right)_{\eta=0} = a\frac{Pr_w^b}{Pr_w}$						
12.99	1.596331	0.859022	1.112062314	1.165705	1.214322	1.298775533	1.369225	1.428397	1.477624
9.3	1.355451	0.86907	0.968900586	1.012233	1.051383	1.119128	1.175400	1.222504	1.261584
6.96	1.176166	0.87788	0.859953477	0.895772	0.928045	0.983702	1.029759	1.068198	1.100014
4.32	0.931281	0.892572	0.707046319	0.732889	0.756068	0.795814	0.828501	0.855647	0.878027
2.97	0.775221	0.904287	0.606510759	0.626223	0.643838	0.673909	0.698516	0.718871	0.735599
2.2	0.66931	0.91378	0.536552489	0.552236	0.566210	0.589978	0.609349	0.625322	0.638415
1.73	0.595025	0.921455	0.486481592	0.499419	0.510919	0.530421	0.546263	0.559292	0.569951

Table 15.2 Predicted deviations ε of the wall similarity temperature gradient from the numerical solutions

Pr_∞	$Mc_{x,\infty} = 0$						
	Pr_w						
	12.99	9.3	6.96	4.32	2.97	2.2	1.73
	ε						
12.99	−0.02346	−0.02084	−0.02014	−0.01731	−0.01243	−0.00808	−0.00536
9.3	−0.00707	−0.00013	−0.00338	−0.00184	−0.00118	−0.00151	−0.00191
6.96	0.007158	0.010049	0.012279	0.009546	0.006953	0.005127	0.001964
4.32	0.0216	0.024238	0.024496	0.022119	0.017478	0.012976	0.007488
2.97	0.024011	0.026789	0.027587	0.025201	0.020591	0.015296	0.008856
2.2	0.015975	0.020801	0.022648	0.021869	0.018095	0.012785	0.006424
1.73	0.003646	0.010221	0.013685	0.015124	0.01276	0.008475	0.002369

Table 15.3 Predicted results of the wall similarity temperature gradient

Pr_∞	a	b	$Mc_{x,\infty} = 0.3$						
			$a_1 = 0.517882$, $a_2 = 0.456662$, $b_1 = 0.954065$, $b_2 = 0.968221$						
			Pr_w						
			12.99	9.3	6.96	4.32	2.97	2.2	1.73
			$\left(-\frac{\partial\theta(\eta,Mc_{x,\infty})}{\partial\eta}\right)_{\eta=0} = a\frac{Pr_w^b}{Pr_w}$						
12.99	1.667376	0.879404	1.223875	1.274203	1.319527	1.397645	1.462248	1.516138	1.560724
9.3	1.431396	0.888793	1.076263	1.117012	1.153601	1.216437	1.268195	1.311234	1.346752
6.96	1.253944	0.897017	0.962931	0.996646	1.026842	1.078535	1.120966	1.156151	1.185123
4.32	1.008537	0.910716	0.802166	0.82646	0.848125	0.88502	0.915129	0.939981	0.960369
2.97	0.849925	0.921625	0.695186	0.713634	0.730030	0.757835	0.78042	0.798993	0.814186
2.2	0.741075	0.930457	0.620037	0.634615	0.647536	0.669373	0.687045	0.701534	0.713358
1.73	0.664044	0.93759	0.565844	0.577769	0.588315	0.60609	0.62043	0.632159	0.641713

Table 15.4 Predicted deviations ε of wall similarity temperature gradient from the numerical solutions

Pr_∞	t_∞, °C	$Mc_{x,\infty} = 0.3$						
		Pr_w						
		12.99	9.3	6.96	4.32	2.97	2.2	1.73
		t_w, °C						
		0	10	20	40	60	80	100
		ε						
12.99	0	−0.017187	−0.00637	−0.004349	−0.00442	−0.00591	−0.006	−0.00826
9.3	10	−0.012237	−0.00149	0.001292	0.00296	0.000976	−0.00091	−0.00395
6.96	20	−0.006871	0.002126	0.005980	0.007492	0.005541	0.002422	−0.00181
4.32	40	−0.002096	0.005215	0.008781	0.009587	0.007834	0.004367	−0.00048
2.97	60	−0.005912	0.000902	0.004505	0.006352	0.004687	0.001487	−0.00325
2.2	80	−0.016207	−0.00919	−0.005142	−0.00219	−0.00286	−0.00547	−0.00951
1.73	100	−0.029760	−0.02212	−0.017360	−0.01292	−0.0123	−0.01376	−0.01716

Table 15.5 Predicted results of the wall similarity temperature gradient

Pr_∞	a	b	$Mc_{x,\infty} = 0.6$						
			$a_1 = 0.56442,\ a_2 = 0.436388,\ b_1 = 0.962858,\ b_2 = 0.970143$						
			Pr_w						
			12.99	9.3	6.96	4.32	2.97	2.2	1.73
			$\left(-\frac{\partial\theta(\eta,Mc_{x,\infty})}{\partial\eta}\right)_{\eta=0} = a\frac{Pr_w^b}{Pr_w}$						
12.99	1.728097	0.891894	1.309725	1.357904	1.401125065	1.47526	1.536244	1.586902	1.628673
9.3	1.493608	0.900837	1.158265	1.197289	1.23220	1.291874	1.340778	1.381278	1.414593
6.96	1.316155	0.908666	1.041351	1.073623	1.102423	1.151505	1.191594	1.224707	1.251888
4.32	1.068858	0.921698	0.874424	0.897606	0.918210	0.953148	0.981527	1.004864	1.023954
2.97	0.907627	0.932067	0.762530	0.780038	0.795548	0.821746	0.842931	0.860292	0.874453
2.2	0.796217	0.940456	0.683475	0.697211	0.709348	0.729781	0.746246	0.7597	0.77065
1.73	0.71694	0.947229	0.626205	0.637345	0.647168	0.663663	0.676916	0.687722	0.6965

Table 15.6 Predicted deviations ε of wall similarity temperature gradient from the numerical solutions

Pr_∞	t_∞, °C	$Mc_{x,\infty} = 0.6$						
		Pr_w						
		12.99	9.3	6.96	4.32	2.97	2.2	1.73
		ε						
12.99	0	−0.011431	0.000609	0.004510	0.00268	−0.00035	−0.00438	−0.00893
9.3	10	−0.012576	−0.00039	0.005049	0.006123	0.00295	−0.00103	−0.00561
6.96	20	−0.008295	0.00221	0.006313	0.008037	0.005518	0.001586	−0.00339
4.32	40	−0.00370	0.003888	0.007668	0.008096	0.006741	0.003006	−0.00206
2.97	60	−0.005907	0.000555	0.003877	0.005398	0.003367	0.000321	−0.00439
2.2	80	−0.014328	−0.00803	−0.004572	−0.00234	−0.00335	−0.00602	−0.01004
1.73	100	−0.026460	−0.0197	−0.015694	−0.01226	−0.01217	−0.01382	−0.01722

15.3.3 For $\mathbf{Mc_{x,\infty}} = 0.6$

For $Mc_{x,\infty}$ = 0.6, the coefficients and exponents a_1, a_2, b_1 and b_2, as well as the calculation results for the wall similarity temperature gradient are listed as below.

Compared with the corresponding numerical solutions at $Mc_{x,\infty} = 0.6$ reported in Chap. 12, the deviations of the predicted data in Table 15.5 for the wall similarity temperature gradient of laminar mixed convection of water on a vertical flat plate are evaluated, and shown in Table 15.6.

It is seen from Table 15.6 that the maximum predicted deviation by using the present correlation equations for laminar mixed convection of water on a vertical flat plate is less than 1.72 % at $Mc_{x,\infty} = 0.6$.

15.3.4 For $\mathbf{Mc_{x,\infty}} = 1$

For $Mc_{x,\infty}$ = 1, the coefficients and exponents a_1, a_2, b_1 and b_2, as well as the calculation results for the wall similarity temperature gradient are listed in Table 15.7.

Compared with the corresponding numerical solutions at $Mc_{x,\infty} = 1$ reported in Chap. 12, the deviations of the predicted data in Table 15.7 for the wall similarity temperature gradient of laminar mixed convection of water on a vertical flat plate are evaluated, and shown in Table 15.8.

It is seen from Table 15.8 that the maximum predicted deviation by using the present correlation equations for laminar mixed convection of water on a vertical flat plate is less than 1.71 % at $Mc_{x,\infty} = 1$.

15.3.5 For $\mathbf{Mc_{x,\infty}} = 3$

For $Mc_{x,\infty}$ = 3, the coefficients and exponents a_1, a_2, b_1 and b_2, as well as the calculation results for the wall similarity temperature gradient are listed in Table 15.9.

Compared with the corresponding numerical solutions at $Mc_{x,\infty} = 3$ reported in Chap. 12, the deviations of the predicted data in Table 15.9 for the wall temperature gradient of laminar mixed convection of water on a vertical flat plate are evaluated, and shown in Table 15.10.

It is seen from Table 15.10 that the maximum predicted deviation by using the present correlation equations for laminar mixed convection of water on a vertical flat plate is less than 1.92 % at $Mc_{x,\infty} = 3$.

Table 15.7 Predicted results of the wall similarity temperature gradient

Pr_∞	a	b	$Mc_{x,\infty} = 1$						
			$a_1 = 0.614225$, $a_2 = 0.4191$, $b_1 = 0.9699$, $b_2 = 0.97185$						
			Pr_w						
			12.99	9.3	6.96	4.32	2.97	2.2	1.73
			$\left(-\frac{\partial\theta(\eta,Mc_{x,\infty})}{\partial\eta}\right)_{\eta=0} = a\frac{Pr_w^b}{Pr_w}$						
12.99	1.799041	0.902358	1.400574	1.447026	1.488562	1.559521	1.617634	1.665736	1.705288
9.3	1.563935	0.910886	1.244459	1.282075	1.315620	1.37274	1.41935	1.457821	1.48938
6.96	1.385049	0.918348	1.123407	1.154481	1.182128	1.229071	1.267254	1.298691	1.324428
4.32	1.134119	0.930761	0.949627	0.971856	0.991555	1.024845	1.051781	1.073865	1.091884
2.97	0.969303	0.94063	0.832424	0.849104	0.863841	0.888651	0.908641	0.924975	0.938268
2.2	0.854746	0.94861	0.749218	0.762196	0.773633	0.792829	0.808243	0.820805	0.831005
1.73	0.772845	0.95505	0.688708	0.699132	0.708299	0.723648	0.735939	0.745934	0.754036

Table 15.8 Predicted deviations ε of wall temperature temperature gradient from the numerical solutions

Pr_∞	t_∞, °C	$Mc_{x,\infty} = 1$						
		Pr_w						
		12.99	9.3	6.96	4.32	2.97	2.2	1.73
		t_w, °C						
		0	10	20	40	60	80	100
		ε						
12.99	0	−0.007724	0.007554	0.011423	0.008263	0.002283	−0.00302	−0.00937
9.3	10	−0.011499	0.001203	0.007741	0.008337	0.004488	−0.0007	−0.00661
6.96	20	−0.007592	0.003338	0.007258	0.009315	0.005954	0.00137	−0.00451
4.32	40	−0.001576	0.005778	0.009218	0.009362	0.007299	0.003132	−0.0023
2.97	60	−0.001361	0.004272	0.006964	0.007611	0.005387	0.001609	−0.0033
2.2	80	−0.007275	−0.00216	0.000423	0.001454	−0.00025	−0.00326	−0.0075
1.73	100	−0.017104	−0.01177	−0.008831	−0.00687	−0.00763	−0.00976	−0.01326

Table 15.9 Predicted results of the wall similarity temperature gradient

Pr_∞	a	b	$Mc_{x,\infty} = 3$						
			$a_1 = 0.765231$, $a_2 = 0.3863$, $b_1 = 0.98$, $b_2 = 0.975625$						
			Pr_w						
			12.99	9.3	6.96	4.32	2.97	2.2	1.73
			$\left(-\frac{\partial\theta(\eta,Mc_{x,\infty})}{\partial\eta}\right)_{\eta=0} = a\frac{Pr_w^b}{Pr_w}$						
12.99	2.060534	0.920623	1.681066	1.726253	1.766428	1.834582	1.889965	1.935527	1.972806
9.3	1.810996	0.928152	1.506286	1.542888	1.575354	1.63027	1.674754	1.711257	1.741063
6.96	1.61917	0.934733	1.369652	1.399853	1.426585	1.47169	1.508124	1.537955	1.562269
4.32	1.346728	0.945662	1.171573	1.19304	1.211978	1.243796	1.26938	1.290249	1.307209
2.97	1.165248	0.954339	1.036501	1.052438	1.066458	1.089937	1.108745	1.124043	1.136446
2.2	1.037697	0.961346	0.939776	0.951994	0.962720	0.980632	0.994939	1.006548	1.015942
1.73	0.945692	0.966994	0.868948	0.878585	0.887030	0.901104	0.912317	0.921399	0.928737

Table 15.10 Predicted deviations ε of wall similarity temperature gradient from the numerical solutions

Pr_∞	t_∞, °C	$Mc_{x,\infty} = 3$						
		Pr_w						
		12.99	9.3	6.96	4.32	2.97	2.2	1.73
		t_w, °C						
		0	10	20	40	60	80	100
		ε						
12.99	0	−0.004935	0.014347	0.019223	0.015603	0.006988	−0.00137	−0.01027
9.3	10	−0.013114	0.002724	0.009404	0.010012	0.004932	−0.00163	−0.00918
6.96	20	−0.010109	0.002161	0.006538	0.008788	0.004952	−0.00053	−0.00723
4.32	40	9.091E-05	0.0071	0.010026	0.009805	0.00717	0.002773	−0.00283
2.97	60	0.005567	0.010126	0.011660	0.011151	0.008647	0.004306	−0.00057
2.2	80	0.004729	0.00852	0.009392	0.008805	0.006287	0.003232	−0.00119
1.73	100	−0.000571	0.003334	0.004137	0.004134	0.002356	−0.00019	−0.00334

Table 15.11 Predicted results of the wall temperature gradient

Pr_∞	a	b	$Mc_{x,\infty} = 6$						
			$a_1 = 0.889273$, $a_2 = 0.3731$, $b_1 = 0.980686$, $b_2 = 0.977886$						
			Pr_w						
			12.99	9.3	6.96	4.32	2.97	2.2	1.73
			$\left(-\frac{\partial\theta(\eta,Mc_{x,\infty})}{\partial\eta}\right)_{\eta=0} = a\frac{Pr_w^b}{Pr_w}$						
12.99	2.314849	0.926624	1.917833	1.965438	2.007685	2.079187	2.137144	2.184727	2.223596
9.3	2.043507	0.933497	1.723129	1.761851	1.796140	1.854021	1.9008	1.939117	1.970359
6.96	1.834056	0.939499	1.570502	1.602577	1.630926	1.678671	1.717159	1.748622	1.774233
4.32	1.535091	0.94946	1.348506	1.371473	1.391711	1.425664	1.452918	1.475123	1.49315
2.97	1.334813	0.95736	1.196566	1.213737	1.228830	1.254076	1.274273	1.290683	1.303978
2.2	1.193419	0.963735	1.087447	1.100705	1.112336	1.131741	1.147225	1.159779	1.169931
1.73	1.091064	0.968871	1.007359	1.017893	1.027118	1.042481	1.054711	1.06461	1.072605

Table 15.12 Predicted deviations ε of wall similarity temperature gradient from the numerical solutions

Pr_∞	t_∞, °C	$Mc_{x,\infty} = 6$						
		Pr_w						
		12.99	9.3	6.96	4.32	2.97	2.2	1.73
		ε						
12.99	0	−0.010847	0.011785	0.017814	0.014983	0.006762	−0.00212	−0.01157
9.3	10	−0.022143	−0.00438	0.003823	0.005749	0.00134	−0.00493	−0.0125
6.96	20	−0.019451	−0.00589	−0.000784	0.00301	−2.8E-05	−0.00493	−0.01132
4.32	40	−0.008118	−0.00063	0.003001	0.003335	0.002005	−0.00178	−0.00676
2.97	60	−0.000970	0.00371	0.005876	0.006169	0.004256	0.00085	−0.00332
2.2	80	−0.000215	0.003376	0.005013	0.005135	0.003377	0.000814	−0.00258
1.73	100	−0.004083	−0.00062	0.001112	0.001768	0.00073	−0.00105	−0.00384

15.3.6 *For* $\mathbf{Mc_{x,\infty}} = 6$

For $Mc_{x,\infty}$ = 6, the coefficients and exponents a_1, a_2, b_1 and b_2 as well as the calculation results for the wall similarity temperature gradient are listed in Table 15.11.

Compared with the corresponding numerical solutions at $Mc_{x,\infty} = 6$ reported in Chap. 12, the deviations of the predicted data in Table 15.11 for the wall temperature gradient of laminar mixed convection of water on a vertical flat plate are evaluated, and shown in Table 15.12.

It is seen from Table 15.12 that the maximum predicted deviation by using the present correlation equations for laminar mixed convection of water on a vertical flat plate is less than 1.95 % at $Mc_{x,\infty} = 6$.

15.3.7 *For* $\mathbf{Mc_{x,\infty}} = 10$

For $Mc_{x,\infty}$ = 10, the coefficients and exponents a_1, a_2, b_1 and b_2, as well as the calculation results for the wall similarity temperature gradient are listed in Table 15.13.

Compared with the corresponding numerical solutions at $Mc_{x,\infty} = 10$ reported in Chap. 12, the deviations of the predicted data in Table 15.13 for the wall similarity temperature gradient of laminar mixed convection of water on a vertical flat plate are evaluated, and shown in Table 15.14.

It is seen from Table 14.14 that the maximum predicted deviation by using the present correlation equations for laminar mixed convection of water on a vertical flat plate is less than 2.1 % at $Mc_{x,\infty} = 10$.

It is seen that the prediction of the wall similarity temperature gradient of laminar mixed convection of water on a vertical flat plate is so reliable that the maximum evaluation deviation is lower than 3 % for $0 \leq Mc_{x,\infty} \leq 10$ compared with the related systems of numerical solution. Meanwhile, there are 94 % of the evaluated values of the wall similarity temperature gradient with the predicted deviation which is located under 2 %.

On the other hand, all such systems of numerical solutions are based on consideration of coupled effect of variable physical properties, and then, have solid theoretical and practical value. Therefore the provided optimal formalized equations of Nusselt number based on the systems of numerical solutions have solid theoretical and practical value too.

Table 15.13 Predicted results of the wall similarity temperature gradient

Pr_∞	a	b	$Mc_{x,\infty} = 10$						
			a_1 = 1.002466, a_2 = 0.363136, b_1 = 0.983564, b_2 = 0.979745						
			Pr_w						
			12.99	9.3	6.96	4.32	2.97	2.2	1.73
			$\left(-\frac{\partial\theta(\eta,Mc_{x,\infty})}{\partial\eta}\right)_{\eta=0} = a\frac{Pr_w^b}{Pr_w}$						
12.99	2.543673	0.933784	2.146459	2.194483	2.237006	2.308778	2.366776	2.414279	2.453007
9.3	2.252997	0.940126	1.932343	1.971395	2.005904	2.064009	2.110837	2.149109	2.180258
6.96	2.027923	0.945661	1.764165	1.796492	1.825009	1.872923	1.911448	1.942874	1.968413
4.32	1.705441	0.954841	1.518962	1.542058	1.562374	1.596389	1.623631	1.645785	1.663745
2.97	1.488485	0.962115	1.350689	1.367897	1.383000	1.408216	1.428348	1.444681	1.457895
2.2	1.334798	0.967981	1.229586	1.242813	1.254400	1.273703	1.289076	1.301522	1.311577
1.73	1.223243	0.972705	1.140556	1.151006	1.160148	1.175349	1.187432	1.197199	1.205078

Table 15.14 Predicted deviations ε of wall similarity temperature gradient from the numerical solutions

Pr_∞	$Mc_{x,\infty} = 10$						
	Pr_w						
	12.99	9.3	6.96	4.32	2.97	2.2	1.73
	ε						
12.99	−0.007459	0.015131	0.020961	0.017043	0.007467	−0.00289	−0.01362
9.3	−0.019996	−0.0025	0.005245	0.006137	0.000753	−0.0066	−0.01487
6.96	−0.016924	−0.00399	0.000644	0.003269	−0.00061	−0.0062	−0.01323
4.32	−0.004296	0.002319	0.005292	0.004955	0.002446	−0.00193	−0.00739
2.97	0.004279	0.008045	0.009522	0.008773	0.00623	0.002251	−0.00224
2.2	0.006383	0.009063	0.010038	0.009151	0.00673	0.003745	8.13E-05
1.73	0.003694	0.006248	0.007358	0.007041	0.005373	0.003196	5.32E-05

15.4 Calculation Example 1

15.4.1 Question

A flat plate with $b = 0.1$ m in width and $x = 0.10$ m in length is suspended vertically in the space of water. The bulk velocity is $w_{x,\infty} = 0.1$ m/s parallel to plate (see Fig. 3.1). The bulk temperature is $t_\infty = 0$ °C, and the plate temperature is $t_w = 20$ °C. Suppose the mixed convection is laminar, please calculate the mixed convection heat transfer on the plate.

15.4.2 Solution

1. Analysis of heat transfer calculation

The theoretical equations of average Nusselt number of laminar water mixed convection are expressed as follows:

The average Nusselt number with definition $\overline{Nu}_{x,w} = \frac{\overline{\alpha_{x,w}} \cdot x}{\lambda_w}$ is expressed as

$$\overline{Nu}_{x,w} = \sqrt{2}(Re_{x,\infty})^{1/2}\left(-\frac{\partial\theta(\eta, Mc_{x,\infty})}{\partial\eta}\right)_{\eta=0}$$

Here, the wall similarity temperature gradient $(-\frac{\partial\theta(\eta,Mc)}{\partial\eta})_{\eta=0}$ is the only unknown variable. Then, evaluation of Nusselt number is attributed to the issue for evaluation of the wall similarity temperature gradient. It can be expressed as

$$\left(-\frac{\partial\theta(\eta, Mc_{x,\infty})}{\partial\eta}\right)_{\eta=0} = a\,Pr_w^{b-1}$$

where

$$a = a_1 Pr_\infty^{a_2}$$

$$b = b_1 Pr_\infty^{b_2}$$

where the coefficients and exponents a_1, a_2, b_1 and b_2 are evaluated by the following equations:

$$a_1 = \frac{0.0003Mc_{x,\infty}^3 - 0.0053Mc_{x,\infty}^2 + 0.583Mc_{x,\infty} + 0.455}{(1 + Mc_{x,\infty})^{0.75}}$$

$$a_2 = \frac{-0.0002Mc_{x,\infty}^3 + 0.0024Mc_{x,\infty}^2 + 0.3465Mc_{x,\infty} + 0.4895}{1 + Mc_{x,\infty}}$$

$$b_1 = \frac{0.0003Mc_{x,\infty}^3 - 0.0047Mc_{x,\infty}^2 + 1.005Mc_{x,\infty} + 0.9392}{1 + Mc_{x,\infty}}$$

$$b_2 = \frac{0.0003Mc_{x,\infty}^2 + 0.9782Mc_{x,\infty} + 0.9652}{1 + Mc_{x,\infty}}$$

From the above complete correlation equations for optimal equations of Nusselt number, it is clear how to calculate heat transfer of laminar water mixed convection.

2. Decision of physical properties and parameters, namely local Prandtl number Pr_w, local Prandtl number Pr_∞ and local mixed convection parameter $Mc_{x,\infty}$.

According to the Appendix we have Pr_w = 6.96 at t_w = 20 °C, Pr_∞ = 12.99 at t_∞ = 0 °C for water.

For local mixed convection parameter $Mc_{x,\infty}$ we have

$$Mc = Gr_{x,\infty}Re_{x,\infty}^{-2}$$

where

$$Re_{x,\infty} = \frac{w_{x,\infty}x}{v_\infty} \quad \text{and} \quad Gr_{x,\infty} = \frac{g(\rho_\infty/\rho_w - 1)x^3}{v_\infty^2}$$

Here, some telated local physical properties need to be determined.

According to the Appendix we have $\lambda_w = 0.602\,\mathrm{W/(m\,°C)}$ and ρ_w = 998.2 kg/m^3 at t_w = 20 °C, and ρ_∞ = 999.9 kg/m^3 and $v_\infty = 1.7527 \times 10^{-6}\,\mathrm{m^2/s}$ at t_∞ = 0 °C. Then,

$$Re_{x,\infty} = \frac{w_{x,\infty}x}{v_\infty} = \frac{0.1 \times 0.1}{1.7527 \times 10^{-6}} = 5705.5$$

$$Gr_{x,\infty} = \frac{g(\rho_\infty/\rho_w - 1)x^3}{v_\infty^2} = \frac{9.8 \times (999.9/998.2 - 1) \times 0.1^3}{(1.7527 \times 10^{-6})^2} = 5,433,031.9$$

$$Mc_{x,\infty} = Gr_{x,\infty}Re_{x,\infty}^{-2} = 5,433,031.9/5705.5^2 = 0.1669$$

3. Evaluation of the wall similarity temperature gradient.

$$
\begin{aligned}
a_1 &= \frac{0.0003Mc_{x,\infty}^3 - 0.0053Mc_{x,\infty}^2 + 0.583Mc_{x,\infty} + 0.455}{(1+Mc_{x,\infty})^{0.75}} \\
&= \frac{0.0003 \times 0.1669^3 - 0.0053 \times 0.1669^2 + 0.583 \times 0.1669 + 0.455}{(1+0.1669)^{0.75}} \\
&= 0.507137 \\
a_2 &= \frac{-0.0002Mc_{x,\infty}^3 + 0.0024Mc_{x,\infty}^2 + 0.3465Mc_{x,\infty} + 0.4895}{1+Mc_{x,\infty}} \\
&= \frac{-0.0002 \times 0.1669^3 + 0.0024 \times 0.1669^2 + 0.3465 \times 0.1669 + 0.4895}{1+0.1669} \\
&= 0.469103 \\
b_1 &= \frac{0.0003Mc_{x,\infty}^3 - 0.0047Mc_{x,\infty}^2 + 1.005Mc_{x,\infty} + 0.9392}{1+Mc_{x,\infty}} \\
&= \frac{0.0003 \times 0.1669^3 - 0.0047 \times 0.1669^2 + 1.005 \times 0.1669 + 0.9392}{1+0.1669} \\
&= 0.948500 \\
b_2 &= \frac{0.0003Mc_{x,\infty}^2 + 0.9782Mc_{x,\infty} + 0.9652}{1+Mc_{x,\infty}} \\
&= \frac{0.0003 \times 0.1669^2 + 0.9782 \times 0.1669 + 0.9652}{1+0.1669} \\
&= 0.9670665
\end{aligned}
$$

Then,

$$
\begin{aligned}
a &= a_1 Pr_\infty^{a_2} = 0.507137 \times 12.99^{0.469103} = 1.688584 \\
b &= b_1 \frac{Pr_\infty^{b_2}}{Pr_\infty} = 0.948500 \times \frac{12.99^{0.9670665}}{12.99} = 0.871692 \\
\left(-\frac{\partial\theta(\eta, Mc_{x,\infty})}{\partial\eta}\right)_{\eta=0} &= a\frac{Pr_w^b}{Pr_w} = 1.688584 \times \frac{6.96^{0.871692}}{6.96} = 1.316465
\end{aligned}
$$

4. Evaluation of heat transfer from the plate

The average Nusselt number with definition $\overline{Nu}_{x,w} = \frac{\overline{\alpha_{x,w}} \cdot x}{\lambda_w}$ is calculated by

$$
\overline{Nu}_{x,w} = \sqrt{2}(Re_{x,\infty})^{1/2}\left(-\frac{\partial\theta(\eta, Mc_{x,\infty})}{\partial\eta}\right)_{\eta=0}
$$

Then,

$$\begin{aligned}
\overline{Nu}_{x,w} &= \sqrt{2}(Re_{x,\infty})^{1/2}\left(-\frac{\partial\theta(\eta, Mc_{x,\infty})}{\partial\eta}\right)_{\eta=0} \\
&= \sqrt{2}(5705.5)^{1/2} \times 1.316465 \\
&= 140.6278 \\
Q_x &= \bar{\alpha}_x(t_w - t_\infty) \times x \times b \\
&= \frac{\lambda_w}{x}\overline{Nu}_{x,w}(t_w - t_\infty) \times x \times b \\
&= \lambda_w \overline{Nu}_{x,w}(t_w - t_\infty) \times b \\
&= 0.602 \times 140.6278 \times (20 - 0) \times 0.1 \\
&= 169.3W
\end{aligned}$$

Question 1 here in this chapter is actually same as the question 1 in Chap. 6. From the calculated results it is seen that the deviation of heat transfer rate Q_x for consideration of Boussinesq approximation is 8.39 % to that for consideration of fluid's variable physical properties. It clearly proves that Boussinesq approximation or ignoring fluid's variable physical properties will severely weaken the theoretical and practical value for study of convection heat transfer, and only reasonable consideration of coupled effect of variable physical properties has the theoretical and practical value.

15.5 Calculation Example 2

15.5.1 Question

All geometric and physical conditions in example 1 are kept in the present question except t_w= 40 °C. Suppose the mixed convection is laminar, please calculate the mixed convection heat transfer on the plate.

15.5.2 Solution

1. Heat transfer analysis is same as that in the above solution.
2. Decision of some local physical properties and parameters.

According to the Appendix we have Pr_w = 4.32 at t_w = 40 °C, Pr_∞ = 12.99 at t_∞ = 0 °C for water.

For local mixed convection parameter $Mc_{x,\infty}$ we have

$$Mc = Gr_{x,\infty}Re_{x,\infty}^{-2}$$

where

$$Re_{x,\infty} = \frac{w_{x,\infty} x}{v_\infty} \quad \text{and} \quad Gr_{x,\infty} = \frac{g(\rho_\infty/\rho_w - 1)x^3}{v_\infty^2}$$

According to the Appendix we have $\lambda_w = 0.630\,\mathrm{W/(m\,°C)}$ and $\rho_w = 992.2\,\mathrm{kg/m^3}$ at $t_w = 40$ °C, and $\rho_\infty = 999.9\,\mathrm{kg/m^3}$ and $v_\infty = 1.7527 \times 10^{-6}\,\mathrm{m^2/s}$ at $t_\infty = 0$ °C. Then,

$$Re_{x,\infty} = \frac{w_{x,\infty} x}{v_\infty} = \frac{0.1 \times 0.1}{1.7527 \times 10^{-6}} = 5705.5$$

$$Gr_{x,\infty} = \frac{g(\rho_\infty/\rho_w - 1)x^3}{v_\infty^2} = \frac{9.8 \times (999.9/992.2 - 1) \times 0.1^3}{(1.7527 \times 10^{-6})^2} = 24,757,250$$

$$Mc_{x,\infty} = Gr_{x,\infty} Re_{x,\infty}^{-2} = 24,757,250/5705.5^2 = 0.760528$$

3. Evaluation of the wall similarity temperature gradient.

$$a_1 = \frac{0.0003Mc_{x,\infty}^3 - 0.0053Mc_{x,\infty}^2 + 0.583Mc_{x,\infty} + 0.455}{(1 + Mc_{x,\infty})^{0.75}}$$

$$= \frac{0.0003 \times 0.760528^3 - 0.0053 \times 0.760528^2 + 0.583 \times 0.760528 + 0.455}{(1 + 0.760528)^{0.75}}$$

$$= 0.585883$$

$$a_2 = \frac{-0.0002Mc_{x,\infty}^3 + 0.0024Mc_{x,\infty}^2 + 0.3465Mc_{x,\infty} + 0.4895}{1 + Mc_{x,\infty}}$$

$$= \frac{-0.0002 \times 0.760528^3 + 0.0024 \times 0.760528^2 + 0.3465 \times 0.760528 + 0.4895}{1 + 0.760528}$$

$$= 0.428464$$

$$b_1 = \frac{0.0003Mc_{x,\infty}^3 - 0.0047Mc_{x,\infty}^2 + 1.005Mc_{x,\infty} + 0.9392}{1 + Mc_{x,\infty}}$$

$$= \frac{0.0003 \times 0.760528^3 - 0.0047 \times 0.760528^2 + 1.005 \times 0.760528 + 0.9392}{1 + 0.760528}$$

$$= 0.966156$$

$$b_2 = \frac{0.0003Mc_{x,\infty}^2 + 0.9782Mc_{x,\infty} + 0.9652}{1 + Mc_{x,\infty}}$$

$$= \frac{0.0003 \times 0.760528^2 + 0.9782 \times 0.760528 + 0.9652}{1 + 0.760528}$$

$$= 0.970914$$

Then,

$$a = a_1 Pr_\infty^{a_2} = 0.585883 \times 12.99^{0.428464} = 1.757731$$
$$b = b_1 \frac{Pr_\infty^{b_2}}{Pr_\infty} = 0.966156 \times \frac{12.99^{0.970914}}{12.99} = 0.89672$$
$$\left(-\frac{\partial\theta(\eta, Mc_{x,\infty})}{\partial\eta}\right)_{\eta=0} = a\frac{Pr_w^b}{Pr_w} = 1.757731 \times \frac{4.32^{0.89672}}{4.32} = 1.511192$$

4. Evaluation of heat transfer from the plate

The average Nusselt number defined as $\overline{Nu}_{x,w} = \frac{\overline{\alpha}_{x,w} \cdot x}{\lambda_w}$ is evaluated by

$$\overline{Nu}_{x,w} = \sqrt{2}(Re_{x,\infty})^{1/2}\left(-\frac{\partial\theta(\eta, Mc_{x,\infty})}{\partial\eta}\right)_{\eta=0}$$

Then,

$$\begin{aligned}
\overline{Nu}_{x,w} &= \sqrt{2}(Re_{x,\infty})^{1/2}\left(-\frac{\partial\theta(\eta, Mc_{x,\infty})}{\partial\eta}\right)_{\eta=0} \\
&= \sqrt{2}(5705.5)^{1/2} \times 1.511192 \\
&= 161.429 \\
Q_x &= \bar{\alpha}_x(t_w - t_\infty) \times x \times b \\
&= \frac{\lambda_w}{x}\overline{Nu}_{x,w}(t_w - t_\infty) \times x \times b \\
&= \lambda_w \overline{Nu}_{x,w}(t_w - t_\infty) \times b \\
&= 0.630 \times 161.429 \times (40 - 0) \times 0.1 \\
&= 406.8W
\end{aligned}$$

Question 2 here in this chapter is actually same as the question 2 in Chap. 6. From the calculated results it is seen that the deviation of heat transfer rate Q_x for consideration of Boussinesq approximation is 5.28 % to that for consideration of fluid's variable physical properties.

15.6 Calculation Example 3

15.6.1 Question

All geometric and physical conditions in example 1 are kept except t_w = 40 °C and t_∞ = 20 °C. Suppose the mixed convection is laminar, please calculate the mixed convection heat transfer on the plate.

15.6.2 Solution

1. Heat transfer analysis is same as that in the above solution.
2. Decision of some local physical properties and parameters.

According to the Appendix we have Pr_w = 4.32 at t_w = 40 °C, Pr_∞ = 6.96 at t_∞ = 20 °C for water.

For local mixed convection parameter $Mc_{x,\infty}$ we have

$$Mc_{x,\infty} = Gr_{x,\infty} Re_{x,\infty}^{-2}$$

where

$$Re_{x,\infty} = \frac{w_{x,\infty} x}{v_\infty} \quad \text{and} \quad Gr_{x,\infty} = \frac{g(\rho_\infty/\rho_w - 1)x^3}{v_\infty^2}$$

Here, the physical properties ρ_∞, ρ_w and v_∞ need to be determined.

According to the Appendix we have $\lambda_w = 0.630\,\mathrm{W/(m\,°C)}$ and $\rho_w = 992.2\,\mathrm{kg/m^3}$ at t_w = 40 °C, and $\rho_\infty = 998.2\,\mathrm{kg/m^3}$ and $v_\infty = 1.0033 \times 10^{-6}\,\mathrm{m^2/s}$ at t_∞ = 20 °C. Then,

$$Re_{x,\infty} = \frac{w_{x,\infty} x}{v_\infty} = \frac{0.1 \times 0.1}{1.0033 \times 10^{-6}} = 9967$$

$$Gr_{x,\infty} = \frac{g(\rho_\infty/\rho_w - 1)x^3}{v_\infty^2} = \frac{9.8 \times (998.2/992.2 - 1) \times 0.1^3}{(1.0033 \times 10^{-6})^2} = 58,873,042$$

$$Mc_{x,\infty} = Gr_{x,\infty} Re_{x,\infty}^{-2} = 58,873,042/9967^2 = 0.5926$$

3. Evaluation of the wall similarity temperature gradient.

$$a_1 = \frac{0.0003Mc_{x,\infty}^3 - 0.0053Mc_{x,\infty}^2 + 0.583Mc_{x,\infty} + 0.455}{(1+Mc_{x,\infty})^{0.75}}$$
$$= \frac{0.0003 \times 0.5926^3 - 0.0053 \times 0.5926^2 + 0.583 \times 0.5926 + 0.455}{(1+0.5926)^{0.75}}$$
$$= 0.563374$$
$$a_2 = \frac{-0.0002Mc_{x,\infty}^3 + 0.0024Mc_{x,\infty}^2 + 0.3465Mc_{x,\infty} + 0.4895}{1+Mc_{x,\infty}}$$
$$= \frac{-0.0002 \times 0.5926^3 + 0.0024 \times 0.5926^2 + 0.3465 \times 0.5926 + 0.4895}{1+0.5926}$$
$$= 0.436793$$
$$b_1 = \frac{0.0003Mc_{x,\infty}^3 - 0.0047Mc_{x,\infty}^2 + 1.005Mc_{x,\infty} + 0.9392}{1+Mc_{x,\infty}}$$
$$= \frac{0.0003 \times 0.5926^3 - 0.0047 \times 0.5926^2 + 1.005 \times 0.5926 + 0.9392}{1+0.5926}$$
$$= 0.962687$$
$$b_2 = \frac{0.0003Mc_{x,\infty}^2 + 0.9782Mc_{x,\infty} + 0.9652}{1+Mc_{x,\infty}}$$
$$= \frac{0.0003 \times 0.5926^2 + 0.9782 \times 0.5926 + 0.9652}{1+0.5926}$$
$$= 0.970103$$

Then,

$$a = a_1 Pr_\infty^{a_2} = 0.563374 \times 6.96^{0.436793} = 1.314238$$
$$b = b_1 \frac{Pr_\infty^{b_2}}{Pr_\infty} = 0.962687 \times \frac{6.96^{0.970103}}{6.96} = 0.908434$$
$$\left(-\frac{\partial\theta(\eta, Mc_{x,\infty})}{\partial\eta}\right)_{\eta=0} = a\frac{Pr_w^b}{Pr_w} = 1.314238 \times \frac{4.32^{0.908434}}{4.32} = 1.14903$$

4. Evaluation of heat transfer from the plate

From Chap. 11, we have

The average Nusselt number defined as $\overline{Nu}_{x,w} = \frac{\overline{\alpha}_{x,w} \cdot x}{\lambda_w}$ can be calculated by

$$\overline{Nu}_{x,w} = \sqrt{2}(Re_{x,\infty})^{1/2}\left(-\frac{\partial\theta(\eta, Mc_{x,\infty})}{\partial\eta}\right)_{\eta=0}$$

Then,

$$\begin{aligned}
\overline{Nu}_{x,w} &= \sqrt{2}(Re_{x,\infty})^{1/2}\left(-\frac{\partial\theta(\eta, Mc_{x,\infty})}{\partial\eta}\right)_{\eta=0} \\
&= \sqrt{2}(9967)^{1/2} \times 1.14903 \\
&= 162.23 \\
Q_x &= \bar{\alpha}_x(t_w - t_\infty) \times x \times b \\
&= \frac{\lambda_w}{x}\overline{Nu}_{x,w}(t_w - t_\infty) \times x \times b \\
&= \lambda_w \overline{Nu}_{x,w}(t_w - t_\infty) \times b \\
&= 0.630 \times 162.23 \times (40 - 20) \times 0.1 \\
&= 204.41\,\text{W}
\end{aligned}$$

Question 3 here in this chapter is actually same as the question 3 in Chap. 6. From the calculated results it is seen that the deviation of heat transfer rate Q_x for consideration of Boussinesq approximation is 4.2 % to that for consideration of fluid's variable physical properties.

Comparing the evaluated results on heat transfer by using the optimal formalized equations in this chapter for consideration of variable physical properties with those in Chap. 6 evaluated by using the optimal formalized equations for consideration Boussinesq approximation, the following conclusions can be obtained:

Boussinesq approximation will lead to the evaluation deviation of heat transfer because the variable physical properties are not taken into account. Such evaluation deviation of heat transfer will increase with decreasing the bulk temperature t_∞ (i.e. increasing Pr_∞), and can be up to over 8 % for a lower bulk temperature t_∞. In addition, the evaluation deviation of heat transfer will increase with decreasing the wall temperature t_w (i.e. increasing Pr_w) also. However, the effect of the bulk temperature t_∞ on heat transfer coefficient much higher than that of the wall temperature t_w. It clearly proves that Boussinesq approximation or ignoring fluid's variable physical properties will severely weaken the theoretical and practical value for study of convection heat transfer, and only reasonable consideration of coupled effect of variable physical properties has the theoretical and practical value. Therefore, it is necessary to consider coupled effect of variable physical properties for assurance of the theoretical and practical value of the research on convection heat transfer.

15.7 Remarks

In this chapter, the accuracy of the formulated correlation equations on the wall similarity temperature gradient was verified by using the comparison to the system of numerical solutions. Furthermore, since such correlation equations are based on the numerical solutions related to consideration of coupled effect of variable

physical properties, it can be confirmed that the formulated correlation equations on the wall similarity temperature gradient and heat transfer of laminar water mixed convection have practical application value.

At the end of this chapter, a calculation example by using the formalized equations of Nusselt number on laminar water mixed convection was performed, and the following conclusions are obtained:

1. Boussinesq approximation will lead to evaluation deviation of heat transfer due to the variable physical properties are not taken into account. With increasing the difference $Pr_\infty - Pr_w$, such deviation will increase. The detailed regulation of the effect of the difference $Pr_\infty - Pr_w$ on the evaluation deviation of heat transfer need to be further investigated.
2. Boussinesq approximation or ignoring fluid's variable physical properties will severely weaken the theoretical and practical value for study of convection heat transfer, and only reasonable consideration of coupled effect of variable physical properties has the theoretical and practical value.

Appendix A
Tables with Physical Properties

Appendix A.1
Physical Properties of Gases at Atmospheric Pressure

T (K)	ρ (kg/m^3)	c_p [kJ/(kg °C)]	$\mu \times 10^6$ [kg/(m s)]	$v \times 10^6$ (m^2/s)	λ [W/(m °C)]	$a \times 10^6$ (m^2/s)	Pr
Air [1]							
100	3.5562	1.032	7.11	1.999	0.00934	2.54	0.786
150	2.3364	1.012	10.34	4.426	0.0138	5.84	0.758
200	1.7458	1.007	13.25	7.59	0.0181	10.3	0.737
250	1.3947	1.006	15.96	11.443	0.0223	15.9	0.720
300	1.1614	1.007	18.46	15.895	0.0263	22.5	0.707
350	0.9950	1.009	20.82	20.925	0.0300	29.9	0.7
400	0.8711	1.014	23.01	26.415	0.0338	38.3	0.69
450	0.7740	1.021	25.07	32.39	0.0373	47.2	0.686
500	0.6964	1.030	27.01	38.785	0.0407	56.7	0.684
550	0.6329	1.040	28.84	45.568	0.0439	66.7	0.683
600	0.5804	1.051	30.58	52.688	0.0469	76.9	0.685
650	0.5356	1.063	32.25	60.213	0.0497	87.3	0.69
700	0.4975	1.075	33.88	68.101	0.05240	98	0.695
750	0.4643	1.087	35.46	76.373	0.0549	109	0.702
800	0.4354	1.099	36.98	84.933	0.0573	120	0.709
850	0.4097	1.11	38.43	93.8	0.0596	131	0.716
900	0.3868	1.121	39.81	102.921	0.0620	143	0.720
950	0.3666	1.131	41.13	112.193	0.0643	155	0.723
1000	0.3482	1.141	42.44	121.884	0.0667	168	0.726
1100	0.3166	1.159	44.9	141.819	0.0715	195	0.728
1200	0.2920	1.175	47.3	161.986	0.0763	224	0.728

(continued)

D.-Y. Shang and L.-C. Zhong, *Heat Transfer of Laminar Mixed Convection of Liquid*, Heat and Mass Transfer, DOI 10.1007/978-3-319-27959-6

T (K)	ρ (kg/m^3)	c_p [kJ/(kg °C)]	$\mu \times 10^6$ [kg/(m s)]	$\nu \times 10^6$ (m^2/s)	λ [W/(m °C)]	$a \times 10^6$ (m^2/s)	Pr
Monoxide, CO [1]							
200	1.6888	1.045	12.7	7.5201	0.017	9.63	0.781
220	1.5341	1.044	13.7	8.9303	0.0190	11.9	0.753
240	1.4055	1.043	14.7	10.4589	0.0206	14.1	0.744
260	1.2967	1.043	15.7	12.1077	0.0221	16.3	0.741
280	1.2038	1.042	16.6	13.7897	0.0236	18.8	0.733
300	1.1233	1.043	17.5	15.5791	0.025	21.3	0.730
320	1.0529	1.043	18.4	17.4755	0.0263	23.9	0.730
340	0.9909	1.044	19.3	19.4772	0.0278	26.9	0.725
360	0.9357	1.045	20.2	21.5881	0.0291	29.8	0.729
380	0.8864	1.047	21	23.6913	0.0305	32.9	0.719
400	0.8421	1.049	21.8	25.8877	0.0318	36.0	0.719
450	0.7483	1.055	23.7	31.6718	0.0350	44.3	0.714
500	0.67352	1.065	25.4	37.7123	0.0381	53.1	0.710
550	0.61226	1.076	27.1	44.2622	0.0411	62.4	0.710
600	0.56126	1.088	28.6	50.9568	0.0440	72.1	0.707
650	0.51806	1.101	30.1	58.1014	0.0470	82.4	0.705
700	0.48102	1.114	31.5	65.4858	0.0500	93.3	0.702
750	0.44899	1.127	32.9	73.2756	0.0528	104	0.702
800	0.42095	1.140	34.3	81.4824	0.0555	116	0.705
Helium, He [1]							
100	0.4871	5.193	9.63	19.77	0.073	28.9	0.686
120	0.406	5.193	10.7	26.36	0.0819	38.8	0.679
140	0.3481	5.193	11.8	33.90	0.0907	50.2	0.676
160	0.30945	5.193	12.9	41.69	0.0992	63.2	0.6745
180	0.2708	5.193	13.9	51.33	0.1072	76.2	0.673
200	0.2462	5.193	15	60.93	0.1151	91.6	0.674
220	0.2216	5.193	16	72.20	0.1231	107	0.675
240	0.20455	5.193	17	83.11	0.13	124	0.6785
260	0.1875	5.193	18	96	0.137	141	0.682
280	0.175	5.193	19	108.57	0.145	160.5	0.681
300	0.1625	5.193	19.9	122.46	0.152	180	0.68
350	0.1422	5.193	22.1	155.42	0.17	237.5	0.6775
400	0.1219	5.193	24.3	199.34	0.187	295	0.675
450	0.10972	5.193	26.3	239.70	0.204	364.5	0.6715
500	0.09754	5.193	28.3	290.14	0.22	434	0.668
600	0.083615	5.193	32	382.71	0.252	601	0.661
700	0.06969	5.193	35	502.22	0.278	768	0.654
800		5.193	38.2		0.304		
900		5.193	41.4		0.33		
1000	0.04879	5.193	44.6	914.12	0.354	1400	0.654

(continued)

T (K)	ρ (kg/m^3)	c_p [kJ/(kg °C)]	$\mu \times 10^6$ [kg/(m s)]	$\nu \times 10^6$ (m^2/s)	λ [W/(m °C)]	$a \times 10^6$ (m^2/s)	Pr
Hydrogen, H_2 [1]							
100	0.24255	11.23	4.21	19.77	0.067	24.6	0.707
200	0.12115	13.54	6.81	26.35	0.131	79.9	0.704
300	0.08078	14.31	8.96	33.90	0.183	158	0.701
400	0.06059	14.48	10.82	41.69	0.226	258	0.695
500	0.04848	14.52	12.64	51.33	0.266	378	0.691
600	0.0404	14.55	14.24	60.93	0.305	519	0.678
700	0.03463	14.61	15.78	72.20	0.342	676	0.675
800	0.0303	14.7	17.24	83.11	0.378	849	0.67
900	0.02694	14.83	18.65	96	0.412	1030	0.671
1000	0.02424	14.99	20.13	108.57	0.448	1230	0.673
1100	0.02204	15.17	21.3	122.46	0.488	1460	0.662
200	0.0202	15.37	22.62	155.41	0.528	1700	0.659
1300	0.01865	15.59	23.85	199.34	0.569	1955	0.655
1400	0.01732	15.81	25.07	239.70	0.61	2230	0.65
1500	0.01616	16.02	26.27	290.14	0.655	2530	0.643
1600	0.0152	16.28	27.37	382.70	0.697	2815	0.639
Nitrogen, N_2 [1]							
100	3.4388	1.07	6.88	2.000	0.0958	2.6	0.768
150	2.2594	1.05	10.06	4.45	0.0139	5.86	0.759
200	1.6883	1.043	12.02	7.126	0.0183	10.4	0.736
250	1.3488	1.042	15.49	11.48	0.0222	15.8	0.727
300	1.1233	1.041	17.82	15.86	0.0259	22.1	0.716
350	0.9625	1.042	20	20.78	0.0293	29.2	0.711
400	0.8425	1.045	22.04	26.16	0.0327	37.1	0.704
450	0.7485	1.05	23.96	32.01	0.0358	45.6	0.703
500	0.6739	1.056	25.77	38.24	0.0389	54.7	0.7
550	0.6124	1.065	27.47	44.86	0.0417	63.9	0.702
600	0.5615	1.075	29.08	51.79	0.0416	73.9	0.701
700	0.4812	1.098	32.1	66.71	0.0499	94.4	0.706
800	0.4211	1.122	34.91	82.91	0.0548	116	0.715
900	0.3743	1.146	37.53	100.27	0.0597	139	0.721
1000	0.3368	1.167	39.99	118.74	0.0647	165	0.721
1100	0.3062	1.187	42.32	138.21	0.07	193	0.718
1200	0.2807	1.204	44.53	158.64	0.0758	224	0.707
1300	0.2591	1.219	46.62	179.93	0.081	256	0.701
Oxygen, O_2 [1]							
100	3.945	0.962	7.64	1.936629	0.00925	2.44	0.796
150	2.585	0.921	11.48	4.441006	0.0138	5.8	0.766
200	1.93	0.915	14.75	7.642487	0.0183	10.4	0.737

(continued)

T (K)	ρ (kg/m^3)	c_p [kJ/(kg °C)]	$\mu \times 10^6$ [kg/(m s)]	$v \times 10^6$ (m^2/s)	λ [W/(m °C)]	$a \times 10^6$ (m^2/s)	Pr
250	1.542	0.915	17.86	11.58236	0.0226	16	0.723
300	1.284	0.92	20.72	16.13707	0.0268	22.7	0.711
350	1.1	0.929	23.35	21.22727	0.0296	29	0.733
400	0.962	0.942	25.82	26.83992	0.033	36.4	0.737
450	0.8554	0.956	28.14	32.89689	0.0363	44.4	0.741
500	0.7698	0.972	30.33	39.39984	0.0412	55.1	0.716
550	0.6998	0.988	32.4	46.29894	0.0441	63.8	0.726
600	0.6414	1.003	34.37	53.58591	0.0473	73.5	0.729
700	0.5498	1.031	38.08	69.26155	0.0523	93.1	0.744
800	0.481	1.054	41.52	86.32017	0.0589	116	0.743
900	0.4275	1.074	44.72	104.6082	0.0649	141	0.74
1000	0.3848	1.09	47.7	123.9605	0.071	169	0.733
1100	0.3498	1.103	50.55	144.5111	0.0758	196	0.736
1200	0.3206	1.115	53.25	166.0948	0.0819	229	0.725
1300	0.206	1.125	58.84	285.6311	0.0871	262	0.721
Carbon dioxide, CO_2 [1]							
220	2.4733	0.783	11.105	4.490	0.010805	5.92	0.818
250	2.1675	0.804	12.59	5.809	0.012884	7.401	0.793
300	1.7973	0.871	14.958	8.322	0.016572	10.588	0.77
350	1.5362	0.9	17.205	11.200	0.02047	14.808	0.755
400	1.3424	0.942	19.32	14.392	0.02461	19.463	0.738
450	1.1918	0.98	21.34	17.906	0.02897	24.813	0.721
500	1.0732	1.013	23.26	21.67	0.03352	30.84	0.702
550	0.9739	1.047	25.08	25.752	0.03821	37.5	0.695
600	0.8938	1.076	26.83	30.018	0.04311	44.83	0.668
Ammonia, NH_3 [2]							
220	0.3828	2.198	7.255	18.952	0.0171	20.54	0.93
273	0.7929	2.177	9.353	11.796	0.022	13.08	0.9
323	0.6487	2.177	11.035	17.011	0.027	19.2	0.88
373	0.559	2.236	12.886	23.052	0.0327	26.19	0.87
423	0.4934	2.315	14.672	29.736	0.0391	34.32	0.87
473	0.4405	2.395	16.49	37.435	0.0476	44.21	0.84
Water vapor [2]							
380	0.5863	2.06	1.271	2.168	0.0246	20.36	1.06
400	0.5542	2.014	1.344	2.425	0.0261	23.38	1.04
450	0.4902	1.98	1.525	3.111	0.0299	30.7	1.01
500	0.4405	1.985	1.704	3.868	0.0339	38.7	0.996
550	0.4005	1.997	1.884	4.704	0.0379	47.5	0.991
600	0.3652	2.026	2.067	5.660	0.0422	57.3	0.986
650	0.338	2.056	2.247	6.648	0.0464	66.6	0.995
700	0.314	2.085	2.426	7.726	0.0505	77.2	1

(continued)

T (K)	ρ (kg/m^3)	c_p [kJ/(kg °C)]	$\mu \times 10^6$ [kg/(m s)]	$\nu \times 10^6$ (m^2/s)	λ [W/(m °C)]	$a \times 10^6$ (m^2/s)	Pr
750	0.2931	2.119	2.604	8.884	0.0549	88.3	1.05
800	0.2739	2.152	2.786	10.172	0.0592	100.1	1.01
850	0.2579	2.186	2.969	11.51221	0.0637	113	1.019
Gas mixture [3]							
0	1.295	1.042	15.8	12.2	0.0228	12.2	0.72
100	0.95	1.068	20.4	21.47	0.0313	21.54	0.69
200	0.748	1.097	24.5	32.75	0.0401	32.8	0.67
300	0.617	1.122	28.2	45.71	0.0484	45.81	0.65
400	0.525	1.151	31.7	60.38	0.057	60.38	0.64
500	0.457	1.185	34.8	76.15	0.0656	76.3	0.63
600	0.405	1.214	37.9	93.58	0.0742	93.61	0.62
700	0.363	1.239	40.7	112.12	0.0827	112.1	0.61
800	0.33	1.264	43.4	131.52	0.0915	131.8	0.6
900	0.301	1.29	45.9	152.49	0.1	152.5	0.59
1000	0.275	1.306	48.4	176	0.109	174.3	0.58
1100	0.257	1.323	50.7	197.28	0.1175	197.1	0.57
1200	0.24	1.34	53	220.83	0.1262	221	0.56
Water vapor [2]							
380	0.5863	2.06	12.71	21.68	0.0246	20.36	1.06
400	0.5542	2.014	13.44	24.25	0.0261	23.38	1.04
450	0.4902	1.98	15.25	31.11	0.0299	30.7	1.01
500	0.4405	1.985	17.04	38.68	0.0339	38.7	0.996
550	0.4005	1.997	18.84	47.04	0.0379	47.5	0.991
600	0.3652	2.026	20.67	56.6	0.0422	57.3	0.986
650	0.338	2.056	22.47	66.48	0.0464	66.6	0.995
700	0.314	2.085	24.26	77.26	0.0505	77.2	1
750	0.2931	2.119	26.04	88.84	0.0549	88.3	1.05
800	0.2739	2.152	27.86	101.72	0.0592	100.1	1.01
850	0.2579	2.186	29.69	115.12	0.0637	113	1.019
380	0.5863	2.06	12.71	21.68	0.0246	20.36	1.06
400	0.5542	2.014	13.44	24.25	0.0261	23.38	1.04
450	0.4902	1.98	15.25	31.11	0.0299	30.7	1.01
500	0.4405	1.985	17.04	38.68	0.0339	38.7	0.996
550	0.4005	1.997	18.84	47.04	0.0379	47.5	0.991
600	0.3652	2.026	20.67	56.6	0.0422	57.3	0.986
650	0.338	2.056	22.47	66.48	0.0464	66.6	0.995
700	0.314	2.085	24.26	77.26	0.0505	77.2	1
750	0.2931	2.119	26.04	88.84	0.0549	88.3	1.05
800	0.2739	2.152	27.86	101.72	0.0592	100.1	1.01
850	0.2579	2.186	29.69	115.12	0.0637	113	1.019

Appendix A.2
Physical Properties of Some Saturated Liquid

t (°C)	ρ (kg/m^3)	c_p [kJ/(kg °C)]	$\mu \times 10^6$ [kg/(m s)]	$v \times 10^6$ (m^2/s)	λ [W/(m °C)]	$a \times 10^7$ (m^2/s)	Pr
Ammonia, NH_3 [4]							
−50	703.69	4.463	306.11	0.435	0.547	1.742	2.6
−40	691.68	4.467	280.82	0.406	0.547	1.775	2.28
−30	679.34	4.467	262.9	0.387	0.549	1.801	2.15
−20	666.69	4.509	254.01	0.381	0.547	1.819	2.09
−10	653.55	4.564	247.04	0.378	0.543	1.825	2.07
0	640.1	4.635	238.76	0.373	0.54	1.819	2.05
10	626.16	4.714	230.43	0.368	0.531	1.801	2.04
20	611.75	4.798	219.62	0.359	0.521	1.775	2.02
30	596.37	4.89	208.13	0.349	0.507	1.742	2.01
40	580.99	4.999	197.54	0.34	0.493	1.701	2
50	564.33	5.116	186.23	0.33	0.476	1.654	1.99
Carbon dioxide, CO_2 [4]							
−50	1156.34	1.84	137.61	0.119	0.085	0.4021	2.96
−40	1117.77	1.88	131.9	0.118	0.1011	0.481	2.45
−30	1076.76	1.97	125.98	0.117	0.1116	0.5272	2.22
−20	1032.39	2.05	118.72	0.115	0.1151	0.5445	2.12
−10	983.38	2.18	111.12	0.113	0.1099	0.5133	2.2
0	926.99	2.47	100.11	0.108	0.1045	0.4578	2.38
10	860.03	3.14	86.86	0.101	0.0971	0.3608	2.8
20	772.57	5	70.3	0.091	0.0872	0.2219	4.1
30	597.81	36.4	47.82	0.08	0.0703	0.0279	28.7
Sulphur dioxide, SO_2 [4]							
−50	1560.84	1.3595	755.45	0.484	0.242	1.141	4.24
−40	1536.81	1.3607	651.61	0.424	0.235	1.130	3.74
−30	1520.64	1.3616	564.16	0.371	0.230	1.117	3.31
−20	1488.60	1.3624	482.31	0.324	0.225	1.107	2.93
−10	1463.61	1.3628	421.52	0.288	0.218	1.097	2.62
0	1438.46	1.3636	369.68	0.257	0.211	1.081	2.38
10	1412.51	1.3645	327.7	0.232	0.204	1.066	2.18
20	1386.40	1.3653	291.14	0.210	0.199	1.050	2.00
30	1359.33	1.3662	258.27	0.190	0.192	1.035	1.83
40	1329.22	1.3674	229.96	0.173	0.185	1.019	1.70
50	1299.10	1.3683	210.45	0.162	0.177	0.999	1.61

(continued)

t (°C)	ρ (kg/m^3)	c_p [kJ/(kg °C)]	$\mu \times 10^6$ [kg/(m s)]	$\nu \times 10^6$ (m^2/s)	λ [W/(m °C)]	$a \times 10^7$ (m^2/s)	Pr
Freon 12, CCl_2F_2 [4]							
−50	1546.75	0.8750	479.49	0.310	0.067	0.501	6.2
−40	1518.71	0.8847	423.72	0.279	0.069	0.514	5.4
−30	1489.56	0.8956	376.86	0.253	0.069	0.526	4.8
−20	1460.57	0.9073	343.23	0.235	0.071	0.539	4.4
−10	1429.49	0.9203	315.92	0.221	0.073	0.550	4.0
0	1397.45	0.9345	299.05	0.214	0.073	0.557	3.8
10	1364.30	0.9496	276.95	0.203	0.073	0.560	3.6
20	1330.18	0.9659	263.38	0.198	0.073	0.560	3.5
30	1295.10	0.9835	251.25	0.194	0.071	0.560	3.5
40	1257.13	1.019	240.11	0.191	0.069	0.555	3.5
50	1215.96	1.0216	231.03	0.190	0.067	0.545	3.5
$C_2H_4(OH)_2$ [4]							
0	1130.75	2.294	65052.05	57.53	0.242	0.934	615
20	1116.65	2.382	21417.35	19.18	0.249	0.939	204
40	1101.43	2.474	9571.427	8.69	0.256	0.939	93
60	1087.66	2.562	5166.385	4.75	0.260	0.932	51
80	1077.56	2.650	3211.129	2.98	0.261	0.921	32.4
100	1058.50	2.742	2148.755	2.03	0.263	0.908	22.4
Mercury, Hg [4]							
0	13628.22	0.1403	1689.9	0.124	8.2	42.99	0.0288
20	13579.04	0.1394	1548.01	0.114	8.69	46.04	0.0249
50	13505.84	0.1386	1404.61	0.104	9.40	50.22	0.0207
100	13384.58	0.1373	1242.09	0.0928	10.51	57.16	0.0162
150	13264.28	0.1365	1131.44	0.0853	11.49	63.54	0.0134
200	13144.94	0.1570	1054.22	0.0802	12.34	69.08	0.0116
250	13025.60	0.1357	996.46	0.0765	13.07	74.06	0.0103
315.5	12847.00	0.134	864.6	0.0673	14.02	81.50	0.0083

t (°C)	ρ (kg/m^3)	c_p [kJ/(kg °C)]	$\mu \times 10^6$ [kg/(m s)]	$\nu \times 10^6$ (m^2/s)	λ [W/(m °C)]	$a \times 10^6$ (m^2/s)	$\beta \times 10^{-4}$ K^{-1}	Pr
Water, H_2O [2]								
0	999.9	4.217	1752.5	1.7527	0.552	0.13494	−0.81	13.39
10	999.7	4.193	1299.2	1.2996	0.576	0.1398	0.87	9.46
20	998.2	4.182	1001.5	1.0033	0.602	0.1442	2.09	6.96
30	995.7	4.179	797	0.8004	0.617	0.14828	3.05	5.4
40	992.2	4.179	651.3	0.6564	0.63	0.14953	3.86	4.32
50	988.1	4.181	544	0.545	0.643	0.15408	4.57	3.54
60	983.2	4.185	460	0.4679	0.653	0.1587	5.22	2.97
70	977.8	4.19	400.5	0.4014	0.662	0.15834	5.83	2.53
80	971.8	4.197	351	0.3612	0.669	0.16403	6.4	2.2
90	965.3	4.205	311.3	0.3225	0.675	0.16629	6.96	1.94
100	958.4	4.216	279	0.2911	0.68	0.16829	7.5	1.73
110	951	4.229	252.2	0.2652	0.683	0.16983	8.04	1.56
120	943.1	4.245	230	0.2439	0.685	0.1711	8.58	1.43
130	934.8	4.263	211	0.2257	0.687	0.17239	9.12	1.31
140	926.1	4.285	195	0.2106	0.687	0.17312	9.68	1.22
150	917	4.31	181	0.1974	0.686	0.17357	10.26	1.14
160	907.4	4.339	169	0.1862	0.684	0.17373	10.87	1.07
170	897.3	4.371	158.5	0.1766	0.681	0.17363	11.52	1.02
180	886.9	4.408	149.3	0.1683	0.676	0.17291	12.21	0.97
190	876	4.449	141.2	0.1612	0.671	0.17217	12.96	0.94
200	863	4.497	133.8	0.155	0.664	0.17109	13.77	0.91
210	852.3	4.551	127.3	0.1494	0.657	0.16938	14.67	0.88
220	840.3	4.614	121.5	0.1446	0.648	0.16713	15.67	87

(continued)

t (°C)	ρ (kg/m^3)	c_p [kJ/(kg °C)]	$\mu \times 10^6$ [kg/(m s)]	$\nu \times 10^6$ (m^2/s)	λ [W/(m °C)]	$a \times 10^6$ (m^2/s)	$\beta \times 10^{-4}$ K^{-1}	Pr
230	827.3	4.686	119.7	0.145	0.639	0.16483	16.8	0.85
240	813.6	4.77	111.4	0.1369	0.629	0.16208	18.08	0.84
250	799	4.869	107	0.1339	0.617	0.1586	19.55	0.84
260	784	4.985	103	0.1314	0.604	0.15455	21.27	0.85
270	767.9	5.13	99.4	0.1294	0.589	0.14952	23.31	0.87
280	750.7	5.3	96.1	0.128	0.573	0.14402	25.79	0.89
290	732.3	5.51	93	0.127	0.558	0.143	28.84	0.92
300	712.5	5.77	90.1	0.1265	0.54	0.13136	32.73	0.96

Temperature Parameters of Gases

Gas	n_μ	n_λ	$n_{\mu\lambda}$	n_{c_p}	Temperature range (K)	Recommended *Pr*
Ar	0.72	0.73	0.7255	0.01	220–1500	0.622
He	0.66	0.725	0.69575	0.01	273–873	0.675
H_2	0.68	0.8	0.746	0.042	220–700	0.68
Air	0.68	0.81	0.7515	0.078	230–1000	0.7
CO	0.71	0.83	0.776	0.068	220–600	0.72
N_2	0.67	0.76	0.7195	0.07	220–1200	0.71
O_2	0.694	0.86	0.7853	0.108	230–600	0.733
Water vapor	1.04	1.185	1.11975	0.003	380–800	1
Gas mixture	0.75	1.02	0.8985	0.134	273–1173	0.63
CO_2	0.88	1.3	1.111	0.34	220–700	0.73
CH_4	0.78	1.29	1.0605	0.534	273–1000	0.74
CCl_4	0.912	1.29	1.1199	0.28	260–400	0.8
SO_2	0.91	1.323	1.13715	0.257	250–900	0.81
H_2S	1	1.29	1.1595	0.18	270–400	0.85
NH_3	1.04	1.375	1.22425	0.34	250–900	0.87

References

1. Incropera, F.P., Dewitt, D.P.: Fundamentals of Heat Transfer. Wiley, New York (1981)
2. Eckert, E.R.G., Drake, R.M.: Heat and Mass Transfer, 2nd edn. McGraw-Hill Book Company, New York (1959)

Index

D.-Y. Shang and L.-C. Zhong, *Heat Transfer of Laminar Mixed Convection of Liquid*, Heat and Mass Transfer, DOI 10.1007/978-3-319-27959-6